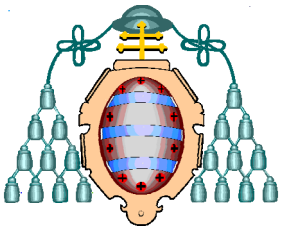

Universidad de Oviedo

Departamento de Bioquímica y Biología Molecular

Identificación de nuevos componentes del degradoma y estudio de la regulación biológica por miRNAs en un modelo animal deficiente en la metaloproteasa Face-1

Tesis Doctoral

Alejandro Piñeiro Ugalde

Oviedo 2011

Director de la Tesis

Carlos López-Otín

ABREVIATURAS, SIGLAS Y SÍMBOLOS

ADAM	metaloproteasa y desintegrina
ADAMTS	ADAM con dominios trombospondina
cDNA	DNA copia
Ci	curio
dCTP	desoxicitidina trifosfato
DNA	ácido desoxirribonucleico
dNTPs	desoxinucleósidos trifosfato
GH	hormona de crecimiento
HGPS	síndrome de Hutchinson-Gilford
IGF-1	factor de crecimiento similar a insulina 1
kb	kilobase
MBS	sitio de unión de microRNAs
MMP	metaloproteasa de matriz
miRNA	microRNA
mRNA	RNA mensajero
pb	pares de bases
PCR	reacción en cadena de la polimerasa
RNA	ácido ribonucleico
ROS	especie reactiva del oxígeno
RISC	complejo de silenciamiento inducido por RNA
SSC	tampón citrato sódico
TAE	tampón Tris/acetato con EDTA
TBE	tampón Tris/borato con EDTA
TE	tampón Tris con EDTA
TIMP	inhibidor tisular de metaloproteasa
Tris	tris(hidroximetil)-aminometano

ÍNDICE

Introducción 1

Los sistemas proteolíticos 4

Metaloproteasas 6

Aminopeptidasas 9

Metzinquinas 12

Envejecimiento 15

Síndromes progeroides 19

Laminopatías 21

Eje somatotrofo 25

microRNAs 28

Biogénesis y mecanismos de acción de los miRNAs 29

Relevancia funcional de los miRNAs 33

Objetivos 37

Material y métodos 41

Material 43

Técnicas de Biología Molecular 45

Técnicas de Biología Celular 52

Ensayos en animales de experimentación 56

Técnicas bioinformáticas 57

Resultados 59

I. Metaloproteasas y el degradoma 61

II. Identificación y caracterización de la aminopeptidasa O humana 91

III. Aminopeptidasa O 101

IV. Identificación y caracterización de las arqueometzinquinas 1 y 2 humanas 113

V. Señalización del eje somatotrofo y contribución de los miRNAs a su regulación en el envejecimiento acelerado 125

VI. Efecto rejuvenecedor de la señalización somatotrofa en el envejecimiento acelerado 135

VII. Análisis de la función de los miRNAs en el envejecimiento 143

VIII. Otros trabajos relacionados con la Tesis 163

Discusión 165

Conclusiones 189

Bibliografía 193

INTRODUCCIÓN

Los elementos reguladores de la actividad celular son responsables del desarrollo, la homeostasis, la plasticidad e incluso el envejecimiento de los organismos y han sido señalados como principal vehículo de la evolución de las especies. Estos elementos constituyen una proporción considerable del genoma de los organismos y se encargan de coordinar la información contenida en el DNA para adaptar el comportamiento celular a las distintas circunstancias exigidas en el espacio y en el tiempo. Este año se cumple el cincuenta aniversario del modelo del operón publicado por François Jacob y Jacques Monod en el que se introducía por primera el concepto de los genes reguladores y se definía un modelo plausible de control de la expresión génica (Jacob y Monod, 1961). La elaboración de este modelo se considera uno de los grandes hitos de la biología molecular de la segunda mitad del siglo XX al señalar el camino que dio lugar al actual conocimiento sobre los sistemas reguladores de la expresión génica. Desde entonces, el modelo originalmente propuesto para bacterias se ha refinado sucesivamente y se han añadido numerosos niveles adicionales de regulación en organismos eucariotas. Así, además del control de la expresión génica mediante factores de transcripción que se unen a secuencias reguladoras situadas en los promotores de los genes, existen sistemas remodeladores de la cromatina que añaden información heredable a la secuencia primaria del DNA en un proceso denominado modificación epigenética (Feinberg, 2007). De igual forma, en las últimas décadas se han identificado diversos grupos de genes que codifican importantes elementos reguladores que actúan a nivel post-transcripcional, ya sea sobre los mRNAs o sobre las proteínas. Entre estos sistemas de regulación post-transcripcional, las proteasas, al igual que las quinasas o fosfatasas, se han revelado como un importante grupo de enzimas que, además de participar en procesos biosintéticos o catabólicos, constituyen un nivel de regulación adicional al de la expresión génica al controlar numerosas propiedades de las proteínas (López-Otín y Hunter, 2010). Por último, el comienzo del siglo XXI ha supuesto una nueva revolución en el campo del control de la actividad génica, con el descubrimiento de miles de moléculas de RNA reguladoras, entre las que destacan los microRNAs y los lincRNAs (*large intervening non-coding RNAs*) (Lee y col., 1993; Guttman y col., 2009).

La interacción entre todos estos sistemas de regulación da lugar a una intrincada red de conexiones que permite que un mismo genoma sea capaz de generar y coordinar la notable variedad de tipos celulares especializados que conforman un organismo vivo, así como adaptar sus funciones a las distintas condiciones que se puedan presentar. Dada su importancia vital, en la presente Tesis Doctoral abordaremos el estudio de los sistemas de regulación biológica mediante una serie de objetivos dirigidos a la identificación de nuevas proteasas y al análisis de la función reguladora de los microRNAs en procesos de envejecimiento normal y patológico.

Los Sistemas Proteolíticos

Las proteasas constituyen un grupo de enzimas presente en todos los seres vivos, desde virus hasta mamíferos. La característica común de este conjunto de enzimas es la hidrólisis del enlace peptídico, un proceso históricamente asociado a la degradación inespecífica de proteínas, pero que en los últimos años se ha revelado como un evento clave en la regulación de múltiples procesos biológicos. Así, hoy sabemos que la proteólisis constituye un sistema altamente selectivo de modificación post-traduccional que condiciona numerosas propiedades de las proteínas, ofreciendo un amplio abanico de posibilidades de regulación. Este tipo de hidrólisis específica de determinados enlaces peptídicos de proteínas concretas se denomina procesamiento proteolítico y su impacto sobre las proteínas es muy diverso, permitiendo modular características tales como su localización subcelular, su estado de actividad, su interacción con otras proteínas o su vida media, entre otras (López-Otín y Overall, 2002). Consecuentemente, las proteasas influyen decisivamente en procesos tan importantes como la replicación del DNA, el control del ciclo celular, la proliferación y migración celulares, la diferenciación celular o la muerte celular programada. Asimismo, la proteólisis afecta a numerosas funciones del organismo, como la morfogénesis y remodelación tisulares, la cicatrización de tejidos, la ovulación y fertilización, la angiogénesis, la hemostasis o la inmunidad (López-Otín y Bond, 2008).

Dada su relevancia funcional, los sistemas proteolíticos requieren una estricta regulación que garantice su correcta actividad espacio-temporal. Por esta razón, además de los mecanismos de modulación de la expresión génica, las proteasas poseen diversos sistemas de regulación a nivel post-traduccional, entre los que destacan la compartimentalización, la síntesis en forma de precursores inactivos o la regulación de su actividad mediante moléculas inhibidoras (Overall y López-Otín, 2002). Sin embargo, pese a la existencia de estos mecanismos, las alteraciones en el equilibrio de los sistemas proteolíticos pueden comprometer gravemente la homeostasis de los tejidos y dar lugar al desarrollo de numerosas patologías humanas, tales como la osteoporosis, las enfermedades neurodegenerativas y cardiovasculares, la artritis reumatoide o el cáncer (Puente y col., 2003). Asimismo, mutaciones en genes de proteasas que conlleven cambios en sus propiedades pueden desembocar en el desarrollo de graves enfermedades. Así, se conoce la existencia de más de 90 enfermedades hereditarias humanas causadas por mutaciones en genes de proteasas (*http://degradome.uniovi.es*). En este sentido, merece especial atención el papel crucial que juegan las proteasas en el desarrollo y progresión del cáncer. Históricamente, estos enzimas se habían considerado como factores pro-tumorales implicados en las etapas de invasión y metástasis del cáncer, dada su capacidad de degradar la matriz extracelular. Sin embargo, tal y como cabría esperar a raíz de su relevancia funcional, el conocimiento adquirido durante los últimos años ha revelado una contribución mucho más compleja de los sistemas proteolíticos en la progresión tumoral. Así, hoy sabemos que las proteasas no solo participan de manera clave en todas las etapas del desarrollo tumoral, sino que muchos de estos enzimas ejercen importantes funciones como proteínas supresoras de tumores, existiendo incluso proteasas que se comportan como factores pro- o anti-tumorales dependiendo del contexto en el que ejerzan su función (López-Otín y Matrisian, 2007).

La creciente complejidad de los sistemas proteolíticos en términos de diversidad y relevancia funcionales, y su extensa implicación en patologías humanas pusieron de manifiesto la necesidad de modificar el abordaje de su estudio hacia un enfoque global e incorporar nuevos conceptos. Así, se ha

introducido el término *degradoma* para designar al conjunto de proteasas expresadas en un momento dado por una célula, tejido u organismo. De manera análoga, se ha definido la *degradómica* como el conjunto de aproximaciones genómicas, transcriptómicas y proteómicas destinadas a la identificación y caracterización de las proteasas, sus sustratos y sus inhibidores, en un determinado organismo (López-Otín y Overall, 2002). En este sentido, el conocimiento de los sistemas proteolíticos ha avanzado notablemente en los últimos años gracias a la disponibilidad de las secuencias genómicas humana y de otros organismos, y al desarrollo de las correspondientes técnicas bioinformáticas para su análisis. El interés de nuestro laboratorio por los sistemas proteolíticos nos impulsó a contribuir a su estudio desde un enfoque global mediante la búsqueda bioinformática de genes de proteasas en los genomas de diversos organismos, aproximación que condujo a la descripción de los degradomas humano y de otros mamíferos como el ratón, la rata, el chimpancé, el orangután y el ornitorrinco (Puente y col., 2003; Puente y López-Otín, 2004; Puente y col., 2005; Ordoñez y col., 2008; Locke y col., 2011). La utilización de estas metodologías permitió a nuestro laboratorio la identificación de numerosas proteasas desconocidas y la anotación en el genoma humano de un total de 570 genes codificantes de proteasas u homólogos de proteasas y de más de 150 genes de inhibidores de proteasas. Estos datos indican que el degradoma humano comprende un 2% del total de genes del genoma, poniendo una vez más de manifiesto la importancia de los sistemas proteolíticos en nuestra biología. Además, los estudios comparativos de degradomas han permitido establecer claves sobre la evolución de las proteasas e incluso de los propios organismos, ofreciendo resultados tan interesantes como el inesperado mayor tamaño de los degradomas de roedores, pese a que su genoma es un 15% más pequeño.

Metaloproteasas

Aunque el mecanismo general de proteólisis consiste en el ataque nucleofílico al carbono carbonilo del enlace peptídico, la evolución ha generado diferentes alternativas para ejecutar esta reacción, lo cual permite la

clasificación de las proteasas en 6 grandes grupos o clases catalíticas. Por un lado se encuentran las serín-, treonín- y cisteín-proteasas, en las que el nucleófilo consiste en un grupo hidroxilo (serín- y treonín-proteasas) o sulfhidrilo (cisteín-proteasas) de la cadena lateral de uno de estos aminoácidos que dan nombre a la clase. Por el contrario, las aspartil-, glutamil- y metaloproteasas utilizan una solución alternativa que consiste en el empleo de una molécula de agua que se encuentra polarizada en el centro activo, de manera que el oxígeno puede actuar como nucleófilo en la reacción.

Las metaloproteasas constituyen un grupo heterogéneo de enzimas proteolíticos caracterizado por la utilización de iones metálicos, comúnmente zinc, para la consecución de la catálisis enzimática. Sin embargo, la forma de coordinar los iones metálicos y acomodar los sustratos ha encontrado múltiples soluciones durante la evolución de esta clase catalítica, lo que permite clasificar a las metaloproteasas en una organización de clanes y familias definidas por sus secuencias de aminoácidos, sus estructuras tridimensionales o mediante estudios mutacionales (Rawlings y Barrett, 1993). Así, la versión 9.4 de una de las bases de datos de referencia de enzimas proteolíticos, MEROPs (*http:// merops.sanger.ac.uk*), recoge un total de 63.670 secuencias de este grupo de proteasas, organizadas en 15 clanes y 55 familias. En la mayoría de metaloproteasas, la estructura básica del centro activo está compuesta por un ion zinc, encargado de polarizar la molécula de agua, coordinado a través de dos residuos de histidina de la cadena polipeptídica y un tercer residuo de naturaleza ácida que puede ser glutamato o aspartato. Además de estos tres aminoácidos de unión al zinc, existe un cuarto aminoácido esencial que se comporta como una base general en el proceso de la catálisis y que suele ser un glutamato (Gomis-Ruth, 2003). Estos cuatro residuos conforman el motivo básico de catálisis y su posición en la secuencia suele ser invariable para los miembros de un mismo clan. Aunque estos cuatro aminoácidos son cruciales para la catálisis, existen otros residuos que muestran más variabilidad entre proteasas y que influyen en la eficiencia del enzima o su especificidad, al participar en procesos como la acomodación del sustrato, la estabilización de intermediarios de reacción o el correcto plegamiento de la proteína.

Las metaloproteasas representan la clase catalítica más numerosa del degradoma de muchos mamíferos, incluido el ser humano, cuyo genoma codifica al menos 191 miembros de esta clase de enzimas (**Figura 1**). Además, las metaloproteasas son una de las clases catalíticas más estudiadas, no solo por su abundancia y relevancia funcional, sino por sus profundas implicaciones en diversas patologías y, especialmente, en el cáncer. La mayor parte de las metaloproteasas pertenecen al clan MA, cuyo motivo característico de unión al zinc es HEXXH, donde los dos residuos de histidina se encargan de coordinar el ion metálico y el glutamato actúa como base general. Asimismo, las proteasas de este clan se clasifican en tres grandes grupos: gluzinquinas, aspzinquinas y metzinquinas. Los dos primeros grupos reciben su nombre de acuerdo al residuo que ocupa la tercera posición de coordinación del zinc, glutamato y aspartato, respectivamente, mientras que el término metzinquinas ha sido acuñado en base a un residuo de metionina conservado que forma parte de una estructura denominada giro-metionina. En este sentido, la primera parte del trabajo realizado en esta Tesis Doctoral se centra en la caracterización de una nueva aminopeptidasa del subclan de las gluzinquinas y de dos metaloproteasas no descritas hasta el momento de iniciar nuestro

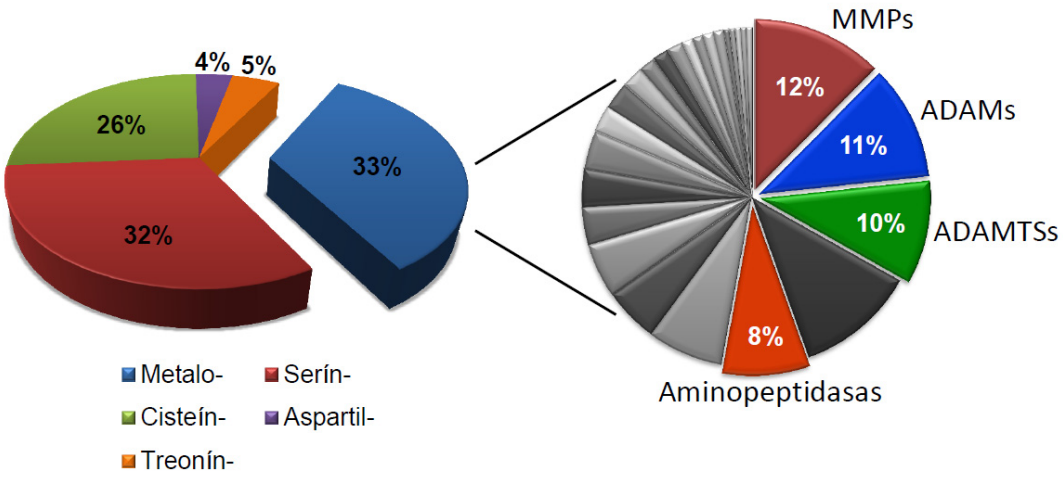

Figura 1. Distribución de las clases catalíticas del degradoma humano (izquierda) mostrando la proporción relativa de las principales familias de metaloproteasas discutidas en la presente Tesis Doctoral (derecha). MMPs, metaloproteasas de matriz extracelular; ADAMs, metaloproteasas con dominios desintegrina; ADAMTSs, ADAMs con dominios trombospondina.

trabajo y cuya identificación y caracterización nos ha permitido definir una nueva familia de metzinquinas humanas.

Aminopeptidasas

Las aminopeptidasas son un tipo de enzimas proteolíticos que actúan sobre el extremo amino terminal de péptidos o proteínas y producen la liberación secuencial de aminoácidos. Las principales aminopeptidasas animales pertenecen a la familia M1 de metaloproteasas, la cual se encuentra incluida en el subclan MA(E) de gluzinquinas (**Figura 1**).

Además de la familia M1, las gluzinquinas comprenden otras cinco familias con representantes en humanos (M2, M3, M13, M41 y M48), las cuales muestran una gran variedad de actividades y funciones. La familia M2 está compuesta exclusivamente por carboxipeptidasas que, en contraposición a las aminopeptidasas, liberan aminoácidos del extremo carboxilo terminal de péptidos o proteínas. Un miembro destacado de esta familia es el enzima convertidor de angiotensina, que produce angiotensina II a partir de angiotensina I y por tanto contribuye de forma clave a la regulación de la presión sanguínea, razón por la cual ha sido diana del desarrollo de diversos inhibidores para el tratamiento de la hipertensión (Danilczyk y col., 2003). El resto de familias de gluzinquinas presentan actividad endopeptidasa, es decir, escinden enlaces peptídicos situados en el interior de péptidos o proteínas, produciendo la liberación de dos nuevos fragmentos. Las familias M3 y M13 están formadas por oligopeptidasas (endopeptidasas que actúan sobre pequeños péptidos) involucradas en el procesamiento de una gran variedad de péptidos bioactivos de los sistemas nervioso, inmune y cardiovascular, así como en la regulación del sistema de clase I de presentación antigénica o en la maduración de proteínas mitocondriales (Chew y col., 1997; Turner y col., 2001; Lim y col., 2007). La familia M41 contiene exclusivamente proteasas que, aunque codificadas en el genoma nuclear, son transportadas a la mitocondria donde participan activamente en la homeostasis de este orgánulo (Koppen y Langer, 2007). Por último, la familia M48 contiene dos endopeptidasas transmembrana humanas: OMA1, situada en la mitocondria, y ZMPSTE-

24/FACE-1, cuyo único sustrato conocido es la prelamina nuclear (Pendás y col., 2002). Cabe destacar que esta familia de metaloproteasas ha adquirido gran protagonismo en los últimos años debido al hallazgo de que mutaciones en el gen *FACE1* o en el gen que codifica su sustrato, la prelamina A, son responsables del desarrollo de síndromes de envejecimiento acelerado, tal como se discutirá más adelante.

La familia M1 está constituida por aminopeptidasas ampliamente distribuidas desde arqueobacterias a mamíferos. Estructuralmente, estos enzimas están definidos por la secuencia consenso de unión al zinc, $HEXXHX_{(18)}E$, así como por la presencia de un motivo exclusivo de la familia denominado "caja GXMENX" que participa en la acomodación del sustrato y en la estabilización de intermediarios de reacción (Vazeux y col., 1998; Iturrioz y col., 2001). El degradoma humano consta de 13 de estas aminopeptidasas cuyo estudio resulta de notable interés, no solo por su relevancia en la fisiología y patología humanas, sino por su diversidad en términos de especificidad de sustrato, localización subcelular y funciones (**Tabla 1**). Así, por ejemplo, la aminopeptidasa A (APA) se encuentra unida a membrana y procesa preferentemente residuos ácidos de los extremos N-terminal de diversos péptidos entre los que se encuentra la angiotensina II, lo que convierte este enzima en un importante regulador del sistema renina-angiotensina en el cerebro (Reaux y col., 1999). La aminopeptidasa N (APN), que muestra afinidad por residuos neutros, también participa en la regulación del sistema renina-angiotensina a través del procesamiento de la angiotensina III (Danziger, 2008). Además, es destacable que la APN es el receptor de ciertos tipos de coronavirus y su expresión se encuentra alterada en varios tumores sólidos asociándose con un incremento en la capacidad de invasión y metástasis (Lachance y col., 1998; Inagaki y col., 2010). Por otra parte, la aminopeptidasa TRHDE, que se encuentra soluble en suero o unida a membrana, muestra una gran selectividad de sustrato, siendo solo activa frente a la hormona liberadora de tirotropina (Schauder y col., 1994). En contraposición, la aminopeptidasa asociada a retículo endoplasmático (ERAP1), posee unos requerimientos de sustrato peculiares, ya que procesa una amplia variedad de aminoácidos del extremo amino terminal, pero solo si

los péptidos son mayores de ocho aminoácidos. Esta proteasa participa en la presentación de antígenos de clase I, siendo el enzima responsable del "*trimming*" o "recorte" de los péptidos generados en el proteasoma (Serwold y col., 2002). Otro miembro atípico de esta familia es la aminopeptidasa LTA4H, un enzima tanto citoplasmático como nuclear que, además de su actividad proteolítica, hidroliza específicamente el grupo epóxido del lípido leucotrieno A4 (LTA4) convirtiéndolo en LTB4, un potente quimioatrayente de leucocitos (Haeggstrom y col., 1990). Por último, otro miembro que merece especial

Tabla 1. Aminopeptidasas humanas de la familia M1 de metaloproteasas.

Aminopeptidasa	Símbolo oficial	Locus	Identificador MEROPS
Aminopeptidasa N	ANPEP	15q26	M01.001
Aminopeptidasa A	ENPEP	4q26	M01.003
Leucotrieno A4 hidrolasa	LTA4H	12q23	M01.004
Ectoenzima degradador de TRH	TRHDE	12q21	M01.008
Aminopeptidasa sensible a puromicina	NPEPPS	17q21	M01.010
Leucil-cistinil aminopeptidasa	LNPEP	5q15	M01.011
Aminopeptidasa B	RNPEP	1q32	M01.014
Aminopeptidasa de retículo endoplásmico 1	ERAP1	5q15	M01.018
Aminopeptidasa B2	RNPEPL1	2q37	M01.022
Aminopeptidasa de retículo endoplásmico 2	ERAP2	5q15	M01.024
Aminopeptidasa Q	AQPEP	5q23	M01.026
Aminopeptidasa O	AOPEP	9q22	M01.028
Aminopeptidasa sensible a puromicina 2	NPEPPSL1	17q12	M01.xxx

mención por su diversidad de funciones es la aminopeptidasa placentaria P-LAP, también conocida como aminopeptidasa regulada por insulina (IRAP). Por una parte, este enzima es la principal oxitocinasa encargada de degradar la oxitocina durante el embarazo, previniendo las contracciones uterinas hasta el momento del parto (Tsujimoto y col., 1992). Por otro lado, también se ha descrito que, en órganos diana de insulina como páncreas y músculo, esta aminopeptidasa se encuentra asociada a receptores GLUT4 en vesículas intracelulares que son translocadas a la membrana plasmática en respuesta a insulina, aunque se desconoce la relevancia funcional de este proceso (Keller y col., 1995). Además, hace una década se demostró que esta aminopeptidasa

era el receptor de angiotensina IV, desempeñando una importante función en la regulación de la memoria cognitiva, lo que la ha convertido en diana terapéutica para el tratamiento de desórdenes neurológicos como la enfermedad de Alzheimer (Albiston y col., 2001; Hallberg, 2009).

Metzinquinas

Las metzinquinas comprenden un extenso y complejo conjunto de metaloproteasas ampliamente distribuidas en todos los organismos y de gran interés en la fisiología y patología de mamíferos. Los determinantes estructurales que agrupan a este conjunto de proteasas son la presencia de un motivo consenso de unión al zinc, HEXXHXXGXXH/D, así como la existencia, en todos sus miembros, de una estructura característica denominada giro metionina (Gomis-Ruth, 2003). Al igual que en el resto de metaloproteasas, las dos histidinas y el glutamato de la secuencia HEXXH actúan como residuos de unión al zinc y base general, respectivamente, pero de forma específica en este grupo de metaloproteasas, el tercer residuo de unión al zinc lo constituye una histidina o un residuo de aspártico que se conecta al centro activo a través del giro de la cadena polipeptídica en torno a un residuo de glicina altamente conservado. Además, una metionina conservada y separada del centro activo por una región amino terminal de extensión variable produce un giro beta del esqueleto peptídico que crea una cavidad hidrofóbica en torno al ion zinc. Su centro activo presenta una organización óptima para alojar grandes sustratos, estando constituido por dos lóbulos laterales que dejan una larga cavidad central con el ion zinc situado en el fondo. Como consecuencia de esta característica, las metzinquinas son endopeptidasas, con la posible excepción de las arqueometzinquinas, tema que será tratado en los resultados y discusión de la presente Tesis. Las metzinquinas contienen algunas de las familias de proteasas más numerosas y estudiadas de mamíferos como son las MMPs (metaloproteasas de matriz extracelular), las ADAMs (metaloproteasas con dominios desintegrina) y las ADAMTSs (ADAMs con dominios trombospondina) (**Figura 1**). Estas familias de metzinquinas, que en conjunto representan el 33% del total de metaloproteasas humanas, se caracterizan por una enorme

diversidad estructural, de manera que, aun compartiendo dominios catalíticos similares, la incorporación de distintos módulos proteicos adicionales les aporta nuevas propiedades y los convierte en unos enzimas muy versátiles involucrados en numerosos procesos fisiológicos y patológicos, incluyendo la progresión tumoral.

Las MMPs constituyen un grupo de enzimas que cuenta con 24 representantes en el genoma humano y cuya principal característica es la capacidad para degradar distintos componentes de la matriz extracelular. Su arquitectura básica se compone de un péptido señal que dirige el enzima a la ruta secretora, un dominio catalítico que se mantiene inactivo gracias a la existencia de una región propéptido, una región bisagra y un dominio hemopexina que contribuye a la especificidad de sustrato y participa en la interacción con sus inhibidores endógenos (TIMPs) (Fanjul-Fernández y col., 2010). Sin embargo, algunas MMPs como las pertenecientes al grupo de las MT-MMPs, disponen de regiones transmembrana o de unión a glicosilfosfatidilinositol que las mantienen ancladas en el exterior de la superficie celular. Además, existen MMPs que carecen del módulo hemopexina, como las matrilisinas, o que disponen de dominos tipo II de fibronectina que les permite unirse al colágeno, como es el caso de las gelatinasas. Estas características contribuyen a que las MMPs participen en un gran número de procesos de remodelación tisular, como la osificación, la angiogénesis, la adipogénesis, la morfogénesis de la glándula mamaria en la pubertad o la cicatrización de heridas (Folgueras y col., 2004). Sin embargo, no solo es su capacidad de degradar la matriz extracelular y favorecer la migración celular lo que les otorga estas funciones, sino que las MMPs generan o liberan un gran número de moléculas bioactivas que modifican las señales presentes en el microambiente extracelular afectando al comportamiento de la célula. Como consecuencia de su relevancia funcional, la desregulación de estos enzimas tiene efectos dramáticos para el organismo, habiéndose descrito su implicación en procesos como el cáncer, la artritis y las enfermedades respiratorias, vasculares y neurológicas (Fanjul-Fernández y col., 2010).

Por otra parte, las ADAMs y ADAMTSs constituyen dos grupos

estructuralmente relacionados de enzimas de la familia de las reprolisinas. Las ADAMs son mayoritariamente proteínas transmembrana que constan de un prodominio que mantiene latente su actividad hidrolítica, una unidad catalítica, un dominio desintegrina, un módulo similar a EGF (factor de crecimiento epidérmico), una región transmembrana y una cola citoplasmática. El genoma humano contiene genes para 21 de estos enzimas, mientras que el de ratón dispone de 35 debido principalmente a la expansión del subgrupo de las denominadas testasas. Las ADAMs ejercen importantes funciones de adhesión y comunicación celular a través de sus dominios desintegrina y del "*shedding*" o proteólisis de los dominios extracelulares de una gran variedad de proteínas de membrana incluyendo citoquinas, factores de crecimiento y moléculas de adhesión. Así, se ha descrito su implicación en procesos como la proliferación y migración celulares, la fertilización, la inmunidad, el desarrollo, la angiogénesis o la regeneración de los tejidos (Reiss y Saftig, 2009). Por su parte, las ADAMTSs tienen 19 representantes en el genoma humano y, aunque guardan gran similitud con las ADAMs, carecen de las regiones transmembrana y citoplasmática, y en su lugar poseen un dominio central trombospondina tipo I, seguido de una región espaciadora y un número variable de dominios trombospondina (Porter y col., 2005). Como consecuencia, las ADAMTSs son secretadas al medio extracelular donde se unen a distintos componentes a través de sus dominios trombospondina y desarrollan sus funciones. Así, por ejemplo, las agrecanasas constituyen un grupo de ADAMTSs con capacidad de degradar diversos proteoglicanos como el agrecano en el cartílago, el brevicano en el sistema nervioso central o el versicano del sistema vascular. Otro grupo de ADAMTSs bien caracterizado lo forman las denominadas N-proteinasas de procolágeno, que participan en la maduración del procolágeno mediante el procesamiento de la región amino terminal de este precursor. Por último, cabe también destacar la ADAMTS13, que procesa el factor de coagulación de von Willebrand y cuya deficiencia es responsable de la púrpura trombocitopénica trombótica caracterizada por la formación de microcoágulos en los tejidos (Levy y col., 2001).

Es importante mencionar que las metzinquinas comprenden también varias familias de proteasas que, aunque no están presenten en mamíferos,

poseen un gran impacto en la biología humana al constituir factores determinantes en la infección por varios microorganismos (Gomis-Ruth, 2003). Así, la familia de las serralisinas incluye varios factores de virulencia bacterianos, como la serralisina de *Serratia marcescens*, la mirabilisina de *Proteus mirabilis*, o la aeruginolisina de *Pseudomonas aeruginosa.* Análogamente, la familia de leishmanolisinas está constituida por varias proteasas que participan en la infección, invasión o supervivencia en el hospedador de varios protozoos parásitos de los géneros *Leishmania* y *Trypanosoma,* causantes de patologías como la enfermedad de Chagas o del sueño.

En resumen, dado el elevado número de metaloproteasas humanas y su enorme diversidad y relevancia funcional en mamíferos, el estudio detallado de los sustratos, mecanismos de regulación y funciones de este grupo de proteasas aportará conocimientos clave para la comprensión de numerosos aspectos de la fisiología, patología y evolución humanas.

Envejecimiento

El envejecimiento se puede definir como el progresivo decaimiento con la edad de las funciones del organismo, asociado a un aumento de la mortalidad. En las sociedades modernas, este progresivo deterioro del organismo ocasiona un aumento en la prevalencia de un cierto número de enfermedades asociadas a la edad, como la diabetes tipo 2, las alteraciones vasculares y neurodegenerativas, y el cáncer. El estudio de los mecanismos moleculares subyacentes al envejecimiento podría aportar importantes pistas sobre las causas de estas enfermedades y ayudar a establecer estrategias encaminadas a su paliación o prevención. Aunque existen múltiples teorías para explicar la existencia de envejecimiento en los organismos, una de las que ha cobrado más apoyos es la teoría del soma prescindible, según la cual el envejecimiento es el resultado del compromiso entre la inversión en la reproducción y el mantenimiento del organismo (Kirkwood y Holliday, 1979).

Esta teoría se basa en esencia en el concepto de antagonismo pleiotrópico, que describe cómo se pueden fijar en la población alelos con efectos negativos sobre el envejecimiento como consecuencia del solapamiento con funciones positivas en la edad reproductora. Además, la adaptación de este concepto a la teoría del soma prescindible también permite explicar la existencia de presiones evolutivas negativas hacia la fijación de alelos ventajosos en edades avanzadas, ya que la inversión en el mantenimiento compromete la inversión en reproducción y, por lo tanto, el éxito en la producción de descendencia. En contraposición al antagonismo pleiotrópico, aunque no mutuamente excluyente, la teoría de la acumulación de mutaciones ofrece una alternativa mecanística según la cual, algunas mutaciones perjudiciales en edades avanzadas se fijan pasivamente en la población como consecuencia de la neutralidad de la selección natural una vez superada la edad reproductora.

Independientemente de los mecanismos evolutivos, el envejecimiento es el resultado de la progresiva acumulación de daño molecular y celular como consecuencia directa de las limitaciones en los mecanismos de reparación y mantenimiento. Uno de los primeros mecanismos señalados como responsables del envejecimiento fue la senescencia celular. La senescencia fue descrita por Hayflick y colaboradores en 1961 como un estado irreversible de quiescencia celular en el que entraban los fibroblastos humanos cultivados *in vitro* al alcanzar un cierto número de divisiones. Aun desconociendo los mecanismos moleculares subyacentes, la observación de que las células tumorales adquirían la capacidad de dividirse de manera indefinida, llevó a Hayflick y colaboradores a postular, de forma muy acertada, que la senescencia constituía un mecanismo de protección tumoral que impedía a las células proliferar indefinidamente, lo cual a su vez podría ser en parte responsable del envejecimiento de los organismos (Hayflick y Moorhead, 1961). Cincuenta años después no han variado mucho los planteamientos de Hayflick y así hoy sabemos que la senescencia forma parte, junto con la apoptosis, de los mecanismos de respuesta a daño genético, siendo la interacción entre estos mecanismos y el daño en el DNA los principales responsables de las alteraciones asociadas al envejecimiento.

Es ampliamente reconocido que con el paso del tiempo los organismos acumulan daño en el DNA, debido en parte a causas externas como la radiación ionizante y ultravioleta, pero principalmente como consecuencia de procesos inherentes a la célula entre los que destacan el acortamiento de los telómeros y la oxidación del DNA por las especies reactivas del oxígeno (ROS). El acortamiento de telómeros es el responsable de la senescencia replicativa de fibroblastos humanos observada por Hayflick. Los telómeros consisten en repeticiones de secuencias de DNA situadas en los extremos de los cromosomas, que protegen al DNA de la degradación y recombinación. El problema surge por la imposibilidad intrínseca de la maquinaria de replicación de sintetizar correctamente los extremos de moléculas lineales de DNA, lo que provoca un acortamiento progresivo de los telómeros en cada ronda de replicación. Cuando se llega a un acortamiento crítico, los telómeros son reconocidos por los mecanismos de protección del DNA como roturas de doble hebra y se dispara una respuesta que desencadena la senescencia celular. Sin embargo, no todas las células sufren este proceso, sino que las células germinales y las células madre producen un complejo ribonucleoproteico denominado telomerasa que les permite extender los telómeros previniendo su acortamiento y escapando a la senescencia. Por lo tanto, el acortamiento de los telómeros no es un fallo evolutivo de la maquinaria de replicación, sino que supone un ejemplo muy ilustrativo del concepto de antagonismo pleiotrópico, constituyendo en edades tempranas un sistema de protección frente al cáncer que limita el potencial proliferativo de las células, pero comprometiendo la capacidad regenerativa de los distintos tejidos a edades avanzadas a la vez que aumenta el riesgo de transformación neoplásica como consecuencia de la inestabilidad genómica generada. Consecuentemente, el 80% de los tumores adquieren capacidad para prevenir el acortamiento de los telómeros, generalmente mediante la expresión de telomerasa (Collado y col., 2007). Asimismo, los ratones deficientes en telomerasa no solo presentan resistencia al desarrollo de tumores sino que envejecen prematuramente (Blasco y col., 1997).

Sin embargo, la observación de que los fibroblastos murinos, pese a tener telómeros más largos, entraban en senescencia más rápidamente que los

de origen humano, puso de manifiesto la existencia de otro elemento potencialmente responsable del envejecimiento celular, las especies reactivas del oxígeno (ROS) (Chen y col., 2007). Las ROS se producen en el metabolismo celular, principalmente durante la respiración mitocondrial, y, cuando exceden la capacidad de los mecanismos celulares de destoxificación, ocasionan daño oxidativo en el DNA, el cual a su vez dispara la respuesta a daño genético y provoca la senescencia celular. Así, se ha detectado aumento de ROS con la edad en diversos tejidos humanos, atribuido tanto a un decaimiento de los mecanismos destoxificantes como a la pérdida de eficiencia de los componentes de la cadena respiratoria. Sin embargo, algunos trabajos recientes muestran resultados contradictorios sobre la contribución de las ROS en el envejecimiento. Así, sorprendentemente, la deficiencia en *Caenorhabditis elegans* de uno de los principales enzimas destoxificantes, la superóxido dismutasa mitocondrial (Sod-2), a pesar de aumentar la producción de ROS extiende la longevidad (Van Raamsdonk y Hekimi, 2009). En el mismo sentido, la sobreexpresión de los principales enzimas destoxificantes en ratones no se traduce en ningún aumento de la longevidad (Perez y col., 2009). Aunque no está claro en qué grado contribuyen las ROS al envejecimiento, hay que destacar que el daño oxidativo no es la única fuente de lesiones del DNA, existiendo también alteraciones espontáneas debidas a fallos en la incorporación de nucleótidos durante la replicación, interconversión de bases causadas por desaminación, pérdida de bases por despurinización, o modificación de bases por alquilación. En total, se estima que cada célula experimenta hasta 10.000 lesiones espontáneas cada día (Hoeijmakers, 2009).

Sin embargo, tal como se ha comentado anteriormente, el daño por sí mismo no es el responsable directo del envejecimiento, sino que es la interacción con los sistemas de respuesta a daño en el DNA lo que dispara una respuesta senescente o apoptótica que conduce a la pérdida del potencial proliferativo de los tejidos. La respuesta a daño en el DNA constituye parte de los sistemas de mantenimiento del genoma, que incluyen también elementos de detección de daño y de reparación (López-Contreras y Fernández-Capetillo, 2010). Así, cuando se produce una lesión en el DNA los sistemas de detección indican la presencia de esta situación a los elementos de reparación, que son

reclutados a la zona dañada. Si el nivel de lesiones es muy elevado o el daño es irreparable, la respuesta a daño en el DNA desencadena la senescencia o la apoptosis. De esta manera, se puede establecer una conexión entre el cáncer y el envejecimiento, según la cual ambos procesos convergen en su etiología, el daño en el DNA, pero divergen en la respuesta a este daño. Consistentemente, las mutaciones conductoras del cáncer suceden frecuentemente en genes de los propios sistemas de mantenimiento del genoma, lo cual permite a las células crecer indefinidamente pese a la existencia de un gran número de mutaciones y aberraciones cromosómicas. En sentido inverso, la sobreexpresión de estos elementos conduce frecuentemente a una mayor susceptibilidad celular a lesiones en el DNA y a una reducción del potencial proliferativo asociado a un aumento en la senescencia. Un ejemplo muy ilustrativo es el supresor de tumores *TP53*, uno de los genes más frecuentemente mutados en cáncer (Hoogervorst y col., 2005). El producto de este gen, la proteína p53, constituye uno de los principales efectores de la respuesta a daño al DNA y su activación mediante una amplia variedad de modificaciones post-traduccionales ocasiona parada del ciclo celular, senescencia o apoptosis. Consecuentemente, los ratones deficientes o heterocigotos para este gen son completamente normales, pero muestran una clara predisposición a desarrollar una gran variedad de tumores (Donehower y col., 1992). Por el contrario, ratones modificados genéticamente que sobreexpresan este supresor tumoral envejecen prematuramente y son resistentes al cáncer, aunque cabe destacar que el incremento controlado de la señalización de p53 en otro modelo de ratón modificado genéticamente protege frente al cáncer sin afectar a la longevidad (García-Cao y col., 2002; Tyner y col., 2002).

Síndromes progeroides

El descubrimiento de enfermedades humanas de envejecimiento acelerado en las que aparecen de forma prematura múltiples alteraciones asociadas a la edad ha ayudado a esclarecer los mecanismos moleculares subyacentes al envejecimiento fisiológico. Estas progerias se desarrollan tanto

en niños como en adultos y recapitulan en mayor o menor grado alteraciones del envejecimiento como el encanecimiento o la alopecia, la distribución anormal de grasa subcutánea, la atrofia muscular, la osteoporosis, la diabetes tipo 2, las enfermedades cardiacas o neurodegenerativas y el cáncer. Uno de los aspectos más reveladores en este sentido es que la mayoría de estos síndromes se deben a mutaciones en genes de mantenimiento del genoma o en genes implicados en la organización de la envuelta nuclear.

Los síndromes pertenecientes al primero de estos grupos son un claro ejemplo de la implicación del daño en el DNA y los mecanismos de respuesta a este daño en el envejecimiento y el cáncer. Así, según el tipo de elementos de los sistemas de mantenimiento del genoma que se encuentren afectados, estos síndromes pueden estar acompañados o no de predisposición a cáncer, e incluso presentar resistencia a su desarrollo. Por ejemplo, mutaciones en el gen *WRN* causan el síndrome de Werner, caracterizado tanto por un envejecimiento acelerado como por una predisposición al cáncer (Machwe y col., 2006). La proteína WRN es una helicasa involucrada en la reparación por recombinación homóloga y en el mantenimiento de los telómeros. En esta patología, la acumulación de lesiones no reparadas genera inestabilidad genómica, lo cual aumenta la probabilidad de padecer cáncer a la vez que dispara los mecanismos de senescencia y apoptosis produciendo envejecimiento acelerado. Sin embargo, la tricotiodistrofia o el síndrome de Cockayne producen envejecimiento acelerado y una aparente protección frente al cáncer (Hoeijmakers, 2009). Este hecho se debe a que los genes afectados en estas patologías pertenecen al sistema de reparación por escisión acoplado a la transcripción (TC-NER), que se restringe a la resolución de bloqueos durante la transcripción. Por ello, el fallo en este sistema tiene pocos efectos mutagénicos en el genoma, pero desencadena la señalización de daño al DNA que conduce a la senescencia o apoptosis celular, acelerando el envejecimiento y protegiendo frente al cáncer. Interesantemente, algunas mutaciones en los genes del sistema de reparación por escisión de nucleótidos que afectan también al mantenimiento global del genoma, causan el síndrome de xeroderma pigmentoso, caracterizado por el envejecimiento acelerado y un importante aumento del riesgo de cáncer de piel, así como otros tumores

internos. En el otro extremo, si las mutaciones afectan a elementos implicados en la elaboración de la respuesta al daño se producen síndromes que, aunque recapitulan algunos síntomas del envejecimiento, su principal característica es la predisposición a desarrollar tumores. Un ejemplo de este tipo de síndromes es la ataxia-telangiectasia, producida por mutaciones en el gen ATM, uno de los principales mediadores tanto de la señalización del daño como de la elaboración de la respuesta (Ciccia y Elledge, 2010). La pérdida de funcionalidad de la proteína ATM permite la acumulación progresiva de mutaciones a la vez que compromete la elaboración de una respuesta senescente o apoptótica. En consecuencia, este síndrome predispone al cáncer más que al envejecimiento.

Laminopatías

El segundo grupo de progerias humanas asociadas a defectos en el procesamiento de la lamina A nuclear se engloban bajo el término laminopatías (Ramírez y col., 2007). La mayor parte de estas patologías se producen por mutaciones en el propio gen codificante de la lamina A (*LMNA*) o en el de la proteasa FACE-1/ZMPSTE24 responsable de su procesamiento, e incluyen síndromes de envejecimiento acelerado como la progeria de Hutchinson-Gilford, la dermopatía restrictiva, la displasia mandibuloacral y el síndrome atípico de Werner. Además de estos síndromes, las laminopatías comprenden diversas patologías humanas debidas a mutaciones en estos genes o en otras proteínas de la envuelta nuclear, como la lamina B o la emerina, entre otras. En este sentido, cabe destacar la reciente identificación en nuestro laboratorio de una nueva laminopatía progeroide causada por mutaciones en la proteína de la envuelta nuclear BANF1 (Puente y col., 2011).

Las laminas son proteínas fibrilares que componen el nucleoesqueleto celular confiriendo resistencia mecánica a la envuelta nuclear a la vez que interaccionan directa o indirectamente con diversos componentes del nucleoplasma y regulan procesos como la organización de la cromatina, la expresión génica o la progresión del ciclo celular (Gruenbaum y col., 2005). A través del ayuste alternativo de intrones, el gen *LMNA* codifica dos proteínas de

distinto tamaño, la prelamina A y una isoforma más corta denominada lamina C. A diferencia de la lamina C, la prelamina A posee en su extremo carboxilo terminal el motivo aminoacídico CaaX (C, cisteína; a, aminoácido alifático; X, cualquier aminoácido), conservado en diversas proteínas y diana de una serie de modificaciones post-traduccionales necesarias para su maduración (**Figura 2**). El primer evento consiste en la prenilación o adición de un grupo lipídico farnesilo mediante unión covalente a la cisteína conservada. A continuación, la prelamina A sufre un corte catalítico que libera el tripéptido –aaX, para que, posteriormente, una metiltransferasa adicione un grupo metilo a la cisteína. Este procesamiento es común a todas las proteínas preniladas, sin embargo, la lamina A sufre un segundo corte catalítico mediado por la metaloproteasa FACE-1/ZMPSTE24, por el cual se libera un péptido carboxilo terminal conteniendo la cisteína farnesilada (Osorio y col., 2009).

Una de las laminopatías más comunes y estudiadas es la progeria de Hutchinson-Gilford, que se produce en el 80% de los casos debido a una mutación *de novo* en el gen *LMNA* que activa un sitio donador de ayuste. El transcrito alternativo resultante presenta una deleción de 150 pares de bases del exón 11, región que codifica el segundo sitio de corte de FACE-1/ZMPSTE24. Como consecuencia, la lamina A no puede completar su maduración y permanece farnesilada, constituyendo la proteína conocida como progerina. Los pacientes con este síndrome sufren de alopecia, ateroesclerosis, alteraciones óseas y musculares, lipodistrofia, voz aguda y mueren prematuramente a una edad media de 13 años por fallos cardiacos (Cadiñanos y col., 2005). Las células de estos pacientes presentan graves defectos nucleares que incluyen engrosamiento de la envuelta nuclear, anormalidades en la forma del núcleo caracterizadas por extrusiones denominadas “blebs” y una distribución anormal de la cromatina (**Figura 2**). Aunque no se conoce con exactitud el mecanismo por el cual la progerina provoca estos defectos, se ha sugerido que el estado farnesilado de la progerina aumenta su afinidad por la membrana nuclear interna, lo que provoca su acumulación en esta zona y la pérdida de localización en el nucleoplasma, a la vez que interfiere con la lamina B, que se encuentra prenilada naturalmente, causando cambios en la arquitectura del núcleo (Ramírez y col., 2007). Estos

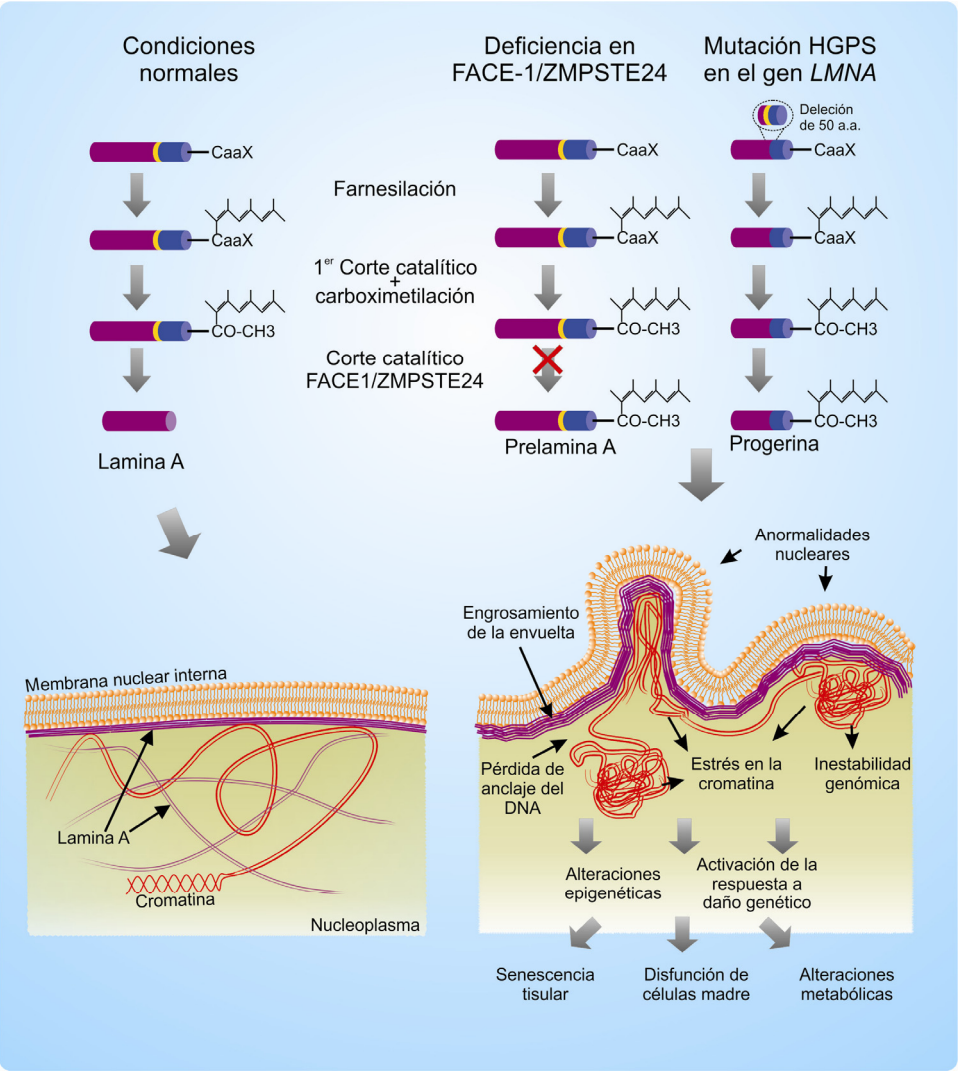

Figura 2. Representación gráfica de la maduración post-traduccional de la prelamina A y de las consecuencias de los defectos en su procesamiento.

defectos provocan a su vez un aumento de la inestabilidad genómica y retraso en la reparación de lesiones en el DNA, lo que se traduce en una pérdida de capacidad proliferativa y aumento de la senescencia celular que conducen al envejecimiento acelerado de los pacientes.

La utilización de modelos murinos que mimetizan las alteraciones presentes en estos pacientes ha aportado importantes datos sobre la conexión entre la lámina nuclear y el envejecimiento. En este sentido, el interés de nuestro laboratorio por los sistemas proteolíticos nos impulsó a la generación de ratones deficientes en la metaloproteasa Zmpste24 (Pendás y col., 2002) como modelo para el estudio del envejecimiento acelerado. Aunque la deficiencia en esta proteasa en humanos produce el síndrome de dermopatía

restrictiva, caracterizado por muerte neonatal, los ratones deficientes en Zmpste24 son viables y recapitulan varias de las alteraciones presentes en los pacientes con HGPS, como alopecia, defectos óseos y cardiacos, lipodistrofia, distrofia muscular y muerte prematura, proporcionando un buen modelo para el estudio de los mecanismos moleculares de los síndromes progeroides y su extrapolación al envejecimiento fisiológico. De forma similar a las células de pacientes HGPS, los fibroblastos de ratones deficientes en Zmpste24 acumulan prelamina A farnesilada y presentan graves anomalías en la estructura nuclear y alteraciones en los patrones de heterocromatina, asociadas a una pérdida de capacidad proliferativa y al desarrollo de un fenotipo senescente (**Figura 2**). El estudio de estos ratones ha revelado datos muy interesantes sobre las consecuencias de la acumulación de prelamina farnesilada. Así, hemos demostrado que el envejecimiento acelerado de estos ratones está asociado a la activación de la respuesta a daño en el DNA, ya que, no solo los ratones mutantes presentan altos niveles de expresión de varios genes diana de p53, sino que además, la eliminación de p53 mediante manipulación genética retrasa el envejecimiento de estos ratones y mejora sus alteraciones patológicas (Varela y col., 2005). Además, este modelo también nos ha permitido concluir que el causante directo de las alteraciones nucleares es la acumulación de prelamina farnesilada y no la ausencia de lamina A madura, ya que los ratones deficientes en Zmpste24 y heterocigotos para el gen *Lmna* muestran una recuperación total de los síntomas de envejecimiento y son indistinguibles de los ratones control (Varela y col., 2005). Estos resultados también nos han permitido definir una estrategia farmacológica trasladable a humanos que reduce la toxicidad de la prelamina A mediante la inhibición de su prenilación y que conduce a una clara mejoría de los síntomas de envejecimiento (Varela y col., 2008). Por otra parte, hemos demostrado que los ratones deficientes en Zmpste24 muestran una activación anómala de la autofagia y una serie de cambios en el metabolismo de lípidos y glúcidos similares a los presentes en modelos animales con longevidad extendida, lo que refleja la posibilidad de que estos ratones desarrollen una respuesta metabólica encaminada a la supervivencia que termina tornándose perjudicial debido a su activación crónica (Mariño y col., 2008). Además, hemos observado que la acumulación de prelamina A produce un gran impacto en la

capacidad proliferativa y de movilización de las células madre adultas epidérmicas, contribuyendo a la pérdida de potencial regenerativo de los tejidos (Espada y col., 2008). Por último, el análisis de estos ratones también ha revelado que la desorganización de la cromatina genera un patrón epigenético similar al descrito en el envejecimiento normal y que incluye una hipermetilación de las repeticiones de DNA ribosómico y una hipometilación de las histonas H2B y H4 (Osorio y col., 2010).

Eje somatotrofo

Además de las lesiones en el DNA y en sus sistemas de respuesta, en los últimos años ha cobrado gran relevancia en el envejecimiento el estudio de los mecanismos de adaptación a recursos nutricionales. Estos procesos, conservados evolutivamente, se encargan de adaptar el metabolismo de los organismos en situaciones de estrés desviando la energía disponible hacia la protección celular y el mantenimiento, en lugar de destinarlas al crecimiento y la reproducción. El ejemplo más evidente de estas respuestas frente al estrés es el aumento en la longevidad que se produce en múltiples organismos cuando son sometidos a restricción calórica (Kenyon, 2010). El estudio de los cambios metabólicos, hormonales y transcriptómicos de diversos organismos bajo estas condiciones ha permitido identificar algunas de las rutas moleculares que orquestan estas respuestas adaptativas y demostrar su influencia en el envejecimiento. En este sentido, el eje somatotrofo se ha revelado como una de las rutas clave en estos procesos.

El eje somatotrofo es un sistema endocrino constituido por la hormona de crecimiento (GH), el factor de crecimiento similar a insulina -1 (IGF-1) y sus efectores intracelulares. La GH es producida en la pituitaria anterior en respuesta a factores hipotalámicos y una vez en la circulación estimula la secreción hepática de IGF-1, o actúa directamente en diversos tejidos (Brown-Borg, 2009). Por su parte, el IGF-1 también puede producirse localmente en tejidos periféricos donde ejerce funciones auto y paracrinas. Tanto la GH como el IGF-1 controlan el desarrollo y crecimiento del organismo, así como el metabolismo de lípidos, glúcidos y proteínas. La transducción de señales de

IGF-1 en las células implica su unión a un receptor tirosín-quinasa que dispara una cascada de fosforilación en la que participan las quinasas PI3K (fosfoinositol 3-quinasa) y AKT/PKD (proteín quinasa D) y que culmina en la regulación negativa de los factores de transcripción FOXO (forkhead box O). El descubrimiento de la contribución de este sistema hormonal a la regulación del envejecimiento surgió a partir de la observación de que, en *C. elegans*, la pérdida de función de *daf-2*, el gen homólogo del receptor de IGF-1 de mamíferos, duplicaba su longevidad (Kenyon y col., 1993). Desde entonces, numerosos modelos animales han demostrado que la disminución de la señalización de esta ruta extiende la longevidad, del mismo modo que se han encontrado bajos niveles de GH e IGF-1 en animales sometidos a restricción calórica y en organismos muy longevos (Haigis y Yankner, 2010). Así, por ejemplo, los ratones deficientes en el receptor de GH presentan menor tamaño, retraso en la pubertad y viven significativamente más que sus controles, al igual que sucede con los ratones Ames y Snell, que portan mutaciones que afectan a la secreción pituitaria de GH, prolactina y tirotropina (Brown-Borg, 2009). Curiosamente, la inhibición de la señalización de IGF-1 va acompañada de un descenso en la incidencia de tumores, probablemente como consecuencia de la disminución de las señales mitogénicas de este sistema hormonal. Reciprocamente, la estimulación de esta vía en ratones transgénicos que sobreexpresan GH produce un aumento del tamaño corporal, una disminución de la esperanza de vida y una mayor incidencia de tumores (Brown-Borg, 2009). En humanos, se han encontrado mutaciones o polimorfismos en el receptor de IGF-1, en AKT y en FOXO3a en individuos muy longevos (Kenyon, 2010). Los beneficios de la disminución de la señalización de GH-IGF-1 se atribuyen a los cambios transcripcionales desencadenados por la activación de los factores FOXO, que provocan una activación de genes implicados en el metabolismo de carbohidratos, en la reparación del DNA, en sistemas antioxidantes y en genes estimuladores de la apoptosis y parada del ciclo celular (Greer y Brunet, 2005).

No obstante, ciertas observaciones no parecen ajustarse al paradigma de la señalización de IGF-1. Por ejemplo, en mamíferos se ha descrito que durante el envejecimiento se produce un descenso en los niveles de GH e IGF-

1 y que este acontecimiento está directamente relacionado con la atrofia del tejido muscular, óseo y cardiaco (Hinkal y Donehower, 2008). Además, el tratamiento de individuos de edad avanzada con GH mejora la forma física, la densidad ósea y otros marcadores de envejecimiento, aunque con ciertos efectos adversos (Liu y col., 2007). Sin embargo, en los últimos años, dos reveladores trabajos han aportado pistas muy importantes que pueden ayudar a entender el papel de la señalización del eje somatotrofo en el envejecimiento. Niedernhofer y col., y posteriormente van der Pluijm y col., han descrito que ratones con fenotipos progeroides causados por deficiencias en el sistema de reparación por escisión de nucleótidos presentan bajos niveles de IGF-1 en plasma y un perfil transcriptómico similar al de organismos con longevidad extendida, caracterizado por activación de genes del metabolismo oxidativo y de carbohidratos, de reparación del DNA, anti-oxidantes y de apoptosis y parada del ciclo celular (Niedernhofer y col., 2006; van der Pluijm y col., 2007). Además, ambos grupos han demostrado que la inducción de daño en el DNA mediante agentes genotóxicos en ratones control disminuye los niveles de IGF-1 en plasma y activa un programa transcripcional similar al de los ratones progeroides. Estos trabajos suponen una conexión directa entre dos rutas fundamentales implicadas en el envejecimiento, la respuesta al daño en el DNA y el eje somatotrofo, a la vez que manifiestan la existencia de una respuesta hormonal al daño en el DNA que desvía la energía del crecimiento hacia el mantenimiento y la reparación. Sin embargo, el aumento de expresión de genes apoptóticos y de senescencia en esta respuesta adaptativa deja abierta la cuestión de si su contribución es beneficiosa o perjudicial para el fenotipo de estos ratones. De igual forma, se desconocen los mediadores de la conexión entre las lesiones en el DNA y el eje somatotrofo, aunque diversas observaciones señalan a la ruta de p53 como uno de los candidatos más probables. Así, la actividad de este supresor tumoral está significativamente aumentada en diversos modelos con envejecimiento acelerado y, como se ha comentado anteriormente, la sobreactivación mediante manipulación genética de p53 protege frente al cáncer y causa una disminución de la longevidad. Además, el análisis de estos ratones ha revelado la existencia de niveles bajos de IGF-1 en plasma (Gatza y col., 2008). Por último, se ha descrito que p53 puede interferir con la señalización de IGF-1 en varios puntos. Así, p53 activa

la transcripción de IGF-BP3 (IGF-1 binding protein 3), una proteína que se une al IGF-1 circulante y bloquea su acción, reprimiendo la expresión del receptor de IGF-1. Además, p53 puede reducir la señalización intracelular de IGF-1 mediante inhibición directa o indirecta de PI3K (Hinkal y Donehower, 2008).

En resumen, aunque se han producido grandes avances en la identificación de los factores desencadenantes del envejecimiento permanecen sin resolver un gran número de cuestiones. Del mismo modo, aún se conoce poco sobre el papel que desempeñan en este proceso los nuevos elementos que progresivamente se van sumando a la complicada red de conexiones moleculares que componen los organismos, como son los microRNAs o los lincRNAs. En este sentido, el empleo de modelos animales progeroides se ha revelado como una herramienta muy eficaz para el avance en el conocimiento de los mecanismos moleculares que operan en el envejecimiento fisiológico de los organismos.

microRNAs

Los microRNAs (miRNAs) constituyen un revolucionario sistema de regulación génica que había pasado desapercibido hasta hace aproximadamente una década. No obstante, los primeros pasos que llevaron a su identificación comenzaron ya en los años 90 en el laboratorio de Victor Ambros. Durante un estudio encaminado a buscar nuevos genes implicados en la transición de larva a adulto del nematodo *C. elegans*, habían descubierto un nuevo gen, *lin-4*, que actuaba como represor del gen *lin-14*, codificante de una nueva proteína (Ambros, 1989). En principio, no pareció representar un hallazgo muy relevante, hasta que en 1993 ese mismo grupo descubrió que el gen *lin-4* no codificaba una proteína represora, sino que producía un pequeño RNA de 22 nucleótidos complementario a una secuencia situada en la región 3' no traducida (3'UTR) del gen *lin-14* (Lee y col., 1993). Este descubrimiento pasó inadvertido como un hecho aislado, hasta que siete años después el grupo de Gary Ruvkum reveló la existencia de otro de estos genes en

nematodos, el gen *let-7*, y demostró su conservación evolutiva hasta humanos (Pasquinelli y col., 2000). A raíz de este trabajo varios laboratorios comenzaron una búsqueda exhaustiva de moléculas de RNA de pequeño tamaño en diversos organismos, que condujeron a la publicación simultánea en el año 2001 de tres estudios que describían la identificación de decenas de estas moléculas en nematodos, moscas y humanos, y proponían la existencia de una nueva clase de RNAs reguladores de la expresión génica (Lagos-Quintana y col., 2001; Lau y col., 2001; Lee y Ambros, 2001). Desde entonces, nuestro conocimiento de los miRNAs ha crecido de forma exponencial y hoy sabemos que este sistema de regulación tiene un gran impacto en prácticamente cualquier proceso de la célula y del organismo. La regulación génica por miRNAs es un mecanismo ampliamente extendido en vertebrados e invertebrados, así como en plantas, aunque ausente en hongos. Esta peculiar distribución sugiere que los miRNAs surgieron de forma independiente en plantas y animales, y de hecho, ambos sistemas presentan diferencias sustanciales en su maquinaria y sus mecanismos de acción (Gatza y col., 2008).

Biogénesis y mecanismos de acción de los miRNAs

Una década después de su descubrimiento, sabemos que los miRNAs son pequeñas moléculas de RNA de una sola hebra, de entre 21 y 23 nucleótidos de longitud, que se unen por complementariedad a secuencias situadas en las regiones 3'UTR de sus RNA mensajeros diana (mRNAs) e inhiben la síntesis proteica mediante el bloqueo de la traducción o la degradación del mRNA. Los miRNAs están codificados en el genoma, principalmente en regiones intergénicas, aunque también se encuentran en intrones de genes codificantes de proteínas y, ocasionalmente, en el 3'UTR o en regiones codificantes (Winter y col., 2009). La gran mayoría de miRNAs intergénicos presentan una estructura génica similar a la de cualquier gen codificante de proteínas, constituida por un promotor para la RNA polimerasa II con secuencias reguladoras, un cierto número de exones y una secuencia de poliadenilación. En el caso de los miRNAs intragénicos, la regulación de su

expresión viene marcada por el promotor del gen hospedador, aunque en algunos casos se transcriben a partir de la hebra antisentido del gen y, por lo tanto, poseen sus propios mecanismos de regulación. Tras su expresión en el núcleo como largos transcritos primarios (pri-miRNAs), los miRNAs deben sufrir un proceso de maduración para dar lugar al miRNA maduro (**Figura 3**). En este sentido, cabe destacar que, con frecuencia, los miRNAs se organizan en grupos denominados clústeres, transcritos como una sola molécula de RNA policistrónico que, posteriormente, origina varios miRNAs maduros. El primer evento de su maduración sucede en el núcleo, donde la región del transcrito primario que dará lugar al miRNA maduro adquiere una estructura secundaria en forma de lazo caracterizada por una región de unos 33 nucleótidos de RNA de doble hebra y un bucle terminal y unas regiones flanqueantes 5' y 3' de RNA de hebra simple. Esta estructura es reconocida por un complejo con actividad nucleasa formado por la RNAsa III Drosha y la proteína DGR8 (diGeorge

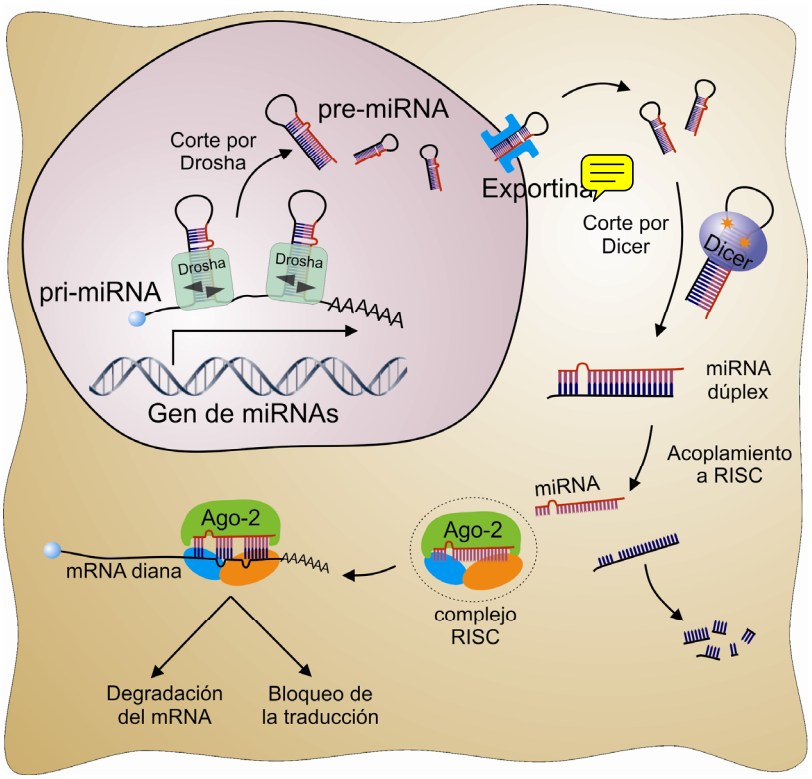

Figura 3. Biogénesis y mecanismos de acción de los microRNAs.

critical region 8). Ambas proteínas poseen dominios de unión a RNA bicatenario que reconocen la estructura en forma de lazo y realizan un corte asimétrico en ambas hebras a 11 nucleótidos del comienzo de la región de doble hebra, generando lo que se conoce como precursor de miRNA (pre-miRNA). El procesamiento por el complejo Drosha/DGR8 acontece de forma simultánea a la transcripción y, en el caso de miRNAs intrónicos, se produce antes de que tenga lugar el ayuste de intrones. El pre-miRNA generado posee 2 nucleótidos protruyentes en su extremo 3', lo que permite su reconocimiento por el complejo exportina-5/Ran-GTP, que media su transporte al citoplasma donde continuará su maduración.

Una vez en el citoplasma, un complejo formado por la RNAasa III Dicer y las proteínas de unión a RNA de doble hebra TRBP (*Tar RNA binding protein*) y PACT (*protein activator of PKR*) realizan un segundo corte en el pre-miRNA, dando lugar a un RNA de doble hebra de unos 22 nucleótidos con extremos 3' protruyentes denominado miRNA dúplex. Posteriormente, este dúplex se une al complejo de silenciamiento o RISC (*RNA-induced silencing complex*), cuyo principal efector es la proteína argonauta-2 (Ago2). La unión a este complejo desencadena la degradación de la hebra pasajera y el acoplamiento de la hebra funcional (complementaría al mRNA), que constituye ya el miRNA maduro y se encargará de guiar al complejo de silenciamiento hacia los mRNAs diana. Aunque en principio el miRNA dúplex podría dar lugar a dos miRNAs maduros, solo una de las hebras es seleccionada por el complejo RISC y, normalmente, es aquella que muestra mayor estabilidad en su extremo 5' (Schwarz y col., 2003).

El reconocimiento de los mRNAs diana y los mecanismos de silenciamiento mediados por RISC difieren entre plantas y animales (Huntzinger y Izaurralde, 2011). En plantas, los miRNAs presentan un mecanismo de acción similar a los RNAi, uniéndose a secuencias perfectamente complementarias situadas en las regiones codificantes de los mRNAs y desencadenando su degradación. Sin embargo, en animales el mecanismo es mucho más complejo, ya que los miRNAs se unen a secuencias parcialmente complementarias situadas en las regiones 3'UTR de los mRNAs,

existiendo tres posibilidades de silenciamiento: la degradación directa del mensajero, su desadenilación y posterior degradación por mecanismos generales de la célula o la inhibición de su traducción a proteínas. La complementariedad parcial entre el mRNA y el miRNA es uno de los aspectos que más ha obstaculizado el avance en el conocimiento de las funciones de los miRNAs en animales, debido a que no parece ajustarse a un único patrón, lo que imposibilita la deducción de los genes diana de los miRNA usando metodologías sencillas de alineamiento de secuencias como sucede en plantas. No obstante, el conocimiento adquirido en los últimos años ha puesto de manifiesto que una región clave de los miRNAs en el reconocimiento de los genes diana es la denominada región semilla (del inglés "seed"), correspondiente a los 9 primeros nucleótidos del extremo 5' (Lewis y col., 2005). Así, se ha comprobado que los sitios de unión de miRNAs (MBSs) más comunes en los mRNAs son aquellos que presentan complementariedad continuada con al menos 7 nucleótidos de la región semilla del miRNA. Aunque menos frecuentes, también existen MBSs funcionales con tan solo 6 nucleótidos emparejados con la región semilla e incluso algunos poseen discontinuidades en la complementariedad de dicha región que son compensadas con un extenso alineamiento en la región 3'. Consecuentemente, la predicción de genes diana usando estos determinantes es una tarea compleja que implica la obtención de un gran número de falsos positivos derivados de la elevada probabilidad de encontrar al azar una secuencia de seis nucleótidos complementaria a la región semilla (Bartel, 2009). Para reducir el número de falsos positivos se han desarrollado programas de predicción que utilizan la información de conservación entre especies bajo la hipótesis de que los MBSs funcionales estarán sometidos a presiones selectivas y por lo tanto aparecerán en varias especies con mayor probabilidad que por azar (Grimson y col., 2007). De igual modo, otros programas incorporan parámetros como la presencia de varios MBSs en el mismo gen, la energía termodinámica del alineamiento, la compensación del emparejamiento en el extremo 3' o la estructura secundaria del mRNA, para lograr el mejor compromiso entre sensibilidad y fiabilidad.

Relevancia funcional de los miRNAs

Independientemente del tipo de mecanismo de silenciamiento, el resultado final de la acción de los miRNAs es una disminución en los niveles de las proteínas codificadas por los genes diana. De esta manera, los miRNAs pueden actuar bien como interruptores, encendiendo o apagando una determinada ruta, como elementos moduladores adicionales a la regulación de la expresión génica, o formando bucles de retroalimentación (Bartel, 2009). Teniendo en cuenta que cada miRNA tiene el potencial de regular entre decenas y cientos de genes, y considerando que se han identificado más de 500 miRNAs en el genoma humano, se estima que un 20-30% de los genes codificantes de proteínas están sometidos a este tipo de regulación (Lewis y col., 2005). En este sentido, un estudio más reciente ha revelado que más del 50% de los transcritos de mamíferos están sometidos a presiones selectivas dirigidas a la conservación de sus MBSs (Friedman y col., 2009). Por otra parte, dado el elevado número de dianas que presentan, un mismo miRNA puede causar un gran impacto en única ruta celular mediante la intervención a varios niveles, o controlar múltiples procesos simultáneamente. Así, para algunos miRNAs se han encontrado relaciones funcionales entre sus genes diana, lo que sugiere su especialización en un proceso concreto. Un ejemplo son los miRNAs del clúster miR-17~96, cuyas dianas muestran un claro enriquecimiento en genes reguladores del crecimiento y que se han revelado como un elemento crucial en el desarrollo embrionario con potentes propiedades oncogénicas en adultos (Ventura y col., 2008). Este ejemplo también pone de manifiesto la cooperación funcional que se puede dar entre miRNAs coexpresados en un mismo clúster, lo que permite regular una gran cantidad de genes mediante el solapamiento entre sus dianas. Sin embargo, es frecuente que los miRNAs no presenten conexiones evidentes entre sus genes diana, lo que parece indicar que pueden desempeñar múltiples funciones dependiendo del tejido o del momento en el que se expresen. Otro aspecto a tener en cuenta en este sistema de regulación es la redundancia funcional que ocurre entre miRNAs que comparten la misma región semilla o entre miRNAs que presentan varias copias idénticas con distinta localización genómica. Por lo tanto, en un escenario como este, se puede concluir que cualquier proceso

celular es susceptible de cierto grado de regulación por miRNAs en algún tipo celular o en alguna condición concreta.

Una de las principales funciones atribuidas a los miRNAs ya desde el descubrimiento de *lin-4* es la regulación del desarrollo embrionario. De hecho, ratones deficientes en cualquiera de los genes implicados en la ruta biosintética de miRNAs, como Drosha, Dicer, DGR8 o Arg-2, mueren prematuramente con graves defectos en su morfogénesis (Park y col., 2010). La generación de modelos murinos deficientes en miRNAs individuales o en clústeres de los mismos ha aportado una valiosa información acerca del impacto real de los miRNAs en la biología de los organismos y ha confirmado su importante contribución a los procesos de programación celular que acontecen durante el desarrollo embrionario. Así, ratones deficientes en miR-17~92 presentan letalidad postnatal con defectos pulmonares y cardiacos, y la haploinsuficiencia de miR-1 o la ausencia de miR-126 ocasionan un 50% de letalidad embrionaria asociada a defectos cardiacos y vasculares, respectivamente (Park y col., 2010). Aunque el número de modelos murinos deficientes en miRNAs es todavía reducido, la gran mayoría de ellos presentan algún tipo de alteración, que va desde defectos en la respuesta inmune o en la diferenciación de los linajes eritroides o mieloides, a retraso en el crecimiento, osteoartritis, anomalías vasculares, o hiperglucemia (Park y col., 2010). Además, estos estudios también han confirmado los fenómenos de redundancia o cooperación funcional entre miRNAs relacionados o coexpresados. Así, los ratones deficientes en miR-133a-1 o miR-133a-2, dos copias idénticas del mismo miRNA, no muestran ningún fenotipo obvio, mientras que la ausencia simultánea de ambos origina letalidad perinatal en aproximadamente el 50% de los casos, asociada a severos defectos cardiacos (Liu y col., 2008). De forma similar, el antes mencionado clúster miR-17~92 presenta otros dos clústeres parálogos, el miR-106a~363 y el miR-106b~25, sumando entre todos 15 miRNAs de 4 familias distintas. Mientras que la ausencia de cualquiera de los dos últimos clústeres no produce ningún fenotipo aparente, su deficiencia combinada con el miR-17~92 agrava en gran medida su fenotipo provocando letalidad ya en etapas muy tempranas del desarrollo (Ventura y col., 2008).

Acorde con su profundo impacto en la biología de los organismos, diversas alteraciones en los sistemas de regulación mediados por miRNAs se asocian frecuentemente al desarrollo de patologías humanas, entre las que destacan enfermedades vasculares e inmunes y el cáncer (Li y col., 2009). La contribución de este sistema de regulación a la progresión tumoral se ha estudiado extensamente en los últimos años y ha revelado un papel fundamental de los miRNAs en esta patología. Existen múltiples alteraciones en la regulación mediada por miRNAs que pueden conducir al desarrollo de tumores, como cambios en su expresión, variación en el número de copias, mutaciones en sus secuencias o en los MBSs de sus genes diana, o alteraciones en los mecanismos de biogénesis. Así, algunos estudios señalan que más del 50% de los miRNAs se encuentran situados en regiones genómicas asociadas al desarrollo del cáncer o cercanos a puntos de rotura cromosómica (Calin y col., 2004). De igual forma, numerosos trabajos han encontrado expresión diferencial de miRNAs en una gran variedad de tumores. En este sentido, en algunos tipos de cáncer, los patrones de expresión de miRNAs se han revelado como una herramienta de clasificación tumoral más efectiva que los perfiles de expresión de mRNAs, lo que ha convertido a los miRNAs en biomarcadores útiles para el diagnóstico y pronóstico del cáncer, permitiendo diferenciar el tejido tumoral del sano o determinar el origen, grado de diferenciación, potencial metastásico o la respuesta a tratamientos anti-tumorales (Brase y col., 2010). Por otro lado, varios trabajos iniciales revelaron la existencia de mutaciones en genes implicados en la biosíntesis de miRNAs en un abundante número de tumores, lo que condujo a la consideración inicial de que los miRNAs desempeñaban un papel principalmente anti-tumoral en la progresión del cáncer (Deng y col., 2008). Sin embargo, la información acumulada durante los últimos años derivada de experimentos de sobreexpresión o inhibición de miRNAs *in vitro* e *in vivo*, ha puesto de manifiesto que los miRNAs contribuyen a múltiples etapas de la progresión tumoral, comportándose tanto como oncogenes como genes supresores de tumores, o desempeñando funciones duales dependiendo del origen y características del tumor (Zhang y col., 2007).

El elevado número de genes diana de cada miRNA, su impacto en los

procesos celulares y su frecuente contribución a diversas patologías ha llevado a su consideración como posibles dianas terapéuticas para el tratamiento de diversas enfermedades y, especialmente, el cáncer. Aunque todavía nos encontramos en los inicios de estas aproximaciones, varios trabajos en ratones y primates han conseguido modificar sustancialmente los niveles de miRNAs utilizando oligonucleótidos que mimetizan o bloquean la acción de los miRNAs endógenos. Así, por ejemplo, la inyección intravenosa en monos verdes africanos de oligonucleótidos antisentido frente a miR-122, un miRNA implicado en el metabolismo del colesterol, ha logrado disminuir los niveles hepáticos de este miRNA durante tres meses, acompañado de un descenso en los niveles de colesterol en ese periodo (Elmen y col., 2008).

En conclusión, el descubrimiento de los miRNAs ha supuesto un hito en la historia de la ciencia al añadir un nuevo nivel de regulación molecular que podría permitirnos explicar muchos aspectos de la biología de los organismos que permanecían sin respuesta. Aunque el conocimiento adquirido durante los últimos años ha aportado pruebas evidentes sobre su profundo impacto en la biología de los mamíferos, todavía existen muchos interrogantes en torno a la regulación por miRNAs, y será necesario reevaluar la contribución que este sistema de regulación desempeña en los distintos procesos fisiológicos y patológicos de los organismos.

OBJETIVOS

Dado el elevado número de proteasas humanas, su diversidad y su relevancia funcional como componentes de sistemas de regulación post-transcripcional, es previsible que una amplia caracterización de estos enzimas pueda aportar importantes conocimientos sobre distintos aspectos de la biología, patología y evolución humanas. Análogamente, el reciente descubrimiento de los miRNAs como una nueva clase de moléculas reguladoras capaces de controlar la expresión de miles de genes codificantes de proteínas, abre un nuevo campo de investigación que podría ayudar a explicar múltiples aspectos de la fisiología y patología humanas. De acuerdo con estas premisas y dada la experiencia de nuestro laboratorio en el estudio de los sistemas proteolíticos en distintos procesos, incluyendo el envejecimiento, en este trabajo nos planteamos profundizar en el estudio de ambos sistemas de regulación biológica mediante la búsqueda de nuevos enzimas proteolíticos y el análisis de la contribución de los miRNAs al envejecimiento.

Los objetivos concretos de este trabajo fueron:

1. Identificación de nuevos genes humanos codificantes de enzimas proteolíticos.
2. Caracterización de los productos de los genes identificados mediante ensayos *in vitro* de actividad y búsqueda de posibles sustratos.
3. Estudio de la implicación de los miRNAs en el envejecimiento mediante el empleo de un modelo animal deficiente en la metaloproteasa Face-1.

MATERIAL Y MÉTODOS

Material

Enzimas de restricción

Los enzimas de restricción, así como otros enzimas utilizados en la clonación molecular (polinucleótido quinasa de T4, DNA ligasa de T4, fragmento Klenow, Taq DNA polimerasa, etc.) se adquirieron a New England Biolabs, Roche Molecular Biochemicals, Amersham Biosciences, Invitrogen Life Technologies y TAKARA BIO Inc.

Reactivos de electroforesis

La separación de DNA en geles de agarosa se realizó utilizando agarosa de grado Biología Molecular de Roche Molecular Biochemicals. La acrilamida/ N,N'-metilenbisacrilamida, la N,N,N',N'-tetrametiletilendiamina (TEMED) y el persulfato amónico utilizados para la separación electroforética de proteínas en geles de poliacrilamida con SDS se obtuvieron de Bio-Rad.

Anticuerpos

El anticuerpo policlonal anti-GST se produjo en nuestro laboratorio tal como se ha descrito previamente (Llamazares y col., 2003). Los anticuerpos anti-Jak2 total y fosforilado, anti-Stat3 total y fosforilado, anti-p42/p44 total y fosforilado, y anti-p53 total y fosforilado (Ser-15) se adquirieron a Cell Signaling. El anticuerpo anti-β-actina y anti-flag se adquirió a Sigma. El anticuerpo anti-γ-H2AX fue suministrado por Millipore. El anticuerpo anti-PPM1D se adquirió a Bethyl Laboratories.

Reactivos para ensayos enzimáticos

Los sustratos fluorogénicos y los péptidos biológicamente activos (neurogranina, angiotensina I, angiotensina II y angiotensina III) se adquirieron

a Bachem. Los inhibidores de proteasas, el AMC (7-amino-4-metil-coumarina), la albúmina, el colágeno fibrilar, la gelatina, el plasminógeno y la aprotinina se obtuvieron de Sigma. La aminopeptidasa N y la leucil aminopeptidasa porcina se adquirieron a Calbiochem.

Animales de experimentación

Los ratones deficientes en FACE-1 se generaron en nuestro laboratorio mediante la técnica de recombinación homóloga en células pluripotenciales embrionarias de ratón utilizando un vector de reemplazamiento con un "cassette" β-Geo que reemplazó los exones II y III de la secuencia genómica (Pendás y col., 2002). Los ratones deficientes en p53 fueron cedidos por el Dr. M. Serrano (CNIO, Madrid) y los ratones deficientes en ATM y los ratones ATR-seckel fueron cedidos por el Dr. O. Fernández-Capetillo (CNIO, Madrid). Los ratones se criaron y mantuvieron en las instalaciones especializadas del animalario de la Universidad de Oviedo y todos los procedimientos se realizaron siguiendo los protocolos aprobados por la Universidad de Oviedo. Finalmente, los animales se sacrificaron por dislocación cervical y sus tejidos se extrajeron y se congelaron a -80 ºC hasta su uso.

Otro material

Las librerías de cDNA humano y los filtros de nylon que contenían RNAs poliadenilados de diferentes tejidos fueron suministrados por Clontech. La doxorrubicina se adquirió a Calbiochem, mientras que la 4-nitroquinolona-1-óxido (4-NQO) y el peróxido de hidrógeno fueron suministrados por Sigma. Las disoluciones tampón utilizadas (TE, SSC, TBE, TAE, SSPE, disolución de Denhardt, etc…) se prepararon como se ha descrito anteriormente (Sambrook y Russell, 2001). Los productos empleados fueron de calidad analítica y se adquirieron a Merck, Sigma, Applied Biosystems, Probus y Prolabo, fundamentalmente. El agua utilizada fue de grado reactivo MilliQ-plus (Millipore). Otros productos utilizados se indican en los siguientes apartados.

Técnicas de Biología Molecular

Técnicas básicas de Biología Molecular

Las técnicas básicas de biología molecular utilizadas en este trabajo que no se detallan (digestiones con enzimas de restricción, ligación de fragmentos de DNA, electroforesis en geles de agarosa, etc…) se realizaron según se describe en la bibliografía (Sambrook y Russell, 2001) o siguiendo las instrucciones de las casas comerciales distribuidoras de los distintos enzimas. Los oligonucleótidos utilizados se diseñaron usando la herramienta PrimerBlast del NCBI (*National Center for Biotechnology Information*) y fueron suministrados por Sigma.

Purificación de fragmentos de DNA

Los fragmentos de DNA, obtenidos por PCR y/o digestión con enzimas de restricción de los diferentes vectores recombinantes, se separaron por electroforesis en geles de agarosa en tampón TBE o TAE y se purificaron mediante columnas de sílica (kit "High Pure PCR Purification", Roche Molecular Biochemicals).

Preparación de sondas radiactivas

Los fragmentos de DNA bicatenario utilizados como sondas se marcaron con [α-^{32}P]dCTP (3000 Ci/mmol, 10 mCi/mL) mediante síntesis a partir de cebadores aleatorios utilizando el kit comercial Rediprime (GE Healthcare). A continuación, la mezcla de marcaje resultante se centrifugó a través de una columna de Sephadex G-25 (GE Healthcare) para retirar los nucleótidos no incorporados a la sonda (Sambrook y Russell, 2001).

Mutagénesis dirigida

Las mutacion dirigida de los sitios de unión de los miRNAs en la región semilla de los genes *PPM1D*, *NARF* e *IGF1* se realizó utilizando el kit "Quikchange XL site-directed mutagénesis" (Stratagene) y las bacterias ultra

competentes XL10-Gold (Stratagene), siguiendo el protocolo del proveedor. En todos los casos, el resultado de la mutagénesis se confirmó mediante secuenciación de la región 3'UTR.

Análisis Northern

Para los análisis Northern, el RNA total de tejidos murinos se obtuvo mediante el procedimiento de Chomczynski y Sacchi (Chomczynski y Sacchi, 1987). Aproximadamente 20 µg de RNA total de cada muestra se separaron en geles de 1,2% de agarosa-formaldehído y se transfirieron a filtros de nylon Hybond N+ (Amersham Biosciences). Tanto estos filtros como los comerciales, que contienen 2 µg de RNA poliadenilado humano, se prehibridaron durante 3 h a 42 ºC en formamida 50%, SSPE 5x, disolución de Denhardt 10x, SDS 2% y DNA desnaturalizado de esperma de salmón 100 µg/mL. La hibridación se realizó en la misma disolución, añadiendo como sonda el cDNA de interés marcado radiactivamente. Tras 12 h de hibridación a 42 ºC, los filtros se lavaron dos veces a temperatura ambiente con SSC 2x, SDS 0,05% durante 20 min, y dos veces a 50 ºC con SSC 0.1x, SDS 0,1% durante otros 20 min. Finalmente, la membrana se expuso durante varios días a películas de autorradiografía y pantallas intensificadoras Biomax MS (Kodak). La integridad y el control de carga de los Northern se comprobaron mediante la hibridación con una sonda específica para β-actina o para gliceraldehido-3-fosfato deshidrogenasa.

Reacción en cadena de la polimerasa (PCR)

Los experimentos de PCR se efectuaron en termocicladores de Perkin Elmer (modelo 9700) y Applied Biosystems (modelo Verity), indistintamente. Para las reacciones se utilizaron 10 µmol de dNTPs, 150 pmol de cada oligonucleótido y 1 unidad de *Taq* DNA polimerasa en un volumen final de 50 µL. Los oligonucleótidos específicos para la amplificación de un DNA particular se diseñaron de acuerdo con la secuencia a amplificar. Los productos obtenidos se analizaron mediante digestión con enzimas de restricción y electroforesis en geles de agarosa en TBE.

Transcripción reversa de RNA acoplada a PCR (RT-PCR)

La RT-PCR semicuantitativa de muestras de ratón se llevó a cabo mediante el kit GeneAmp (PerkinElmer Life Sciences) utilizando un 1 μg de RNA total extraído de testículos de ratón a diferentes edades. El cDNA resultante se amplificó mediante PCR durante 25 ciclos utilizando oligonucleótidos específicos. Como control de carga e integridad se amplificó la β-actina bajo las mismas condiciones y los fragmentos generados se analizaron mediante electroforesis en geles de agarosa en TBE.

Análisis transcripcional mediante RT-PCR en tiempo real

El RNA se obtuvo de tejido congelado y líneas celulares utilizando TRIzol (Invitrogen) y el kit comercial RNeasy (QIAGEN). Se usó 1 μg de RNA total para la síntesis de cDNA de doble hebra y la transcripción reversa se llevó a cabo utilizando oligo dT y siguiendo las instrucciones de los kits comerciales "ThermoScript RT-PCR" de Invitrogen y "High Capacity cDNA Reverse Transcription" de Applied Biosystems. Los análisis de expresión por RT-PCR a tiempo real de los genes seleccionados se llevaron a cabo usando ensayos de expresión Taqman (Applied Biosystems) en un sistema de detección "7500HT Fast Real-Time PCR" o "7300 Real-Time PCR System" (Applied Biosystems), siguiendo las instrucciones del fabricante. Los resultados se analizaron mediante cuantificación relativa frente al control endógeno β-actina empleando el Software SDS 1.4 y 2.1 de Applied Biosystems.

Secuenciación de ácidos nucleicos

Todas las reacciones de secuenciación capilar, tanto de productos de PCR como de plásmidos, se llevaron a cabo usando el kit "DR terminator *Taq*FS" y el secuenciador automático de DNA ABI-PRISM 310 (Applied Biosystems), con oligonucleótidos específicos como cebadores.

Electroforesis en geles de poliacrilamida-SDS

Las muestras se mezclaron con tampón de disociación (Tris-HCl 62,5

mM, pH 6,8, SDS 2%, glicerol 10% y azul de bromofenol 0,0005%) y se calentaron a 95 ºC durante 5 min antes de cargarlas en el gel. La electroforesis se realizó en tampón Tris-HCl 24,8 mM, glicina 192 mM, SDS 0,1%, pH 8,8 a un amperaje constante de 25 mA por gel, hasta que el azul de bromofenol alcanzó el final del gel. Las proteínas se fijaron con ácido tricloroacético al 20% durante 5 min a 55 ºC, se tiñeron con azul de Coomassie al 0,25% en metanol:ácido acético:agua (45:10:45) durante 10 min a 55 ºC. Los geles se destiñeron con metanol:ácido acético:agua (10:7,5:82,5) a 55 ºC.

Extracción de proteínas

Los cultivos celulares se lavaron con PBS y se homogenizaron mediante la adición del volumen adecuado de un tampón Tris 20 mM, pH 7,4, NaCl 150 mM, 1% Triton X-100, EDTA 10 mM, que contenía coctel completo de inhibidores de proteasas ("Complete protease inhibitor cocktail", Roche Molecular Biochemicals) y los inhibidores de fosfatasas ortovanadato sódico 200 μM y β-glicerofosfato 1 mM. Los tejidos congelados de ratones se homogenizaron directamente mediante un homogenizador Ultraturrax T-8 (IKA) en un volumen apropiado del tampón anterior. Los lisados celulares o de tejidos se sometieron a centrifugación a 12.000 x *g* a 4ºC para eliminar las partículas insolubles y se recolectaron los sobrenadantes para su análisis. La concentración de proteínas de los sobrenadantes se determinó mediante la técnica del ácido bicinconínico ("BCA Protein Assay Kit", Pierce). Para su posterior análisis Western se emplearon 5 μg o 25 μg de los lisados celulares o de tejidos, respectivamente.

Análisis Western

Las muestras a analizar se separaron mediante electroforesis en un gel de poliacrilamida-SDS del porcentaje adecuado al tamaño de las proteínas a detectar (8-13%). El gel se incubó en tampón de transferencia (CAPS 10 mM, NaOH 4 mM, metanol 20%) durante 30 min. La transferencia a membranas de nitrocelulosa (Hybond ECL, Amersham Biosciences) o polifluoruro de vinilideno (PVDF) (Immobilon-P, 0,45 μM, Biorad) se realizó en el mismo tampón de

transferencia durante 60 min a 50 V en un soporte Miniprotean II (Bio-Rad). Una vez transferidas las proteínas, se bloquearan las membranas en PT (PBS 1x, Tween-20 0,1%) con leche en polvo desnatada al 5% durante 1 h, tras lo cual la membrana se incubó de 1 a 12 h con el anticuerpo primario diluido en leche en polvo desnatada (Biorad) o albúmina bovina (Roche Molecular Biochemicals) al 3% en PT. La membrana se lavó tres veces con PT durante 5 min y posteriormente se incubó 1 h con el anticuerpo secundario diluido en leche en polvo desnatada al 1,5% en PT. Tras lavar de nuevo con PT, se llevó a cabo la detección de los complejos antígeno-anticuerpo mediante generación de quimio-luminiscencia con un sustrato comercial (Millipore).

Producción y purificación de proteínas recombinantes

Los cDNAs de los dominios catalíticos de APO (posiciones 180-589), AMZ1 (posiciones 1-320) y AMZ2 (posiciones 1-300) se amplificaron mediante PCR utilizando oligonucleótidos específicos que contenían sitios de restricción utilizando el kit de amplificación "Expand long template high fidelity". Posteriormente, se digirieron los productos de la PCR con los correspondientes enzimas de restricción y se clonaron en los sitios apropiados del vector de expresión pGEX-5x-2. La construcción resultante se transformó en células competentes de *Escherichia coli* de la cepa BL21(DE3)-pLysE y su expresión se indujo mediante la adición de isopropil-1-tio-β-D-galactopiranósido (a una concentración final de 1 mM), seguido de una incubación a 28 ºC durante 3 h. Transcurrido este tiempo, se centrifugaron las células, se lavaron con tampón PBS, y se lisaron por incubación a 4 ºC durante 12 h en un tampón PBS que contenía 100 µg/mL de lisozima, 10 µg/mL de DNasa, y 0,1% de Tritón X-100. En el caso de AMZ1 y AMZ2, el lisado resultante se centrifugó y se reservó para su posterior purificación. En el caso de la APO, tras la centrifugación del lisado, se lavó el precipitado tres veces con PBS y se disolvió en un tampón Tris 20 mM, pH 7,4 que contenía cloruro de guanidina 6 M. La proteína recombinante del domino catalítico de la APO se replegó mediante dos pasos de diálisis a 4 ºC durante 24 h, primero con un tampón Tris 50 mM, pH 7,5, NaCl 150 mM, ditiotreitol 2 mM, urea 2 M, y posteriormente dos veces en un tampón Tris 50 mM, pH 7,5, NaCl 150 mM. Tanto la APO recombinante

replegada como las AMZs recombinantes contenidas en el sobrenadante del lisado se purificaron por cromatografía de afinidad utilizando una columna de glutatión sefarosa. Finalmente, la identidad de las proteínas recombinantes se confirmó utilizando análisis Western y digestión con tripsina seguida de análisis por espectrometría de masas.

Digestión con tripsina

Las proteínas se separaron mediante SDS-PAGE y se tiñeron con azul de Coomassie. A continuación, se recortaron manualmente las bandas correspondientes del gel en cuadrados de aproximadamente 1 mm^3, se colocaron en tubos de 0,5 mL, y se lavaron tres veces durante 45 min con 180 µL de bicarbonato amónico 25 mM/acetonitrilo (70:30) (v/v). A continuación, se deshidrataron a 90 ºC durante 15 min y se incubaron con tripsina 12 µg/mL (Promega) en una solución de bicarbonato amónico 25 mM durante 1 h a 60 ºC. Las digestiones resultantes se mantuvieron en hielo 2 min y se les añadió 2 µL de ácido tricloroacético al 10%. Posteriormente, se desalaron las muestras mediante cromatografía de fase reversa C18 (ZipTip, Millipore). Para la elución de los péptidos digeridos se emplearon 2 µL de 10 mg/mL de ácido α-ciano-4-hidroxicinámico en acetonitrilo y trifluoroacético 0,1% (50:50) (v/v). Finalmente, se analizó 1 µL del eluido mediante espectrometría de masas.

Espectrometría de masas

El análisis por espectrometría de masas se realizó utilizando ionización-desorción láser asistida por matriz (MALDI) en un equipo de espectrometría de masas de tiempo de vuelo con una fuente láser de nitrógeno (Voyager-DE STR; Applied Biosystems). Para cada espectro se realizaron entre 50 y 200 disparos láser (error estándar ± 20 ppm).

Ensayos enzimáticos

La actividad enzimática de los dominios catalíticos recombinantes de APO, AMZ1 y AMZ2 se ensayó utilizando derivados de aminoácidos conjugados a AMC. Además, se analizó la actividad de las AMZ1 y AMZ2

recombinantes frente a los péptidos fluorogénicos QF35 (*AMC-Pro-Leu-Ala-Nva-Dpa-Ala-Arg-NH_2*) y QF41 (*AMC-Pro-Cha-Gly-Nva-His-Ala-Dpa-NH_2*), donde AMC es ácido acético-(7-metoxicumarin-4il), Nva es L-norvalina, Dpa es ácido propiónico-L-dinitrofenil-diamino y Cha es ciclohexil-alanina. Los ensayos se realizaron a 37 ºC utilizando una concentración final de 5 µM de sustrato en un tampón que contenía 50 mM de Tris-HCl, 150 mM de NaCl, y 0,05% de Brij-35, ajustado a pH 7,5. La fluorescencia se midió en un espectrofluorímetro LS55 PerkinElmer Life Sciences (para AMC λ_{ex} = 360 nm y λ_{em} = 460 nm, y para los péptidos que contienen MCA λ_{ex} = 328 y λ_{em} = 393). La calibración de la fluorescencia se realizó utilizando concentraciones conocidas de AMC y MCA. Para los experimentos de inhibición, se preincubaron las proteínas recombinantes 30 min a 37 ºC con los correspondientes inhibidores y a continuación se midió la actividad hidrolítica mediante un ensayo fluorogénico como el descrito arriba, empleando como sustratos Arg-AMC para APO, Ala-AMC para AMZ1 y Arg-AMC para AMZ2. Los estudios cinéticos se realizaron usando diferentes concentraciones de los sustratos fluorogénicos (0,5-100 µM) en un volumen final de 100 µL de la solución tamponada que contenía los enzimas recombinantes (5 nM). La hidrólisis de los péptidos se calculó como el aumento de fluorescencia a 37 ºC a tiempo final. Los ensayos con proteínas purificadas (albúmina, colágeno fibrilar, gelatina, plasminógeno, o aprotinina) y con péptidos bioactivos (neurogranina, angiotensina I, angiotensina II, y angiotensina III) se efectuaron incubando las proteínas recombinantes (2,5 mM) con cada sustrato (10 µM). Los ensayos se incubaron a 37 ºC en un tampón que contenía 50 mM de Tris-HCl y 150 mM NaCl, pH 7,5, durante 12 h para las proteínas purificadas y durante 2, 6 y 24 h para los péptidos bioactivos. La hidrólisis de las proteínas purificadas se analizó por SDS-PAGE y la de los péptidos bioactivos por espectrometría de masas.

Análisis de expresión de miRNAs

El análisis de los patrones de expresión del conjunto de todos los miRNAs de ratón se realizó como se ha descrito previamente (Lu y col., 2005) utilizando RNA total extraído con TRIzol (Invitrogen). Para la cuantificación de los niveles individuales de los miRNAs de interés, el RNA de tejidos o líneas

celulares se preparó empleando el kit “miRVANA miRNA isolation” (Ambion), y la calidad y concentración de las muestras se determinó utilizando un espectrofotómetro NanoDrop ND-1000. La determinación de los niveles relativos de cada miRNA se realizó mediante RT-PCR a tiempo real utilizando ensayos “Taqman microRNA expression assays” (Applied Biosystems). Para ello, se generó cDNA de doble hebra a partir de 10 ng de RNA total mediante el kit de transcripción reversa “Taqman miRNA reverse transcription kit” (Applied Biosystems). El cDNA resultante se amplificó mediante PCR a tiempo real en un sistema de detección “7300 Real-Time PCR System” (Applied Biosystems) siguiendo las instrucciones del fabricante. Los resultados se analizaron mediante cuantificación relativa frente al control endógeno RNU6B (para muestras humanas) o snoRNA202 (para muestras de ratón) empleando el Software SDS 1.4 y 2.1 de Applied Biosystems.

Técnicas de Biología Celular

Cultivos celulares y ensayos de proliferación

Para el establecimiento de cultivos primarios de fibroblastos de ratón, las orejas de ratones de 12 semanas de edad fueron esterilizadas con etanol, lavadas en PBS y trituradas con cuchillas. El material triturado se incubó con 600 µL de una disolución de colagenasa D (Roche Molecular Biochemicals) 4 mg/mL y dispasa II (Roche Molecular Biochemicals) 4 mg/mL en DMEM (Gibco) durante 45 min a 37 ºC y 5% de CO_2. Posteriormente se le añadieron 6 mL de DMEM con 10% de suero bovino fetal (Gibco) y 1% de antibiótico antimicótico (Gibco) y se incubó durante toda la noche a 37 ºC y 5% de CO_2. Finalmente, la mezcla se filtró, se lavó y se sembró en placas de 10 cm. A partir de entonces, se pasaron un millón de células en placas de 10 cm de diámetro cada tres días en incubadores con 20% de oxígeno. Para el contaje celular, se utilizó un hematocitómetro Bright-Line (Hausser Scientific) siguiendo las instrucciones del fabricante. Las células HEK-293 y U2OS fueron suministradas por el Dr. P.P. Durán (CNIO, Madrid) y las células HCT-116 por el Dr. B

Vogelstein (Ludwig Center, Baltimore, MD, USA), mientras que los fibroblastos humanos control (GM00038) y los derivados de pacientes de HGPS que contenían la mutación G608G (AG11498) se obtuvieron del repositorio de líneas celulares "Coriel Cell Repository". Todas las líneas celulares se cultivaron en medio DMEM (Gibco) suplementado con 10% de suero bovino fetal (Gibco) y 1% de penicilina/estreptomicina/glutamina (Gibco).

Experimentos funcionales de miRNAs

La sobreexpresión de miRNAs en células U2OS o en fibroblastos se llevó a cabo mediante el uso de moléculas de RNA miméticas "miRIDIAN microRNA mimics" (Dharmacon), mientras que la inhibición se realizó con moléculas de RNA complementarias al miRNA maduro "miRCURY LNA microRNA power inhibitors" (Exiqon). La transfección de estas moléculas en células U2OS y fibroblastos se llevó a cabo utilizando lipofectamina RNAiMAX (Invitrogen) siguiendo el protocolo de transfección directa suministrado por el proveedor. Para los ensayos de proliferación de fibroblastos en placas de 10 cm se realizaron dos transfecciones consecutivas y en el caso de los ensayos de proliferación MTT, las transfecciones se realizaron empleando el protocolo de transfección reversa suministrado por el proveedor. En todos los casos, los miméticos e inhibidores de miRNAs se utilizaron a una concentración final de 25 nM y 20 nM, respectivamente. Asimismo, en todos los experimentos, las células control se trataron con una concentración equivalente de un mimético o inhibidor de miRNAs control suministrado por los proveedores.

Ensayos de actividad luciferasa

Para la validación de los mRNAs diana de los miRNAs, se clonaron las regiones 3'UTR completas de los genes seleccionados en el plásmido psiCHECK-2 (cedido por el Dr. A. Rodríguez, *The Welcome Trust Sanger Institute*, Cambridge, UK) utilizando los enzimas de restricción *XhoI* y *NotI*. Las construcciones resultantes (250 ng) se transfectaron en células HEK-293, previamente sembradas para alcanzar una confluencia aproximada del 50%, en combinación con miméticos o inhibidores de los miRNAs de interés o de un miRNA control (20 nM) utilizando lipofectamina 2000 según las instrucciones

del proveedor. En este caso, se utilizaron miméticos de miRNAs ("Pre-miR microRNA precursor molecules", Ambion) o inhibidores de miRNAs ("Anti-miR microRNA inhibitors", Ambion). Tras la transfección, se reemplazó el medio con medio de crecimiento fresco o medio que contenía 0,5 μM de doxorrubicina durante 18 h antes de ensayar la actividad luciferasa. Para los experimentos con promotores, se clonaron las regiones genómicas indicadas en el plásmido pGL3 basic (Promega) utilizando el enzima de restricción *SmaI*. Las construcciones resultantes (250 ng) se transfectaron junto con el plásmido pRLTK (Promega) (12,5 ng) en células HCT-116, previamente sembradas en placas de 24 pocillos, utilizando lipofectamina 2000 según las instrucciones del fabricante. Tras la transfección, se reemplazó el medio de transfección por medio de crecimiento fresco que contenía doxorrubicina (0,5 μM), 4-NQO (0,5 μM) o H_2O_2 (20 μM), y las células se mantuvieron en esas condiciones durante 24 h antes de ensayar la actividad luciferasa. Para la determinación de la actividad luciferasa se empleó el kit "Dual-luciferase Reporter Assay System" (Promega) siguiendo el protocolo del fabricante. Una vez concluido el tratamiento de las células, se aspiró el medio de las placas de 24 pocillos y se lisaron mediante la adición de 80 μL de "Passive Lysis Buffer" y empleando un agitador orbital. A continuación, la actividad de las luciferasas de *Photinus pyralis* y *Renilla reniformis* se determinó utilizando 10 μL del lisado en un luminómetro TD-20/20 (Turner Biosystems). En todos los casos se utilizó la relación entre la actividad de ambas luciferasas para su representación.

Análisis de senescencia celular e inmunofluorescencia

La senescencia celular se analizó mediante detección de la actividad β-galactosidasa a pH 6,0 usando un kit de Cell Signaling diseñado para este fin y siguiendo las instrucciones del fabricante. La cuantificación de las células senescentes se llevó a cabo mediante el contaje del número de células positivas para la tinción a una magnificación 10x utilizando un microscopio de contraste de fases. Para los estudios inmunocitoquímicos, las células se crecieron sobre cubreobjetos estériles tratados con gelatina y posteriormente se lavaron con PBS y se fijaron con paraformaldehído al 4% en PBS. A continuación, se permeabilizaron con 0,5% de Triton X-100 en PBS durante 5

min a 25 ºC. Seguidamente, las muestras se bloquearon con 5% de albúmina bovina en PBS durante 45 min a 25 ºC. La incubación con los distintos anticuerpos primarios se llevó a cabo a las concentraciones recomendadas por los distintos fabricantes de cada anticuerpo durante 12 h a 4 ºC utilizando 5% de albúmina bovina en PBS como bloqueante. Finalmente, tras varios lavados con PBS, las muestras se incubaron con los correspondientes anticuerpos secundarios conjugados con distintos fluorocromos. Las preparaciones se contratiñeron con DAPI (4',6-diamidino-2-fenilindol) (Sigma-Aldrich) y se montaron con el medio de montaje Vectashield (Vector). Las microfotografías digitalizadas se tomaron utilizando un microscopio Axiovert 200M (Zeiss). La cuantificación de células positivas para γ-H2AX se realizó mediante el contaje de al menos 300 células en campos de visión aleatorios a una magnificación de 40 x.

Producción de retrovirus e infección

Las células HEK-293T creciendo en placas de 6 pocillos se transfectaron transitoriamente con el reactivo TransIT-LT1 (Mirus), la construcción derivada del vector pLEMIR conteniendo el transcrito primario de miR-29b-2~29c y los vectores "*helper*" PMD y CMV-VSVG (cedidos por el Dr. J. M. Silva, Universidad de Columbia, Nueva York, E.E.U.U.). Transcurridas 18-24 h se retiró el medio de transfección y se reemplazó con medio de crecimiento fresco. El medio de cultivo se recogió 24 h después de la transfección, se filtró con filtros Millex de 0,45 µm (Millipore) para recoger las partículas retrovirales y se congeló a -20 ºC para su futura utilización. Para la infección, se añadió 1 mL del sobrenadante viral a células U2OS que se habían sembrado 24 h antes en placas de 6 pocillos para que alcanzasen una confluencia del 30-50% en el momento de la infección, y se añadió polibreno a una concentración final de 5 µg/mL. La infección se dejó transcurrir durante 12 h y se repitió este proceso una segunda vez pero en ausencia de polibreno. Las células se cultivaron en medio de crecimiento fresco durante 24 h antes de reemplazarlo por un medio de selección que contenía 2 µg/mL de puromicina. La selección se mantuvo durante 24-48 h y finalmente, las células se dejaron recuperar 48 h en medio de crecimiento antes de realizar los experimentos.

Ensayo de proliferación MTT

Para cuantificar la proliferación celular se usó el kit "Cell Titer 96 Non Radioactive cell proliferation kit" de Promega. Se sembraron 2.500 fibroblastos o 5.000 células U2OS por pocillo en placas de 96 pocillos (100 µL) y se incubaron a 37 ºC y 5% de CO_2. La proliferación celular se midió mediante la conversión de 3-(4,5-dimetiltiazol-2-il)-5-(3-carboximetoxifenil)-2-(4-sulfofenil)-2H-tetrazol (MTS) en formazán soluble en agua por enzimas deshidrogenasas presentes en las células. Tres horas antes de cada tiempo prefijado (0, 24, 48 y 72 h) se añadieron 15 µL de colorante a cada pocillo y se continuó la incubación a 37 ºC. Después de 3 h, se añadió la solución de solubilización y tras una incubación de 1 h a 37 ºC se midió la absorbancia a 570 nm en un lector de placas "Power Wave XS" de Biotek.

Ensayos en animales de experimentación

Todos los ensayos realizados utilizando animales de experimentación se llevaron a cabo de acuerdo con la normativa establecida por el Comité de Experimentación Animal de la Universidad de Oviedo.

Administración de IGF-1 recombinante

Los ratones fueron tratados con una dosis diaria de 1 mg de IGF-1 recombinante humana por kg de masa corporal. Para ello se utilizaron bombas osmóticas (modelo 1004, Alzet) con una tasa de bombeo de 0,125 mL/h mantenida durante 28 días. Las bombas se cargaron con 8,3 mg/mL de IGF-1 recombinante disuelto en tampón salino isotónico conteniendo 10 mM de HCl y se equilibraron durante 24 h en tampón salino isotónico a 37 ºC antes de su utilización. Para su implantación, los ratones fueron anestesiados con isofluorano, se les realizó una incisión en la piel en la mitad de la curvatura espinal y se les creó un bolsillo subcutáneo mediante disección roma con tijeras quirúrgicas. Las bombas se insertaron en el bolsillo subcutáneo con el regulador de flujo orientado distalmente y la incisión se suturó mediante grapas

Michel. Transcurridos 28 días, se reemplazaron las bombas por unidades nuevas utilizando el mismo procedimiento. Durante el reemplazamiento, se comprobó que las bombas retiradas habían liberado su contenido.

Análisis de parámetros sanguíneos

Los ratones fueron ayunados durante 5 h antes de la recolección de las muestras para evitar cualquier interferencia debido a la ingesta de alimento. Los animales se anestesiaron utilizando isofluorano y se recolectaron aproximadamente 100 μL de sangre mediante punción en el seno transversal utilizando una aguja de 23G. Para la obtención de plasma, se utilizaron tubos Vacutainer (BD) tratados con ácido etilendiaminotetraacético (EDTA). La sangre recolectada se centrifugó a 900 x *g* en una centrífuga refrigerada a 4 ºC y el sobrenadante se reservó a -80 ºC para su posterior análisis. La concentración de IGF-1 en plasma se determinó utilizando el kit de ELISA Quantikine (R&D Systems), mientras que para los niveles de GH en plasma se empleó un kit de ELISA adquirido a Linco Research.

Análisis de la respuesta a GH

Para este fin se utilizaron ratones de 3 meses y medio ayunados 12 h, a los que se les administró una dosis intravenosa de 5 mg/kg de GH recombinante humana. Transcurridos 10 min, se sacrificaron los ratones y se recolectaron las muestras hepáticas y se congelaron instantáneamente en nitrógeno líquido. La respuesta a GH se examinó mediante análisis Western con anticuerpos específicos.

Técnicas Bioinformáticas

Búsqueda de genes de proteasas y análisis filogenético

Utilizando el programa BLAST se analizaron las bases de datos pública (www.ncbi.nlm.nih.gov) y privada (www.celera.com) del genoma humano

buscando regiones con secuencia similar a genes de metaloproteasas de organismos procariotas. La búsqueda en múltiples especies de secuencias similares a las proteasas humanas de interés se llevó a cabo empleando el algoritmo TBLASTN. Las secuencias obtenidas se alinearon automáticamente con ClustalX 1.8 (www.igbmc.u-strasbq.fr/BioInfo/ClustalX) y manualmente con GeneDoc 2.6 (www.psc.edu /biomed/genedoc). Como control externo del análisis se incluyó una metaloproteasa de la enterobacteria *Yersinia pestis,* que no está relacionada con las arqueometzinquinas. El árbol de máxima parsimonia de este alineamiento se calculó con el programa Protpars incluido en el paquete Phylip 3.6 (evolution.genetics.washington.edu/phylip/getme.html). A continuación se representó el árbol obtenido utilizando TreePlot (www.bioinformatics.nl/tools/plottree.html). Además, se construyó un árbol de las especies seleccionadas, basado en diversas fuentes de información filogenética (www.ncbi.nlm.nih.gov/Taxonomy/CommonTree/wwwcmt.cgi).

Análisis bioinformático y estadístico

La predicción computacional de las dianas de miRNA se realizó mediante la combinación de los siguientes programas bioinformáticos: TargetScan (www.targetscan.org), Microcosm (www.ebi.ac.uk/enright-srv/microcosm) y PicTar (pictar.mdc-berlin.de). Para el análisis estadístico de los datos experimentales se emplearon el programa Prism (GraphPad software, Inc) o el programa Excel del paquete Microsoft Office. Las velocidades iniciales de los ensayos enzimáticos se dedujeron utilizando el paquete de análisis FL WinLab 2.01 (PerkinElmer Life Sciences) y los datos se ajustaron a la ecuación de Michaelis-Menten usando GraFit 4.0 (Erithacus). Los datos experimentales se muestran como el valor medio calculado a partir de los mismos, y las barras de error representan el error estándar de la media.

RESULTADOS

I. Metaloproteasas y el degradoma

Las metaloproteasas constituyen un grupo heterogéneo de enzimas proteolíticos caracterizado por la utilización de iones metálicos, comúnmente zinc, para la consecución de la catálisis enzimática. Estos enzimas representan una de las clases catalíticas de proteasas más numerosa en múltiples organismos y desempeñan un papel esencial en multitud de procesos biológicos. En este trabajo de revisión, hemos llevado a cabo una descripción general de la complejidad de las metaloproteasas en el marco del degradoma para posteriormente discutir la relevancia de estos enzimas en los procesos biológicos y patológicos de los organismos. Finalmente, hemos analizado en mayor profundidad tres grupos de metaloproteasas, MMPs, ADAMs y ADAMTSs, que han adquirido una gran relevancia por su implicación en diversas patologías humanas.

Artículo 1: **Alejandro P. Ugalde**, Gonzalo R. Ordóñez, Pedro M. Quirós, Xose A. Puente y Carlos López-Otín. "Metalloproteases and the Degradome"

Methods in Molecular Biology, **622**: 3-29 (2010)

Aportación personal al trabajo

En este trabajo realicé la tarea de recopilar y organizar la información disponible acerca de los distintos aspectos de las metaloproteasas discutidos en este capítulo. Además, participé en la elaboración del manuscrito y de las figuras bajo la supervisión de los Drs. Carlos López-Otín y Xose Antón Suárez Puente y con la colaboración del resto de los coautores.

Chapter 1

Metalloproteases and the Degradome

Alejandro P. Ugalde, Gonzalo R. Ordóñez, Pedro M. Quirós, Xose S. Puente, and Carlos López-Otín

Abstract

Metalloproteases comprise a heterogeneous group of proteolytic enzymes whose main characteristic is the utilization of a metal ion to polarize a water molecule and perform hydrolytic reactions. These enzymes represent the most densely populated catalytic class of proteases in many organisms and play essential roles in multiple biological processes. In this chapter, we will first present a general description of the complexity of metalloproteases in the context of the degradome, which is defined as the complete set of protease genes encoded by the genome of a certain organism. We will also discuss the functional relevance of these enzymes in a large variety of biological and pathological conditions. Finally, we will analyze in more detail three families of metalloproteases: ADAMs (a disintegrin and metalloproteinase), ADAMTSs (ADAMs with thrombospondin domains), and MMPs (matrix metalloproteinases) which have a growing relevance in a number of human pathologies including cancer, arthritis, neurodegenerative disorders, and cardiovascular diseases.

Key words: Enzyme, proteolysis, metzincin, cancer, metastasis, arthritis.

1. Introduction

Since their initial discovery, concepts on proteases have evolved from the consideration of these enzymes as proteins merely implicated in the non-specific degradation of dietary proteins to their wide recognition as members of complex systems which modulate multiple biological processes through cleavage of specific substrates (1). By performing these proteolytic processing reactions, proteases regulate a wide range of cellular processes such as DNA replication, cell-cycle progression, cell proliferation, differentiation and migration, apoptosis, senescence, and autophagy. In metazoans, proteolytic systems are also involved

I.M. Clark (ed.), D.A. Young, A.D. Rowan (Consulting editors), *Matrix Metalloproteinase Protocols*,
Methods in Molecular Biology 622, DOI 10.1007/978-1-60327-299-5_1,
© Springer Science+Business Media, LLC 2001, 2010

in the maintenance of tissue homeostasis and in the regulation of different physiological processes such as fertilization and fecundation, embryonic development, immune response, wound healing, tissue remodeling, and angiogenesis.

The importance of proteolysis is underscored by the fact that proteases can be found in all kingdoms of life, from archaea and eubacteria to plants and animals, as well as in numerous viruses Additionally, alterations in the structure or regulation of proteolytic systems can have dramatic consequences on the whole organism and underlie many human pathologies such as neurodegenerative diseases, progeroid syndromes, or cancer (2). To understand the increasing complexity of proteolytic enzymes from a global perspective, the term degradome has been recently coined to define the entire complement of protease genes encoded by the genome of one organism (1). The recent availability of genome sequences from several organisms has allowed the annotation and comparison of their respective degradomes. Thus, a highly curated protease database (http://www.uniovi.es/degradome), which does not incorporate protease pseudogenes or retrovirus-derived protease-like sequences, currently annotates 569 human proteases and homologues classified in 68 families. The chimpanzee degradome is very similar to the human degradome despite notable variations in immune defense proteases like caspase-12 which is absent or non-functional in humans but is present in chimpanzee and all other mammals (3). Interestingly, mouse and rat degradomes are much larger (644 and 629 protease genes, respectively) than the human degradome despite their genomes are smaller. These differences mainly derive from the specific expansion in rodents or the specific inactivation in humans of members of protease families – such as placental cathepsins and kallikreins – involved in reproductive and immunological functions (2). The recent analysis of the degradome of other mammals such as the duck-billed platypus has revealed not only the presence of more than 500 protease genes but also a lack of all genes encoding gastric pepsins, which are highly conserved digestive proteases present in the rest of mammals (4). Birds, amphibians, and fish also contain large numbers of protease genes (more than 300 in every analyzed genome), although the protease annotation work in these species has not been as detailed as in mammals. Remarkably, analysis of the degradome of invertebrates such as *Drosophila melanogaster* – a model organism with a gene content considerably lower than vertebrates – has shown the presence of more than 600 protease genes (5). This relatively large number of insect proteases mainly derives from the genomic expansion of a family of serine proteases genes implicated in embryonic development and immune defense. Comparative genomic analysis has also facilitated the annotation of the protease repertoire of model plants such as *Arabidopsis thaliana* which contains more than 700 pro-

tease genes (6). Finally, there is a growing interest in the careful analysis of the degradomes of bacteria, viruses, fungi, and parasites to define novel therapeutic targets. In this regard, the annotation in the MEROPS database (http://merops.sanger.ac.uk) of more than 100 protease genes in the genome of bacteria such as *Yersinia pestis* and in the malaria parasite *Plasmodium falciparum*, which cause important human diseases, is noteworthy.

In summary, these recent genomic studies have provided a first global view of the complexity of proteolytic systems in all living organisms. Although all these proteases catalyze the same biochemical reaction – the hydrolysis of a peptide bond – different mechanistic solutions have been developed during evolution to efficiently perform this type of reaction. Attending to their catalytic mechanism, proteolytic enzymes can be grouped into six different classes: aspartic, glutamic, serine, cysteine, threonine, and metalloproteases. The general mechanism for all of them consists in the nucleophilic attack to the carbonyl carbon of the peptide bond. In aspartic, glutamic, and metalloproteases, a polarized water molecule located in the active center acts directly as a nucleophile. By contrast, in the other three classes the reactive element consists of a hydroxyl (serine and threonine) or sulfydryl (cysteine) group from the corresponding side chain of these residues at the catalytic core. In this chapter we will focus on the analysis of metalloproteases, which represent the most densely populated catalytic class of proteases in many organisms including mammals (**Fig. 1.1**). We will first present a general description of the complexity of this large group of enzymes. We will also discuss different functions of metalloproteases in both normal and pathological conditions. Finally, we will analyze in more detail the ADAM (a disintegrin and metalloproteinase domain), ADAMTS (ADAMs with thrombospondin domains), and MMP (matrix metalloproteinases) families of enzymes which are of special relevance in the context of this book.

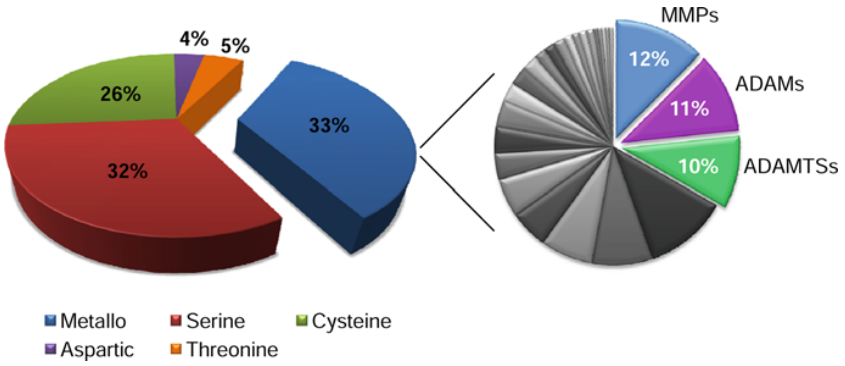

Fig. 1.1. Distribution of proteases in the human degradome.

2. Metalloprotease Classification

Metalloproteases comprise a heterogeneous group of proteases that can be classified at various levels, according to their catalytic mechanism, their substrates and products, or their structural homology (**Fig. 1.2**). Similar to other protease classes, a first classification scheme can be established attending to the cleavage position in the substrate. Following this criterion, metalloproteases can be classified as endopeptidases or exopeptidases. Endopeptidases comprise those enzymes with ability to cleave inner peptide bonds of proteins, whereas exopeptidases cleave a peptide bond located not further than three amino acids from the N-terminal (aminopeptidases) or C-terminal end (carboxypeptidases) of the protein.

The main characteristic of metalloproteases is the utilization of a metal ion – usually Zn – to polarize a water molecule and perform the hydrolysis reaction. The problem of coordinating a metal ion and accommodate the substrate in a polypeptide scaffold has found different solutions throughout evolution. As

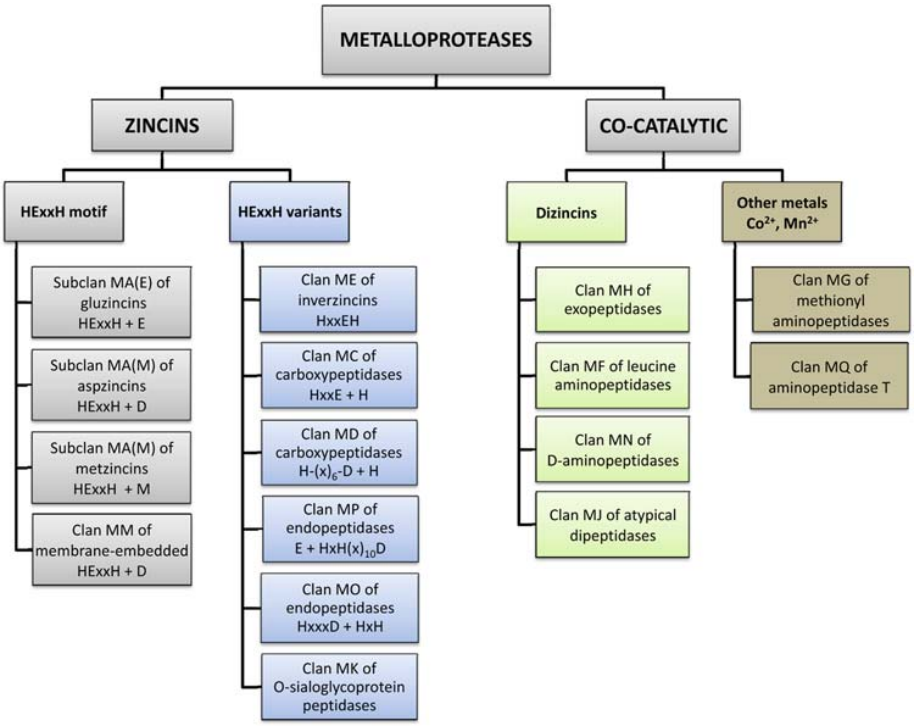

Fig. 1.2. Classification of metalloproteases. The figure shows an overview of the different catalytic mechanisms employed by metalloproteases.

a result, metalloproteases can be classified in different groups, termed clans or families, based on structural and sequence homology. The last MEROPS database release (8.00) contains 32,275 sequences of metalloproteases, which can be grouped into at least 14 clans and 54 different families. **Figure 1.2** shows a simple classification of metalloproteases based on the nature and sequence of the active site as well as other structural determinants. The metal ion present in the active center of metalloproteases is usually coordinated with the polypeptide backbone through the binding to two histidines and a third residue which can be another histidine or an acidic residue (Asp, Glu). In addition to these three metal-binding residues, a catalytic residue is absolutely necessary for the enzymatic activity of the protease. This residue acts as a general base, first accepting a proton from water and then transferring it to the scissile bond. The positions of these key four residues are usually conserved among members of a clan and can be deduced from the alignment of primary sequences or, more accurately, through the study of 3D structures. Although the three zinc-binding residues and the general base are crucial for the activity of metalloproteases, other residues can influence enzyme efficiency by participating in different aspects of catalysis such as carboxyanion stability, substrate accommodation, and protein fold.

3. The HExxH Motif and Its Variants

The most conserved zinc-binding motif in metalloproteases is the HExxH sequence. In this short motif, the two histidines coordinate the zinc ion and the glutamate acts as a general base in the catalytic reaction. This structural motif characterizes the MA clan, the largest clan of metalloproteases, which contains two subclans and 40 families of peptidases, including MMPs, ADAMs, and ADAMTSs which will be further discussed in this chapter. In this group of enzymes, the third coordination position of the zinc ion is occupied by another residue situated at a distal position from the core sequence (**Fig. 1.2**). This residue can be a glutamate, an aspartate, or another histidine. Additionally, the HExxH motif can also be found in the MM clan of membrane-embedded metalloproteases, although they have been placed in a separate clan because of their transmembrane-spanning segments that carry the zinc-binding residues (7). These peculiar metalloproteases are able to cleave the transmembrane-spanning helical regions of membrane proteins within the lipid bilayer, thus participating in a signal transduction system termed *regulated intramembrane proteolysis*. A representative member of this metalloprotease clan is the site-2 protease (MBTPS2) which regulates

the level of cholesterol in cell membranes through the processing of the sterol regulatory element-binding protein (8). Therefore, the HExxH sequence motif constitutes the most successful solution to the zinc coordination problem and has been employed by more than 40 different families of metalloproteases.

A simple variation of the HExxH motif is present in the ME clan of peptidases, whose members display an HxxEH motif, an inversion of the zinc-binding sequence presented above. Additionally, an aspartate residue acts as the third ligand for the metal ion. Due to the inversion of the structural motif, this group of enzymes has been named inverzincins. There are four functional inverzincins encoded in the human genome: the insulin-degrading enzyme insulysin, the convertase nardilysin, and the mitochondrial presequence peptidases eupitrilysin and MPP (mitochondrial processing peptidase beta-subunit) (9). In addition, there are three clans (MC, MP, and MK) of non-HExxH metalloproteases distributed in humans. The MC clan comprises a unique family of carboxypeptidases (M14), with a consensus motif HxxE, where glutamate and histidine act as zinc-binding residues, together with a third His located 103–143 residues toward the C terminus. In humans, there are 19 members of this family involved in the digestion of dietary proteins in the intestine, protein degradation by mast cells, or proteolytic processing of different bioactive peptides (10, 11). The MP clan includes the family M67 containing enzymes that chelate the zinc ion through two histidines and an aspartic acid situated within the motif $HSHP(x)_9D$. There are seven human MP members which participate in the detachment of the ubiquitin tag from proteins marked for proteasome degradation (12). The MK clan has a unique family of endopeptidases (M22) which cleaves *O*-sialoglycosylated proteins and contains two members in the human genome: *O*-sialoglycosylated endopeptidase (OSGEP) and OSGEP-2 with an HxExH motif. Finally, there are two additional clans of metalloproteases (MD and MO) without the HExxH motif. Both of them are broadly distributed in bacteria and display major roles in bacterial wall synthesis and homeostasis. MD clan contains metalloproteases with an alternative consensus sequence HxxxxxxD and a distal histidine (13). MO clan proteases also employ two histidines and an aspartic acid as metal ligands, but they occur within the motifs HxxxD and HxH (13).

4. Co-catalytic Metalloproteases

All of the above-described metalloproteases contain a unique zinc ion in their active center and are known as zincins, but there is a second group of metalloproteases termed dizincins or co-catalytic zincins which are characterized by an active center that

coordinates two zinc ions. As in zincins, each metal ion is coordinated with three residues of the protein, but in dizincins, at least one of them acts as a bridge between the two zinc ions. Co-catalytic proteases can be grouped into two main classes. The first class contains clan MF aminopeptidases involved in processes such as MHC-I antigen presentation or lens crystallin protein turnover (14). The two zinc ions are coordinated through six residues, and an arginine in the active center interacts with a bicarbonate ion that functions as a general base. The second group of dizincins includes aminopeptidases from clans MH and MN whose zinc-binding structure is composed of five residues and a glutamate or a histidine residue acting as a general base. Peptidases from clan MN are D-amino acid-specific aminopeptidases distributed only in bacteria and archaea and implicated in peptidoglycan synthesis (15). The MH clan is composed of four families (M18, M20, M28, and M42) of amino- and carboxypeptidases present in animals, with the exception of family M42, which is restricted to archaea and bacteria. Human members of this family include aspartyl aminopeptidase, the only member of family M18 in mammals, carnosine dipeptidases I and II from family M20, and several glutamate carboxypeptidases from M28 family. Finally, a third group of co-catalytic metalloproteases that require other bivalent ions like Mn(II), Co(II), or Fe(II) for their activity is formed by clans MQ and MG. Proteases from the MQ clan are only distributed in plants, bacteria, and archaea, but several members of the MG clan can be found in mammals (family M24). Human members include three methionyl aminopeptidases, which release the N-terminal methionine of nascent proteins and X-Pro dipeptidases involved in the turnover of collagen degradation products (16).

5. The MA Clan of Metalloproteases

As mentioned above, most metalloproteases belong to the MA clan. Peptidases from this clan contain an active center fold related to that of thermolysin and are classically divided into three groups: *gluzincins*, *aspzincins*, and *metzincins* (17–19). The first two groups were named according to the third zinc-binding amino acid, glutamate and aspartate, respectively, whereas the metzincin group was defined attending to a conserved methionine residue in a structure called Met-turn (20). Metzincins usually employ a histidine as the third zinc-binding residue, although an aspartate can be found at this position in some members. Metzincins and aspzincins are grouped together in the same MA(M) subclan, while gluzincins are classified into subclan MA(E).

5.1. Gluzincins

The gluzincin superfamily contains 18 families of both exopeptidases and endopeptidases and is widely distributed throughout all kingdoms of life. Among them, only six families (M1, -2, -3, -13, -41, and -48) are present in animals. Members of the M1 family are aminopeptidases which participate in the processing of different bioactive peptides and proteins, thus regulating important aspects of the organism physiology such as blood pressure, embryonic implantation, placental homeostasis, inflammation, or angiogenesis (21). On the other hand, members of the M2 family of metalloproteases show carboxypeptidase activity with only two representatives in humans: angiotensin-converting enzymes-1 and -2 (ACE and ACE2). ACE has gained enormous interest due to its role in the regulation of blood pressure by processing angiotensin I to angiotensin II (22). The importance of this enzyme in the control of blood pressure is highlighted by the fact that inhibitors targeting ACE are widely used for the treatment of hypertension and congestive heart failure. An additional characteristic feature of ACE is the presence, in the same polypeptide chain, of two different gluzincin domains. This structure is extremely unusual among metalloproteases, because only carboxypeptidase D contains two different metalloprotease domains within the same polypeptide chain. The four other families of gluzincins present in humans are endopeptidases. Members of the M3 and M13 families are oligopeptidases involved in the processing of bioactive peptides. The M3 family only contains three members: thimet oligopeptidase, which is implicated in the regulation of the MHC-I system of antigen presentation; neurolysin, which degrades intracellular bioactive peptides as neurotensin; and the mitochondrial intermediate peptidase that participates in the maturation of several nuclear-encoded mitochondrial proteins (23, 24). The M13 family is formed by seven members: neprilysins -1 and -2, endothelin-converting enzymes -1 and -2, Kell blood group antigen, and DINE and PHEX peptidases, all of them membrane peptidases involved in the metabolism of a great variety of regulatory peptides of nervous, cardiovascular, or immune systems (25). The M41 family contains nuclear-encoded mitochondrial metalloproteases that play important roles in mitochondrial homeostasis (26). By contrast, the M48 family is composed of two transmembrane endopeptidases: ZMPSTE24/FACE-1 which participates in the processing of farnesylated proteins (27) and the mitochondrial protease OMA1. This family of gluzincins has gained considerable interest after the finding that mutations in the genes encoding FACE-1 or its substrate (lamin A) are responsible for different premature ageing syndromes including Hutchinson–Gilford progeria or mandibuloacral dysplasia (28–30).

In addition to these families of gluzincins widely distributed in animals, there are several metalloproteases belonging to

families absent in metazoans but of notable relevance because they behave as virulence factors for a large variety of pathogenic bacteria and fungi. A good example is the M4 thermolysin family, which is composed of secreted proteases produced by different bacterial strains. Some members of this family such as *Pseudomonas aeruginosa* pseudolysin, *Legionella* sp. Msp peptidase or *Vibrio cholerae* vibriolysin are important virulence factors (31). The M27 family of tetanus and botulism toxins is another example of a group of microbial metalloproteases that participate in the pathogenicity mechanism, as well as the anthrax lethal factor from *Bacillus anthracis* (family M34) (19). Bacterial collagenases from *Vibrio* and *Clostridium* degrade extracellular components of host interstitial tissue causing gas gangrene and septicemia and are frequently used in molecular biotechnology (32). Fungi metalloproteases belong to the M36 family and include fungalysin, an elastinolytic enzyme from *Aspergillus fumigates*, and several keratinases from fungi dermatophytes (33, 34).

5.2. Aspzincins

Aspzincins comprise a unique family of zincins (M35) constituted by deuterolysins from molds and bacteria. Most of them are neutral proteinases that participate in organism nutrition using as substrates, basic nuclear proteins like histones and protamines (17). Deuterolysins from *A. oryzae* and *A. sojae* have special interest since they are secreted by these molds during soybean fermentation. Sequence alignment of members of this family reveals an HExxH zinc-binding motif while the third zinc ligand is an aspartate residue situated 10 residues C-terminal to the second histidine (17). Although some metzincins from families M6 and M7 also contain an aspartate as third ligand, aspzincins are considered a different group due to the lack of a Met-turn and the absence of significant sequence homology with metzincins. This distinction is less clear in the M64 family of IgA peptidases from *Clostridium* (35). These enzymes also have an aspartate as the third zinc-binding residue and lack the consensus methionine present in metzincins, but contain a highly conserved glycine residue within the sequence HExxHxxxG which resembles the consensus sequence of metzincins. Therefore, it will be necessary to solve the 3D structure of these metalloproteases in order to determine the importance of each position and define with which group each is more akin.

5.3. Metzincins

The superfamily of metzincins is composed of metalloproteases with the HExxHxxxGxxH/D consensus zinc-binding sequence in their active center, where the first two histidines coordinate the zinc ion, and the glutamate acts as a general base. The conserved glycine serves as a hinge for a turn that brings the third metal ligand (His or Asp) near the zinc ion. An N-terminal segment of variable length connects the third ligand residue with the

invariant methionine which forms part of the 1,4-β-turn, generating a hydrophobic pillow for the zinc ion (18, 20, 36). The catalytic domain of metzincins consists of two lobes leaving a central groove which contains the zinc ion at its bottom, resulting in an optimum configuration for accommodating elongated substrates. All metzincins are metalloendopeptidases, with the possible exception of archaeometzincins, a family of aminopeptidases from the MA(M) clan widely distributed in archaea and vertebrates but whose structures remain undetermined (37). Metzincin families with reported 3D structures include *astacins*, *serralysins*, *adamalysins/reprolysins*, *matrixins/MMPs*, *snapalysins*, and *leishmanolysins*.

The *astacin* subfamily (M12A) receives its name from the crayfish digestive enzyme astacin, the first discovered member of this group of enzymes. Astacins are broadly distributed among the animal kingdom as well as in eubacteria, fungi, or protozoans and perform diverse functions different from digestion. These additional astacins include a group of metalloproteases present in a variety of animal species and termed hatching enzymes, due to their function during the breakdown of the egg envelope (38, 39). Another important group of astacins includes BMP-1/tolloid-like peptidases from *Xenopus*, *Drosophila*, and mammals. These enzymes are extracellular proteases able to target various extracellular matrix (ECM) components, growth factors, and enzymes (40). Accordingly, BMPs are implicated in processes such as bone formation, collagen assembly, embryonic development, differentiation, and TGF-β signaling (39, 41). Meprins constitute another group of astacins, widely distributed among chordates and displaying a membrane-bound localization in the brush border of the small intestine and kidney, as well as in leukocytes. Most of them are glycoproteins involved in the processing of bioactive peptides, like bradykinin, substance P, bombesin, and gastrin, as well as different basement membrane components such as collagen IV, nidogen-1, and fibronectin (38, 39). Interestingly, most astacins contain additional C-terminal modules such as EGF (epidermal growth factor)-like, CUB (complement subcomponents C1r/C1 s, embryonic sea urchin protein Uegf, BMP-1), and MATH (meprin and TRAF homology) (39).

Serralysins (M10B) and *snapalysins* (M7) are metzincins restricted to bacterial species. The former receives its name from the *Serratia marcescens* serralysin, which, like the rest of members of this family, acts as a virulence factor. Other examples are mirabilysin from *Proteus mirabilis*, aeruginolysin from *Pseudomonas aeruginosa*, and peptidases from *Erwinia chrysanthemi or Yersinia pestis*. These microorganisms are the causal agents of several human pathologies such as meningitis, endocarditis, otitis, pneumonia, conjunctivitis, and urinary infections that mainly affect immunocompromised hosts. Serralysins play

important roles in host invasion and virulence by degrading host defense mediators, such as interleukins, immunoglobulins, coagulation factors, and antimicrobial peptides (42–45). Snapalysins are secreted peptidases from various species of *Streptomyces* characterized by having an aspartic acid as third zinc ligand, a feature shared with peptidases from the M6 family. This family is formed by immune inhibitors from different *Bacillus* species that infect insects, including the immune inhibitor A from *Bacillus thuringensis*, which cleaves antibacterial humoral proteins produced by the immune system of insects (20, 46).

The *leishmanolysin* family of metzincins (M8) is a group of peptidases identified as the major surface glycoproteins (MSPs) of different protozoan parasites, mainly from genders *Leishmania* and *Trypanosoma*. These organisms are responsible for several anthroponotic diseases, such as the sleeping sickness, Chagas' disease, and various leishmaniosis (47). Leishmanolysins are expressed in the amastigote and promastigote stage of the parasite and contribute to different aspects of protozoan survival and host invasion. MSPs are extracellular membrane-anchored peptidases that bind complement component C3, or cleave CD4 molecules, immunoglobulins, and other components of the host immune system, favoring resistance to complement-mediated lysis, attachment, entrance, and survival into the macrophages (48, 49). Recently, several mammalian and insect homologues have been discovered, such as invadolysin, which plays important roles in cell division and development in *Drosophila* (50). Mammalian homologues of invadolysin have been named leishmanolysin-2 and -3 and their functions remain unknown.

The *reprolysins/adamalysins* form the second group of M12 peptidases (M12B), which comprises snake venom metalloproteases (SVMPs), ADAMs, and ADAMTSs. The name reprolysin reflects the fact that the first family members were identified in reptiles and in mammalian reproductive tissues. Currently, there are more than 140 reprolysin entries in MEROPS database, broadly distributed throughout the animal kingdom and expressed in a wide variety of tissues. The minimum structure of an adamalysin is found in some snake venom proteases which only contain the peptidase unit. However, most members of this group of metalloproteases contain additional domains which contribute to various aspects of their specificity, localization, or activation. SVMPs are toxic proteins present in snake venom which cause some of the symptoms associated with snake venom intoxication, such as hemorrhage, necrosis, edema, and inflammation. These metalloproteases exert their functions through degradation of proteins of the endothelial basement membrane, such as fibronectin, collagen, nidogen, or laminin, as well as by processing of plasma coagulation factors like fibrinogen and von Willebrand factor (20, 51). In addition to SVMPS, the reprolysins

also include ADAMs and ADAMTSs, two groups of metalloproteases of growing interest in multiple physiological and pathological conditions. Accordingly, both subfamilies will be discussed in detail in the following sections.

5.3.1. ADAMs (A Disintegrin and Metalloprotease)

The ADAM subfamily of reprolysins is composed of a variety of widely distributed enzymes that share a structural domain organization, constituted by a peptidase unit followed by a disintegrin domain, an EGF-like module, a transmembrane region, and a cytoplasmic tail (**Fig. 1.3**). The peptidase unit also contains an N-terminal signal peptide and a pro-domain which keeps ADAMs inactive through interaction with the active center via a conserved cysteine residue, in a mechanism known as cysteine switch. Interestingly, the pro-domain may also have a secondary function as a chaperone, favoring the proper fold of these metalloproteases (52). The signal peptide directs ADAMs to the endoplasmic reticulum where the pro-domain is cleaved off by furin-like pro-protein convertases. Some ADAMs are located at the Golgi but most show a cellular surface localization or are

Protease	Human gene	Mouse gene	Human locus
Decysin	*ADAMDEC1*	+	8p21
ADAM-1a / Fertilin-α	*ADAM1 (ps)*	+	12q24
ADAM-1b	-------	+	
ADAM-2 / Fertilin-β (np)	*ADAM2*	+	8p11
ADAM-3B / Cyritestin (np)	*ADAM3B (ps)*	+	16q12
ADAM-4 (np)	*ADAM4 (ps)*	+	14q24
ADAM-4B (np)	*ADAM4B (ps)*	+	14q24
ADAM-5 (np)	*ADAM5 (ps)*	+	8p11
ADAM-6 (np)	*ADAM6 (ps)*	+	14q24
ADAM-6B (np)	-------	+	
ADAM-7 (np)	*ADAM7*	+	8p21
ADAM-8	*ADAM8*	+	10q26
ADAM-9 / Meltrin-γ	*ADAM9*	+	8p11
ADAM-10	*ADAM10*	+	15q21
ADAM-11 (np)	*ADAM11*	+	17q21
ADAM-12 / Meltrin-α	*ADAM12*	+	10q26
ADAM-15 / Metargidin	*ADAM15*	+	1q21
ADAM-17 / TACE	*ADAM17*	+	2p25
ADAM-18 (np)	*ADAM18*	+	8p11
ADAM-19 /Meltrin-β	*ADAM19*	+	5q33
ADAM-20	*ADAM20*	-	14q24
ADAM-21	*ADAM21*	+	14q24
ADAM-22 (np)	*ADAM22*	+	7q21
ADAM-23 (np)	*ADAM23*	+	2q33
Testase -1	-------	+	
Testase-2	*ADAM25 (ps)*	+	8p22
Testase-3	-------	+	
ADAM-28	*ADAM28*	+	8p21
ADAM-29 (np)	*ADAM29*	+	4q34
ADAM-30	*ADAM30*	+	1p11
ADAM-32 (np)	*ADAM32*	+	8p11
ADAM-33	*ADAM33*	+	20p13
Testase-4	-------	+	
Testase-5	-------		
Testase-6	-------	+	
Testase-7	-------	+	
Testase-8	-------	+	
Testase-9	-------	+	

Protease	Human gene	Mouse gene	Human locus
ADAMTS-1	*ADAMTS1*	+	21q21
ADAMTS-2	*ADAMTS2*	+	5q35
ADAMTS-3	*ADAMTS3*	+	4q21
ADAMTS-4 / Aggrecanase-1	*ADAMTS4*	+	1q23
ADAMTS-5/11/ Aggrecanase-2	*ADAMTS5*	+	21q21
ADAMTS-6	*ADAMTS6*	+	5q12
ADAMTS-7	*ADAMTS7*	+	15q24
ADAMTS-8	*ADAMTS8*	+	11q24
ADAMTS-9	*ADAMTS9*	+	3p14
ADAMTS-10	*ADAMTS10*	+	19p13
ADAMTS-12	*ADAMTS12*	+	5p13
ADAMTS-13 / vWF-CP	*ADAMTS13*	+	9q34
ADAMTS-14	*ADAMTS14*	+	10q22
ADAMTS-15	*ADAMTS15*	+	11q24
ADAMTS-16	*ADAMTS16*	+	5p15
ADAMTS-17	*ADAMTS17*	+	15q26
ADAMTS-18	*ADAMTS18*	+	16q23
ADAMTS-19	*ADAMTS19*	+	5q23
ADAMTS-20	*ADAMTS20*	+	12q12

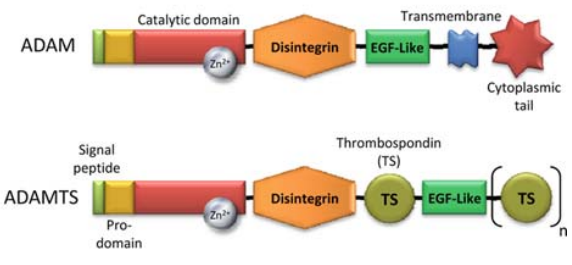

Fig. 1.3. Human and mouse ADAMs and ADAMTSs. The figure shows the domain organization of both groups of proteolytic enzymes; (np) indicates non-protease homologues; genes, and pseudogenes (ps) absent in one species are *shadowed* in *gray* and *green*, respectively.

secreted. Nevertheless, several family members, such as ADAM-12, undergo alternative splicing events giving rise to a large cell-surface protein and a short secreted isoform (53). In humans there are 21 ADAMs out of the 38 members identified in mammals, whereas a total of 37 family members have been identified in the mouse genome (**Fig. 1.3**). It is remarkable that several mouse ADAMs, such as ADAM-1, -3, -4, and -25, are pseudogenes in the human genome (2). This situation also occurs in rat, whose genome lacks three mouse ADAM orthologs and presents three pseudogenes that are functional in mice (54). Moreover, ADAM-20 is a human-specific gene which is absent in rodent genomes. The main subgroup of ADAMs expanded in the mouse genome is that of testases, whose name derives from their predominant expression in testis and their functions in reproduction. In mice there are nine testase genes, all of them being absent in humans with the exception of testase-2 which in humans is a pseudogene. Although ADAMs are expressed in various somatic tissues, most of them show expression in reproductive tissues. Other ADAMs are detected predominantly in male reproductive organs, such as ADAM-2, -3, -5, -18, -24, -25, -26, or -32, whereas some family members, like ADAM-11, -22, or -23, are mainly expressed in the central nervous system (55).

The main function of several ADAMs is the ectodomain shedding from the cell surface of a variety of transmembrane proteins, such as cytokines, growth factors and their receptors, and adhesion proteins. A well-known example is ADAM-17, also known as TNF-α converting enzyme (TACE). TNF-α is a key regulator of the immune response that exists in two alternative forms, a small secreted isoform and a large membrane-anchored protein. ADAM-17, as well as ADAM-9 and -10, can release the ectodomain of the membrane-bound TNF-α, leading to its activation (56). However, the fact that only *Adam17*-deficient mice display a significantly inhibited TNF-α shedding has led to the proposal that ADAM-17 is the major TNF-α sheddase (57). The EGF family of growth factors is also susceptible to ADAM-mediated shedding. EGF-like growth factors are synthesized as membrane-bound precursors that, upon proteolytic cleavage, release a soluble mitogenic form that binds to its receptor at the cell surface. ADAM-17 can shed various EGF-like growth factors, such as amphiregulin, epiregulin, heparin-binding EGF, neuregulin, and TGF-α. Similarly, other ADAMs such as ADAM-9, -12, and -19 can cleave some of these substrates. This functional overlapping is supported by the fact that *Adam8*, *-9*, and *-15* knockout mice develop normally, whereas *Adam12*-deficient mice display minor development defects (58). Furthermore, mice simultaneously lacking functional ADAM-9, -12, and -15 are viable and fertile, with no apparent pathology (59). ADAMs also regulate growth factor and cytokine signaling

pathways at the receptor level. For example, shedding of IL-1, IL-6, and TNF-α receptors is impaired in *Adam17*-null cells. Growth factor receptors such as HER4JM-a isoform, hepatocyte growth factor receptor Met, and nerve growth factor receptors are also susceptible to shedding by ADAM-17 (56). Another function associated with ADAMs is the α-secretase activity against amyloid precursor protein (APP), which generates a soluble α-APP with neurotrophic effects, instead of the harmful effects derived from β-amyloid production. It has been reported that ADAM-9, ADAM-10, and ADAM-17 are able to generate α-APP in physiological conditions. However, only *Adam17*-null cells are unable to produce soluble α-APP, indicating that this ADAM may be the main α-secretase. Other important substrates of ADAMs are insulin-like growth factor binding proteins (IGFBPs) and Notch receptor. ADAM12 cleaves IGFBP-3 and -5 and may be responsible for the increased levels of active IGF in plasma during pregnancy (60). Finally, *Adam10*-deficient mice die at day 9.5 of embryogenesis due to multiple defects in nervous and cardiovascular systems development associated with a downregulation of Notch signaling (61).

As a consequence of their ability to target this variety of substrates, ADAMs influence cell behavior at several different levels, including regulation of the balance between survival and apoptotic signals, promotion of cell migration, or induction of angiogenesis (62). For example, ADAM-15 disintegrin domain constitutes a potent anti-angiogenic factor with capacity of disrupting the association between integrin $\alpha_v\beta_3$ and vitronectin (63). In this regard, it is necessary to emphasize that the proteolytic activity is not an absolute requirement for certain functions of ADAMs. This is reflected by the fact that many ADAMs have changes in their consensus catalytic sequence that impair their catalytic properties but do not affect other essential functions of these enzymes. This is the case of ADAM-2, a non-protease ADAM whose deficiency in mice causes infertility, resembling the phenotype of the ADAM-3 knockout. Recent studies have proved that ADAM-2 is necessary for the correct stability and location of ADAM-3 (64). Another interesting example is ADAM-23, which promotes cell adhesion via interaction of its disintegrin domain with $\alpha_v\beta_3$ integrin (65).

One remarkable feature of ADAM activity is that, in most cases, ADAMs require an activation signal, like that provided by phorbol esters, to exert their effects. This phenomenon is related to the ability of ADAMs to mediate the transactivation of EGF receptors. Angiotensin II, endothelin-1, lysophosphatidic acid, or carbachol are examples of molecules that can activate EGF receptors without direct interaction with them (66). These ligands bind to G protein-coupled receptors (GPCRs) and initiate a signal transduction pathway that leads to ADAM activation. Activation

of ADAM is thought to be due to protein–protein interactions and phosphorylation at the cytoplasmic tail of these enzymes. The cytoplasmic tails of several ADAMs contain binding sites for SH3 domain proteins as well as phosphorylation sites for protein kinases (56). The activation mechanisms are not well defined, but various second messengers such as c-Src, PKC, Ca^{2+}, and ROS have been found to be implicated in the signaling of shedding processes (66). The two major pathways associated with activation of ADAM-mediated shedding are the Erk and p38 mitogen-activated protein kinases (MAPK). ADAM activity is also subjected to regulation by inhibitor molecules. Tissue inhibitors of metalloproteases (TIMPs) are endogenous molecules classically linked to MMP inhibition, but various works support a cross-reaction with ADAMs. For example, ADAM-17 is inhibited by TIMP-3, whereas ADAM-10 is susceptible to TIMP-1 and -3 blockade. By contrast other ADAMs such as ADAM-8 and -9 are not controlled by TIMPs (67).

Finally, it is remarkable that these structural and functional studies on ADAMs have an additional dimension after the description of ADAMTSs, a related group of reprolysins that share some features with ADAMs and also exhibit distinctive properties which will be discussed in the next section.

5.3.2. ADAMTSs (A Disintegrin and Metalloprotease with Thrombospondin Motifs)

This group of secreted reprolysins share some ADAM domains but lack the transmembrane and cytoplasmic tail and contain additional domains, including a central thrombospondin (TS) type-1 motif and a series of C-terminal TS repeats, ranging from zero in ADAMTS-4 to 14 in the case of ADAMTS-20 (68, 69). ADAMTS-7 and -12 have a mucin domain between the third and fourth of their seven C-terminal TS repeats. ADAMTS-20 and ADAMTS-9 have a GON domain, and ADAMTS-13 has two CUB domains. A PLAC (protease and lacunin) domain is also present in several ADAMTSs (**Fig. 1.3**) (70). One feature that distinguishes ADAMTSs from ADAMs is their ability to bind to the ECM through their central and C-terminal TS domains or through their spacer regions (71). Nascent ADAMTSs undergo N-terminal processing first in the endoplasmic reticulum by a signal peptidase and second in the trans-Golgi network by a proprotein convertase. Latency of pro-ADAMTSs may not be due to a cysteine-switch mechanism like in ADAM or MMPs, because only six ADAMTSs contain a conserved cysteine residue in their pro-domains. In addition, ADAMTSs can be processed at their C-terminal end, mainly within the spacer region or in the mucin domain in the case of ADAMTS-12. This processing affects ECM binding and substrate specificity of these enzymes. Thus, full-length ADAMTS-4 undergoes C-terminal processing generating two short-length isoforms that are not bound to the ECM. The full-length isoform cleaves aggrecan at a different position than

the short isoforms and is inhibited by addition of fibronectin, indicating that the spacer region is responsible for ECM binding and substrate specificity (71). Another interesting example is ADAMTS-1, which shows a potent anti-angiogenic activity which is absent in shorter isoforms lacking the C-terminal TS repeats and part of the spacer region (71). This C-terminal processing of ADAMTSs is carried out by members of the MMP family, such as MMP-2, -8, -15, and -17 (70).

ADAMTSs are expressed in a wide range of adult tissues, being more restricted in fetal tissues. ADAMTS-1, -4, -5, -8, -9, and -15 constitute a subgroup of enzymes with ability to degrade aggrecan, the major cartilage proteoglycan. Accordingly, these ADAMTSs are known as aggrecanases, although they can also degrade brevican, mainly expressed in the CNS, and versican, a blood vessel-specific proteoglycan. Aggrecanases contribute to the development of osteoarthritis and other pathologies not related to cartilage metabolism, such as growth retardation, impaired adipogenesis, and decreased fertility (72). ADAMTS-2, -3, and -14 are procollagen N-proteinases implicated in the releasing of the N-terminal propeptides of procollagen. ADAMTS-2 acts on procollagen I, II, and III, but ADAMTS-3 and ADAMTS-14 are restricted to procollagen II and I, respectively. ADAMTS-2 mutations cause Ehlers–Danlos syndrome in humans, characterized by skin fragility and joint laxity (73). Likewise, ADAMTS-10 mutations are responsible of human Weill–Marchesani syndrome, another pathology associated with altered ECM homeostasis and characterized by short stature, brachydactyly, joint stiffness, eye anomalies, and heart defects (74). ADAMTS-9 and -20 contain a GON domain and show structural similarity with the *Caenorhabditis elegans* gon-1, an ADAMTS associated with gonadal development in this organism. *Adamts20*-mutant mice are viable but display defects in melanocyte development (75). To date, it is unknown whether ADAMTS-9 controls gonadal formation in mammals, although a high-level expression in various embryonic tissues has been reported (76). The only ADAMTS-containing CUB domain is ADAMTS-13, also known as von Willebrand factor cleaving protease (vWFCP), whose deficiency is responsible for thrombotic thrombocytopenic purpura, characterized by the formation of microvascular thrombi and the development of anemia, renal failure, and neurological dysfunction (77). ADAMTS-1 and -8 stand out by their anti-angiogenic properties, as both can inhibit angiogenesis through VEGF binding and sequestration by their TS motifs (78). Another recently reported anti-angiogenic ADAMTS is ADAMTS-12, which is able to abolish tubule formation when exogenously added to epithelial cells (79). Interestingly, ADAMTS-12 also has anti-tumorigenic properties, decreasing tumor growth by preventing neovascularization (79).

Likewise, ADAMTS-1, -8, -9 -15, and -18 have also been proposed to play antitumor roles (80).

In addition to ADAMs and ADAMTSs, there is a third group of metzincins called MMPs that have been subjected to an exhaustive research due to their relevance in multiple normal and pathological conditions, especially in cancer and arthritis. The next section will review the nature, functions, and implications in disease of this group of metalloproteases.

5.3.3. MMPs (Matrix Metalloproteinases)

MMPs or matrixins are a group of secreted or membrane-anchored enzymes with at least 25 members distributed among vertebrates (**Fig. 1.4**) (81). Similar to reprolysins, MMPs have a HExxHxxGxxH peptidase motif in their proteolytic domain, an N-terminal signal peptide, and a pro-domain. This minimum domain structure is characteristic of matrilysins (MMP-7 and MMP-26). However, the archetypal domain organization of MMP contains an additional C-terminal hinge region followed by several hemopexin domains. This organization

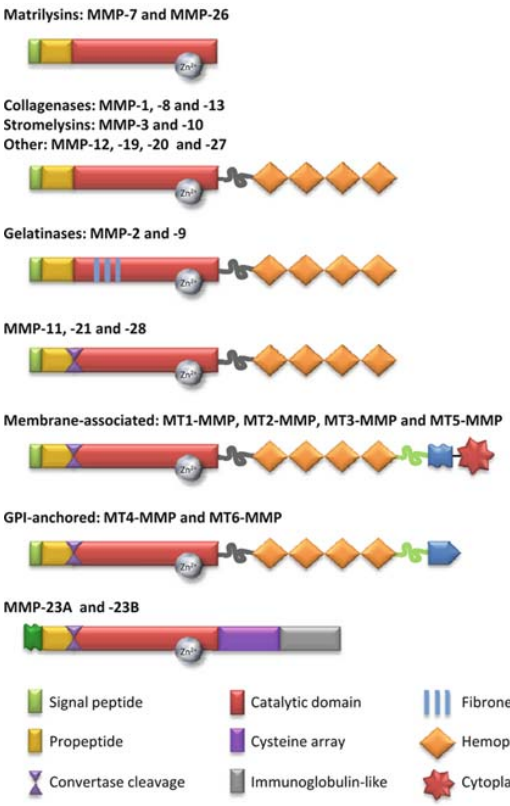

Protease	Human gene	Mouse gene	Human locus
Collagenase-like B	-------	+	
Collagenase -1	*MMP1*	+	11q22
Gelatinase -A	*MMP2*	+	16q22
Stromelysin-1	*MMP3*	+	11q22
Matrilysin	*MMP7*	+	11q22
Collagenase-2	*MMP8*	+	11q22
Gelatinase-B	*MMP9*	+	20q13
Stromelysin-2	*MMP10*	+	11q22
Stromelysin-3	*MMP11*	+	22q11
Macrophage elastase	*MMP12*	+	11q22
Collagenase-3	*MMP13*	+	11q22
MT1-MMP	*MMP14*	+	14q11
MT2-MMP	*MMP15*	+	16q22
MT3-MMP	*MMP16*	+	8q22
MT4-MMP	*MMP17*	+	12q24
MMP-19	*MMP19*	+	12q13
Enamelysin	*MMP20*	+	11q22
MMP-21	*MMP21*	+	10q26
MMP-23A	*MMP23A*	+	1p36
MMP-23B	*MMP23B*	-	1p36
MT5-MMP	*MMP24*	+	20q11
MT6-MMP	*MMP25*	+	16p12
Matrilysin-2	*MMP26*	-	11p15
MMP-27	*MMP27*	+	11q22
Epilysin	*MMP28*	+	17q12

Fig. 1.4. The MMP family of matrix metalloproteases. Schematic domain organization and human and mouse family members.

is present in stromelysin-1 and -2 (MMP-3 and -10), collagenases (MMP-1, -8, and -13), metalloelastase (MMP-12), enamelysin (MMP-20), and MMP-27. A similar domain structure is present in stromelysin-3 (MMP-11), epilysin (MMP-28), and MMP-21, but these enzymes have a furin-like target sequence inserted in their pro-domains, and constitute the group of secreted convertase-activatable MMPs. Other convertase-activatable MMPs are membrane-anchored by a glycosylphosphatidylinositol (GPI), or by type I or type II transmembrane segments, constituting a group called membrane-type MMPs (MT-MMPs). MMP-23A and 23 B also belong to this group, but contain an N-terminal type II transmembrane region and a cysteine array and immunoglobulin domains in their C-terminal end. Finally, MMP-2 and MMP-9 are secreted MMPs with gelatinolytic activity and characterized by the presence of fibronectin type II modules inserted into the peptidase domain (**Fig. 1.4**) (81).

MMP activity regulation has been widely studied with the finding of three main levels of endogenous control: gene transcription, proenzyme activation, and activity inhibition. Transcription regulation of MMPs is a complex mechanism in which no single factor is responsible for induction of MMP expression. However, cytokines such as TNF-α or IL-1 and growth factors such as TGF-β have been widely associated with the regulation of MMP expression. Likewise, several signal transduction pathways are implicated in the control of MMP transcription, like the p38 MAPK, which displays a dual role, enhancing or repressing MMP expression depending on the cell type (82). From the large variety of stimuli influencing MMP expression, several transcription factors have been found to mediate transcriptional changes in these metalloprotease genes. For example, most promoters of MMP genes contain functional binding sites for AP1, a transcription factor composed of dimers of members of the Fos and Jun family of oncoproteins. Other transcription factors associated with regulation of MMP expression are nuclear factor κB (NF-κB), T-cell factor 4 (TCF4), p53, and members of the Ets family of oncoproteins (81–83).

The second general level of regulation of MMP activity is proenzyme activation. MMPs are synthesized as zymogens where a conserved cysteine residue of the pro-domain occupies the active center abolishing its activity. The release of the pro-domain is a complex process that usually involves additional proteolytic enzymes. Thus, there are several MMPs that contain a pro-protein convertase sequence in their pro-domain and are activated in the secretory pathway by furin-like peptidases (84). However, most MMPs are activated at the pericellular space by other MMPs, such as MT-MMPs and MMP-3, or by serine proteases like plasmin, chymase, and tryptase. In most cases, this activation requires two

cleavages: a first one that exposes cryptic parts of the pro-domain and a second one in the exposed pro-domain that finally releases this structure (82). Substrate binding may also be responsible for pro-domain disengagement, triggering protease activation (85). Finally, other non-protease molecules can also be required for MMP activation, as in the case of MMP-2 activation by MT1-MMP, in which TIMP-2 acts as a scaffold protein to locate both MMPs at an adjacent position (82, 85).

The third main point of MMP regulation is the inhibition of the enzymatic activity of these metalloproteases. MMP activity can be blocked by general inhibitors present in plasma or tissue fluids, like α2-macroglobulins, and also by TIMPs which are more specific inhibitors. There are four TIMPs in humans, which differ in their expression pattern and MMP specificity. In addition, other molecules contain domains with structural similarity to TIMPs which allow them to act as MMP inhibitors. These include the C-terminal fragment of the procollagen C-terminal proteinase enhancer protein (PCPE), the NC1 domain of collagen type IV, the reversion-inducing cysteine-rich protein with Kazal motifs (RECK), and the tissue factor pathway inhibitor-2 (TFPI2) (82, 86–88).

Over many years, it has been considered that the main ability of MMPs is the degradation of ECM substrates, such as fibrillar and non-fibrillar collagens, gelatin, aggrecan, fibronectin, laminin, and elastin. However, a large number of non-matrix substrates have been reported for MMPs including cytokines, growth factors, adhesion molecules, other proteases, peptidase inhibitors, clotting factors, and several receptors (89). MMPs play an important role in tissue resorption in several physiological processes, such as endometrial cycling, embryonic development, bone remodeling, postpartum uterine involution, post-lactation mammary involution, and wound healing (81). Nevertheless, many of their effects are not due to tissue destruction since MMPs are implicated in the regulation of a large number of processes via specific processing of a wide range of ECM and non-ECM substrates. These MMP-regulated processes include proliferation, migration, apoptosis, angiogenesis, and inflammation. Several MMPs participate in the regulation of cytokine and chemokine release and activation, which are key steps in the immune response. For example, MMP-1, -2, -3, -7, -9, and -12 are able to process proTNF-α into soluble active TNF-α. MMP-2, -3, and -9 also have the ability to cleave IL-1β, generating a more active form (90). Moreover, MMP-9 controls IL-2-dependent proliferation of T lymphocytes through degradation of IL-2 receptor type-α, and MMP-8, -13, and -14 can cleave IL-8 generating truncated forms with increased activity (91, 92).

Similar to the case of ADAMs, MMPs are also involved in the regulation of cell proliferation by modulating the bioavailability

of active growth factors. Thus, MMP-1 and -3 cleave perlecan and release FGF, whereas MMP-2, -3, and -7 process decorin liberating ECM-anchored TFG-β (93, 94). A good example of non-ECM substrate processed by MMPs that influences the bioavailability of growth factors is the family of IGFBPs, soluble proteins that bind free IGF, and block its activity. All IGFBPs are susceptible to degradation by MMPs: MMP-1 cleaves IGFBP-2 and -3, MMP-2 processes IGFBP-3 and -5, and MMP-7 degrades all of them (89, 95). On the other hand, MMPs can regulate apoptosis via shedding of some death ligands (96) and modulate angiogenesis through the proteolytic exposure of cryptic anti-angiogenic signals present in ECM proteins. For example, arrestin, canstatin, and tumbastin are angioinhibitory peptides generated after MMP cleavage of collagen IV α-1, α-2, and α-3 chain, respectively. Moreover, MMP-7 mediates the release of endostatin from collagen XVIII and MMP-9 liberates tumstatin from collagen IV, both of which are anti-angiogenic molecules. Epithelial migration is a necessary step for new vessel formation and MMPs also participate in this process. MT1-MMP and MMP-2 cleave laminin-5 and generate a cryptic fragment that promotes cell motility. Migration-stimulating factor liberated through MMP-mediated processing of fibronectin also displays cell migration activity. Likewise, ECM degradation mediated by MMPs causes the release of angiogenic factors like VEGF, which is a potent pro-angiogenic molecule and osteoclast chemoattractant. In summary, MMPs perform a broad spectrum of actions influencing important cell processes such as apoptosis, cell migration, and cell proliferation, which ultimately control tissue homeostasis.

Due to the variety of processes in which MMPs are implicated, alterations in the structure or regulation of their genes are frequently associated with the development of several human pathologies, including cancer. Enamelysin (MMP-20) mutations cause amelogenesis imperfecta, an inherited tooth malformation due to defects in enamel maturation (97). Likewise, mutations in MMP-13 are responsible for human spondyloepimetaphyseal dysplasia, an autosomal dominant disorder characterized by defective growth and modeling of vertebrae and long bones (98). Moreover, MMP-2 is mutated in patients with multicentric osteolysis with arthritis, another inherited human skeletal disorder that displays altered bone resorption (99). Furthermore, specific MMP-1 and MMP-3 alleles have been associated with an increased susceptibility to different diseases including cancer (81). On the other hand, and as a direct consequence of their important roles of apoptosis, proliferation, and cell migration, deregulation of MMPs has been associated with tumorigenesis in a great variety of tissues. Growth factors released by MMPs generate proliferative and survival signals required by tumor cells. For example, *Mmp11*-deficient mice develop less

dimethylbenzanthracene-induced carcinomas whereas MMP-11 increases tumorigenicity in a syngenic model of tumorigenesis, both effects attributed to the ability of this MMP to release IGFs (100, 101). Similarly, MMP-7 inhibits cancer cell apoptosis by releasing HB-EGF or cleaving Fas-L. Angiogenesis is another key step in tumor growth which is regulated by MMPs at several levels (102). Thus, MMP-9 increases the bioavailability of VEGF whereas MMP-14 promotes the endothelial migration by degradation of the vessels matrix (103, 104). However, the most classical roles attributed to MMPs in cancer are those associated with tumor invasion and metastasis. Various MMPs have been implicated in cancer metastasis, like MMP-9, whose downregulation in cancer cells reduces the number of metastasis in mice, or MMP-14, which participates in the degradation of laminin-5 during cancer cell migration (105, 106). Furthermore, MMP-1 and MMP-2 are important functional mediators in the generation of pulmonary metastasis from breast carcinomas (107). MMPs may also contribute to cancer cell evasion from immune system. This is the case of MMP-9, which suppresses proliferation of T lymphocytes via degradation of their IL-2 receptors. Other MMPs reduce the neutrophil efflux by chemokine degradation or inhibit the T-lymphocyte response by TGF-β production (81, 82, 108). On the other hand, and contrary to classical ideas in this field, recent works have demonstrated that MMPs are able to inhibit cancer development, thereby acting as tumor suppressors. MMP-8 was the first family member associated with this function after the finding that *Mmp8*-deficient mice develop more skin tumors in a carcinogenesis assay (109). The mechanism by which this protease exerts its effects has been related to an abnormal inflammatory response observed in these mice subjected to chemical carcinogenesis. Likewise, MMP-26 has been associated with favorable clinical outcome when upregulated in hormone-dependent carcinomas (110). Other MMPs, such as MMP-3, -9, -11, -12, and -19, have dual functions in cancer progression, being associated with both favorable and bad prognosis (80).

6. Conclusions

In summary, metalloproteases comprise a diverse and complex group of hydrolytic enzymes that participate in almost every biochemical process of the cell and in the tissue homeostasis and physiology of pluricellular organisms. In particular, three groups of metalloproteases, MMPs, ADAMs, and ADAMTSs, have been subjected to intensive research as a consequence of their wide presence in mammals and their important roles in normal

physiology and in pathogenic processes, including cancer and arthritis. Accumulative discoveries have revealed the enormous complexity of these three families, which makes it necessary to adopt a global perspective for their study, including the analysis of their inhibitors and regulatory elements. Therefore, it will be necessary to combine classical molecular tools with high-throughput degradomic approaches to shed new light in the functional roles of these proteolytic enzymes in physiology and disease.

Acknowledgments

We thank all members of our group for helpful comments and advice. Our work is supported by grants from Ministerio de Educación y Ciencia-Spain, Fundación Lilly, Fundación La Caixa; Fundación "M. Botín"; and the European Union (FP7). The Instituto Universitario de Oncología is supported by Obra Social Cajastur-Asturias, Spain.

References

1. Lopez-Otin, C. and Overall, C. M. (2002) Protease degradomics: a new challenge for proteomics. *Nat Rev Mol Cell Biol* **3**, 509–519.
2. Puente, X. S., Sanchez, L. M., Overall, C. M., and Lopez-Otin, C. (2003) Human and mouse proteases: a comparative genomic approach. *Nat Rev Genet* **4**, 544–558.
3. Puente, X. S., Gutierrez-Fernandez, A., Ordonez, G. R., Hillier, L. W., and Lopez-Otin, C. (2005) Comparative genomic analysis of human and chimpanzee proteases. *Genomics* **86**, 638–647.
4. Ordoñez, G. R., Hillier, L. W., Warren, W. C., Grützner, F., Lopez-Otin, C., and Puente, X. S. (2008) Loss of genes implicated in gastric function during platypus evolution. *Genome Biol* **9**, R81.
5. Shah, P. K., Tripathi, L. P., Jensen, L. J., Gahnim, M., Mason, C., Furlong, E. E., Rodrigues, V., White, K. P., Bork, P., and Sowdhamini, R. (2008) Enhanced function annotations for Drosophila serine proteases: a case study for systematic annotation of multimember gene families. *Gene* **407**, 199–215.
6. Garcia-Lorenzo, M., Sjodin, A., Jansson, S., and Funk, C. (2006) Protease gene families in Populus and Arabidopsis. *BMC Plant Biol* **6**, 30.
7. Kinch, L. N., Ginalski, K., and Grishin, N. V. (2006) Site-2 protease regulated intramembrane proteolysis: sequence homologs suggest an ancient signaling cascade. *Protein Sci* **15**, 84–93.
8. Brown, M. S. and Goldstein, J. L. (1999) A proteolytic pathway that controls the cholesterol content of membranes, cells, and blood. *Proc Natl Acad Sci U S A* **96**, 11041–11048.
9. Rawlings, N. D. and Barrett, A. J. (1995) Evolutionary families of metallopeptidases. *Methods Enzymol* **248**, 183–228.
10. Reznik, S. E. and Fricker, L. D. (2001) Carboxypeptidases from A to z: implications in embryonic development and Wnt binding. *Cell Mol Life Sci* **58**, 1790–1804.
11. Arolas, J. L., Vendrell, J., Aviles, F. X., and Fricker, L. D. (2007) Metallocarboxypeptidases: emerging drug targets in biomedicine. *Curr Pharm Des* **13**, 349–366.
12. Ambroggio, X. I., Rees, D. C., and Deshaies, R. J. (2004) JAMM: a metalloprotease-like zinc site in the proteasome and signalosome. *PLoS Biol* **2**, E2.
13. Bochtler, M., Odintsov, S. G., Marcyjaniak, M., and Sabala, I. (2004) Similar active sites in lysostaphins and D-Ala-D-Ala metallopeptidases. *Protein Sci* **13**, 854–861.
14. Matsui, M., Fowler, J. H., and Walling, L. L. (2006) Leucine aminopeptidases: diversity in structure and function. *Biol Chem* **387**, 1535–1544.

15. Holz, R. C., Bzymek, K. P., and Swierczek, S. I. (2003) Co-catalytic metallopeptidases as pharmaceutical targets. *Curr Opin Chem Biol* **7**, 197–206.
16. Leopoldini, M., Russo, N., and Toscano, M. (2007) Which one among Zn(II), Co(II), Mn(II), and Fe(II) is the most efficient ion for the methionine aminopeptidase catalyzed reaction? *J Am Chem Soc* **129**, 7776–7784.
17. Fushimi, N., Ee, C. E., Nakajima, T., and Ichishima, E. (1999) Aspzincin, a family of metalloendopeptidases with a new zinc-binding motif. Identification of new zinc-binding sites (His(128), His(132), and Asp(164)) and three catalytically crucial residues (Glu(129), Asp(143), and Tyr(106)) of deuterolysin from Aspergillus oryzae by site-directed mutagenesis. *J Biol Chem* **274**, 24195–24201.
18. Bode, W., Gomis-Ruth, F. X., and Stockler, W. (1993) Astacins, serralysins, snake venom and matrix metalloproteinases exhibit identical zinc-binding environments (HEXXHXXGXXH and Met-turn) and topologies and should be grouped into a common family, the 'metzincins'. *FEBS Lett* **331**, 134–140.
19. Hooper, N. M. (1994) Families of zinc metalloproteases. *FEBS Lett* **354**, 1–6.
20. Gomis-Ruth, F. X. (2003) Structural aspects of the metzincin clan of metalloendopeptidases. *Mol Biotechnol* **24**, 157–202.
21. Albiston, A. L., Ye, S., and Chai, S. Y. (2004) Membrane bound members of the M1 family: more than aminopeptidases. *Protein Pept Lett* **11**, 491–500.
22. Danilczyk, U., Eriksson, U., Crackower, M. A., and Penninger, J. M. (2003) A story of two ACEs. *J Mol Med* **81**, 227–234.
23. Lim, E. J., Sampath, S., Coll-Rodriguez, J., Schmidt, J., Ray, K., and Rodgers, D. W. (2007) Swapping the substrate specificities of the neuropeptidases neurolysin and thimet oligopeptidase. *J Biol Chem* **282**, 9722–9732.
24. Chew, A., Buck, E. A., Peretz, S., Sirugo, G., Rinaldo, P., and Isaya, G. (1997) Cloning, expression, and chromosomal assignment of the human mitochondrial intermediate peptidase gene (MIPEP). *Genomics* **40**, 493–496.
25. Turner, A. J., Isaac, R. E., and Coates, D. (2001) The neprilysin (NEP) family of zinc metalloendopeptidases: genomics and function. *Bioessays* **23**, 261–269.
26. Koppen, M. and Langer, T. (2007) Protein degradation within mitochondria: versatile activities of AAA proteases and other peptidases. *Crit Rev Biochem Mol Biol* **42**, 221–242.
27. Pendas, A. M., Zhou, Z., Cadinanos, J., Freije, J. M., Wang, J., Hultenby, K., Astudillo, A., Wernerson, A., Rodriguez, F., Tryggvason, K., and Lopez-Otin, C. (2002) Defective prelamin A processing and muscular and adipocyte alterations in Zmpste24 metalloproteinase-deficient mice. *Nat Genet* **31**, 94–99.
28. Navarro, C. L., Cadinanos, J., De Sandre-Giovannoli, A., Bernard, R., Courrier, S., Boccaccio, I., Boyer, A., Kleijer, W. J., Wagner, A., Giuliano, F., Beemer, F. A., Freije, J. M., Cau, P., Hennekam, R. C., Lopez-Otin, C., Badens, C., and Levy, N. (2005) Loss of ZMPSTE24 (FACE-1) causes autosomal recessive restrictive dermopathy and accumulation of Lamin A precursors. *Hum Mol Genet* **14**, 1503–1513.
29. Varela, I., Cadinanos, J., Pendas, A. M., Gutierrez-Fernandez, A., Folgueras, A. R., Sanchez, L. M., Zhou, Z., Rodriguez, F. J., Stewart, C. L., Vega, J. A., Tryggvason, K., Freije, J. M., and Lopez-Otin, C. (2005) Accelerated ageing in mice deficient in Zmpste24 protease is linked to p53 signalling activation. *Nature* **437**, 564–568.
30. Ramirez, C. L., Cadinanos, J., Varela, I., Freije, J. M., and Lopez-Otin, C. (2007) Human progeroid syndromes, aging and cancer: new genetic and epigenetic insights into old questions. *Cell Mol Life Sci* **64**, 155–170.
31. Hase, C. C. and Finkelstein, R. A. (1993) Bacterial extracellular zinc-containing metalloproteases. *Microbiol Rev* **57**, 823–837.
32. Harrington, D. J. (1996) Bacterial collagenases and collagen-degrading enzymes and their potential role in human disease. *Infect Immun* **64**, 1885–1891.
33. Markaryan, A., Morozova, I., Yu, H., and Kolattukudy, P. E. (1994) Purification and characterization of an elastinolytic metalloprotease from Aspergillus fumigatus and immunoelectron microscopic evidence of secretion of this enzyme by the fungus invading the murine lung. *Infect Immun* **62**, 2149–2157.
34. Jousson, O., Lechenne, B., Bontems, O., Capoccia, S., Mignon, B., Barblan, J., Quadroni, M., and Monod, M. (2004) Multiplication of an ancestral gene encoding secreted fungalysin preceded species differentiation in the dermatophytes Trichophyton and Microsporum. *Microbiology* **150**, 301–310.
35. Kosowska, K., Reinholdt, J., Rasmussen, L. K., Sabat, A., Potempa, J., Kilian, M., and Poulsen, K. (2002) The Clostridium ramosum IgA proteinase represents a novel type

of metalloendopeptidase. *J Biol Chem* **277**, 11987–11994.
36. Stocker, W., Grams, F., Baumann, U., Reinemer, P., Gomis-Ruth, F. X., McKay, D. B., and Bode, W. (1995) The metzincins – topological and sequential relations between the astacins, adamalysins, serralysins, and matrixins (collagenases) define a superfamily of zinc-peptidases. *Protein Sci* **4**, 823–840.
37. Diaz-Perales, A., Quesada, V., Peinado, J. R., Ugalde, A. P., Alvarez, J., Suarez, M. F., Gomis-Ruth, F. X., and Lopez-Otin, C. (2005) Identification and characterization of human archaemetzincin-1 and -2, two novel members of a family of metalloproteases widely distributed in Archaea. *J Biol Chem* **280**, 30367–30375.
38. Quesada, V., Sanchez, L. M., Alvarez, J., and Lopez-Otin, C. (2004) Identification and characterization of human and mouse ovastacin: a novel metalloproteinase similar to hatching enzymes from arthropods, birds, amphibians, and fish. *J Biol Chem* **279**, 26627–26634.
39. Bond, J. S. and Beynon, R. J. (1995) The astacin family of metalloendopeptidases. *Protein Sci* **4**, 1247–1261.
40. Hopkins, D. R., Keles, S., and Greenspan, D. S. (2007) The bone morphogenetic protein 1/Tolloid-like metalloproteinases. *Matrix Biol* **26**, 508–523.
41. Angerer, L., Hussain, S., Wei, Z., and Livingston, B. T. (2006) Sea urchin metalloproteases: a genomic survey of the BMP-1/tolloid-like, MMP and ADAM families. *Dev Biol* **300**, 267–281.
42. McCoy, A. J., Liu, H., Falla, T. J., and Gunn, J. S. (2001) Identification of Proteus mirabilis mutants with increased sensitivity to antimicrobial peptides. *Antimicrob Agents Chemother* **45**, 2030–2037.
43. Kida, Y., Inoue, H., Shimizu, T., and Kuwano, K. (2007) Serratia marcescens serralysin induces inflammatory responses through protease-activated receptor 2. *Infect Immun* **75**, 164–174.
44. Driscoll, J. A., Brody, S. L., and Kollef, M. H. (2007) The epidemiology, pathogenesis and treatment of Pseudomonas aeruginosa infections. *Drugs* **67**, 351–368.
45. Matheson, N. R., Potempa, J., and Travis, J. (2006) Interaction of a novel form of Pseudomonas aeruginosa alkaline protease (aeruginolysin) with interleukin-6 and interleukin-8. *Biol Chem* **387**, 911–915.
46. Grandvalet, C., Gominet, M., and Lereclus, D. (2001) Identification of genes involved in the activation of the Bacillus thuringiensis inhA metalloprotease gene at the onset of sporulation. *Microbiology* **147**, 1805–1813.
47. Gelb, M. H. and Hol, W. G. (2002) Parasitology. Drugs to combat tropical protozoan parasites. *Science* **297**, 343–344.
48. Grandgenett, P. M., Otsu, K., Wilson, H. R., Wilson, M. E., and Donelson, J. E. (2007) A function for a specific zinc metalloprotease of African trypanosomes. *PLoS Pathog* **3**, 1432–1445.
49. Yao, C., Donelson, J. E., and Wilson, M. E. (2003) The major surface protease (MSP or GP63) of Leishmania sp. Biosynthesis, regulation of expression, and function. *Mol Biochem Parasitol* **132**, 1–16.
50. McHugh, B., Krause, S. A., Yu, B., Deans, A. M., Heasman, S., McLaughlin, P., and Heck, M. M. (2004) Invadolysin: a novel, conserved metalloprotease links mitotic structural rearrangements with cell migration. *J Cell Biol* **167**, 673–686.
51. Ramos, O. H. and Selistre-de-Araujo, H. S. (2006) Snake venom metalloproteases – structure and function of catalytic and disintegrin domains. *Comp Biochem Physiol C Toxicol Pharmacol* **142**, 328–346.
52. Milla, M. E., Leesnitzer, M. A., Moss, M. L., Clay, W. C., Carter, H. L., Miller, A. B., Su, J. L., Lambert, M. H., Willard, D. H., Sheeley, D. M., Kost, T. A., Burkhart, W., Moyer, M., Blackburn, R. K., Pahel, G. L., Mitchell, J. L., Hoffman, C. R., and Becherer, J. D. (1999) Specific sequence elements are required for the expression of functional tumor necrosis factor-alpha-converting enzyme (TACE). *J Biol Chem* **274**, 30563–30570.
53. Hougaard, S., Loechel, F., Xu, X., Tajima, R., Albrechtsen, R., and Wewer, U. M. (2000) Trafficking of human ADAM 12-L: retention in the trans-Golgi network. *Biochem Biophys Res Commun* **275**, 261–267.
54. Puente, X. S. and Lopez-Otin, C. (2004) A genomic analysis of rat proteases and protease inhibitors. *Genome Res* **14**, 609–622.
55. Sagane, K., Yamazaki, K., Mizui, Y., and Tanaka, I. (1999) Cloning and chromosomal mapping of mouse ADAM11, ADAM22 and ADAM23. *Gene* **236**, 79–86.
56. Seals, D. F. and Courtneidge, S. A. (2003) The ADAMs family of metalloproteases: multidomain proteins with multiple functions. *Genes Dev* **17**, 7–30.
57. Zheng, Y., Saftig, P., Hartmann, D., and Blobel, C. (2004) Evaluation of the contribution of different ADAMs to tumor necrosis factor alpha (TNFalpha) shedding and of the function of the TNFalpha ectodomain in ensuring selective stimulated shedding by the

TNFalpha convertase (TACE/ADAM17). *J Biol Chem* **279**, 42898–42906.
58. Kurisaki, T., Masuda, A., Sudo, K., Sakagami, J., Higashiyama, S., Matsuda, Y., Nagabukuro, A., Tsuji, A., Nabeshima, Y., Asano, M., Iwakura, Y., and Sehara-Fujisawa, A. (2003) Phenotypic analysis of Meltrin alpha (ADAM12)-deficient mice: involvement of Meltrin alpha in adipogenesis and myogenesis. *Mol Cell Biol* **23**, 55–61.
59. Huovila, A. P., Turner, A. J., Pelto-Huikko, M., Karkkainen, I., and Ortiz, R. M. (2005) Shedding light on ADAM metalloproteinases. *Trends Biochem Sci* **30**, 413–422.
60. Loechel, F., Fox, J. W., Murphy, G., Albrechtsen, R., and Wewer, U. M. (2000) ADAM 12-S cleaves IGFBP-3 and IGFBP-5 and is inhibited by TIMP-3. *Biochem Biophys Res Commun* **278**, 511–515.
61. Hartmann, D., de Strooper, B., Serneels, L., Craessaerts, K., Herreman, A., Annaert, W., Umans, L., Lubke, T., Lena Illert, A., von Figura, K., and Saftig, P. (2002) The disintegrin/metalloprotease ADAM 10 is essential for Notch signalling but not for alpha-secretase activity in fibroblasts. *Hum Mol Genet* **11**, 2615–2624.
62. Maretzky, T., Reiss, K., Ludwig, A., Buchholz, J., Scholz, F., Proksch, E., de Strooper, B., Hartmann, D., and Saftig, P. (2005) ADAM10 mediates E-cadherin shedding and regulates epithelial cell-cell adhesion, migration, and beta-catenin translocation. *Proc Natl Acad Sci U S A* **102**, 9182–9187.
63. Beck, V., Herold, H., Benge, A., Luber, B., Hutzler, P., Tschesche, H., Kessler, H., Schmitt, M., Geppert, H. G., and Reuning, U. (2005) ADAM15 decreases integrin alphavbeta3/vitronectin-mediated ovarian cancer cell adhesion and motility in an RGD-dependent fashion. *Int J Biochem Cell Biol* **37**, 590–603.
64. Nishimura, H., Myles, D. G., and Primakoff, P. (2007) Identification of an ADAM2-ADAM3 complex on the surface of mouse testicular germ cells and cauda epididymal sperm. *J Biol Chem* **282**, 17900–17907.
65. Cal, S., Freije, J. M., Lopez, J. M., Takada, Y., and Lopez-Otin, C. (2000) ADAM 23/MDC3, a human disintegrin that promotes cell adhesion via interaction with the alphavbeta3 integrin through an RGD-independent mechanism. *Mol Biol Cell* **11**, 1457–1469.
66. Ohtsu, H., Dempsey, P. J., and Eguchi, S. (2006) ADAMs as mediators of EGF receptor transactivation by G protein-coupled receptors. *Am J Physiol Cell Physiol* **291**, C1–C10.
67. Rocks, N., Paulissen, G., El Hour, M., Quesada, F., Crahay, C., Gueders, M., Foidart, J. M., Noel, A., and Cataldo, D. (2007) Emerging roles of ADAM and ADAMTS metalloproteinases in cancer. *Biochimie* 90(2), 369–379.
68. Llamazares, M., Cal, S., Quesada, V., and Lopez-Otin, C. (2003) Identification and characterization of ADAMTS-20 defines a novel subfamily of metalloproteinases-disintegrins with multiple thrombospondin-1 repeats and a unique GON domain. *J Biol Chem* **278**, 13382–13389.
69. Cal, S., Obaya, A. J., Llamazares, M., Garabaya, C., Quesada, V., and Lopez-Otin, C. (2002) Cloning, expression analysis, and structural characterization of seven novel human ADAMTSs, a family of metalloproteinases with disintegrin and thrombospondin-1 domains. *Gene* **283**, 49–62.
70. Porter, S., Clark, I. M., Kevorkian, L., and Edwards, D. R. (2005) The ADAMTS metalloproteinases. *Biochem J* **386**, 15–27.
71. Hashimoto, G., Shimoda, M., and Okada, Y. (2004) ADAMTS4 (aggrecanase-1) interaction with the C-terminal domain of fibronectin inhibits proteolysis of aggrecan. *J Biol Chem* **279**, 32483–32491.
72. Little, C. B., Meeker, C. T., Golub, S. B., Lawlor, K. E., Farmer, P. J., Smith, S. M., and Fosang, A. J. (2007) Blocking aggrecanase cleavage in the aggrecan interglobular domain abrogates cartilage erosion and promotes cartilage repair. *J Clin Invest* **117**, 1627–1636.
73. Colige, A., Nuytinck, L., Hausser, I., van Essen, A. J., Thiry, M., Herens, C., Ades, L. C., Malfait, F., Paepe, A. D., Franck, P., Wolff, G., Oosterwijk, J. C., Smitt, J. H., Lapiere, C. M., and Nusgens, B. V. (2004) Novel types of mutation responsible for the dermatosparactic type of Ehlers-Danlos syndrome (Type VIIC) and common polymorphisms in the ADAMTS2 gene. *J Invest Dermatol* **123**, 656–663.
74. Dagoneau, N., Benoist-Lasselin, C., Huber, C., Faivre, L., Megarbane, A., Alswaid, A., Dollfus, H., Alembik, Y., Munnich, A., Legeai-Mallet, L., and Cormier-Daire, V. (2004) ADAMTS10 mutations in autosomal recessive Weill-Marchesani syndrome. *Am J Hum Genet* **75**, 801–806.
75. Rao, C., Foernzler, D., Loftus, S. K., Liu, S., McPherson, J. D., Jungers, K. A., Apte, S. S., Pavan, W. J., and Beier, D. R. (2003) A defect in a novel ADAMTS family member is the cause of the belted white-spotting mutation. *Development* **130**, 4665–4672.

76. Jungers, K. A., Le Goff, C., Somerville, R. P., and Apte, S. S. (2005) Adamts9 is widely expressed during mouse embryo development. *Gene Expr Patterns* **5**, 609–617.
77. Levy, G. G., Nichols, W. C., Lian, E. C., Foroud, T., McClintick, J. N., McGee, B. M., Yang, A. Y., Siemieniak, D. R., Stark, K. R., Gruppo, R., Sarode, R., Shurin, S. B., Chandrasekaran, V., Stabler, S. P., Sabio, H., Bouhassira, E. E., Upshaw, J. D., Jr., Ginsburg, D., and Tsai, H. M. (2001) Mutations in a member of the ADAMTS gene family cause thrombotic thrombocytopenic purpura. *Nature* **413**, 488–494.
78. Luque, A., Carpizo, D. R., and Iruela-Arispe, M. L. (2003) ADAMTS1/METH1 inhibits endothelial cell proliferation by direct binding and sequestration of VEGF165. *J Biol Chem* **278**, 23656–23665.
79. Llamazares, M., Obaya, A. J., Moncada-Pazos, A., Heljasvaara, R., Espada, J., Lopez-Otin, C., and Cal, S. (2007) The ADAMTS12 metalloproteinase exhibits anti-tumorigenic properties through modulation of the Ras-dependent ERK signalling pathway. *J Cell Sci* **120**, 3544–3552.
80. Lopez-Otin, C. and Matrisian, L. M. (2007) Emerging roles of proteases in tumour suppression. *Nat Rev Cancer* **7**, 800–808.
81. Folgueras, A. R., Pendas, A. M., Sanchez, L. M., and Lopez-Otin, C. (2004) Matrix metalloproteinases in cancer: from new functions to improved inhibition strategies. *Int J Dev Biol* **48**, 411–424.
82. Overall, C. M. and Lopez-Otin, C. (2002) Strategies for MMP inhibition in cancer: innovations for the post-trial era. *Nat Rev Cancer* **2**, 657–672.
83. Clark, I. M., Swingler, T. E., Sampieri, C. L., and Edwards, D. R. (2007) The regulation of matrix metalloproteinases and their inhibitors. *Int J Biochem Cell Biol* 40(6–7), 1362–1378.
84. Pei, D. and Weiss, S. J. (1995) Furin-dependent intracellular activation of the human stromelysin-3 zymogen. *Nature* **375**, 244–247.
85. Kinoshita, T., Sato, H., Takino, T., Itoh, M., Akizawa, T., and Seiki, M. (1996) Processing of a precursor of 72-kilodalton type IV collagenase/gelatinase A by a recombinant membrane-type 1 matrix metalloproteinase. *Cancer Res* **56**, 2535–2538.
86. Oh, J., Takahashi, R., Kondo, S., Mizoguchi, A., Adachi, E., Sasahara, R. M., Nishimura, S., Imamura, Y., Kitayama, H., Alexander, D. B., Ide, C., Horan, T. P., Arakawa, T., Yoshida, H., Nishikawa, S., Itoh, Y., Seiki, M., Itohara, S., Takahashi, C., and Noda, M. (2001) The membrane-anchored MMP inhibitor RECK is a key regulator of extracellular matrix integrity and angiogenesis. *Cell* **107**, 789–800.
87. Herman, M. P., Sukhova, G. K., Kisiel, W., Foster, D., Kehry, M. R., Libby, P., and Schonbeck, U. (2001) Tissue factor pathway inhibitor-2 is a novel inhibitor of matrix metalloproteinases with implications for atherosclerosis. *J Clin Invest* **107**, 1117–1126.
88. Mott, J. D., Thomas, C. L., Rosenbach, M. T., Takahara, K., Greenspan, D. S., and Banda, M. J. (2000) Post-translational proteolytic processing of procollagen C-terminal proteinase enhancer releases a metalloproteinase inhibitor. *J Biol Chem* **275**, 1384–1390.
89. McCawley, L. J. and Matrisian, L. M. (2001) Matrix metalloproteinases: they're not just for matrix anymore! *Curr Opin Cell Biol* **13**, 534–540.
90. Schonbeck, U., Mach, F., and Libby, P. (1998) Generation of biologically active IL-1 beta by matrix metalloproteinases: a novel caspase-1-independent pathway of IL-1 beta processing. *J Immunol* **161**, 3340–3346.
91. Van Lint, P. and Libert, C. (2007) Chemokine and cytokine processing by matrix metalloproteinases and its effect on leukocyte migration and inflammation. *J Leukoc Biol* **82**, 1375–1381.
92. Sheu, B. C., Hsu, S. M., Ho, H. N., Lien, H. C., Huang, S. C., and Lin, R. H. (2001) A novel role of metalloproteinase in cancer-mediated immunosuppression. *Cancer Res* **61**, 237–242.
93. Imai, K., Hiramatsu, A., Fukushima, D., Pierschbacher, M. D., and Okada, Y. (1997) Degradation of decorin by matrix metalloproteinases: identification of the cleavage sites, kinetic analyses and transforming growth factor-beta1 release. *Biochem J* **322** (Pt 3), 809–814.
94. Whitelock, J. M., Murdoch, A. D., Iozzo, R. V., and Underwood, P. A. (1996) The degradation of human endothelial cell-derived perlecan and release of bound basic fibroblast growth factor by stromelysin, collagenase, plasmin, and heparanases. *J Biol Chem* **271**, 10079–10086.
95. Nakamura, M., Miyamoto, S., Maeda, H., Ishii, G., Hasebe, T., Chiba, T., Asaka, M., and Ochiai, A. (2005) Matrix metalloproteinase-7 degrades all insulin-like growth factor binding proteins and facilitates insulin-like growth factor bioavailability. *Biochem Biophys Res Commun* **333**, 1011–1016.

96. Ii, M., Yamamoto, H., Adachi, Y., Maruyama, Y., and Shinomura, Y. (2006) Role of matrix metalloproteinase-7 (matrilysin) in human cancer invasion, apoptosis, growth, and angiogenesis. *Exp Biol Med (Maywood)* **231**, 20–27.
97. Papagerakis, P., Lin, H. K., Lee, K. Y., Hu, Y., Simmer, J. P., Bartlett, J. D., and Hu, J. C. (2008) Premature stop codon in MMP20 causing amelogenesis imperfecta. *J Dent Res* **87**, 56–59.
98. Kennedy, A. M., Inada, M., Krane, S. M., Christie, P. T., Harding, B., Lopez-Otin, C., Sanchez, L. M., Pannett, A. A., Dearlove, A., Hartley, C., Byrne, M. H., Reed, A. A., Nesbit, M. A., Whyte, M. P., and Thakker, R. V. (2005) MMP13 mutation causes spondyloepimetaphyseal dysplasia, Missouri type (SEMD(MO)). *J Clin Invest* **115**, 2832–2842.
99. Martignetti, J. A., Aqeel, A. A., Sewairi, W. A., Boumah, C. E., Kambouris, M., Mayouf, S. A., Sheth, K. V., Eid, W. A., Dowling, O., Harris, J., Glucksman, M. J., Bahabri, S., Meyer, B. F., and Desnick, R. J. (2001) Mutation of the matrix metalloproteinase 2 gene (MMP2) causes a multicentric osteolysis and arthritis syndrome. *Nat Genet* **28**, 261–265.
100. Wu, E., Mari, B. P., Wang, F., Anderson, I. C., Sunday, M. E., and Shipp, M. A. (2001) Stromelysin-3 suppresses tumor cell apoptosis in a murine model. *J Cell Biochem* **82**, 549–555.
101. Boulay, A., Masson, R., Chenard, M. P., El Fahime, M., Cassard, L., Bellocq, J. P., Sautes-Fridman, C., Basset, P., and Rio, M. C. (2001) High cancer cell death in syngeneic tumors developed in host mice deficient for the stromelysin-3 matrix metalloproteinase. *Cancer Res* **61**, 2189–2193.
102. Noel, A., Jost, M., and Maquoi, E. (2008) Matrix metalloproteinases at cancer tumor-host interface. *Semin Cell Dev Biol* **19**, 52–60.
103. Bergers, G., Brekken, R., McMahon, G., Vu, T. H., Itoh, T., Tamaki, K., Tanzawa, K., Thorpe, P., Itohara, S., Werb, Z., and Hanahan, D. (2000) Matrix metalloproteinase-9 triggers the angiogenic switch during carcinogenesis. *Nat Cell Biol* **2**, 737–744.
104. Hiraoka, N., Allen, E., Apel, I. J., Gyetko, M. R., and Weiss, S. J. (1998) Matrix metalloproteinases regulate neovascularization by acting as pericellular fibrinolysins. *Cell* **95**, 365–377.
105. Koshikawa, N., Giannelli, G., Cirulli, V., Miyazaki, K., and Quaranta, V. (2000) Role of cell surface metalloprotease MT1-MMP in epithelial cell migration over laminin-5. *J Cell Biol* **148**, 615–624.
106. Itoh, T., Tanioka, M., Matsuda, H., Nishimoto, H., Yoshioka, T., Suzuki, R., and Uehira, M. (1999) Experimental metastasis is suppressed in MMP-9-deficient mice. *Clin Exp Metastasis* **17**, 177–181.
107. Gupta, G. P., Nguyen, D. X., Chiang, A. C., Bos, P. D., Kim, J. Y., Nadal, C., Gomis, R. R., Manova-Todorova, K., and Massague, J. (2007) Mediators of vascular remodelling co-opted for sequential steps in lung metastasis. *Nature* **446**, 765–770.
108. Egeblad, M. and Werb, Z. (2002) New functions for the matrix metalloproteinases in cancer progression. *Nat Rev Cancer* **2**, 161–174.
109. Balbin, M., Fueyo, A., Tester, A. M., Pendas, A. M., Pitiot, A. S., Astudillo, A., Overall, C. M., Shapiro, S. D., and Lopez-Otin, C. (2003) Loss of collagenase-2 confers increased skin tumor susceptibility to male mice. *Nat Genet* **35**, 252–257.
110. Savinov, A. Y., Remacle, A. G., Golubkov, V. S., Krajewska, M., Kennedy, S., Duffy, M. J., Rozanov, D. V., Krajewski, S., and Strongin, A. Y. (2006) Matrix metalloproteinase 26 proteolysis of the NH2-terminal domain of the estrogen receptor beta correlates with the survival of breast cancer patients. *Cancer Res* **66**, 2716–2724.

II. Identificación y caracterización de la aminopeptidasa O humana

La búsqueda bioinformática en el genoma humano nos ha permitido clonar y caracterizar un cDNA que codifica una nueva metaloproteasa humana a la que hemos denominado aminopeptidasa O (AP-O) por su similitud en secuencia y actividad enzimática con los miembros de la familia M1 de aminopeptidasas. Mediante análisis Northern de tejidos humanos hemos demostrado que esta nueva aminopeptidasa se expresa de manera predominante en testículos, páncreas, placenta, corazón e hígado. Asimismo, la producción en bacterias del domino catalítico recombinante de la AP-O nos ha permitido confirmar su actividad proteolítica del tipo aminopeptidasa, con preferencia por residuos de arginina. Además, hemos demostrado que la AP-O recombinante es capaz de convertir la angiotensina III en angiotensina IV, un potente péptido del sistema renina-angiotensina que desempeña múltiples acciones en diversos tejidos, incluyendo hígado, corazón y cerebro.

Artículo 2: Araceli Díaz-Perales, Víctor Quesada, Luis María Sánchez, **Alejandro P. Ugalde,** María F. Suárez, Antonio Fueyo y Carlos López-Otín. "Identification of human aminopeptidase O, a novel metalloprotease with structural similarity to aminopeptidase B and leukotriene A4 hydrolase"

J Biol Chem, **280**(14): 14310-14317 (2005)

Aportación personal al trabajo

La realización de este trabajo coincidió con mi llegada al laboratorio y con él comencé a familiarizarme con las técnicas bioquímicas y de biología molecular empleadas para la clonación, producción y análisis de expresión de nuevos genes. En este artículo, participé en la clonación y análisis de expresión, así como en la producción y purificación de la aminopeptidasa-O.

THE JOURNAL OF BIOLOGICAL CHEMISTRY
Vol. 280, No. 14, Issue of April 8, pp. 14310–14317, 2005
Printed in U.S.A.
© 2005 by The American Society for Biochemistry and Molecular Biology, Inc.

Identification of Human Aminopeptidase O, a Novel Metalloprotease with Structural Similarity to Aminopeptidase B and Leukotriene A_4 Hydrolase*

Received for publication, November 23, 2004, and in revised form, January 27, 2005
Published, JBC Papers in Press, February 1, 2005, DOI 10.1074/jbc.M413222200

Araceli Díaz-Perales‡, Víctor Quesada‡, Luis M. Sánchez‡, Alejandro P. Ugalde‡, María F. Suárez‡, Antonio Fueyo§, and Carlos López-Otín‡¶

From the ‡Departamento de Bioquímica y Biología Molecular and §Biología Funcional, Facultad de Medicina, Instituto Universitario de Oncología, Universidad de Oviedo, 33006 Oviedo, Spain

We have cloned and characterized a human brain cDNA encoding a new metalloprotease that has been called aminopeptidase O (AP-O). AP-O exhibits a series of structural features characteristic of aminopeptidases, including a conserved catalytic domain with a zinc-binding site ($HEXXHX_{18}E$) that allows its classification in the M1 family of metallopeptidases or gluzincins. The structural complexity of AP-O is further increased by the presence of an additional C-terminal domain 170 residues long, which is predicted to have an ARM repeat fold originally identified in the *Drosophila* segment polarity gene product Armadillo. This ARM repeat domain is also present in aminopeptidase B, aminopeptidase B-like, and leukotriene A_4 hydrolase and defines a novel subfamily of aminopeptidases that we have called ARM aminopeptidases. Northern blot analysis revealed that AP-O is mainly expressed in the pancreas, placenta, liver, testis, and heart. Human AP-O was produced in *Escherichia coli*, and the purified recombinant protein hydrolyzed synthetic substrates used for assaying aminopeptidase activity. This activity was abolished by general inhibitors of metalloproteases and specific inhibitors of aminopeptidases. Recombinant AP-O also cleaved angiotensin III to generate angiotensin IV, a bioactive peptide of the renin-angiotensin pathway with multiple actions on diverse tissues, including brain, testis, and heart. On the basis of these results we suggest that AP-O could play a role in the proteolytic processing of bioactive peptides in those tissues where it is expressed.

Aminopeptidases are exopeptidases that have the ability to catalyze the hydrolysis of amino acid residues from the N terminus of peptide or protein substrates. These enzymes are widely distributed in multiple organisms from bacteria to human and play essential roles in protein maturation and regulation of the metabolism of bioactive peptides (1, 2). Furthermore, alterations in the function and regulation of aminopeptidases underlie several human diseases, including cancer and cardiovascular disorders (3–5). Among the different families of human aminopeptidases, there has been a growing interest in the analysis of the biological and pathological relevance of members of the M1 family of zinc metallopeptidases or gluzincins (6, 7). To date, 12 members of this family have been identified in human tissues (www.uniovi.es/degradome) (8). Aminopeptidase A (APA or ENPEP) is a type II membrane-bound protease that cleaves N-terminal amino acid residues from peptides such as cholecystokinin-8 and angiotensin II (9, 10) and contributes to the control of blood pressure and angiogenesis (11–13). Aminopeptidase N (APN,[1] ANPEP, or CD13) is also a membrane-bound exopeptidase associated with angiogenesis regulation (14–16) that acts as a receptor for the coronavirus and tumor-homing peptides (17, 18). Aminopeptidase Q (APQ or laeverin) is structurally related to APN and participates in regulation of the extravillous trophoblast invasion of maternal decidual tissues (8, 19). The thyrotropin-releasing hormone degrading ectoenzyme (TRHDE) is found in serum as a soluble enzyme or anchored to the cell surface of neuronal cells and selectively inactivates TRH, a peptide that stimulates hormone secretion from adenohypophyseal cells (20–22). Placental leucine aminopeptidase (PLAP, LNPEP, or IRAP), puromycin-insensitive, leucyl-specific aminopeptidase (PILS-AP, ERAAP, ERAP1, or ARTS1), and leukocyte-derived arginine aminopeptidase (L-RAP, AMPEP, or LPEP) belong to the subfamily of oxytocinases. Placental leucine aminopeptidase is regulated by insulin and degrades peptide hormones such as oxytocin and vasopressin, maintaining homeostasis during pregnancy (23–28). The puromycin-insensitive, leucyl-specific aminopeptidase and the leukocyte-derived arginine aminopeptidase are involved in the N-terminal trimming of major histocompatibility complex class I-presented peptide precursors (29–31) and the shedding of cytokine receptors (32, 33). The puromycin-sensitive aminopeptidase (PSA or NPEPPS) has a broad substrate specificity and is involved in multiple processes including protein turnover, neuropeptide metabolism, cell cycle control, reproduction, and regulation of anxiety and pain (34–38). Leukotriene A_4 hydrolase (LTA4H) and aminopeptidase B (APB or RNPEP) are structurally related and have been linked to inflammatory processes and tumor progression (39–46). Finally, aminopeptidase B-like (APB-L or RNPEPL1) has been identified in the course of global projects of human genome analysis (8, 47), but to date no functional characterization of this enzyme hasbeen provided.

* This work was supported by grants from Comisión Interministerial de Ciencia y Tecnología-Spain, Gobierno del Principado de Asturias, Fundación La Caixa, European Union (FP5 and FP6), and Daiichi Fine Chemical Co, Ltd (Toyama, Japan). The Instituto Universitario de Oncología is supported by Obra Social Cajastur-Asturias and Red de Centros de Cáncer-Instituto Carlos III, Spain. The costs of publication of this article were defrayed in part by the payment of page charges. This article must therefore be hereby marked "*advertisement*" in accordance with 18 U.S.C. Section 1734 solely to indicate this fact.

The nucleotide sequence(s) reported in this paper has been submitted to the GenBank™/EBI Data Bank with accession number(s) AJ560639, AJ810420, and AJ810421.

¶ To whom correspondence should be addressed. Tel.: 34-985-104201; Fax: 34-985-103564; E-mail: clo@uniovi.es.

[1] The abbreviations used are: APN, aminopeptidase N; APB, aminopeptidase B; APB-L, APB-like; AP-O, aminopeptidase O; AMC, 7-amino-4-methylcoumarin; GST, glutathione *S*-transferase; LTA4H, leukotriene A_4 hydrolase; PAP, porcine leucine aminopeptidase; SH3, Src homology 3.

Recently, as part of our studies aimed at trying to get a complete view of the human degradome, the complete set of proteases produced by human tissues (48), we detected a genomic sequence encoding a putative protein with structural similarity to aminopeptidases of the M1 family of metalloenzymes. In this work we report the cloning and characterization of a cDNA coding for this new aminopeptidase that has been tentatively called aminopeptidase O (AP-O). We also examine the distribution of this enzyme in human tissues and perform an analysis of its enzymatic activity on synthetic and endogenous substrates. Finally, we discuss the putative physiological role of this novel enzyme in the processing of bioactive peptides in heart and reproductive tissues.

EXPERIMENTAL PROCEDURES

Materials—Human cDNA libraries and Northern blots containing polyadenylated RNAs from different tissues were from Clontech. Restriction endonucleases and other reagents used for molecular cloning were from Roche Diagnostics. Double-stranded DNA probes were radiolabeled with [α-^{32}P]dCTP (3000 Ci/mmol) from Amersham Biosciences, using a commercial random-priming kit purchased from the same company. Antibodies against GST were developed in our laboratory as described previously (49). The aminopeptidases APN and porcine leucine aminopeptidase (PAP) were obtained from Calbiochem. The fluorogenic aminopeptidase substrates, as well as angiotensins I, II, and III, were purchased from Bachem, and protease inhibitors and AMC were from Sigma.

Bioinformatic Screening of the Human Genome and cDNA Cloning—The BLAST program was used to search public (www.ncbi.nlm.nih.gov) and private (www.celera.com) human genome databases to look for regions with sequence similarity to previously described M1 aminopeptidases. After identification in human chromosome 9q22 of DNA contigs encoding regions similar to the catalytic domain of these enzymes, we designed specific oligonucleotides to PCR amplify a cDNA for this protein using a brain cDNA library. All PCR amplifications were performed in a GeneAmp 2400 PCR system from PerkinElmer Life Sciences. After cloning the amplified PCR products in pUC19, the identity of the products was confirmed by nucleotide sequencing.

Nucleotide Sequence Analysis—Cloned cDNAs were sequenced by the dideoxy chain termination method using the DR Terminator Taq FS kit and an ABI-Prism 310 DNA sequencer (Applied Biosystems). Computer analysis of DNA and protein sequences was performed with the GCG software package of the University or Wisconsin Genetics Computer Group.

RNA Extraction—Samples were homogenized in guanidinium thiocyanate buffer with a blender. Then, a one-tenth volume of sodium acetate 3 M pH 4.0, 1 volume of phenol/water, and 1 volume of chloroform/isoamylic alcohol (1:25) were added. The resulting mixture was centrifuged at 13,000 rpm for 20 min at 4 °C. The aqueous phase was recovered, and 1 volume of cold 2-propanol was added. After centrifugation, the pellet was washed with 70% ethanol.

Northern Blot Analysis—Nylon filters containing 2 μg of poly(A$^+$) RNA from human tissues or 20 μg of total RNA from mouse tissues were prehybridized at 42 °C for 3 h in 50% formamide, 5× SSPE (1× SSPE is 150 mM NaCl, 10 mM NaH_2PO_4, and 1 mM EDTA, pH 7.4), 10× Denhardt's solution, 2% SDS, and 100 μg/ml denatured herring sperm DNA. Then, filters were hybridized with a radiolabeled human AP-O-specific probe (377 bp) containing nucleotides 2101–2477 of the isolated cDNA. Hybridization was performed for 20 h under the same conditions used for prehybridization. Finally, blots were washed once with 2× SSC, 0.05% SDS for 30 min and three times in 0.1× SSC, 0.1% SDS for 30 min at 50 °C and exposed to autoradiography. RNA integrity and loading was assessed by hybridization with probes specific for β-actin or glyceraldehyde-3-phosphate dehydrogenase.

Reverse Transcription PCR—About 1 μg of total RNA extracted from the testes of mice of different ages was used to carry out reverse-transcriptase reactions using the GeneAmp kit from PerkinElmer Life Sciences. A PCR reaction was then performed with the primers 5′-GAAGAGGTGTTTGAAAAGCTTC-3′ and 5′-GGGAGAGAATCACCTCG-3′ for 25 cycles of denaturation (94 °C for 20 s), annealing (62 °C for 20 s), and extension (72 °C for 30 s). As a control, β-actin was PCR-amplified from all samples under the same conditions.

Production, Refolding, and Purification of Recombinant Proteins—A cDNA containing the catalytic domain of AP-O was obtained by PCR amplification using two oligonucleotides containing BamHI and EcoRI sites, respectively, namely 5′-CATGGATCCAATCTGTGTTAAAAGTCGAGGAGG-3′ and 5′-CAGGAATTCCCCTAGCCCTTTAAATAATGCACCTGC-3′ (where the BamHI and EcoRI sites are underlined). The PCR amplifications were performed with 25 cycles of denaturation (95 °C for 15 s), annealing (58 °C for 10 s), and extension (68 °C for 2 min) using the Expand™ Long High Fidelity PCR system. The PCR product was digested with BamHI and EcoRI and cloned between the corresponding sites of the pGEX-5x-2 expression vector (Amersham Biosciences). The resulting construct was transformed into BL21(DE3)-pLysE-competent *Escherichia coli* cells, and expression was induced by the addition of isopropyl-1-thio-β-D-galactopyranoside (final concentration 1 mM), followed by 5 h of incubation at 28 °C. The cells were then harvested by centrifugation, washed with phosphate-buffered saline, and lysed by incubation in phosphate-buffered saline with 100 μg/ml lysozyme, 10 μg/ml DNase, and 0.1% Triton X-100 overnight at 4 °C. The extract was centrifuged, and the pellet was washed three times with phosphate-buffered saline and dissolved in a buffer containing 20 mM Tris, pH 7.4, and 6 M guanidinium chloride. The recombinant protein was refolded at 4 °C in two dialysis steps, first against a buffer containing 50 mM Tris, pH 7.5, 150 mM NaCl, 2 mM dithiothreitol, and 2 M urea for 48 h and twice against 50 mM Tris, pH 7.5, and 150 mM NaCl for 24 h. Refolded protein was purified by affinity chromatography using a glutathione-Sepharose column. The identity of the recombinant proteins was verified by Western blot and in-gel digestion followed by mass spectrometry analysis.

Western Blot Analysis—The supernatant and the pellet of the bacterial extracts were separated in 10% SDS-PAGE. After electrophoresis, gels were electrotransferred onto nitrocellulose filters, and then the filters were blocked with 5% nonfat dried milk in PBT (phosphate-buffered saline with 0.1% Tween 20) and incubated for 1 h with rabbit anti-GST serum diluted 1:1000 in 3% nonfat dried milk in PBT. After three washes with PBT, filters were incubated with horseradish peroxidase-conjugated goat anti-rabbit IgG at a 1:20000 dilution in 1.5% milk in PBT and developed with a West Pico enhanced chemiluminescence kit (Pierce).

In-gel Digestion—Gel bands were manually excised and placed into 0.5-ml tubes. Gel pieces were washed twice with 180 μl of 25 mM ammonium bicarbonate/acetonitrile (70:30), dried at 90 °C, and incubated with 12 μg/ml trypsin (Promega) in 25 mM ammonium bicarbonate. The digestion was allowed to proceed for 4–12 h at 37 °C. The peptide mixture was then desalted by C_{18} reverse phase chromatography (ZipTip, Millipore) and eluted with α-cyano-4-hydroxycinnamic acid in 50% acetonitrile and 0.05% trifluoroacetic acid. In a typical experiment, 1 μl of this solution was analyzed by mass spectrometry.

Mass Spectrometry Analysis—Matrix-assisted laser desorption ionization was performed on a time-of-flight mass spectrometer equipped with a nitrogen laser source (Voyager-DE STR, Applied Biosystems). Data from 50–200 laser shots were collected to produce a mass spectrum.

Enzyme Assays—Enzymatic activity of the purified recombinant human AP-O was assayed using AMC-coupled amino acids (Asp-AMC, Thr-AMC, Leu-AMC, Glu-AMC, His-AMC, Val-AMC, Asn-AMC, Ser-AMC, Ile-AMC, Trp-AMC, Phe-AMC, Ala-AMC, Gln-AMC, Gly-AMC, Lys-AMC, Tyr-AMC, Pro-AMC, Met-AMC, and Arg-AMC). Assays were carried out at 37 °C at a substrate concentration of 5 μM in a buffer containing 50 mM Tris-HCl, 150 mM NaCl, and 0.05% Brij-35, pH 7.5. The fluorometric measurements were made in an LS55 spectrofluorometer from PerkinElmer Life Sciences (λ_{ex} = 360 nm and λ_{em} = 460 nm). The fluorescent signal was calibrated using known concentrations of AMC. For inhibition experiments, the reaction mixture was preincubated for 30 min at 37 °C with *o*-phenanthroline, E-64, 4-(2-aminoethyl)-benzenesulfonyl fluoride, or arphamenine A (20 μM), and the hydrolyzing activity against Arg-AMC was then determined by fluorometric measurements as described above. Kinetic studies were performed using different concentrations of the fluorogenic compounds (0.5–500 μM) in 100 μl of assay buffer containing 5 nM recombinant AP-O or the commercially available aminopeptidases APN and PAP (5 pM), and peptide hydrolysis was measured as the increase in fluorescence at 37 °C over time. Initial velocities were calculated using the analysis package FL WinLab 2.01 (PerkinElmer Life Sciences), and data were fitted to the Michaelis-Menten equation (50) using GraFit v4.0 (Erithacus). Assays with angiotensin peptides were performed by incubation of 2.5 nM refolded AP-O or 2.5 pM APN and PAP with 10 μM angiotensins I, II, or III. Reactions were carried out at 37 °C in a buffer containing 50 mM Tris-HCl and 150 mM NaCl pH 7.5 for 2, 6, and 24 h. Samples were purified using ZipTip and analyzed by mass spectrometry.

FIG. 1. **Sequence and domain structure of human AP-O.** *A*, nucleotide and amino acid sequences of AP-O. The zinc-binding site characteristic of aminopeptidases is highlighted by a *black background*. The complete catalytic domain is shown in *bold*. The GMEN motif and YXKG box are highlighted by *gray backgrounds*. The SH3-like motif is in *italics* and is *underlined*. The C-terminal ARM repeat domain is *underlined*. *B*, graphic representation of the AP-O domain structure showing the LTA4H-like N-terminal domain, the gluzincin catalytic domain, the SH3-like motif, and the ARM domain.

RESULTS

Identification and Characterization of a New Human Aminopeptidase—An extensive search for DNA genomic sequences encoding novel aminopeptidases allowed us to identify a contig in human chromosome 9q22 containing coding information for the putative catalytic domain of a yet uncharacterized metalloprotease. The full-length cDNA for this enzyme was predicted by comparison with the structure of other aminopeptidases and then amplified by PCR experiments. We used specific oligonucleotides to amplify, from a brain cDNA library, a 2.5-kb fragment containing in frame initiator and stop codons. After cloning and sequencing of the PCR-amplified products, we confirmed by conceptual translation that the generated sequence encoded a new protein (Fig. 1) that we tentatively called aminopeptidase O or AP-O.

Computer analysis of the identified amino acid sequence revealed that it contains a large catalytic domain typical of M1 aminopeptidases flanked by N- and C-terminal extensions, which are 150 and 170 residues long, respectively (Fig. 1). Moreover, the C-terminal extension is connected to the catalytic domain through a hydrophobic loop that resembles SH3 domain recognition sequences (51, 52). The N-terminal extension of AP-O is recognized by the InterPro program (www.ebi.ac.uk/interpro) as being similar to the N-terminal domain of LTA4H despite the low percentage of identities between both regions (about 15%). The C-terminal region is recognized by the

A

```
AP-O    : RVFAPVCLTGACQETLLRLIPPCLS--AAHSVLGAHPFSRLDVLIVPANFPSLGMASPHIMFLSQSILTGG--------NHLCGTRLCHEIAHAWFGLAIGARDWTEEWLSEGFATHLE
APB     : RVWAEPCLIDAAK-EYNGVIEEFLA--TGEKLFGPYVWGRYDLLFMPPSFPPFGGMENPCLTFVTPCLLAGD---------RSLADVIIHEISHSWFGNLVTNANWGEFWLNEGFTMYAQ
APB-L   : RVWAEPCLLPTATSKLSGAVEQWLS--AAERLYGPYMWGRYDIVFLPPSFPIVAMENPCLTFIISSILESD---------EFLVIDVIHEVAHSWFGNAVTNATWEEMWLSEGLATYAQ
LTA4H   : LVWSEKEQVEKSAYEFS-ETESMLK--IAEDLGGPYVWGQYDLLVLPPSFPYGGMENPCLTFVTPTLLAGD---------KSLSNVIAHEISHSWTGNLVTNKTWDHFWLNEGHTVYLE
NPEPPS  : RVYT-PVGKAE-QGKFALEVAAKTLPFYKDYFNVPYPLPKIDLIAIA-DFAAGAMENWGLVTYRETALLIDPKNSCSSSRQWVALVVGHELAHQWFGNLVTMEWWTHLWLNEGFASWIE
APN     : RIWARPSAIAAGHGDYALNVTGPILNFFAGHYDTPYPLPKSDQIGLP-DFNAGAMENWGLVTYRENSLLFDPLSSSSSNKERVVTVIAHELAHQWFGNLVTIEWWNDLWLNEGFASYVE
AMPEP   : SIYASPDKRNQ--THYALQASLKLLDFYEKYFDIYYPLSKLDLIAIP-DFAPGAMENWGLITYRETSLLFDPKTSSASDKLWVTRVIAHELAHQWFGNLVTMEWWNDIWLKEGFAKYME
PPILS   : SVYAVPDKINQ--ADYALDAAVTLLEFYEDYFSIPYPLPKQDLAAIP-DFQSGAMENWGLTTYRESALLFDAEKSSASSKLGITVTVAHELAHQWFGNLVTMEWWNDLWLNEGFAKFME
LNPEP   : SIYAVPENIGQ--VHYALETTVKLLEFFQNYFEIQYPLKKLDLVAIP-DFEAGAMENWGLLTFREETLLYDSNTSSMADRKLVTKIIAHELAHQWFGNLVTMKWWNDLWLNEGFATFME
APA     : TIYVQPEQKHT--AEYAANITKSVFDYFEEYFAMNYSLPKLDKIAIP-DFGTGAMENWGLITYRETNLLYDPKESASSNQQRVATVVAHELVHQWFGNIVTMDWWEDLWLNEGFASFFE
APQ     : RIWARKDAIANGSADFALNITGPIFSFLEDLFNISYSLPKTDIIALP-SFDNHAMENWGLMIFDESGLLLEPKDQLTEKKTLISYVVSHEIGHQWFGNLVTMNWWNNIWLNEGFASYFE
TRHDE   : RLYARPDAIRRGSGDYALHITKRLIEFYEDYFKVPYSLPKLDLLAVP-KHPYAAMENWGLSIFVEQRILLDPSVSSISYLLDVTMVIVHEICHQWFGDLVTPVWWEDVWLKEGFAHYFE
```

B

```
AP-O    : LLPDQLVLLLEHLLEQKTLSPRTLQSLQRTYH--LQDQDAEVRHRWCELIVKHKFTKAYKSVERFLQED--QAMGVYLYGELMVSEDARQQQLARRCFERTKEQMDRSSAQVVAEML---
APB     : WKTYQLVYFLDKILQKSPLPPGNVKKLGDTYPSISNARNAELRLRWGQIVLKNDHQEDFWKVKEFLHNQGKQKYTLPLYHAMMGGSE-VAQTLAKETFASTASQLHSNVVNYVQQI----
APB-L   : WRTFQTALFLDRLLDGSPLPQEVVMSLSKCYSSLLDSMNAEIRIRWLQIEVRNDYYPDLHRVRRFLESQMSRMYTIPLYEDLCTG---ALKSFALEVFYQTQGRLHPNLRRAIQQIL---
LTA4H   : LSSHQLNEPLAQTLQRAPLPLGHIKRMQEVYN-FNAINNSEIRFRWLRLCIQSKWEDAIPLALKMATEQGRMKFTRPLFKDLAAFD--KSHDQAVRTYQEHKASMHPVTAMLVGKDLKVD
```

FIG. 2. **Amino acid sequence alignment of catalytic and ARM repeat domains of AP-O and related enzymes.** *A*, alignment of amino acid sequences around the zinc-binding site of the catalytic domains of human aminopeptidases. Designations not defined in the abbreviations footnote are as follows: *AMPEP*, leukocyte-derived arginine aminopeptidase; *APA*, aminopeptidase A; *APQ*, aminopeptidase Q; *LNPEP*, placental leucine aminopeptidase; *NPEPPS*, puromycin-sensitive aminopeptidase; *PPILS*, puromycin-insensitive, leucyl-specific aminopeptidase; *TRHDE*, thyrotropin-releasing, hormone-degrading ectoenzyme. *B*, alignment of amino acid sequences of the C-terminal domain of aminopeptidases AP-O, APB, APB-like, and LTA4H. Residues common to all of these aminopeptidases are *shaded gray*. The alignment was performed using ClustalX (version 1.81).

SMART program (smart.embl-heidelberg.de) as an ARM repeat domain. This domain was first recognized in the *Drosophila* segment polarity protein known as Armadillo, but it is also present in other proteins such as β-catenin and the tumor suppressor APC (adenomatous polyposis coli) (53–57). Interestingly, detailed structural analysis of all members of the M1 family of aminopeptidases demonstrated that a similar ARM repeat fold is also predicted in the equivalent regions of APB, APB-L, and LTA4H (Fig. 2). In this latter case, the occurrence of this fold has been confirmed by analysis of the three-dimensional structure of the enzyme (52).

Further comparative analysis of the catalytic domain of AP-O revealed a low overall similarity with other members of the family, the highest percentage of identities being with APB and LTA4H (25 and 21%, respectively) (Fig. 2). Nevertheless, and despite this low level of similarity with other gluzincins, the AP-O catalytic domain contains a series of structural features characteristic of this family of enzymes. Thus, it contains the archetypal metalloprotease zinc-binding site ending in a family-specific Glu residue ($HEXXHX_{18}E$) that acts as the third zinc ligand (Figs. 1 and 2). A series of residues around this zinc-binding site are also conserved in AP-O with respect to those of other aminopeptidases. These conserved amino acids include a Glu residue seven residues downstream of the third zinc ligand that is proposed as contributing to subsite interactions of M1 aminopeptidases with basic substrates (58) (Fig. 2). By contrast, the G(G/A)MENP motif present in the catalytic domain of aminopeptidases (59) is not well conserved in AP-O. The equivalent sequence in AP-O is LGMASP, which lacks the conserved glutamic acid residue reported to be important for the activity of these enzymes (59–62). On the other hand, the catalytic domain of AP-O contains a conserved Tyr at the position 595, included in a YXKG box, which has been implicated in transition state stabilization (58, 60, 63, 64). It is also remarkable that all of the structural features of aminopeptidases found in human AP-O are also present in the sequences deduced for its mouse and rat orthologues, which exhibit 80 and 76% identities with the human enzyme (EMBL accession numbers AJ810420 and AJ810421). Interestingly, no AP-O orthologous sequences were found in *Caenorhabditis elegans* or *Drosophila melanogaster*, suggesting that AP-O may be a protease specific to vertebrates.

It is noteworthy that AP-O lacks any recognizable signal sequence or type II transmembrane domain characteristic of other enzymes of the M1 family of aminopeptidases such as oxytocinases (PLAP, the puromycin-insensitive, leucyl-specific aminopeptidase, and the leukocyte-derived arginine aminopeptidase), the thyrotropin-releasing, hormone-degrading ectoenzyme, the puromycin-sensitive aminopeptidase, aminopeptidase A, and APN. Therefore, we suggest that this novel enzyme is a protease with a domain organization similar to that of other family members such as APB, APB-L, and LTA4H. To further explore the structural and evolutionary relationships between AP-O and other members of the M1 aminopeptidase family, we performed a computational phylogenetic tree analysis (Fig. 3). According to this phylogenetic analysis, together with the exclusive presence of a C-terminal ARM repeat fold in these aminopeptidases, we suggest that APB, APB-L, LTA4H, and AP-O form a defined subfamily of M1 metalloproteases that we propose to call ARM aminopeptidases.

Analysis of Aminopeptidase O Distribution in Human Tissues—To investigate the presence of AP-O mRNA transcripts in human tissues, Northern blots containing poly(A^+) RNAs prepared from a variety of human tissues (leukocytes, colon, small intestine, ovary, testis, prostate, thymus, spleen, pancreas, kidney, liver, lung, placenta, brain, and heart) were hybridized with a specific probe for human AP-O. As can be seen in Fig. 4*A*, AP-O mRNA transcripts are present at low levels in several tissues, being predominantly detected in the pancreas, placenta, liver, testis, and heart. Nevertheless, reverse transcription PCR analysis also revealed the expression of AP-O in a number of additional tissues such as brain, lung, and kidney (data not shown). The two mRNA transcripts of 7.5 and 5 kb observed in some tissues are likely derived from alternative splicing events reported previously to occur in other aminopeptidases (28, 29, 33, 65). The detection of AP-O expression in the heart suggests a potential role for this enzyme in the processing of bioactive peptides that regulate cardiac muscle physiology. Likewise, the expression in testis also suggests that this aminopeptidase could be implicated in reproductive functions as described previously for other family members (42). To further study the putative implication of AP-O in testis development, we analyzed the expression of this gene in samples

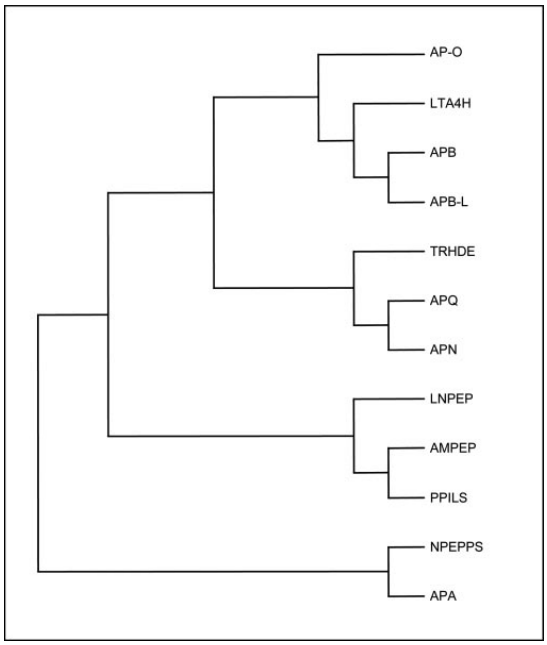

FIG. 3. **Phylogenetic relationships of AP-O and other M1 aminopeptidases.** The sequence of AP-O was aligned to the sequences of the other members of the aminopeptidase family to deduce their phylogenetic relationship. The tree was calculated with the Protpars program of the Phylip program package (version 3.6). *APA*, aminopeptidase A; *APQ*, aminopeptidase Q; *LNPEP*, placental leucine aminopeptidase; *NPEPPS*, puromycin-sensitive aminopeptidase; *PPILS*, puromycin-insensitive, leucyl-specific aminopeptidase; *TRHDE*, thyrotropin-releasing, hormone-degrading ectoenzyme.

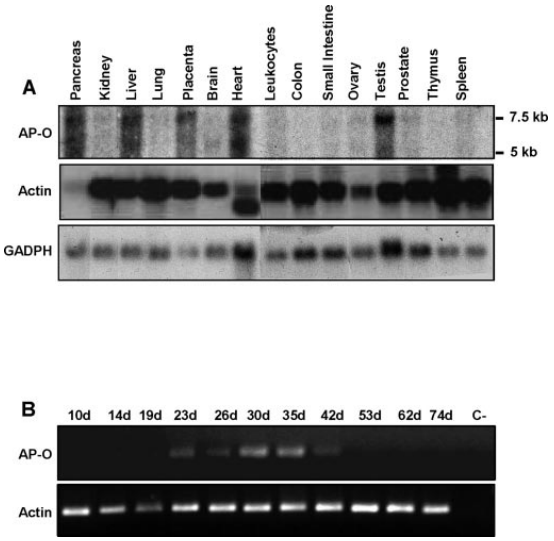

FIG. 4. **Analysis of AP-O expression.** *A*, filters containing ~2 μg of polyadenylated RNAs from human adult tissues were hybridized with a human AP-O-specific probe. Probes for β-actin and glyceraldehyde-3-phosphate dehydrogenase (*GADPH*) were used to assess RNA integrity and equal loading. RNA sizes are indicated in kilobase values. *B*, reverse transcription PCR analysis of testis samples from mice of different ages using specific AP-O primers (*d*, day).

from mice of different ages (from 8 to 74 days). As shown in Fig. 4*B*, AP-O expression was detected in samples from day 23 to day 42, reaching a peak in testis from 30–35-day old mice. This peak of AP-O expression overlaps with the period when mice reach sexual maturity.

Enzymatic Activity of the Recombinant Human Aminopeptidase O—To investigate the enzymatic activity of human AP-O, we produced in *E. coli* a fusion protein containing the putative catalytic domain of the enzyme linked to GST at the N terminus. After isopropyl-1-thio-β-D-galactopyranoside induction of bacterial cells transformed with the plasmid encoding the fusion protein, a band of the expected size (70 kDa) was detected by Western blot analysis of protein extracts with antibodies against GST (Fig. 5*A*). This recombinant GST-aminopeptidase protein was contained in insoluble inclusion bodies, which were solubilized, refolded, and purified by affinity chromatography as described under "Experimental Procedures." As can be seen in Fig. 5*A*, two bands of ~70 and ~30 kDa were detected with anti-GST antibodies in both bacterial extracts and purified recombinant AP-O. To assess the identity of the proteins in these bands, they were digested with trypsin and analyzed by mass spectrometry. The obtained spectra confirmed that the 70-kDa band corresponded to the GST-AP-O fusion protein, whereas the 30-kDa band corresponded to a processed GST-AP-O protein lacking the catalytic site of this enzyme (data not shown).

The recombinant human AP-O was then used in enzymatic assays with fluorescent peptides commonly employed for assaying other aminopeptidases. These assays showed that recombinant AP-O exhibits a significant proteolytic activity against Arg-AMC and, to a lesser extent, against Asn-AMC (Fig. 5*B*). To further characterize this activity, we performed a kinetic analysis of the Arg-AMC proteolysis catalyzed by AP-O (Fig. 5*C*). The fitting of the resulting data to the Michaelis-Menten equation yielded k_{cat} and K_m values of 4×10^{-4} s^{-1} and 6 μM, respectively. Similar experiments with purified APN and PAP showed higher k_{cat} (9 and 7 s^{-1}, respectively) and K_m (140 and 210 μM) values. We then tested the ability of different protease inhibitors to block the enzymatic activity of AP-O. This activity was strongly inhibited by *o*-phenanthroline, a metalloprotease inhibitor, but not by 4-(2-aminoethyl)-benzenesulfonyl fluoride and E-64 (Fig. 5*D*), which are common inhibitors of serine- and cysteine proteases, respectively. Furthermore, AP-O activity was significantly inhibited by arphamenine A, which is a potent inhibitor of aminopeptidases such as APB and LTA4H (66–68), thereby reinforcing the proposal that this new enzyme belongs to this family of metalloproteases.

The expression of the AP-O gene in heart and testis prompted us to evaluate the possibility that this aminopeptidase could participate in the proteolytic processing of peptides involved in the regulation of cardiac and male reproductive physiology (5, 69). To this purpose, we incubated angiotensins I, II, and III with 2.5 nM recombinant AP-O or the commercially available aminopeptidases APN and PAP (2.5 pM), and the resulting fragments were analyzed by mass spectrometry. As shown in Fig. 6*A*, angiotensin III was detected by this method as a 932-Da peak, corresponding to the sequence RVYIHPF. By contrast, incubation with AP-O or APN produced an additional 775-Da peak corresponding to angiotensin IV (VYIHPF) (Fig. 6, *B* and *C*, respectively), although the AP-O-catalyzed reaction was significantly slower. However, PAP failed to hydrolyze angiotensin III (data not shown). Similar experiments using angiotensins I and II yielded no additional peaks when incubated with AP-O (data not shown).

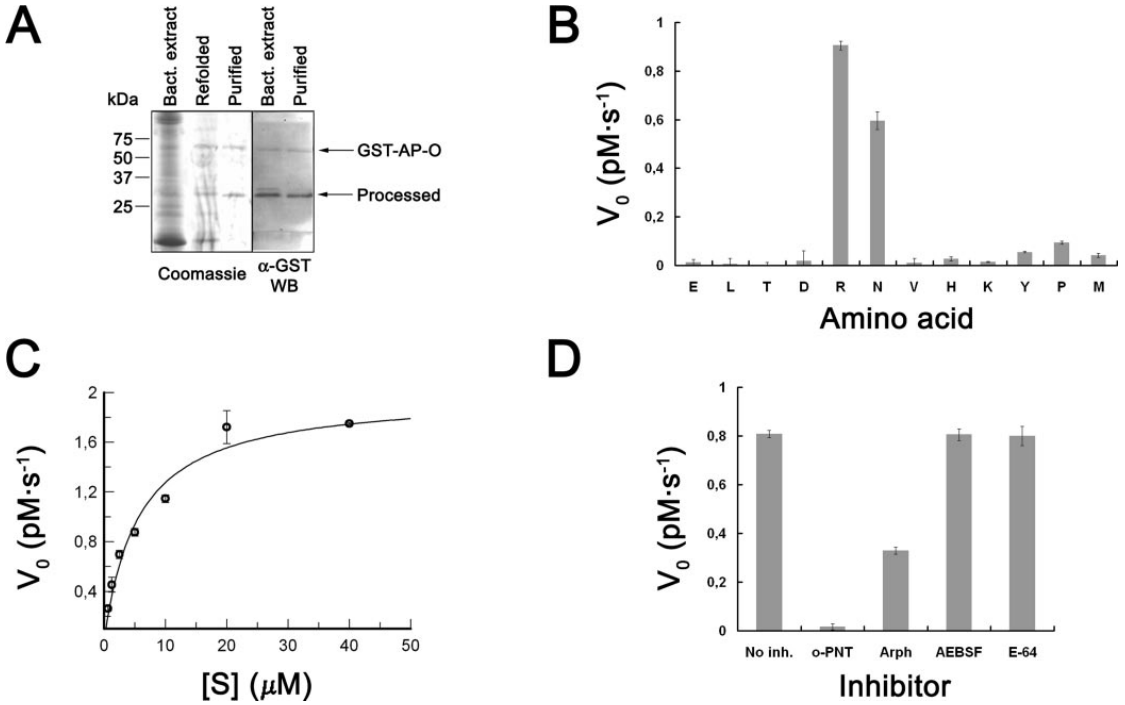

FIG. 5. **Production and enzymatic analysis of recombinant human AP-O.** *A*, a Coomassie Blue-stained SDS-PAGE and a Western blot show the results of the expression, refolding, and purification of the recombinant catalytic domain of human AP-O. 5-μl aliquots of the insoluble fraction of the lysate (*Bact. extract*), the refolded supernatant (*Refolded*), and the refolded purified AP-O (*Purified*) were analyzed in each *lane*. The two *far right lanes* correspond to the Western blot analysis of bacterial pellet and purified AP-O using anti-GST antibodies. The sizes of the molecular size markers are indicated on the *left*. The *upper arrow* on the *right* indicates the position of the fusion protein GST-AP-O. *B,* analysis of the hydrolyzing activity of AP-O using different AMC-bound amino acids. The initial velocity of each reaction (V_0) is represented. *C*, kinetic analysis of the AP-O-catalyzed Arg-AMC proteolysis. Different concentrations of Arg-AMC were incubated with refolded AP-O, and the resulting data were fitted to the Michaelis-Menten equation. *D*, AP-O sensitivity to different inhibitors. Recombinant GST-AP-O was incubated alone (*No inh.*) or in the presence of *o*-phenanthroline (*o-PNT*), arphamenine A (*Arph*), 4-(2-aminoethyl)-benzenesulfonyl fluoride (*AEBSF*), and E-64, and the remaining activity was measured using Arg-AMC as the substrate.

DISCUSSION

In this work we describe the finding in human tissues of a new member of the M1 zinc aminopeptidase family that we have called aminopeptidase O or AP-O. The strategy followed to identify human AP-O was first based on a genomic search of sequences with similarity to those encoding the catalytic domain of known aminopeptidases such as aminopeptidase A, APN, APB, or LTA4H. After the identification of candidate sequences in the human genome and a series of PCR amplification experiments using a cDNA brain library as template, a full-length cDNA coding for human AP-O was finally isolated, cloned, and characterized. Detailed structural analysis of the identified sequence revealed that this protein shows a domain organization characterized by an N-terminal region similar to that present in LTA4H, namely a large catalytic domain, a short SH3 recognition sequence domain, and a C-terminal extension possessing an ARM repeat fold. According to the three-dimensional structural analysis of LTA4H, the N-terminal domain of this enzyme contains a large concave surface exposed to the solvent that could participate in the recognition of specific substrates (52). On the basis of the observed sequence similarity between LTA4H and AP-O at this region, we suggest that the equivalent domain in AP-O plays a similar role. This domain is followed by a typical catalytic domain of the M1-family of zinc-dependent metalloprotease or gluzincins as assessed by the glutamic acid residue located 18 residues C-terminal to the archetypal zinc-binding motif (HE*XX*HX_{18}E). This catalytic domain also contains most of the conserved residues in aminopeptidases that have been linked to substrate recognition and catalysis but lacks specific amino acids such as the Glu residue in the G(G/A)MENP motif, proposed to be important for the catalytic activity of these enzymes (59–62). The catalytic domain of AP-O is followed by a hydrophobic loop that resembles an SH3 domain recognition sequence found in a variety of intracellular or membrane-associated proteins (51). This domain could mediate the putative binding of AP-O with the Pro-rich motifs present in other proteins. Finally, the C-terminal domain of AP-O has been predicted to have an ARM repeat fold. This fold is characterized by a three-dimensional structure containing two layers of parallel α-helices arranged in an antiparallel manner with perpendicular loops containing short helical segments on top (56, 57). This unusual coil of helices seems to be suitable for protein-protein interactions, although it is smaller in aminopeptidases than in other ARM repeat-containing proteins such as Armadillo or HEAT repeats (52). The presence of this ARM domain in AP-O as well as in other aminopeptidases such as LTA4H, APB, and APB-like have prompted us to group these proteins in a novel subfamily of M1-proteases that we have called ARM aminopeptidases.

In this work we have also analyzed the distribution of AP-O in human and mouse tissues. These studies allowed us to detect the expression of the *AP-O* gene in several tissues, mainly in the pancreas, placenta, liver, heart, and testis. This pattern of expression suggests that AP-O is implicated in the develop-

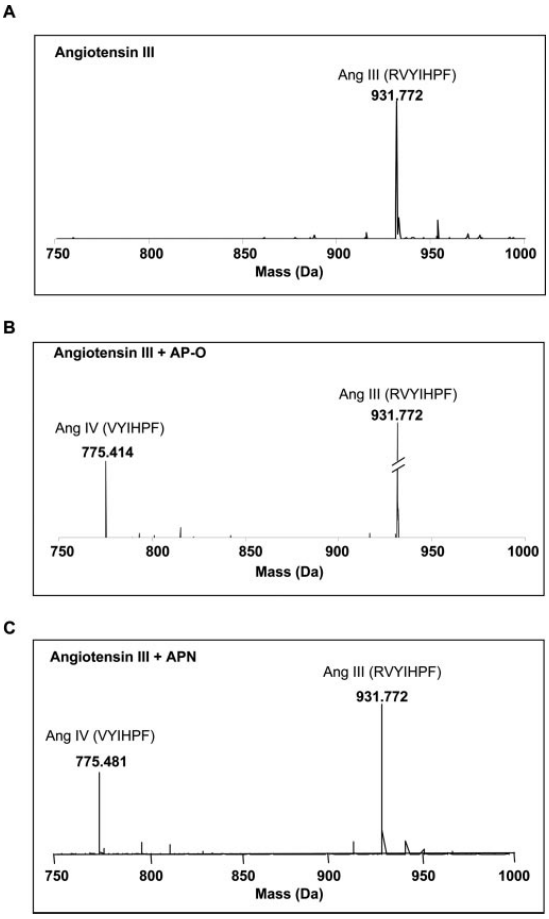

FIG. 6. **Mass spectrometry analysis of the angiotensin III proteolysis catalyzed by AP-O.** Human angiotensin III was incubated alone (*A*) or in the presence of 2.5 nM recombinant GST-AP-O (*B*) or 2.5 pM APN (*C*) for 24 h. The resulting peptide mix was analyzed by mass spectrometry. The peaks corresponding to angiotensin III (*Ang III*) (931.8 Da) and angiotensin IV (*Ang IV*) (775.4 Da) are shown.

ment or physiology of these organs. Interestingly, expression analysis of AP-O in testes from mice of different ages showed a peak of expression in samples from 30–35-day old mice during the sexual maturation stage. This result supports the putative implication of this novel enzyme in testis development as described for APB (42, 70, 71).

To further explore the physiological implications of AP-O, we performed a functional analysis of the recombinant enzyme produced in *E. coli*. This analysis revealed that this protein is a catalytically active aminopeptidase and that this activity is abolished by both general and specific aminopeptidase inhibitors. Remarkably, the preferred substrate of AP-O in these studies was Arg-AMC. This preference for N-terminal Arg residues is similar to that of other aminopeptidases such as APB (39, 46, 68). To further characterize the specificity of AP-O for Arg-AMC, we performed parallel studies with other commercially available aminopeptidases. These studies showed that APN and PAP can also cleave Arg-AMC, although, unlike AP-O, they also cleave Lys-AMC to a similar extent (Fig. 5*B* and data not shown). Interestingly, the K_m value was ~100 times lower in the AP-O-catalyzed Arg-AMC cleavage than in the APN- or PAP-catalyzed reactions. This result would support the possibility that the cleavage of N-terminal Arg residues catalyzed by AP-O could also be of *in vivo* relevance. This possibility, together with the expression of the AP-O gene in the heart and testis, tissues in which the renin-angiotensin system plays important roles (5, 69), prompted us to investigate the putative involvement of AP-O in the processing of peptides of this system. The renin-angiotensin system regulates the homeostasis, blood pressure, endocrine processes, and behavior at the systemic level as well as at the local tissue level (5, 69). Angiotensin peptides derive from a precursor, called angiotensinogen, which is converted to angiotensin I and II by the successive actions of the endopeptidases renin and ACE (angiotensin-converting enzyme). Angiotensin II is an octapeptide involved in homeostasis and hemodynamic processes (72). An aminopeptidase activity, possibly aminopeptidase A (5, 73), converts angiotensin II to angiotensin III, a heptapeptide important in brain and cardiovascular physiology (74). Finally, angiotensin III is converted to angiotensin IV by another aminopeptidase activity (73, 74). Consistent with the specificity of AP-O, this enzyme cleaved the N-terminal residue of angiotensin III *in vitro*, but not that of angiotensin I or II. This finding opens the possibility that AP-O belongs to the group of angiogenic enzymes that play an important role in the biological processes depending on the generation of angiotensin IV in tissues such as brain, testis, and heart (73, 75). However, it must be noticed that AP-O assays were performed with the recombinant catalytic domain of this enzyme, whereas APN and PAP were purified from a natural source. This difference could explain the low k_{cat} value obtained in the AP-O-catalyzed Arg-AMC cleavage, as well as its slow angiotensin III hydrolyzing activity. Thus, further experiments with purified AP-O are required to confirm the putative activity of this enzyme under physiological conditions.

Additionally, AP-O might also process angiogenic peptides as reported previously for other M1 aminopeptidases and have a role in tumor progression (11, 12, 76–78). In this regard, the gene encoding AP-O maps at chromosome 9q22, a region associated with loss of heterozygosity in different malignant tumors including ovarian, bladder, basal cell, and esophageal carcinomas (79–82). Furthermore, 9q22 amplification is associated with cisplatin resistance of human male germ cell tumors (83), whereas a subset of familial colorectal neoplasia kindreds has been linked to 9q22 (84). Unidentified loci located at the region containing AP-O have also been linked to cases of Alzheimer disease (85), schizophrenia (86), and diabetes (87). Finally, duplication of this region leads to learning disability and pyloric stenosis (88). Further studies will be required to ascertain if AP-O could be a direct target of any of these genetic abnormalities resulting in cancer or other pathological conditions.

In summary, we have cloned and characterized AP-O, a novel M1 aminopeptidase that shows a structural organization similar to other members of this group but also shows some structural peculiarities. Notably, we have identified orthologous sequences in mouse and rat, but not in *C. elegans* or *D. melanogaster*, which contain orthologous genes for the remaining members of this aminopeptidase family. We have also shown that AP-O is a proteolytically active enzyme with a profile of activity and sensitivity to inhibitors characteristic of metallopeptidases. The expression of the *AP-O* gene is detected at significant levels in diverse tissues including pancreas, placenta, liver, testis, and heart. Further experimental work, including the generation of mutant mice deficient in this protease, will be necessary to clarify the role of AP-O in physiological processes.

Acknowledgments—We thank Drs. G. Velasco, J. P. Freije, and X. S. Puente for helpful comments and support and S. Álvarez and P. Martín Bringas for excellent technical assistance.

REFERENCES

1. Taylor, A. (1993) *FASEB J.* **7,** 290–298
2. Lowther, W. T., and Matthews, B. W. (2002) *Chem. Rev.* **102,** 4581–4608
3. Nanus, D. M. (2003) *Clin. Cancer Res.* **9,** 6307–6309
4. Sato, Y. (2004) *Biol. Pharm. Bull.* **27,** 772–776
5. Mitsui, T., Nomura, S., Itakura, A., and Mizutani, S. (2004) *Biol. Pharm. Bull.* **27,** 768–771
6. Hooper, N. M. (1994) *FEBS Lett.* **354,** 1–6
7. Gomis-Ruth, F. X. (2003) *Mol. Biotechnol.* **24,** 157–202
8. Puente, X. S., Sanchez, L. M., Overall, C. M., and Lopez-Otin, C. (2003) *Nat. Rev. Genet.* **4,** 544–558
9. Nanus, D. M., Engelstein, D., Gastl, G. A., Gluck, L., Vidal, M. J., Morrison, M., Finstad, C. L., Bander, N. H., and Albino, A. P. (1993) *Proc. Natl. Acad. Sci. U. S. A.* **90,** 7069–7073
10. Zini, S., Fournie-Zaluski, M. C., Chauvel, E., Roques, B. P., Corvol, P., and Llorens-Cortes, C. (1996) *Proc. Natl. Acad. Sci. U. S. A.* **93,** 11968–11973
11. Mitsui, T., Nomura, S., Okada, M., Ohno, Y., Kobayashi, H., Nakashima, Y., Murata, Y., Takeuchi, M., Kuno, N., Nagasaka, T., J, O. W., Cooper, M. D., and Mizutani, S. (2003) *Mol. Med.* **9,** 57–62
12. Marchio, S., Lahdenranta, J., Schlingemann, R. O., Valdembri, D., Wesseling, P., Arap, M. A., Hajitou, A., Ozawa, M. G., Trepel, M., Giordano, R. J., Nanus, D. M., Dijkman, H. B., Oosterwijk, E., Sidman, R. L., Cooper, M. D., Bussolino, F., Pasqualini, R., and Arap, W. (2004) *Cancer Cell* **5,** 151–162
13. Fournie-Zaluski, M. C., Fassot, C., Valentin, B., Djordjijevic, D., Reaux-Le Goazigo, A., Corvol, P., Roques, B. P., and Llorens-Cortes, C. (2004) *Proc. Natl. Acad. Sci. U. S. A.* **101,** 7775–7780
14. Look, A. T., Ashmun, R. A., Shapiro, L. H., and Peiper, S. C. (1989) *J. Clin. Investig.* **83,** 1299–1307
15. Hashida, H., Takabayashi, A., Kanai, M., Adachi, M., Kondo, K., Kohno, N., Yamaoka, Y., and Miyake, M. (2002) *Gastroenterology* **122,** 376–386
16. Petrovic, N., Bhagwat, S. V., Ratzan, W. J., Ostrowski, M. C., and Shapiro, L. H. (2003) *J. Biol. Chem.* **278,** 49358–49368
17. Yeager, C. L., Ashmun, R. A., Williams, R. K., Cardellichio, C. B., Shapiro, L. H., Look, A. T., and Holmes, K. V. (1992) *Nature* **357,** 420–422
18. Pasqualini, R., Koivunen, E., Kain, R., Lahdenranta, J., Sakamoto, M., Stryhn, A., Ashmun, R. A., Shapiro, L. H., Arap, W., and Ruoslahti, E. (2000) *Cancer Res.* **60,** 722–727
19. Fujiwara, H., Higuchi, T., Yamada, S., Hirano, T., Sato, Y., Nishioka, Y., Yoshioka, S., Tatsumi, K., Ueda, M., Maeda, M., and Fujii, S. (2004) *Biochem. Biophys. Res. Commun.* **313,** 962–968
20. Schauder, B., Schomburg, L., Kohrle, J., and Bauer, K. (1994) *Proc. Natl. Acad. Sci. U. S. A.* **91,** 9534–9538
21. Schomburg, L., Turwitt, S., Prescher, G., Lohmann, D., Horsthemke, B., and Bauer, K. (1999) *Eur. J. Biochem.* **265,** 415–422
22. Kelly, J. A., Slator, G. R., Tipton, K. F., Williams, C. H., and Bauer, K. (2000) *J. Biol. Chem.* **275,** 16746–16751
23. Kandror, K. V., Yu, L., and Pilch, P. F. (1994) *J. Biol. Chem.* **269,** 30777–30780
24. Keller, S. R., Scott, H. M., Mastick, C. C., Aebersold, R., and Lienhard, G. E. (1995) *J. Biol. Chem.* **270,** 23612–23618
25. Rogi, T., Tsujimoto, M., Nakazato, H., Mizutani, S., and Tomoda, Y. (1996) *J. Biol. Chem.* **271,** 56–61
26. Keller, S. R., Davis, A. C., and Clairmont, K. B. (2002) *J. Biol. Chem.* **277,** 17677–17686
27. Lew, R. A., Mustafa, T., Ye, S., McDowall, S. G., Chai, S. Y., and Albiston, A. L. (2003) *J. Neurochem.* **86,** 344–350
28. Albiston, A. L., McDowall, S. G., Matsacos, D., Sim, P., Clune, E., Mustafa, T., Lee, J., Mendelsohn, F. A., Simpson, R. J., Connolly, L. M., and Chai, S. Y. (2001) *J. Biol. Chem.* **276,** 48623–48626
29. Serwold, T., Gonzalez, F., Kim, J., Jacob, R., and Shastri, N. (2002) *Nature* **419,** 480–483
30. Saric, T., Chang, S. C., Hattori, A., York, I. A., Markant, S., Rock, K. L., Tsujimoto, M., and Goldberg, A. L. (2002) *Nat. Immunol.* **3,** 1169–1176
31. Tanioka, T., Hattori, A., Masuda, S., Nomura, Y., Nakayama, H., Mizutani, S., and Tsujimoto, M. (2003) *J. Biol. Chem.* **278,** 32275–32283
32. Cui, X., Hawari, F., Alsaaty, S., Lawrence, M., Combs, C. A., Geng, W., Rouhani, F. N., Miskinis, D., and Levine, S. J. (2002) *J. Clin. Investig.* **110,** 515–526
33. Cui, X., Rouhani, F. N., Hawari, F., and Levine, S. J. (2003) *J. Biol. Chem.* **278,** 28677–28685
34. Constam, D. B., Tobler, A. R., Rensing-Ehl, A., Kemler, I., Hersh, L. B., and Fontana, A. (1995) *J. Biol. Chem.* **270,** 26931–26939
35. Huber, G., Thompson, A., Gruninger, F., Mechler, H., Hochstrasser, R., Hauri, H. P., and Malherbe, P. (1999) *J. Neurochem.* **72,** 1215–1223
36. Osada, T., Ikegami, S., Takiguchi-Hayashi, K., Yamazaki, Y., Katoh-Fukui, Y., Higashinakagawa, T., Sakaki, Y., and Takeuchi, T. (1999) *J. Neurosci.* **19,** 6068–6078
37. Osada, T., Watanabe, G., Kondo, S., Toyoda, M., Sakaki, Y., and Takeuchi, T. (2001) *Mol. Endocrinol.* **15,** 960–971
38. Osada, T., Watanabe, G., Sakaki, Y., and Takeuchi, T. (2001) *Mol. Endocrinol.* **15,** 882–893
39. Fukasawa, K. M., Fukasawa, K., Harada, M., Hirose, J., Izumi, T., and Shimizu, T. (1999) *Biochem. J.* **339,** 497–502
40. Funk, C. D., Radmark, O., Fu, J. Y., Matsumoto, T., Jornvall, H., Shimizu, T., and Samuelsson, B. (1987) *Proc. Natl. Acad. Sci. U. S. A.* **84,** 6677–6681
41. Minami, M., Ohno, S., Kawasaki, H., Radmark, O., Samuelsson, B., Jornvall, H., Shimizu, T., Seyama, Y., and Suzuki, K. (1987) *J. Biol. Chem.* **262,** 13873–13876
42. Cadel, S., Foulon, T., Viron, A., Balogh, A., Midol-Monnet, S., Noel, N., and Cohen, P. (1997) *Proc. Natl. Acad. Sci. U. S. A.* **94,** 2963–2968
43. Draoui, M., Bellincampi, L., Hospital, V., Cadel, S., Foulon, T., Prat, A., Barre, N., Reichert, U., Melino, G., and Cohen, P. (1997) *J. Neurooncol.* **31,** 99–106
44. Haeggstrom, J. Z. (2000) *Am. J. Respir. Crit. Care Med.* **161,** S25–S31
45. Chen, X., Li, N., Wang, S., Wu, N., Hong, J., Jiao, X., Krasna, M. J., Beer, D. G., and Yang, C. S. (2003) *J. Natl. Cancer Inst.* **95,** 1053–1061
46. Haeggstrom, J. Z. (2004) *J. Biol. Chem.* **279,** 50639–50642
47. Puente, X. S., and Lopez-Otin, C. (2004) *Genome Res.* **14,** 609–622
48. Lopez-Otin, C., and Overall, C. M. (2002) *Nat. Rev. Mol. Cell Biol.* **3,** 509–519
49. Llamazares, M., Cal, S., Quesada, V., and Lopez-Otin, C. (2003) *J. Biol. Chem.* **278,** 13382–13389
50. Northrop, D. B. (1999) *Adv. Enzymol. Relat. Areas Mol. Biol.* **73,** 25–55
51. Han, L., Wong, D., Dhaka, A., Afar, D., White, M., Xie, W., Herschman, H., Witte, O., and Colicelli, J. (1997) *Proc. Natl. Acad. Sci. U. S. A.* **94,** 4954–4959
52. Thunnissen, M. M., Nordlund, P., and Haeggstrom, J. Z. (2001) *Nat. Struct. Biol.* **8,** 131–135
53. Peifer, M., Orsulic, S., Sweeton, D., and Wieschaus, E. (1993) *Development* **118,** 1191–1207
54. Huber, A. H., Nelson, W. J., and Weis, W. I. (1997) *Cell* **90,** 871–882
55. Groves, M. R., and Barford, D. (1999) *Curr. Opin. Struct. Biol.* **9,** 383–389
56. Andrade, M. A., Petosa, C., O'Donoghue, S. I., Muller, C. W., and Bork, P. (2001) *J. Mol. Biol.* **309,** 1–18
57. Coates, J. C. (2003) *Trends Cell Biol.* **13,** 463–471
58. Thompson, M. W., Govindaswami, M., and Hersh, L. B. (2003) *Arch Biochem. Biophys* **413,** 236–242
59. Luciani, N., Marie-Claire, C., Ruffet, E., Beaumont, A., Roques, B. P., and Fournie-Zaluski, M. C. (1998) *Biochemistry* **37,** 686–692
60. Vazeux, G., Iturrioz, X., Corvol, P., and Llorens-Cortes, C. (1998) *Biochem. J.* **334,** 407–413
61. Laustsen, P. G., Vang, S., and Kristensen, T. (2001) *Eur. J. Biochem.* **268,** 98–104
62. Rudberg, P. C., Tholander, F., Thunnissen, M. M., and Haeggstrom, J. Z. (2002) *J. Biol. Chem.* **277,** 1398–1404
63. Andberg, M. B., Hamberg, M., and Haeggstrom, J. Z. (1997) *J. Biol. Chem.* **272,** 23057–23063
64. Ma, Z., Daquin, A., Yao, J., Rodgers, D., Thompson, M. W., and Hersh, L. B. (2003) *Arch Biochem. Biophys.* **415,** 80–86
65. Keller, S. R. (2004) *Biol. Pharm. Bull.* **27,** 761–764
66. Morty, R. E., and Morehead, J. (2002) *J. Biol. Chem.* **277,** 26057–26065
67. Orning, L., Gierse, J. K., and Fitzpatrick, F. A. (1994) *J. Biol. Chem.* **269,** 11269–11273
68. Petrov, V. V., Fagard, R. H., and Lijnen, P. J. (2004) *Cardiovasc. Res.* **61,** 724–735
69. Leung, P. S., and Sernia, C. (2003) *J. Mol. Endocrinol.* **30,** 263–270
70. Cadel, S., Pierotti, A. R., Foulon, T., Creminon, C., Barre, N., Segretain, D., and Cohen, P. (1995) *Mol. Cell. Endocrinol.* **110,** 149–160
71. Balogh, A., Cadel, S., Foulon, T., Picart, R., Der Garabedian, A., Rousselet, A., Tougard, C., and Cohen, P. (1998) *J. Cell Sci.* **111,** 161–169
72. O'Mahony, O. A., Djahanbahkch, O., Mahmood, T., Puddefoot, J. R., and Vinson, G. P. (2000) *Hum. Reprod.* **15,** 1345–1349
73. von Bohlen und Halbach, O. (2003) *Cell Tissue Res.* **311,** 1–9
74. Lorenzo, O., Ruiz-Ortega, M., Suzuki, Y., Ruperez, M., Esteban, V., Sugaya, T., and Egido, J. (2002) *J. Am. Soc. Nephrol.* **13,** 1162–1171
75. De Godoy, M. A., Dunn, S., and Rattan, S. (2004) *Gastroenterology* **127,** 127–138
76. Bhagwat, S. V., Lahdenranta, J., Giordano, R., Arap, W., Pasqualini, R., and Shapiro, L. H. (2001) *Blood* **97,** 652–659
77. Bhagwat, S. V., Petrovic, N., Okamoto, Y., and Shapiro, L. H. (2003) *Blood* **101,** 1818–1826
78. Oh, P., Li, Y., Yu, J., Durr, E., Krasinska, K. M., Carver, L. A., Testa, J. E., and Schnitzer, J. E. (2004) *Nature* **429,** 629–635
79. Simoneau, M., LaRue, H., Aboulkassim, T. O., Meyer, F., Moore, L., and Fradet, Y. (2000) *Oncogene* **19,** 6317–6323
80. Byrom, J., Mudaliar, V., Redman, C. W., Jones, P., Strange, R. C., and Hoban, P. R. (2004) *Int. J. Oncol.* **24,** 1271–1277
81. Lichun, Y., Ching Tang, C. M., Wai Lau, K., and Lung, M. L. (2004) *Cancer Lett.* **203,** 71–77
82. Obermann, E. C., Meyer, S., Hellge, D., Zaak, D., Filbeck, T., Stoehr, R., Hofstaedter, F., Hartmann, A., and Knuechel, R. (2004) *Oncol. Rep.* **11,** 745–751
83. Rao, P. H., Houldsworth, J., Palanisamy, N., Murty, V. V., Reuter, V. E., Motzer, R. J., Bosl, G. J., and Chaganti, R. S. (1998) *Cancer Res.* **58,** 4260–4263
84. Wiesner, G. L., Daley, D., Lewis, S., Ticknor, C., Platzer, P., Lutterbaugh, J., MacMillen, M., Baliner, B., Willis, J., Elston, R. C., and Markowitz, S. D. (2003) *Proc. Natl. Acad. Sci. U. S. A.* **100,** 12961–12965
85. Blacker, D., Bertram, L., Saunders, A. J., Moscarillo, T. J., Albert, M. S., Wiener, H., Perry, R. T., Collins, J. S., Harrell, L. E., Go, R. C., Mahoney, A., Beaty, T., Fallin, M. D., Avramopoulos, D., Chase, G. A., Folstein, M. F., McInnis, M. G., Bassett, S. S., Doheny, K. J., Pugh, E. W., and Tanzi, R. E. (2003) *Hum. Mol. Genet.* **12,** 23–32
86. Mowry, B. J., Ewen, K. R., Nancarrow, D. J., Lennon, D. P., Nertney, D. A., Jones, H. L., O'Brien, M. S., Thornley, C. E., Walters, M. K., Crowe, R. R., Silverman, J. M., Endicott, J., Sharpe, L., Hayward, N. K., Gladis, M. M., Foote, S. J., and Levinson, D. F. (2000) *Am. J. Med. Genet.* **96,** 864–869
87. Kim, S. H., Ma, X., Klupa, T., Powers, C., Pezzolesi, M., Warram, J. H., Rich, S. S., Krolewski, A. S., and Doria, A. (2003) *Diabetes* **52,** 2182–2186
88. Maraschio, P., Maserati, E., Seghezzi, L., Tupler, R., Verri, M. P., and Tiepolo, L. (1998) *Clin. Genet.* **54,** 159–160

III. Aminopeptidasa O

El libro Handbook of Proteolytic Enzymes editado por Alan J. Barrett, J. Fred Woessner y Neil D. Rawlings es una obra de referencia en la investigación de los sistemas proteolíticos que recoge una exhaustiva y actualizada descripción del conjunto de enzimas proteolíticos. A través de este capítulo, hemos contribuido a la elaboración de la tercera edición de este libro mediante la realización de una revisión actualizada de los conocimientos acumulados acerca de la aminopeptidasa O. Aunque existe escasa información sobre su relevancia funcional, la combinación de nuestros datos y la de trabajos posteriores, sugiere que la AP-O podría desempeñar un papel en la fisiología cardiaca, así como en la homeostasis de la vasculatura de otros órganos, mediante el procesamiento de péptidos biológicamente activos como la angiotensina.

Artículo 3: **Alejandro P. Ugalde,** Araceli Díaz Perales y Carlos López-Otín. "Aminopeptidase-O"

Handbook of Proteolytic Enzymes, 3ª edición. Editores: A. J. Barrett, N. D. Rawlings and J. F. Woessner. Editorial Academic Press (Londres); 2011 (en prensa).

Aportación personal al trabajo

En este trabajo realicé la tarea de recopilar y organizar la información disponible acerca de la aminopeptidasa-O. Asimismo, participé en la elaboración del manuscrito y las figuras bajo la supervisión de la Dra. Araceli Díaz Perales y el Dr. Carlos López-Otín.

AMINOPEPTIDASE O

Alejandro P. Ugalde, Araceli Díaz-Perales and Carlos López-Otín*

Alejandro Piñeiro Ugalde: Departamento de Bioquímica y Biología Molecular, Instituto Universitario de Oncología, Universidad de Oviedo. 33006 - Oviedo, Spain. Phone: +34 985 104 202, Fax: +34 985 103 564.
Email: pineiroalejandro@uniovi.es

Araceli Díaz-Perales: Unidad de Bioquímica, Departamento de Biotecnología, E.T.S. Ingenieros Agrónomos, Universidad Politécnica– Madrid, Spain. Phone: +34 913 365 760, Fax: +34 913 365 757.
Email: araceli.diaz@upm.es

*Corresponding autor: Departamento de Bioquímica y Biología Molecular, Instituto Universitario de Oncología, Universidad de Oviedo. 33006 - Oviedo, Spain. Phone: +34 985 104 201, Fax: +34 985 103 564.
Email: clo@uniovi.es

Glossary

UTR (untranslated region): non-coding sequences present in the 5' or 3' regions of mature mRNAs

Pseudogene: DNA sequence resembling a gene but lacking its genetic function

Proteasome: cytoplasmic protein complex responsible of cell protein turnover

Epoxide: cyclic ether with three ring atoms

Autophagy: catabolic process that degrades intracellular components in the lysosome

Exopeptidase: hydrolytic activity that cleaves single amino acids, dipeptides or tripeptides from the unsubstituted ends of a polypeptide chain

AMC (7-amino-4-methylcoumarin): fluorogenic molecule employed in synthetic substrates proteolytic assays

βGAL (β-galactosidase): bacterial reporter enzyme easily detected by the hydrolysis of synthetic color substrates.

Keywords

ARM-peptidases, bifunctional, degradome, gene-trapping, gluzincins, metalloproteases, MHC-I, microRNAs, nucleosome, oxytocinases, pseudogene, renin-angiotensin

Databanks

***MEROPS name*: aminopeptidase O**

***MEROPS classification*: clan MA(E), family M1, peptidase M01.028**

***Species distribution*: subkingdom Metazoa**

***Reference sequence from*: *Homo sapiens* (UniProt: Q8N6M6)**

Name and History

Aminopeptidase O (**AP-O**) was originally identified by a computational search of putative novel aminopeptidases based on the available sequences of members of the M1 family of exopeptidases [1]. This approach revealed the presence of a putative coding sequence in chromosome 9q22 of a yet uncharacterized metalloprotease. PCR amplification from a brain cDNA library confirmed the existence of a 2.5 kb fragment containing an in-frame initiator and stop codons that encoded a new protein with sequence similarity to other M1 aminopeptidases. According to the *MEROPS* database, the M1 family of aminopeptidases is included in the MA(E) clan of gluzincins [2] which are characterized by the consensus zinc-binding motif $HEXXHX_{18}E$, where the two histidines and the last glutamate act as zinc-binding residues, and the first glutamate behaves as a general base in the catalysis. In addition, M1 aminopeptidases have in their sequence the consensus motif GXMENX, which participates in substrate accommodation and transition state stabilization [3-4]. The M1 family of zinc metalloproteases constitutes a very interesting group of enzymes that play important roles in human physiology [5-10] and whose alterations are associated with several human diseases, including cancer [11-15].

Activity and Specificity

In the work by Diaz-Perales *et al*, an AP-O recombinant fragment containing the catalytic domain linked to GST at the N-terminus was produced in *E. coli* and assayed against several fluorescent peptides [1]. These assays demonstrated that recombinant AP-O exhibits significant proteolytic activity against Arg-AMC and, to a lesser extent, against Asn-AMC, confirming that, despite AP-O lacks the consensus GXMENX motif in the catalytic domain, the enzyme retains

catalytic activity against common aminopeptidase substrates. Moreover, the fact that AP-O recombinant protein displays the highest activity against N-terminal arginine amino acids is in agreement with its classification as an enzyme closely related to LTA4H and APB, since both peptidases show preference for basic N-terminal residues. Accordingly, recombinant AP-O activity is inhibited by general metalloprotease inhibitors and by arphamenine A, a potent selective inhibitor of APB and LTA4H [16-17]. On the other hand, although both LTA4H and APB exhibit high activity against N-terminal lysine, recombinant AP-O lacks this property and gains N-terminal asparagine hydrolytic activity, which could be explained by the specific structural features of AP-O. Further confirmation for arginine preference was supported by the finding that recombinant AP-O is able to remove the N-terminal Arg of angiotensin III to generate angiotensin IV, while displays no activity against angiotensin I or II [1]. Although the experiments were carried out with the recombinant catalytic domain, the specificity against angiotensin III suggests that AP-O could play an *in vivo* role in the regulation of the renin-angiotensin system, as has been described for other M1 aminopeptidases [18-19].

Structural Chemistry

The AP-O protein sequence is 819 amino acids in length and is composed of a large central catalytic domain typical of M1 aminopeptidases flanked by N- and C-terminal extensions (Figure 1). AP-O shows low levels of identity with other members of the M1 family, being aminopeptidase B (APB; Chapter 101) and leukotriene A4 hydrolase (LTA4H; Chapter 100) the most related aminopeptidases, with 23.5% and 20% of identity, respectively. The catalytic domain contains the characteristic motif of the gluzincin metalloproteases, $HEXXHX_{18}E$, but lacks the consensus GXMENX. The equivalent sequence in AP-O is LGMASP, a unique feature among the M1 aminopeptidases [1, 20]. Computational analysis of the C-terminal extension predicts an Armadillo-like (ARM) motif connected to the catalytic domain by a proline-rich region similar to SH3 domain recognition sequence. This C-terminal structure is also found in other members of the M1 family, including LTA4H, APB and aminopeptidase B-like (APB-L; *MEROPS* identifier M01.022). The ARM domain was originally recognized in the *Drosophila* Armadillo protein and is present in proteins like β-catenin and APC (Adenomatous Polyposis Coli), where is thought to play a role in protein-protein interactions [21-22]. Computational analysis of the N-terminal extension

of AP-O also predicts a LTA4H-like domain, although the percentage of identity between the domains of both proteins is relatively low. Similarly, all the structural features found in human AP-O are also present in the sequences deduced for its mouse and rat orthologues, which exhibit 80 and 76% identities with the human enzyme [1]. Collectively, all these features suggest that APO, LTA4H, APB and APB-L are related proteins that share a relatively recent common ancestor. This idea is supported by phylogenetic analysis using the full length sequence of the M1 family, which groups AP-O, LTA4H, APB and APB-L into a separate subgroup with exclusive characteristics among the M1 peptidases (Figure 2). These observations led us to propose the name of ARM aminopeptidases to designate this subgroup of M1 exopeptidases [1]. It is also noteworthy that, like in LTA4H, APB and APB-L, no putative transmembrane domains or signal sequences have been identified in AP-O sequence. However, a more recent work reported the presence of a nucleolar localization signal (NuLS) that is not recognized by the bioinformatic search programs and demonstrated that, when this region is present in the protein, AP-O is transported to the nucleolus [23]. Moreover, it has been proposed that alternative splicing of the exon encoding the NuLS might be one of the mechanisms regulating subcellular localization [23].

Biological Aspects

Expression

Northern blot analysis of human samples shows predominant transcriptional activity in pancreas, placenta, liver, testis and heart. Further experiments revealed that AP-O expression in mouse testis displays a restricted temporal pattern, being detected in a range between 23 and 42 days old and reaching a peak at 30-35 days after birth [1]. In addition, Axton *et al*, by using mice carrying a β-gal gene trapping insertion in the AP-O gene, demonstrated that AP-O expression is restricted to the vasculature of embryo and adult tissues [23]. It is noteworthy that two different transcripts of about 5 and 7.5 Kb were detected in Northern blots of human samples. Accordingly, current databases report the presence of several isoforms, including one that lacks the exon encoding the active center. Similarly, it has been reported alternative splicing of various exons of the mouse AP-O gene, including the exon that encodes the catalytic domain, and the existence of

a second initiator codon at exon 2 [23]. Futhermore, Northern blot analysis has demonstrated that some of the AP-O isoforms are tissue specific.

It is remarkable that the gene encoding AP-O (called *AOPEP* or *C9Orf3*) is the host gene of a microRNA (miRNA) cluster composed of miR-23b, miR-27b, miR-24-1. miRNAs are small non-coding RNA molecules that bind to complementary regions usually present in the 3'-UTR of their target mRNA genes repressing protein synthesis through several mechanisms [24]. Intronic miRNAs share the same promoter as the host gene, being encoded in the pre-mRNA and processed before splicing. Interestingly, miR-27b has been associated with mouse heart development by modulating Mef2c expression [25]. Furthermore, both the miRNAs and the host-gene (*AOPEP*) shows analogous temporal expression patterns in heart, characterized by transcriptional activation from E12.5 and maintained expression in neonates, which supports previous observations [1, 23].

Physiological Function

Although very little is known about the functional roles of AP-O, the available information support the hypothesis that this aminopeptidase might be involved in cardiovascular system homeostasis. First, its expression is restricted to the vasculature of embryonic and adult tissues and strong transcriptional activity is detected in both human and mouse heart tissues [1, 23]. Furthermore, a gene trapping insertion in the *AP-O* gene was found in a screening designed to isolate genes involved in cardiovascular development [23]. It is noteworthy that homozygous mice for the gene trapping insertion are normal and display no obvious phenotype. However, the insertion occurred in the 3'-end of the gene and the resulting protein lacks only the last 46 amino acids of the wild-type AP-O, so it is possible that the APO-βgal fusion retains functionality, although genetic compensation cannot be discarded. Second, *AOPEP* is the host gene of a cluster of miRNAs that play a role in mouse heart development. Considering that both *AOPEP* and the miRNAs are transcribed from the same promoter, complementary roles might be expected for both elements. Finally, it has been shown that, *in vitro*, AP-O cleaves angiotensin III to generate angiotensin IV [1], a bioactive peptide of the renin-angiotensin pathway that plays multiple roles on tissues such as brain, testis, and heart.

Acknowledgements

Our work is supported by grants from Ministerio de Ciencia e Innovación-Spain, Fundación "M. Botín", and the European Union (FP7-Microenvimet). The Instituto Universitario de Oncología is supported by Obra Social Cajastur-Asturias, Spain.

References

[1] Diaz-Perales, A.; Quesada, V.; Sanchez, L. M.; Ugalde, A. P.; Suarez, M. F.; Fueyo, A.; Lopez-Otin, C., Identification of human aminopeptidase O, a novel metalloprotease with structural similarity to aminopeptidase B and leukotriene A4 hydrolase. J Biol Chem (280) (2005) 14310-7.

[2] Rawlings, N. D.; Barrett, A. J.; Bateman, A., MEROPS: the peptidase database. Nucleic Acids Res (38) (2010) D227-33.

[3] Iturrioz, X.; Rozenfeld, R.; Michaud, A.; Corvol, P.; Llorens-Cortes, C., Study of asparagine 353 in aminopeptidase A: characterization of a novel motif (GXMEN) implicated in exopeptidase specificity of monozinc aminopeptidases. Biochemistry (40) (2001) 14440-8.

[4] Vazeux, G.; Iturrioz, X.; Corvol, P.; Llorens-Cortes, C., A glutamate residue contributes to the exopeptidase specificity in aminopeptidase A. Biochem J (334 (Pt 2)) (1998) 407-13.

[5] Bhagwat, S. V.; Lahdenranta, J.; Giordano, R.; Arap, W.; Pasqualini, R.; Shapiro, L. H., CD13/APN is activated by angiogenic signals and is essential for capillary tube formation. Blood (97) (2001) 652-9.

[6] Fournie-Zaluski, M. C.; Fassot, C.; Valentin, B.; Djordjijevic, D.; Reaux-Le Goazigo, A.; Corvol, P.; Roques, B. P.; Llorens-Cortes, C., Brain renin-angiotensin system blockade by systemically active aminopeptidase A inhibitors: a potential treatment of salt-dependent hypertension. Proc Natl Acad Sci U S A (101) (2004) 7775-80.

[7] Fujiwara, H.; Higuchi, T.; Yamada, S.; Hirano, T.; Sato, Y.; Nishioka, Y.; Yoshioka, S.; Tatsumi, K.; Ueda, M.; Maeda, M.; Fujii, S., Human extravillous trophoblasts express laeverin, a novel protein that belongs to membrane-bound gluzincin metallopeptidases. Biochem Biophys Res Commun (313) (2004) 962-8.

[8] Heuer, H.; Schafer, M. K.; Bauer, K., The thyrotropin-releasing hormone-degrading ectoenzyme: the third element of the thyrotropin-releasing hormone-signaling system. Thyroid (8) (1998) 915-20.

[9] Lachance, C.; Arbour, N.; Cashman, N. R.; Talbot, P. J., Involvement of aminopeptidase N (CD13) in infection of human neural cells by human coronavirus 229E. J Virol (72) (1998) 6511-9.

[10] Serwold, T.; Gonzalez, F.; Kim, J.; Jacob, R.; Shastri, N., ERAAP customizes peptides for MHC class I molecules in the endoplasmic reticulum. Nature (419) (2002) 480-3.

[11] Inagaki, Y.; Tang, W.; Zhang, L.; Du, G.; Xu, W.; Kokudo, N., Novel aminopeptidase N (APN/CD13) inhibitor 24F can suppress invasion of hepatocellular carcinoma cells as well as angiogenesis. Biosci Trends (4) (2010) 56-60.

[12] Landau, R.; Laverriere, A.; Bischof, P.; Irion, O.; Morales, M.; Cohen, M., Alteration of circulating Placental Leucine Aminopeptidase (P-LAP) activity in preeclampsia. Neuro Endocrinol Lett (31) (2010) 63-6.

[13] Saiki, I.; Murata, J.; Watanabe, K.; Fujii, H.; Abe, F.; Azuma, I., Inhibition of tumor cell invasion by ubenimex (bestatin) in vitro. Jpn J Cancer Res (80) (1989) 873-8.

[14] Haroon, N.; Inman, R. D., Endoplasmic reticulum aminopeptidases: Biology and pathogenic potential. Nat Rev Rheumatol (6) (2010) 461-7.

[15] Hartiala, J.; Li, D.; Conti, D. V.; Vikman, S.; Patel, Y.; Wilson Tang, W. H.; Brennan, M. L.; Newman, J. W.; Stephensen, C. B.; Armstrong, P.; Hazen, S. L.; Allayee, H., Genetic contribution of the leukotriene pathway to coronary artery disease. Hum Genet (2011).

[16] Umezawa, H.; Aoyagi, T.; Ohuchi, S.; Okuyama, A.; Suda, H.; Takita, T.; Hamada, M.; Takeuchi, T., Arphamenines A and B, new inhibitors of aminopeptidase B, produced by bacteria. J Antibiot (Tokyo) (36) (1983) 1572-5.

[17] Orning, L.; Gierse, J. K.; Fitzpatrick, F. A., The bifunctional enzyme leukotriene-A4 hydrolase is an arginine aminopeptidase of high efficiency and specificity. J Biol Chem (269) (1994) 11269-73.

[18] Reaux, A.; Fournie-Zaluski, M. C.; David, C.; Zini, S.; Roques, B. P.; Corvol, P.; Llorens-Cortes, C., Aminopeptidase A inhibitors as potential central antihypertensive agents. Proc Natl Acad Sci U S A (96) (1999) 13415-20.

[19] Danziger, R. S., Aminopeptidase N in arterial hypertension. Heart Fail Rev (13) (2008) 293-8.

[20 Pham, V. L.; Cadel, M. S.; Gouzy-Darmon, C.; Hanquez, C.; Beinfeld, M. C.; Nicolas, P.; Etchebest, C.; Foulon, T., Aminopeptidase B, a glucagon-processing enzyme: site directed mutagenesis of the Zn2+-binding motif and molecular modelling. BMC Biochem (8) (2007) 21.

[21] Huber, A. H.; Nelson, W. J.; Weis, W. I., Three-dimensional structure of the armadillo repeat region of beta-catenin. Cell (90) (1997) 871-82.

[22] Peifer, M.; Orsulic, S.; Sweeton, D.; Wieschaus, E., A role for the Drosophila segment polarity gene armadillo in cell adhesion and cytoskeletal integrity during oogenesis. Development (118) (1993) 1191-207.

[23] Axton, R.; Wallis, J. A.; Taylor, H.; Hanks, M.; Forrester, L. M., Aminopeptidase O contains a functional nucleolar localization signal and is implicated in vascular biology. J Cell Biochem (103) (2008) 1171-82.

[24] Huntzinger, E.; Izaurralde, E., Gene silencing by microRNAs: contributions of translational repression and mRNA decay. Nat Rev Genet (12) (2011) 99-110.

[25] Chinchilla, A.; Lozano, E.; Daimi, H.; Esteban, F. J.; Crist, C.; Aranega, A. E.; Franco, D., MicroRNA profiling during mouse ventricular maturation: a role for miR-27 modulating Mef2c expression. Cardiovasc Res (89) (2011) 98-108.

List of Relevant web pages

- 'MEROPS the peptidase database' merops.sanger.ac.uk/
- 'The degradome database' www.uniovi.es/degradome
- 'InterPro database of protein domains' www.ebi.ac.uk/interpro
- 'SMART (Web-tool to identify protein domains)' smart.embl-heidelberg.de
- 'Ensembl genome browser' www.ensembl.orgl
- 'UCSC genome browser' genome.ucsc.edu

Further Reading

[1] Ugalde, A. P.; Ordonez, G. R.; Quiros, P. M.; Puente, X. S.; Lopez-Otin, C., Metalloproteases and the degradome. Methods Mol Biol (622) (2010) 3-29.

[2] Matsui, M.; Fowler, J. H.; Walling, L. L., Leucine aminopeptidases: diversity in structure and function. Biol Chem (387) (2006) 1535-44.

[3] Albiston, A. L.; Ye, S.; Chai, S. Y., Membrane bound members of the M1 family: more than aminopeptidases. Protein Pept Lett (11) (2004) 491-500.

[4] Tsujimoto, M.; Hattori, A., The oxytocinase subfamily of M1 aminopeptidases. Biochim Biophys Acta (1751) (2005) 9-18.

[5] Lopez-Otin, C.; Overall, C. M., Protease degradomics: a new challenge for proteomics. Nat Rev Mol Cell Biol (3) (2002) 509-19.

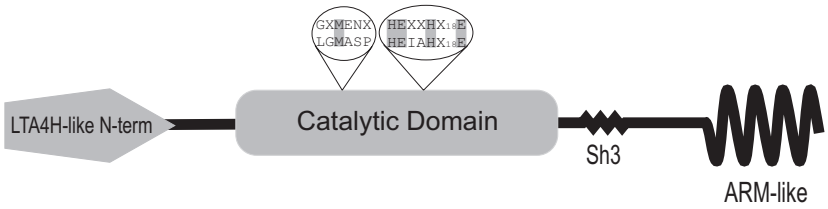

Figure 1. Structure of human AP-O.

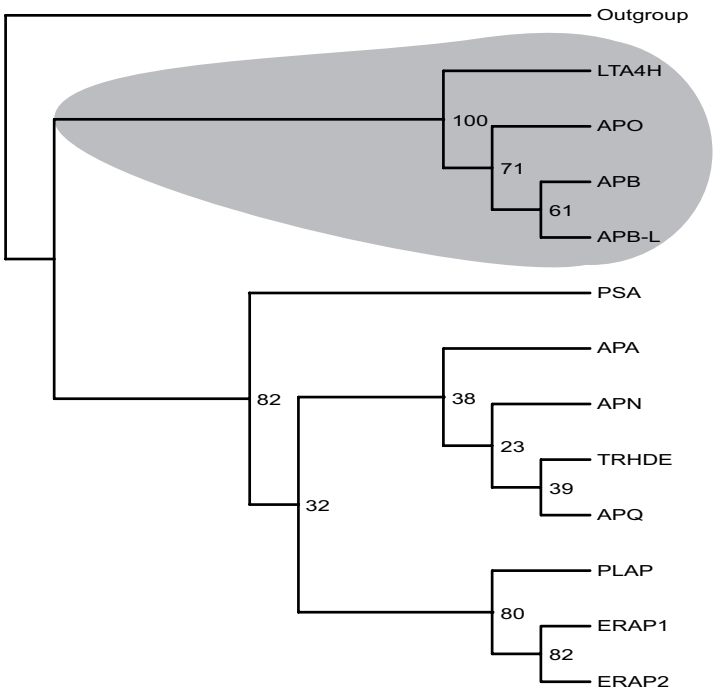

Figure 2. Phylogenetic tree of M1 aminopeptidases.

Ugalde et al

IV. Identificación y caracterización de las arqueometzinquinas 1 y 2 humanas.

La búsqueda bioinformática en el genoma humano nos ha permitido clonar y caracterizar dos nuevas metaloproteasas humanas a las que hemos denominado arqueometzinquinas 1 y 2 (AMZ1 y AMZ2) por su relación con proteasas predichas en el análisis bioinformático de los genomas de arqueobacterias. La búsqueda de secuencias ortólogas en distintos organismos ha demostrado una peculiar evolución de esta familia de proteasas que incluye múltiples pérdidas génicas, así como eventos de transferencia lateral y duplicaciones. Por otra parte, el análisis Northern de tejidos humanos nos ha permitido definir los patrones de expresión de estos nuevos enzimas, siendo la AMZ1 predominantemente detectada en corazón y testículos, y la AMZ2 en corazón e hígado. Por último, la producción en bacterias de los dominios catalíticos de ambas proteasas nos ha permitido demostrar su actividad proteolítica.

Artículo 4: Araceli Díaz Perales, Víctor Quesada, Juan R. Peinado, **Alejandro P. Ugalde,** Jesús Álvarez, María F. Suárez, Xavier Gomis-Rüth y Carlos López-Otín. "Identification and characterization of human archaemetzincin-1 and -2, two novel members of a family of metalloproteases widely distributed in Archaea"

J Biol Chem, **280**(34): 30367-30375 (2005)

Aportación personal al trabajo

La realización de este trabajo coincidió con mi primer año en el laboratorio y con él aprendí las principales técnicas bioquímicas y de biología molecular empleadas para la clonación, producción y análisis de expresión de nuevos genes. En este artículo, contribuí a la clonación y análisis de expresión, así como en la producción, purificación y ensayos de actividad de las arqueometzinquinas.

THE JOURNAL OF BIOLOGICAL CHEMISTRY
Vol. 280, No. 34, Issue of August 26, pp. 30367–30375, 2005
Printed in U.S.A.
© 2005 by The American Society for Biochemistry and Molecular Biology, Inc.

Identification and Characterization of Human Archaemetzincin-1 and -2, Two Novel Members of a Family of Metalloproteases Widely Distributed in Archaea*

Received for publication, April 26, 2005, and in revised form, June 13, 2005
Published, JBC Papers in Press, June 22, 2005, DOI 10.1074/jbc.M504533200

Araceli Díaz-Perales‡, Víctor Quesada‡, Juan R. Peinado‡, Alejandro P. Ugalde‡, Jesús Álvarez§, María F. Suárez‡, F. Xavier Gomis-Rüth¶, and Carlos López-Otín‡‖

From the Departamentos de ‡Bioquímica y Biología Molecular y §Biología Celular, Facultad de Medicina, Instituto Universitario de Oncología, Universidad de Oviedo, 33006 Oviedo, Spain and the ¶Institut de Biología Molecular de Barcelona, Consejo Superior de Investigaciones Cientiíficas, 08034 Barcelona, Spain

Systematic analysis of degradomes, the complete protease repertoires of organisms, has demonstrated the large and growing complexity of proteolytic systems operating in all cells and tissues. We report here the identification of two new human metalloproteases that have been called archaemetzincin-1 (AMZ1) and archaemetzincin-2 (AMZ2) to emphasize their close relationship to putative proteases predicted by bioinformatic analysis of archaeal genomes. Both human proteins contain a catalytic domain with a core motif (HE*XX*H*XX*GX_3CX_4C*X*MX_{17}C*XX*C) that includes an archetypal zinc-binding site, the methionine residue characteristic of metzincins, and four conserved cysteine residues that are not present at the equivalent positions of other human metalloproteases. Analysis of genome sequence databases revealed that AMZs are widely distributed in Archaea and vertebrates and contribute to the defining of a new metalloprotease family that has been called archaemetzincin. However, AMZ-like sequences are absent in a number of model organisms from bacteria to nematodes. Phylogenetic analysis showed that these enzymes have undergone a complex evolutionary process involving a series of lateral gene transfer, gene loss, and genetic duplication events that have shaped this novel family of metalloproteases. Northern blot analysis showed that AMZ1 and AMZ2 exhibit distinct expression patterns in human tissues. AMZ1 is mainly detected in liver and heart whereas AMZ2 is predominantly expressed in testis and heart, although both are also detectable at lower levels in other tissues. Both human enzymes were produced in *Escherichia coli*, and the purified recombinant proteins hydrolyzed synthetic substrates and bioactive peptides, demonstrating that they are functional proteases. Finally, these activities were abolished by inhibitors of metalloproteases, providing further evidence that AMZs belong to this catalytic class of proteolytic enzymes.

Proteases mediate many key physiological processes (1). These enzymes play essential roles in a variety of events that determine cell life and death in all living organisms. Thus, proteases participate in the control of cell cycle progression, tissue morphogenesis and remodeling, cell proliferation and migration, ovulation and fertilization, angiogenesis, host defense, hemostasis, apoptosis, and autophagy (2–9). Because of these crucial roles, strict regulatory mechanisms are necessary to prevent misdirected temporal and spatial proteolytic activities. The failure of these regulatory mechanisms contributes to the development of many pathological processes including arthritis, cardiovascular diseases, neurodegenerative disorders, and cancer (10–15). The recent description of the human degradome, the complete set of human proteases, and the degradomes of other organisms represent preliminary steps to understanding the complexity of protease systems (16). According to our data, there are at least 561 protease and protease-related genes in the human genome (17) (web.uniovi.es/degradome). Likewise, we have annotated >600 protease genes in the mouse and rat genomes (17, 18). This increased complexity in the rodent degradomes is mainly due to the expansion in both mouse and rat genomes of specific gene families encoding proteases implicated in reproduction and host defense. Similarly, the availability of the genome sequences of other model organisms such as *Caenorhabditis elegans*, *Drosophila melanogaster*, or *Arabidopsis thaliana* has allowed us to predict that all of them contain a large number of protease genes ranging from 400 to 600 different members (19) (merops.sanger.ac.uk), thereby emphasizing the complexity of proteolytic systems present in all organisms.

Recently, and as part of our studies aimed at identifying novel human proteases, we have evaluated the possibility that human tissues could produce proteases described previously in evolutionarily distant organisms but whose occurrence in mammals has yet not been reported. This approach led us to identify and characterize human and mouse ovastacin, a novel metalloprotease similar to hatching enzymes from arthropods, birds, amphibians, and fish (20). Following this strategy, we have also tried to explore the putative occurrence in the human genome of genes encoding proteases with sequence similarity to putative metalloproteases annotated in the course of genome sequencing projects of prokaryotic organisms (21). In this work, we report the identification, cloning, and characterization of two novel human metalloproteases called archaemetzincin-1 (AMZ1)[1] and arch-

* This work was supported by grants from Ministerio de Ciencia y Tecnología-Spain, Fundación La Caixa, the European Union (FP5 and FP6-Cancer Degradome), and the Daiichi Fine Chemical Company, Limited. (Toyama, Japan). The Instituto Universitario de Oncología is supported by Obra Social Cajastur-Asturias and Red de Centros de Cáncer-Instituto Carlos III of Spain. The costs of publication of this article were defrayed in part by the payment of page charges. This article must therefore be hereby marked "*advertisement*" in accordance with 18 U.S.C. Section 1734 solely to indicate this fact.

The nucleotide sequence(s) reported in this paper has been submitted to the GenBank™/EBI Data Bank with accession number(s) AJ635357, AJ635358, AJ879912, AJ879913, AJ879914, and AJ879915.

‖ To whom correspondence should be addressed. Tel.: 34-985-104201; Fax: 34-985-103564; E-mail: clo@uniovi.es.

[1] The abbreviations used are: AMZ, archaemetzincin; AMC, 7-amino-4-methylcoumarin; contig, group of overlapping clones; GST, glutathione *S*-transferase; Mca, (7-methoxycoumarin-4-yl)-acetic acid.

aemetzincin-2 (AMZ2), which are closely related to proteins whose sequence has been predicted by bioinformatic analysis of archaeal genomes. We perform a detailed phylogenetic analysis of these enzymes to clarify the origin and complex evolutionary history of this new family of metalloproteases. Finally, we examine the tissue distribution of AMZ1 and AMZ2 in human tissues and analyze their enzymatic properties.

EXPERIMENTAL PROCEDURES

Materials—Restriction endonucleases and other reagents used for molecular cloning were from Roche Diagnostics. Double-stranded DNA probes were radiolabeled with [α-^{32}P]dCTP (3000 Ci/mmol) from Amersham Biosciences, using a commercial random priming kit purchased from the same company. Human cDNA libraries and Northern blots containing polyadenylated RNAs from different tissues were from Clontech. Fluorogenic substrates and biologically active peptides (neurogranin, angiotensin II, and angiotensin III) were purchased from Bachem, and protease inhibitors and AMC were from Sigma. Albumin, fibrillar collagens, gelatin, plasminogen, and aprotinin were also from Sigma. Antibodies against GST were developed in our laboratory as described previously (22).

Bioinformatic Analysis and cDNA Cloning—The BLAST program was used to screen public (www.ncbi.nlm.nih.gov) and private (www.celera.com) human genome databases, searching for regions with sequence similarity to prokaryotic metalloproteinase sequences (21). We found two partial sequences located in the human chromosomes 7p22.3 and 17q24.2 exhibiting similarity to putative metalloproteinase sequences identified during the course of large scale genome-sequencing projects involving Archaea (23–26). After the identification of these human sequences, we designed specific oligonucleotides to PCR amplify the cDNAs for these metalloproteases using a human brain cDNA library as a template. All PCR amplifications were performed in a GeneAmp 2400 PCR system from PerkinElmer Life Sciences. After cloning the PCR products in pBluescript, their identity was confirmed by nucleotide sequencing

Nucleotide Sequence Analysis—Cloned cDNAs were sequenced at the Oviedo University DNA analysis facility using BigDye Terminator (version 3.1) chemistry on an ABI PRISM 3100 genetic analyzer platform (Applied Biosystems). Computer analysis of DNA and protein sequences was performed with the GCG software package of the University of Wisconsin Genetics Computer Group.

Phylogenetic Analysis—The sequences of archaemetzincins from 27 archaeal, bacterial, and eukaryotic organisms were predicted from their genomic sequences with the TBLASTN algorithm. The obtained sequences were aligned automatically with ClustalX version 1.8 (www.igbmc.u-strasbg.fr/BioInfo/ClustalX) and manually with GeneDoc version 2.6. (www.psc.edu/biomed/genedoc). An unrelated metalloprotease from the enterobacteria *Yersinia pestis* was also added to this alignment as an out group. The most parsimonious tree according to this alignment was calculated with the Protpars program included in the Phylip package version 3.6 (evolution.genetics.washington.edu/phylip/getme.html). The resulting tree was plotted with TreePlot (www.bioinformatics.nl/tools/plottree.html). Additionally, a tree of the selected species was constructed based on a diverse array of phylogenetic resources (www.ncbi.nlm.nih.gov/Taxonomy/CommonTree/wwwcmt.cgi).

Northern Blot Analysis—Nylon membranes containing 2 μg of poly(A$^+$) RNA from diverse human tissues were prehybridized at 42 °C for 3 h in 50% formamide, 5× SSPE (1× SSPE is 150 mM NaCl, 10 mM NaH_2PO_4, 1 mM EDTA, pH 7.4) 10× Denhardt's solution, 2% SDS, and 100 μg/ml denatured herring sperm DNA. Membranes were then hybridized with specific radiolabeled probes containing nucleotides from positions 180 to 580 of AMZ1 cDNA and from 340 to 750 of AMZ2 cDNA. Hybridization was performed for 20 h under the same conditions used for prehybridization. Finally, blots were washed once with 2× SSC, 0.05% SDS for 30 min and three times in 0.1× SSC and 0.1% SDS for 30 min at 50 °C and exposed to autoradiography. RNA integrity and loading was assessed by hybridization with an actin probe.

Production and Purification of Recombinant Proteins—cDNAs for the predicted catalytic domains of AMZ1 (positions 1–320) and AMZ2 (positions 1–300) were obtained by PCR amplification using specific oligonucleotide pairs containing defined restriction sites. The AMZ1 catalytic domain oligonucleotides were 5′-GGGGATCCCATGCTGCAGTGTAGACCCGCACAGGA-3′ and 5′-GGGTCGACGATTGAGAGAAGGGGTAGGGTCCCTG-3′, and the AMZ2 catalytic domain oligonucleotides were 5′-GGGGATCCCATGCAAATAATACGGCACTCCG-3′ and 5′-CAGGAATTCAGTAAAAACCTCTTGACGGTCCG-3′ (where the restriction sites are underlined). PCR amplifications were performed with 30 cycles of denaturation (95 °C for 30 s), annealing (60 °C for 30 s), and extension (68 °C for 1 min) using the Expand^{TM} long template, high fidelity PCR system. PCR products were then digested with the corresponding restriction enzymes and cloned in the appropriate sites of the pGEX-5x-2 expression vector (Amersham Biosciences). The resulting constructs were transformed into BL21(DE3)-pLysE-competent *Escherichia coli* cells, and expression was induced by the addition of isopropyl-1-thio-β-D-galactopyranoside (final concentration 1 mM), followed by 3 h of incubation at 28 °C. The cells were then harvested by centrifugation, washed with phosphate-buffered saline, and lysed by incubation in phosphate-buffered saline with 100 μg/ml lysozyme, 10 μg/ml DNase, and 0.1% Triton X-100 overnight at 4 °C. The recombinant catalytic domain proteins contained in the corresponding supernatants were purified by affinity chromatography using a glutathione-Sepharose column. The identity of the recombinant proteins was verified by Western blot and trypsin digestion followed by mass spectrometry analysis.

Trypsin Digestion—Gel bands were manually excised and placed into 0.5-ml tubes. Then, gel pieces were washed three times with 180 μl of 25 mM ammonium bicarbonate/acetonitrile (70:30) (v/v), dried at 90 °C for 15 min, and incubated with 12 μg/ml trypsin (Promega) in 25 mM ammonium bicarbonate at 60 °C for 1 h. Likewise, soluble proteins were incubated with trypsin (12 μg/ml) in 25 mM ammonium bicarbonate for 1 h at 60 °C. The resulting peptide mixtures were placed into ice for 2 min, and 2 μl of 10% trifluoroacetic acid were added to each sample. Samples were then desalted by C18 reverse phase chromatography (ZipTip; Millipore). Peptides were eluted with 2 μl of α-cyano-4-hydroxycinnamic acid in acetonitrile and 0.1% trifluoroacetic acid (50:50) (v/v). In a typical experiment, 1 μl of this solution was analyzed by mass spectrometry.

Mass Spectrometry Analysis—Matrix-assisted laser desorption ionization was performed on a time-of-flight mass spectrometer equipped with a nitrogen laser source (Voyager-DE STR; Applied Biosystems). Data from 50 to 200 laser shots were collected to produce a mass spectrum (S. E ± 20 ppm).

Protease Assays—Enzymatic activity of the purified recombinant human AMZ1 and AMZ2 was assayed using AMC-coupled amino acids (Asp-AMC, Thr-AMC, Leu-AMC, Glu-AMC, His-AMC, Val-AMC, Asn-AMC, Ser-AMC, Ile-AMC, Trp-AMC, Phe-AMC, Ala-AMC, Gln-AMC, Gly-AMC, Lys-AMC, Tyr-AMC, Pro-AMC, Met-AMC, and Arg-AMC) or the fluorogenic peptides QF35 (Mca-Pro-Leu-Ala-Nva-Dpa-Ala-Arg-NH_2) and QF41 (Mca-Pro-Cha-Gly-Nva-His-Ala-Dpa-NH_2), where Mca is (7-methoxycoumarin-4yl)-acetic acid, Nva is norvaline, Dpa is L-dinitrophenyl-diamino propionic acid, and Cha is cyclohexyl alanine. Assays were carried out at 37 °C at a substrate concentration of 5 μM in a buffer containing 50 mM Tris-HCl, 150 mM NaCl, and 0.05% Brij-35, pH 7.5. The fluorometric measurements were made in an LS55 spectrofluorometer from PerkinElmer Life Sciences (λ_{ex} = 360 nm and λ_{em} = 460 nm for AMC-coupled amino acids and λ_{ex} = 328 nm and λ_{em} = 393 nm for Mca-containing peptides). The fluorescent signal was calibrated using known concentrations of AMC and Mca. For inhibition experiments, the recombinant proteins were preincubated for 30 min at 37 °C with *o*-phenantroline, E-64, 4-(2-aminoethyl)-benzenesulfonyl fluoride, batimastat, tissue inhibitor of metalloproteinase-1, -2, -3, and -4, arphamenine A, and amastatin, and then the hydrolyzing activity against Ala-AMC for AMZ1 or against Arg-AMC for AMZ2 was determined by fluorometric measurements as described above. Kinetic studies were performed using different concentrations of the fluorogenic compounds (0.5–100 μM) in 100 μl of assay buffer containing recombinant enzymes (5 nM), and peptide hydrolysis was measured from the increase in fluorescence at 37 °C over time. Initial velocities were calculated using the analysis package FL WinLab 2.01 (PerkinElmer Life Sciences), and data were fitted to the Michaelis-Menten equation (27) using GraFit version 4.0 (Erithacus). Assays with purified proteins (albumin, fibrillar collagens, gelatin, plasminogen, or aprotinin) and bioactive peptides (neurogranin, angiotensin II, and angiotensin III) were performed by incubation of 2.5 nM recombinant AMZ1 or AMZ2 with each substrate (10 μM). Reactions were carried out at 37 °C in a buffer containing 50 mM Tris-HCl and 150 mM NaCl, pH 7.5, overnight for purified proteins or in the course of 2 h for bioactive peptides. The digestions of purified proteins were analyzed by SDS-PAGE. Peptide digestions were purified using a ZipTip and analyzed by mass spectrometry.

RESULTS

Cloning and Characterization of Two Human cDNAs Encoding Novel Metalloproteases Similar to Archaeal Metzincins—A bioinformatic search of the human genome to look for sequences similar to those of archaeal or bacterial metallopro-

teases led us to identify two DNA contigs located in chromosomes 7p22.3 and 17q24.2 and encoding two uncharacterized proteins with sequence similarity to putative archaeal metalloprotease sequences (21, 23–26). The full-length cDNAs for both human enzymes were PCR-amplified using specific oligonucleotides and a brain cDNA library. These experiments led us to the amplification of 1.5- and 1-kb cDNAs, both containing in-frame initiator and stop codons. After cloning and sequencing of the PCR-amplified products, we confirmed by conceptual translation that the generated sequences encoded two novel proteins of 498 and 360 amino acids, respectively (Fig. 1*A*, and GenBank™ accession numbers AJ635357 and AJ635358). Domain analysis with the InterPro (www.ebi.ac.uk/interpro) and SMART (smart.embl-heidelberg.de) programs confirmed the presence in both human protein sequences of a catalytic domain related to neutral zinc metalloproteases. A search for orthologous sequences using the TBLASTN algorithm showed that both human sequences are closely related to members of a family of predicted metalloproteases originally identified during the analysis of archaeal genomes and tentatively called archaemetzincins (21). Accordingly, we propose to call the newly identified proteins human archaemetzincin-1 and -2. The maximum percentages of identities between the catalytic domains of human and archaeal enzymes were 27% between human AMZ1 and the predicted archaemetzincin from the genome sequence of *Thermococcus kodakaraensis* and 39% between human AMZ2 and the corresponding enzyme from *Pyrococcus abyssi* (Fig. 1*B*). Likewise, the percentage of identities between the catalytic domains of human AMZ1 and AMZ2 is ~40%. Further bioinformatic analysis of available genome sequences revealed that archaemetzincins are widely distributed in Archaea as well as in vertebrates including birds, amphibians, and fish (Fig. 1*B*). However, no orthologous sequences were found in a large number of bacterial species, with the exception of *Aquifex aeolicus* and *Myxococcus xanthus*. Likewise, archaemetzincins were also absent from plants and from non-vertebrate Metazoa, such as *C. elegans, D. melanogaster* and *Anopheles gambiae*.

Amino acid sequence alignment of both human archaemetzincins with all related sequences present in different species allowed us to identify a highly conserved core catalytic motif, $\underline{\text{HE}}XX\underline{\text{H}}XXGX_3CX_4CXMX_{17}CXXC$, where the putative metalloprotease zinc-binding site is underlined. The conserved methionine would be part of the "Met-turn" described in the metzincin clan of metalloproteases (21), although it should be noted that the sequences deduced for mouse and rat AMZ1 contain a Leu residue at this position (Fig. 1*B*, and GenBank™ accession numbers AJ879912 and AJ879913, respectively). By contrast, mouse and rat AMZ2 contain the archetypal Met at this position (Fig. 1*B*, and GenBank™ accession numbers AJ879914 and AJ879915, respectively). Notably, human AMZ1 and rodent AMZ1 lack a conserved His residue that is present in human and rodent AMZ2, as well as in archaeal and fungal archaemetzincins (Fig. 1*B*). Accordingly, this His residue can be used as a distinctive structural feature between AMZ1 and AMZ2. It is also noteworthy that the core catalytic motif of these enzymes contains four Cys residues that are absolutely conserved in all archaemetzincins but are absent at the equivalent positions of other metalloproteases. Accordingly, we propose that these four Cys residues can be used as a specific signature to distinguish this family of metalloproteases within the metzincin clan.

Evolutionary Analysis of AMZs—An extensive search of the publicly available genome sequences allowed us to identify AMZ genes in multiple eukaryotic and prokaryotic organisms. However, AMZs are absent in several eukaryotic model organisms, such as *Saccharomyces cerevisiae, A. thaliana*, *D. melanogaster*, and *C. elegans*, as well as in most bacterial organisms. All of the predicted prokaryotic AMZs were classified as AMZ2 because of the presence of a third histidine residue in their catalytic site. Additionally, the archaeal organisms belonging to the Thermococcaceae family presented a second AMZ2 with a highly divergent N-terminal extension that we called AMZ2b. After alignment of these sequences, a phylogenetic tree was calculated and rooted with an unrelated metalloprotease (Fig. 2). The obtained tree shows eukaryotic and prokaryotic AMZs separated into two large groups. Only AMZ2b genes and AMZ2 from bacterial *M. xanthus* stand outside these groups. Interestingly, AMZ2 from *A. aeolicus* groups with AMZs from archaeal organisms, suggesting a relatively late lateral gene transfer event from Archaea to bacteria as was previously proposed for other *A. aeolicus* genes (28, 29). Finally, data from this analysis were fitted to a taxonomic tree to construct a model that could explain the evolution of AMZ genes (Fig. 3). According to this model, the primordial AMZ arose in a common ancestor of Archaea and Eukaryota. Some bacterial species acquired this gene through lateral gene transfer from archaeal organisms. On the other hand, two duplication events would explain the presence of AMZ2b in Thermococcaceae and AMZ1 in Amniota. The lack of AMZ genes in several eukaryotic and archaeal organisms would be likely explained by multiple gene loss events at different times (Fig. 3).

Expression Analysis of AMZ1 and AMZ2 in Human Tissues—To analyze the distribution of both archaemetzincins in human tissues, Northern blots containing poly(A^+) RNAs prepared from a variety of human adult tissues were hybridized with specific probes for human AMZ1 or AMZ2. As can be seen in Fig. 4, AMZ1 mRNA transcripts are detected predominantly in liver and heart, although there are significant mRNA levels in pancreas, kidney, and testis. On the other hand, AMZ2 mRNAs are mainly present in heart and testis, although there are also detectable transcripts in pancreas, kidney, liver, lung, placenta, brain, and prostate. Notably, both human AMZs display several mRNA transcripts, possibly derived from alternative splicing events. On the other hand, both AMZ mRNAs are present in all fetal tissues analyzed (Fig. 4), being mainly detected in kidney and liver in the case of AMZ1 and in kidney and brain in the case of AMZ2.

Enzymatic Properties of Human AMZ1 and AMZ2 Produced in E. coli—To analyze the enzymatic properties of both human AMZs, we produced in *E. coli* two fusion proteins containing the putative catalytic domains of these enzymes linked to GST at their N termini. The catalytic domains were defined based on the alignments of human AMZs with the related archaeal proteins, which showed the maximum degree of conservation in the N-terminal region of these proteins. Then, these constructs (encoding amino acids 1–320 of AMZ1 and 1–300 of AMZ2) were transformed in *E. coli* BL21, and, after isopropyl-1-thio-β-D-galactopyranoside induction, bands of the expected size (55 kDa) were detected by SDS-PAGE and Western blot analysis of protein extracts using antibodies against GST (Fig. 5*A*). These recombinant GST-proteases were then purified by glutathione-Sepharose chromatography. To assess the identity of the proteins present in these bands, they were digested with trypsin and analyzed by mass spectrometry. The obtained spectra confirmed that the 55-kDa bands corresponded to GST-AMZ1 and GST-AMZ2 fusion proteins.

The recombinant human AMZ1 and AMZ2 proteins were then used in enzymatic assays with the fluorescent substrates commonly employed for assaying other proteases. These assays showed that recombinant AMZ1 exhibits a significant hydrolytic activity against Ala-AMC, whereas recombinant AMZ2 preferentially cleaves Arg-AMC (Fig. 5*B*). By contrast, we did

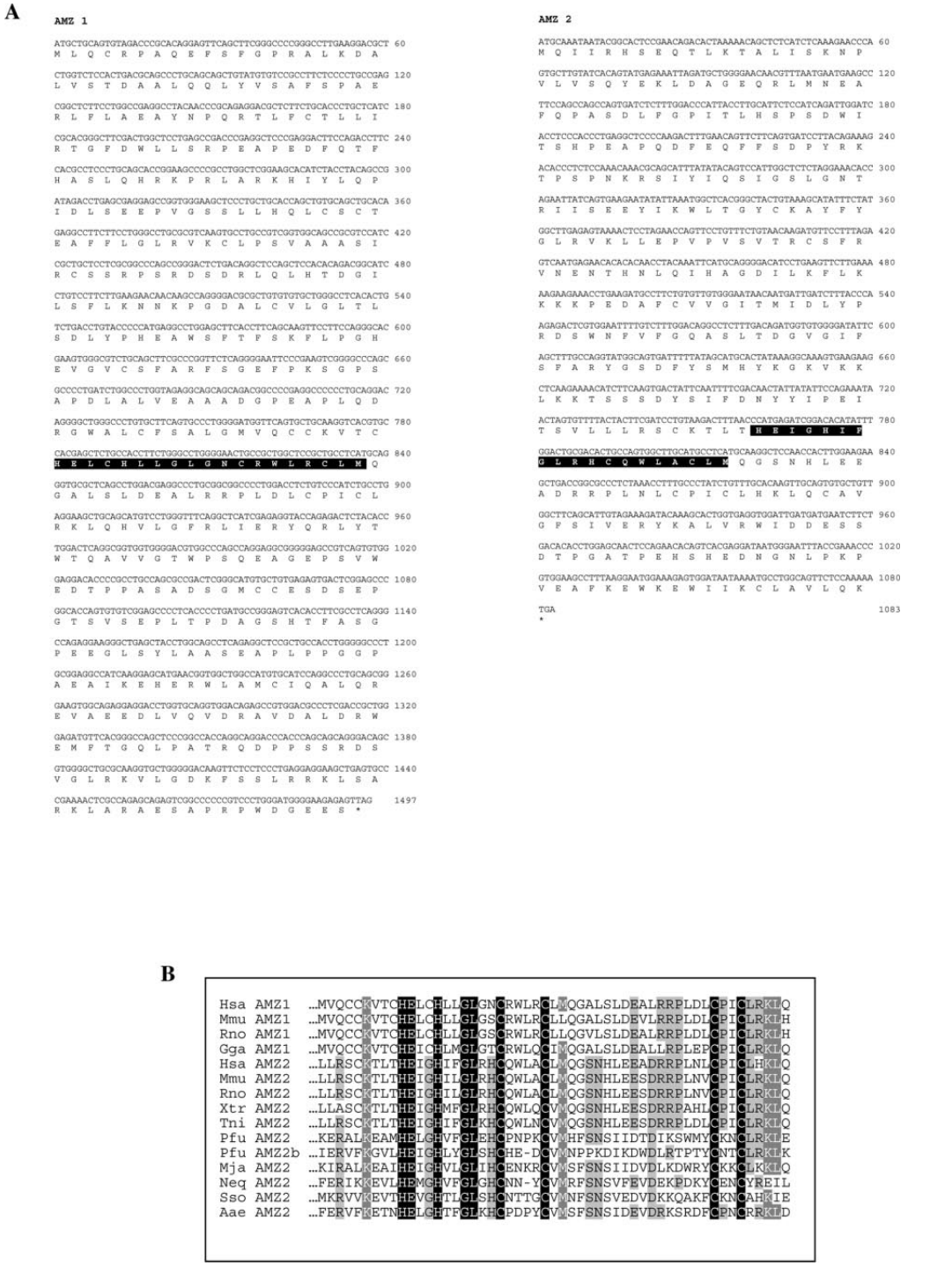

FIG. 1. **Sequences of human AMZs and comparison to proteases from other organisms.** *A*, sequences of human AMZ1 and AMZ2. The nucleotide and amino acid sequences of AMZ1 and AMZ2 are shown. The characteristic core catalytic motif of archaemetzincins, including the zinc-binding site, is in *black*. *B*, amino acid sequence alignment around the zinc-binding site of the catalytic domains of AMZ enzymes. Residues common to all of them are *shaded*. The alignment was performed using ClustalX (version 1.81). *Hsa*, *Homo sapiens*; *Mmu*, *Mus musculus*; *Rno*, *Rattus novergicus*; *Gga*, *Gallus gallus*; *Xtr*, *Xenopus tropicalis*; *Tni*, *Tetraodon nigroviridis*; *Pfu*, *Pyrococcus furiosus*; *Mja*, *Methanoccoccus jannaschii*; *Neq, Nanoarchaeum equitans*; *Sso, Sulfolobus solfataricus*; *Aae, A. aeolicus*.

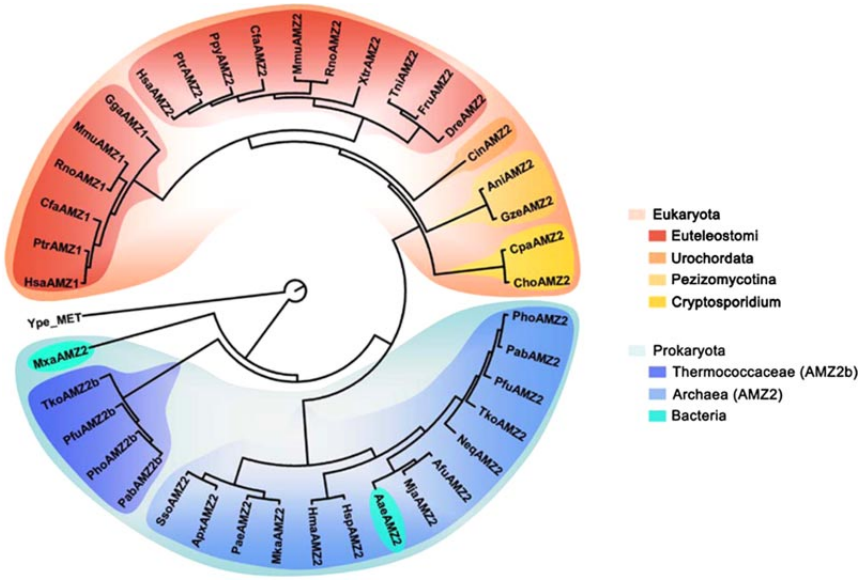

FIG. 2. **Phylogenetic relationships of archaemetzincins.** The tree was calculated with the Protpars program of the Phylip program package (version 3.6). *Hsa*, *Homo sapiens*; *Ptr*, *Pan troglodytes; Ppy*, *Pongo pygmaeus*; *Cfa*, *Canis familiaris*; *Mmu*, *Mus musculus*; *Rno*, *Rattus novergicus*; *Gga*, *Gallus gallus*; *Xtr*, *Xenopus tropicalis*; *Dre*, *Danio rerio*; *Fru*, *Fugu rubripes*; *Tni*, *Tetraodon nigroviridis*; *Cin*, *Ciona intestinalis*; *Ani*, *Aspergillus nidulans*; *Gze*, *Giberella zeae*; *Cho*, *Cryptosporidium hominis*; *Cpa*, *Cryptosporidium parvum*; *Pab*, *Pyrococcus abyssi*; *Tko*, *T. kodakaraensis*; *Afu*, *Archaeoglobus fulgidus*; *Apx*, *Aeropyrum pernix*; *Pfu*, *Pyrococcus furiosus*; *Mja*, *Methanococcus jannaschii*; *Hsp*, *Halobacterium* sp.; *Hma*, *Haloarcula marismortui*; *Neq*, *Nanoarchaeum equitans*; *Pho*, *Pyrococcus horikoshii*; *Sso*, *Sulfolobus solfataricus*; *Mka*, *Methanopyrus kandleri; Pae*, *Pyrobaculum aerophilum*; Aae, *A. aeolicus*; Mxa, *M. xanthus*; Ype, *Y. pestis*.

not detect any significant activity of human recombinant AMZs against QF35 or QF41, two peptides widely used for assaying metalloendopeptidases. Likewise, we did not detect any evidence of endoproteolytic activity of human recombinant AMZs against a number of protein substrates including albumin, fibrillar collagens, gelatin, plasminogen, or aprotinin (data not shown). It is also noteworthy that the two human AMZs exhibited different optimal pH values for their hydrolyzing activities against AMC derivatives. Whereas AMZ1 reaches a maximum of activity at pH 8.0, the optimal pH for AMZ2 activity is 7.0 (Fig. 5*C*). We then tested the ability of different protease inhibitors to block the enzymatic activity of both human AMZs. As can be seen in Fig. 5*D*, the activity of both peptidases was inhibited by the general metalloprotease inhibitors *o*-phenantroline and batimastat, but not by 4-(2-aminoethyl)-benzenesulfonyl fluoride, E-64, and tissue inhibitors of metalloproteinases (TIMPS), which are inhibitors of serine, cysteine, and matrix metalloproteases, respectively. Interestingly, AMZ1 and AMZ2 activities were significantly inhibited by amastatin, which is an inhibitor of aminopeptidases (Fig. 5*D*). We next performed a kinetic analysis of the proteolytic reaction catalyzed by the catalytic domains of AMZ1 and AMZ2 with their preferred substrates (Ala-AMC and Arg-AMC, respectively). The fitting of the resulting data to the Michaelis-Menten equation yielded k_{cat}/K_m values of 46 M^{-1} s^{-1} and 22 M^{-1} s^{-1} for catalytic domain proteins of AMZ1 and AMZ2, respectively, which are similar to the value reported for recombinant aminopeptidase O produced in the same expression system (30). We have also tried to perform similar experiments with the full-length proteins produced in bacterial systems. To date, these experiments have been hampered by the low amounts of full-length AMZs, which can be recovered in active form by using different expression systems. Nevertheless, preliminary experiments performed with full-length AMZ1 and AMZ2 produced as His tail fusion proteins in *E. coli* BL21 pLysS have confirmed the above results for substrate specificity and sensitivity to inhibitors obtained by using the catalytic domains of both enzymes (data not shown).

To further characterize the enzymatic activity of the identified AMZ metalloproteases, several commercially available bioactive peptides were incubated in the presence of purified catalytic domains of AMZ1 or AMZ2, and the resulting samples were analyzed by mass spectrometry. As shown in Fig. 6, these experiments demonstrated that human AMZ1 exhibited aminopeptidase activity against neurogranin, whereas human AMZ2 was active against angiotensin III. Thus, as can be seen in Fig. 6*A*, neurogranin is detected as a 1800.1-Da peak consistent with its amino acid sequence (AAKIQASFRGHMARKK), whereas incubation of neurogranin with AMZ1 produced a single additional peak with a mass of 1657.9 Da, corresponding to the processed peptide KIQASFRGHMARKK (Fig. 6*B*). Notably, AMZ2 did not process neurogranin under the same experimental conditions (data not shown). Similarly, neither AMZ1 nor AMZ2 hydrolyzed angiotensin II (data not shown). However, AMZ2 cleaved the N-terminal Arg residue of angiotensin III (RVYIHPF), albeit with low efficiency, to produce angiotensin IV (VYIHPF) (Fig. 6, *C* and *D*).

DISCUSSION

In this work we describe two new human proteases that have been tentatively called archaemetzincin-1 and -2. According to a series of structural and enzymatic features, these proteins belong to a new family of metalloproteases characterized by a conserved motif (HE*XX*H*XX*GX_3CX_4CXMX_{17}C*XX*C) that contains an archetypal zinc-binding site and four Cys residues that contribute to defining the specific signature of this novel metalloprotease family. Furthermore, enzymatic assays performed with human recombinant AMZs have provided the first evidence that these proteins are catalytically active metalloproteases that exhibit substrate specificity and sensitivity to in-

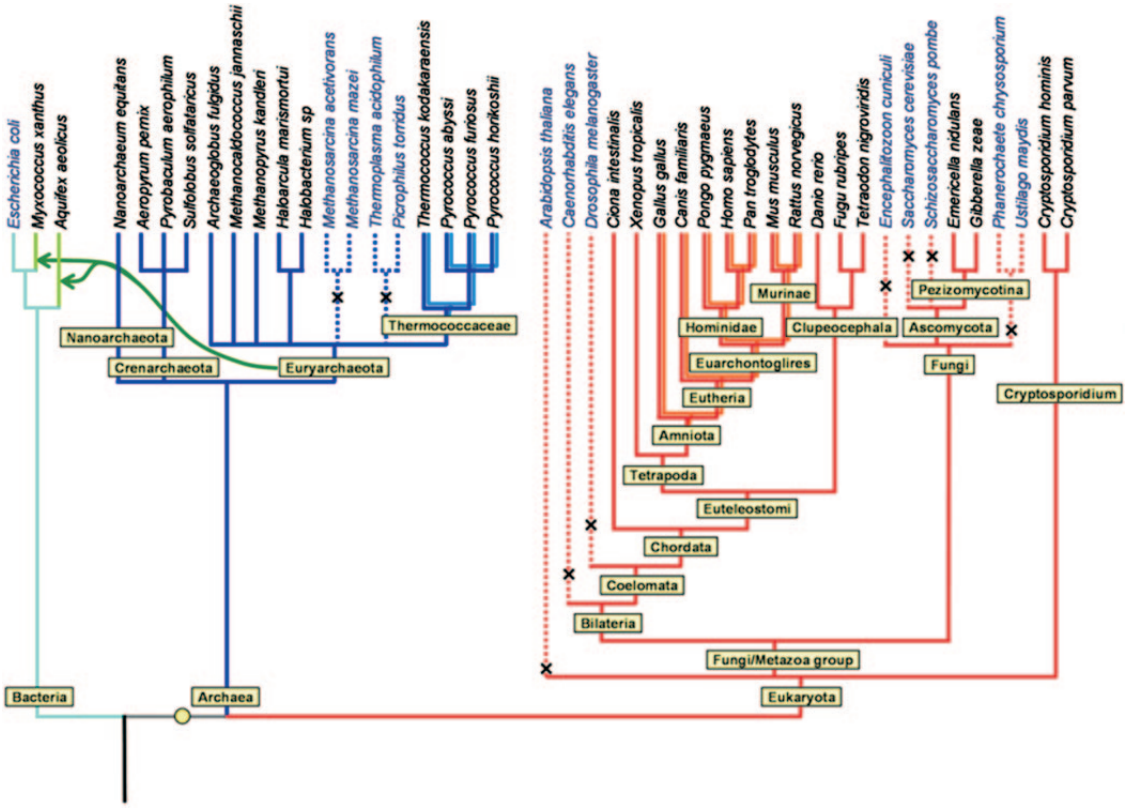

FIG. 3. **Model of the evolution of archaemetzincins.** A common tree based on a diverse array of phylogenetic resources was constructed using the NCBI taxonomy browser. Species lacking any AMZ genes are in *dark blue*. Putative sites of origin (*yellow circle*), duplication (*double line*), lateral transfer (*green arrow*), and loss (*dashed line* and *black cross*) of AMZ genes are shown.

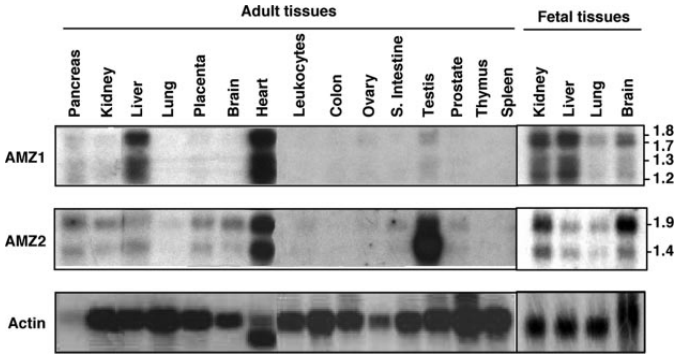

FIG. 4. **Analysis of AMZ1 and AMZ2 expression in adult and fetal human tissues.** Filters containing ~2 μg of polyadenylated RNAs were hybridized with human AMZ1 or AMZ2 specific probes. RNA sizes are indicated in kilobases. *S. Intestine*, small intestine.

hibitors, which appears to indicate that both proteases may act predominantly as aminopeptidases.

An additional distinctive feature of this family of metalloproteases is the complex series of evolutionary events that have contributed to its creation and diversification in different organisms. In fact, our bioinformatic analysis revealed that these enzymes are widely distributed in vertebrate and archaeal organisms but are absent in the genomes of a number of model organisms such as *E. coli*, *S. cerevisiae*, *A. thaliana*, *D. melanogaster*, and *C. elegans*. The occurrence of genes shared by prokaryotes and vertebrates but absent in other eukaryotes has been widely considered as an indication of lateral gene transfer events from prokaryotes to vertebrates (31). Accordingly, AMZs could represent novel and interesting examples of these rare evolutionary events. However, the recent accumulation of data questioning many cases of lateral gene transfer to the vertebrate lineage (32–34) prompted us to perform an exhaustive bioinformatic search for AMZ genes in all available genome sequences. This analysis led us to identify additional AMZ-related sequences in other non-vertebrate eukaryotes and in two bacterial species, as well as to uncover a series of complex evolutionary events underlying the formation of this metalloprotease family (Fig. 3). According to this phylogenetic analysis, the evolutionary history of AMZs is best described by

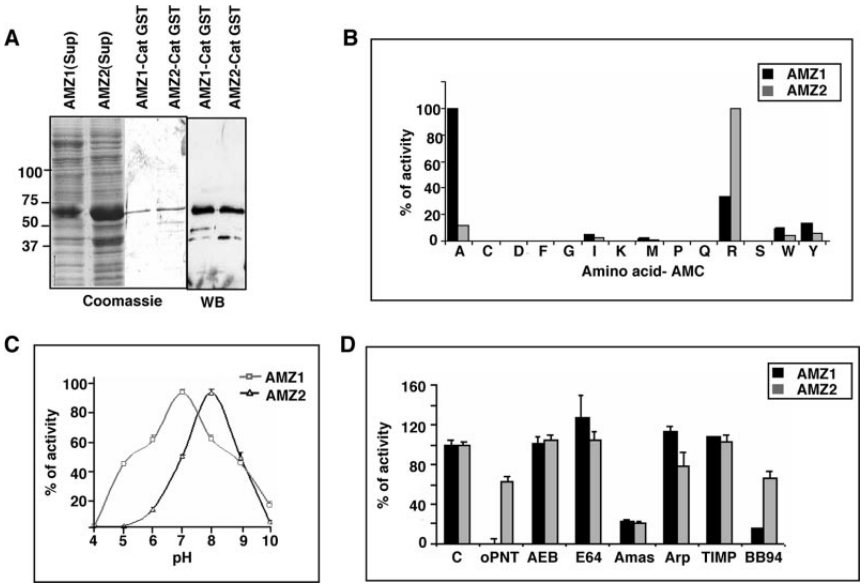

FIG. 5. **Production and enzymatic analysis of recombinant human AMZ1 and AMZ2.** *A*, Coomassie Blue-stained SDS-PAGE and Western blot (*WB*) showing the results of the expression and purification of the recombinant catalytic domains (*Cat*) of human AMZ1 and AMZ2. 5-μl aliquots of soluble fraction (*AMZ1(Sup)* and *AMZ2(Sup)*) and purified AMZ1 and AMZ2 were analyzed in *each lane*. The two *far right lanes* correspond to the Western blot analysis of purified AMZ1 and AMZ2 using anti-GST antibodies. Molecular size markers are shown on the left. *B*, analysis of the hydrolyzing activity of AMZ1 and AMZ2 using different AMC-bound amino acids. *C*, pH optimum analysis using Ala-AMC and Arg-AMC as substrates for AMZ1 and AMZ2, respectively. *D*, AMZ sensitivity to different inhibitors. Recombinant GST-AMZ1 or GST-AMZ2 were incubated alone (*C*) or in the presence of 10 mM *o*-phenantroline (*oPNT*), 20 μM 4-(2-aminoethyl)-benzenesulfonyl fluoride (*AEB*), 20 μM E-64, 20 μM amastatin (*Amas*), 20 μM arphamenine A (*Arp*), 5 nM tissue inhibitor of metalloproteinase-1 (*TIMP*), and 5 μM batimastat (*BB94*); the remaining activity was measured using Ala-AMC or Arg-AMC as substrate.

a scenario in which the primordial AMZ gene, related to current AMZ2 enzymes, arose in a common ancestor of archaeal and eukaryotic organisms. The lack of AMZ genes in virtually all the analyzed bacterial genomes should be fully consistent with the proposed origin of AMZs after the appearance of the primordial bacterial organism. The presence of an AMZ in *A. aeolicus*, a hyperthermophilic bacteria that occupies an ecological niche dominated by Archaea, should be explained by lateral gene transfer from some of these archaeal organisms. Furthermore, the clear phylogenetic relationship between *A. aeolicus* AMZ2 and archaeal AMZs provides additional support to the occurrence of the proposed lateral transmission. Similarly, the finding of AMZ-related sequences in *M. xanthus* should likely be the result of lateral transfer from Archaea, but in this case this event was followed by a rapid accumulation of mutations, which would explain its location as an out group in the phylogenetic tree. The evolutionary history of AMZs in eukaryotic organisms has also involved a series of diverse events since their separation from their common ancestor with Archaea. First, the absence of AMZ genes in plants, nematodes, or insects is remarkable, suggesting the occurrence of multiple gene loss events in these organisms. Consistent with this proposal, codon usage or nucleotide composition analysis of AMZ genes failed to provide any evidence of lateral transmission from Archaea to vertebrates. Finally, our phylogenetic analysis also revealed that eukaryotic AMZ1 diverged from AMZ2 recently, probably by gene duplication, again illustrating the genomic plasticity of this family of metalloproteases.

To further explore the functional relevance of AMZ1 and AMZ2, we performed an enzymatic analysis of both recombinant enzymes produced in *E. coli*. This analysis revealed that the recombinant proteins are catalytically active and that their activities seem to correspond to those of aminopeptidases. However, the two human metalloproteases show different substrate preferences. Whereas AMZ1 preferentially targets substrates that contain Ala at their N termini, AMZ2 mainly hydrolyzes substrates with Arg at that position. Consistent with this finding, AMZ1 could hydrolyze the N-terminal Ala of neurogranin, whereas AMZ2 processed the N-terminal Arg of angiotensin III. Furthermore, AMZ1 and AMZ2 failed to hydrolyze synthetic peptides such as QF35 and QF41, which are used for the analysis of metalloendopeptidases. The activities of both enzymes were abolished by general metalloprotease inhibitors such as *o*-phenantroline and batimastat and by the specific aminopeptidase inhibitor amastatin, providing further evidence that AMZs could be classified as metalloaminopeptidases. Also in this regard, it is remarkable that the activity of the recombinant catalytic domains of AMZs is relatively low, which is somewhat reminiscent of the limited proteolytic activity observed with the catalytic domains of ADAMTSs (a disintegrin and metalloprotease with thrombospondin motifs) but is in contrast to the case of matrix metalloproteinase catalytic domains, which readily hydrolyze linear peptides and gelatin (35–37). On this basis, it is tempting to speculate that the catalytic domains of some metalloproteinases including AMZs and ADAMTSs may have very strict requirements in terms of the presence of additional motifs or domains to exhibit their full potential as proteolytic enzymes.

In this work, we have also analyzed the distribution of AMZ1 and AMZ2 in human tissues. These studies allowed us to detect the predominant expression of AMZ1 in liver and heart, whereas AMZ2 mRNA was mainly detected in heart and testis. This pattern of expression suggests that both AMZs are implicated in the development or physiology of these organs. Nevertheless, further studies will be required to validate at the protein level the observed distribution of AMZ RNAs in human

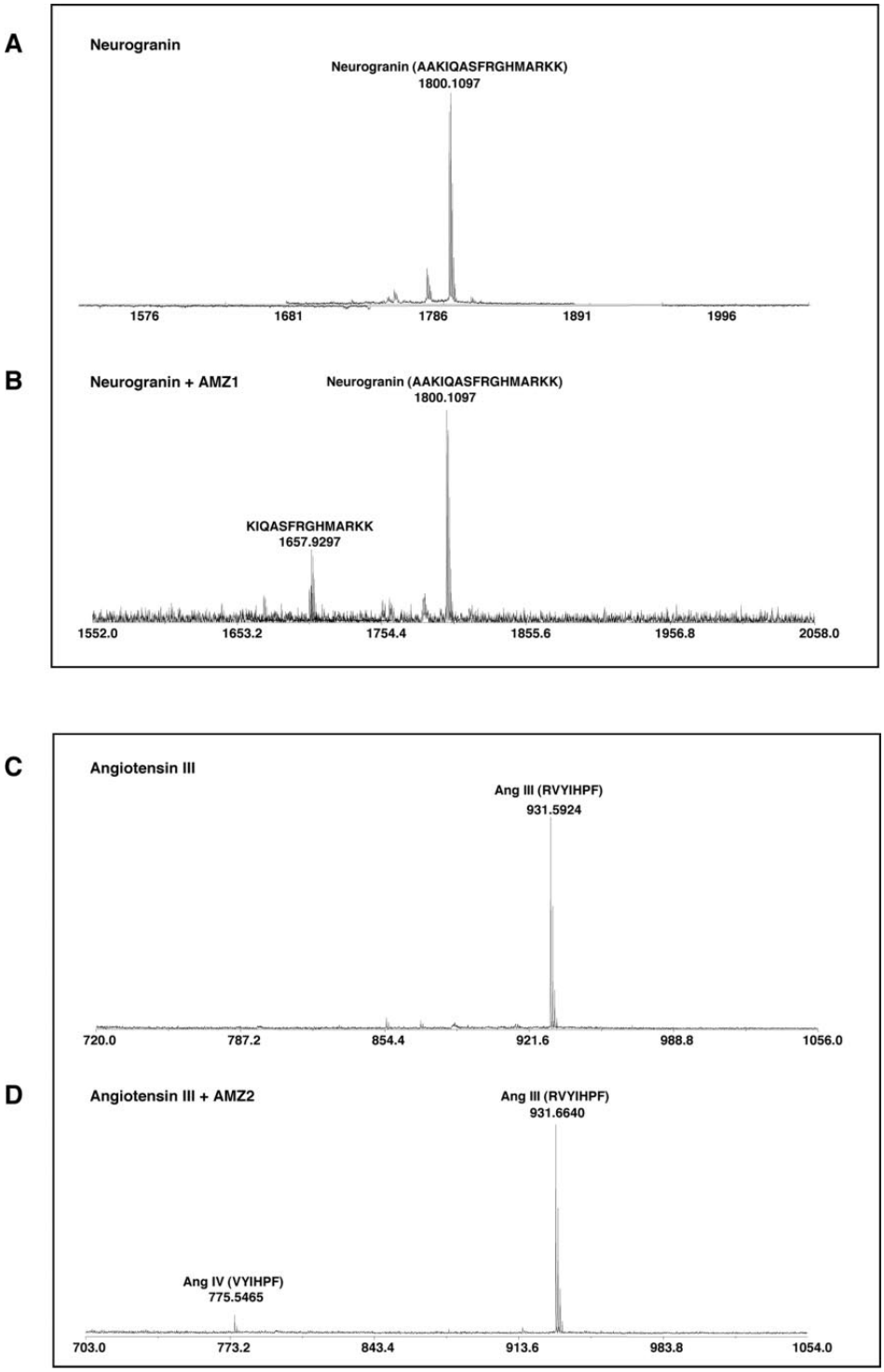

FIG. 6. **Mass spectrometry analysis of the biological peptide proteolysis catalyzed by AMZs.** Human neurogranin or angiotensin III were incubated alone (*A* and *C*, respectively) or in the presence of recombinant GST-AMZ1 (*B*) or GST-AMZ2 (*D*) for 2 h. The resulting peptide mixture was analyzed by mass spectrometry. The peaks corresponding to neurogranin (1800.1 Da), processed neurogranin (1657.9 Da), angiotensin III (931.6 Da), and angiotensin IV (775.4 Da) are shown.

tissues. Additional clues about the physiological and pathological roles of these enzymes may be derived from their chromosome locations at 7p22 and 17q24, respectively. Alterations in these regions have been frequently associated with cancer and other diseases such as hypertension or multiple sclerosis (38–41). Further studies will be required to ascertain whether AMZs could be a direct target of any of these genetic abnormalities resulting in cancer or other pathological conditions. Likewise, further experimental work, including the three-dimensional structural analysis of these enzymes and the generation of mutant organisms deficient in these proteases, will be necessary to clarify their functional roles and to define their precise relevance in the context of the growing complexity of proteolytic systems operating in all living organisms.

Acknowledgments—We thank G. Velasco, J. P. Freije, A. M. Pendás, S. Cal, L. M. Sánchez, and X. S. Puente for helpful comments, and S. Alvarez for excellent technical assistance.

REFERENCES

1. Lopez-Otin, C., and Overall, C. M. (2002) *Nat. Rev. Mol. Cell Biol.* **3,** 509–519
2. Glickman, M. H., and Ciechanover, A. (2002) *Physiol. Rev.* **82,** 373–428
3. Inada, M., Wang, Y., Byrne, M. H., Rahman, M. U., Miyaura, C., Lopez-Otin, C., and Krane, S. M. (2004) *Proc. Natl. Acad. Sci. U. S. A.* **101,** 17192–17197
4. Blobel, C. P. (2005) *Nat. Rev. Mol. Cell Biol.* **6,** 32–43
5. Curry, T. E., Jr., and Osteen, K. G. (2003) *Endocr. Rev.* **24,** 428–465
6. Noel, A., Maillard, C., Rocks, N., Jost, M., Chabottaux, V., Sounni, N. E., Maquoi, E., Cataldo, D., and Foidart, J. M. (2004) *J. Clin. Pathol.* **57,** 577–584
7. Di Cera, E. (2003) *Chest* **124,** 11S–17S
8. Riedl, S. J., and Shi, Y. (2004) *Nat. Rev. Mol. Cell Biol.* **5,** 897–907
9. Marino, G., Uria, J. A., Puente, X. S., Quesada, V., Bordallo, J., and Lopez-Otin, C. (2003) *J. Biol. Chem.* **278,** 3671–3678
10. Baker, A. H., Edwards, D. R., and Murphy, G. (2002) *J. Cell Sci.* **115,** 3719–3727
11. Apte, S. S. (2004) *Int. J. Biochem. Cell Biol.* **36,** 981–985
12. Liu, J., Sukhova, G. K., Sun, J. S., Xu, W. H., Libby, P., and Shi, G. P. (2004) *Arterioscler. Thromb. Vasc. Biol.* **24,** 1359–1366
13. Marjaux, E., Hartmann, D., and De Strooper, B. (2004) *Neuron* **42,** 189–192
14. Overall, C. M., and Lopez-Otin, C. (2002) *Nat. Rev. Cancer* **2,** 657–672
15. Borgono, C. A., and Diamandis, E. P. (2004) *Nat. Rev. Cancer* **4,** 876–890
16. Puente, X. S., Sanchez, L. M., Gutierrez-Fernandez, A., Velasco, G., and Lopez-Otin, C. (2005) *Biochem. Soc. Trans.* **33,** 331–334
17. Puente, X. S., Sanchez, L. M., Overall, C. M., and Lopez-Otin, C. (2003) *Nat. Rev. Genet.* **4,** 544–558
18. Puente, X. S., and Lopez-Otin, C. (2004) *Genome Res.* **14,** 609–622
19. Rawlings, N. D., Tolle, D. P., and Barrett, A. J. (2004) *Nucleic Acids Res.* **32,** D160–D164
20. Quesada, V., Sanchez, L. M., Alvarez, J., and Lopez-Otin, C. (2004) *J. Biol. Chem.* **279,** 26627–26634
21. Gomis-Ruth, F. X. (2003) *Mol. Biotechnol.* **24,** 157–202
22. Llamazares, M., Cal, S., Quesada, V., and Lopez-Otin, C. (2003) *J. Biol. Chem.* **278,** 13382–13389
23. Bult, C. J., White, O., Olsen, G. J., Zhou, L., Fleischmann, R. D., Sutton, G. G., Blake, J. A., FitzGerald, L. M., Clayton, R. A., Gocayne, J. D., Kerlavage, A. R., Dougherty, B. A., Tomb, J. F., Adams, M. D., Reich, C. I., Overbeek, R., Kirkness, E. F., Weinstock, K. G., Merrick, J. M., Glodek, A., Scott, J. L., Geoghagen, N. S. M., and Venter, J. C. (1996) *Science* **273,** 1058–1073
24. Slesarev, A. I., Mezhevaya, K. V., Makarova, K. S., Polushin, N. N., Shcherbinina, O. V., Shakhova, V. V., Belova, G. I., Aravind, L., Natale, D. A., Rogozin, I. B., Tatusov, T. L., Wolf, Y. I., Stetter, K. O., Malykh, A. G., Koonin, E. V., and Kozyavkin, S. A. (2002) *Proc. Natl. Acad. Sci. U. S. A.* **99,** 4644–4649
25. Maeder, D. L., Weiss, R. B., Dunn, D. M., Cherry, J. L., Gonzalez, J. M., DiRuggiero, J., and Robb, F. T. (1999) *Genetics* **152,** 1299–1305
26. Fukui, T., Atomi, H., Kanai, T., Matsumi, R., Fujiwara, S., and Imanaka, T. (2005) *Genome Res.* **15,** 352–363
27. Northrop, D. B. (1999) *Adv. Enzymol Relat. Areas Mol. Biol.* **73,** 25–55
28. Forterre, P., Bouthier De La Tour, C., Philippe, H., and Duguet, M. (2000) *Trends Genet.* **16,** 152–154
29. Nesbo, C. L., L'Haridon, S., Stetter, K. O., and Doolittle, W. F. (2001) *Mol. Biol. Evol.* **18,** 362–375
30. Diaz-Perales, A., Quesada, V., Sanchez, L. M., Ugalde, A. P., Suarez, M. F., Fueyo, A., and Lopez-Otin, C. (2005) *J. Biol. Chem.* **280,** 14310–14317
31. Lander, E. S., Linton, L. M., Birren, B., Nusbaum, C., Zody, M. C., Baldwin, J., Devon, K., Dewar, K., Doyle, M., FitzHugh, W., Funke, R., Gage, D., Harris, K., Heaford, A., Howland, J., Kann, L., Lehoczky, J., LeVine, R., McEwan, P., McKernan, K., Meldrim, J., Mesirov, J. P., Miranda, C., Morris, W., Naylor, J., Raymond, C., Rosetti, M., Santos, R., Sheridan, A., Sougnez, C., Stange-Thomann, N., Stojanovic, N., Subramanian, A., Wyman, D., Rogers, J., Sulston, J., Ainscough, R., Beck, S., Bentley, D., Burton, J., Clee, C., Carter, N., Coulson, A., Deadman, R., Deloukas, P., Dunham, A., Dunham, I., Durbin, R., French, L., Grafham, D., Gregory, S., Hubbard, T., Humphray, S., Hunt, A., Jones, M., Lloyd, C., McMurray, A., Matthews, L., Mercer, S., Milne, S., Mullikin, J. C., Mungall, A., Plumb, R., Ross, M., Shownkeen, R., Sims, S., Waterston, R. H., Wilson, R. K., Hillier, L. W., McPherson, J. D., Marra, M. A., Mardis, E. R., Fulton, L. A., Chinwalla, A. T., Pepin, K. H., Gish, W. R., Chissoe, S. L., Wendl, M. C., Delehaunty, K. D., Miner, T. L., Delehaunty, A., Kramer, J. B., Cook, L. L., Fulton, R. S., Johnson, D. L., Minx, P. J., Clifton, S. W., Hawkins, T., Branscomb, E., Predki, P., Richardson, P., Wenning, S., Slezak, T., Doggett, N., Cheng, J. F., Olsen, A., Lucas, S., Elkin, C., Uberbacher, E., Frazier, M., Gibbs, R. A., Muzny, D. M., Scherer, S. E., Bouck, J. B., Sodergren, E. J., Worley, K. C., Rives, C. M., Gorrell, J. H., Metzker, M. L., Naylor, S. L., Kucherlapati, R. S., Nelson, D. L., Weinstock, G. M., Sakaki, Y., Fujiyama, A., Hattori, M., Yada, T., Toyoda, A., Itoh, T., Kawagoe, C., Watanabe, H., Totoki, Y., Taylor, T., Weissenbach, J., Heilig, R., Saurin, W., Artiguenave, F., Brottier, P., Bruls, T., Pelletier, E., Robert, C., Wincker, P., Smith, D. R., Doucette-Stamm, L., Rubenfield, M., Weinstock, K., Lee, H. M., Dubois, J., Rosenthal, A., Platzer, M., Nyakatura, G., Taudien, S., Rump, A., Yang, H., Yu, J., Wang, J., Huang, G., Gu, J., Hood, L., Rowen, L., Madan, A., Qin, S., Davis, R. W., Federspiel, N. A., Abola, A. P., Proctor, M. J., Myers, R. M., Schmutz, J., Dickson, M., Grimwood, J., Cox, D. R., Olson, M. V., Kaul, R., Shimizu, N., Kawasaki, K., Minoshima, S., Evans, G. A., Athanasiou, M., Schultz, R., Roe, B. A., Chen, F., Pan, H., Ramser, J., Lehrach, H., Reinhardt, R., McCombie, W. R., de la Bastide, M., Dedhia, N., Blocker, H., Hornischer, K., Nordsiek, G., Agarwala, R., Aravind, L., Bailey, J. A., Bateman, A., Batzoglou, S., Birney, E., Bork, P., Brown, D. G., Burge, C. B., Cerutti, L., Chen, H. C., Church, D., Clamp, M., Copley, R. R., Doerks, T., Eddy, S. R., Eichler, E. E., Furey, T. S., Galagan, J., Gilbert, J. G., Harmon, C., Hayashizaki, Y., Haussler, D., Hermjakob, H., Hokamp, K., Jang, W., Johnson, L. S., Jones, T. A., Kasif, S., Kaspryzk, A., Kennedy, S., Kent, W. J., Kitts, P., Koonin, E. V., Korf, I., Kulp, D., Lancet, D., Lowe, T. M., McLysaght, A., Mikkelsen, T., Moran, J. V., Mulder, N., Pollara, V. J., Ponting, C. P., Schuler, G., Schultz, J., Slater, G., Smit, A. F., Stupka, E., Szustakowski, J., Thierry-Mieg, D., Thierry-Mieg, J., Wagner, L., Wallis, J., Wheeler, R., Williams, A., Wolf, Y. I., Wolfe, K. H., Yang, S. P., Yeh, R. F., Collins, F., Guyer, M. S., Peterson, J., Felsenfeld, A., Wetterstrand, K. A., Patrinos, A., Morgan, M. J., Szustakowki, J., de Jong, P., Catanese, J. J., Osoegawa, K., Shizuya, H., Choi, S., and Chen, Y. J. (2001) *Nature* **409,** 860–921
32. Stanhope, M. J., Lupas, A., Italia, M. J., Koretke, K. K., Volker, C., and Brown, J. R. (2001) *Nature* **411,** 940–944
33. Salzberg, S. L., White, O., Peterson, J., and Eisen, J. A. (2001) *Science* **292,** 1903–1906
34. Roelofs, J., and Van Haastert, P. J. (2001) *Nature* **411,** 1013–1014
35. Kashiwagi, M., Enghild, J. J., Gendron, C., Hughes, C., Caterson, B., Itoh, Y., and Nagase, H. (2004) *J. Biol. Chem.* **279,** 10109–10119
36. Murphy, G., Allan, J. A., Willenbrock, F., Cockett, M. I., O'Connell, J. P., and Docherty, A. J. (1992) *J. Biol. Chem.* **267,** 9612–9618
37. Clark, I. M., and Cawston, T. E. (1989) *Biochem. J.* **263,** 201–206
38. Lafferty, A. R., Torpy, D. J., Stowasser, M., Taymans, S. E., Lin, J. P., Huggard, P., Gordon, R. D., and Stratakis, C. A. (2000) *J. Med. Genet.* **37,** 831–835
39. Kalikin, L. M., George, R. A., Keller, M. P., Bort, S., Bowler, N. S., Law, D. J., Chance, P. F., and Petty, E. M. (1999) *Genomics* **57,** 36–42
40. Chen, D. C., Saarela, J., Clark, R. A., Miettinen, T., Chi, A., Eichler, E. E., Peltonen, L., and Palotie, A. (2004) *Genome Res.* **14,** 1483–1492
41. Meuleman, J., Timmerman, V., Van Broeckhoven, C., and De Jonghe, P. (2001) *Neurogenetics* **3,** 115–118

V. Señalización del eje somatotrofo y contribución de los miRNAs a su regulación en el envejecimiento acelerado

Dada la creciente relevancia de la ruta de señalización de IGF-1 en los procesos de envejecimiento, decidimos analizar el estado de esta ruta en los ratones deficientes en la metaloproteasa Zmpste24, un modelo murino de la progeria humana de Hutchinson-Gilford. Estos estudios revelaron que los ratones mutantes presentan graves alteraciones del eje somatotrofo, caracterizadas por un drástico aumento en los niveles de GH y un importante descenso en los niveles de IGF-1. Asimismo, encontramos que la sobreexpresión anómala de miR-1 podría estar contribuyendo a esta desregulación del eje somatotrofo. Para dilucidar si estas alteraciones contribuyen al envejecimiento acelerado de estos ratones, realizamos un tratamiento con IGF-1 recombinante que condujo al restablecimiento del correcto balance de GH e IGF-1, mejoró sustancialmente los defectos asociados al envejecimiento de los ratones mutantes y extendió significativamente su esperanza de vida.

Artículo 5: Guillermo Mariño*, **Alejandro P. Ugalde***, Álvaro F. Fernández, Fernando G. Osorio, Antonio Fueyo, José M. P. Freije y Carlos López-Otín. "Insulin-like growth factor 1 treatment extends longevity in a mouse model of human premature aging by restoring somatotroph axis function"

* *Estos autores contribuyeron por igual a este trabajo*

Proc Natl Acad Sci USA, **107**(37): 16268-16273 (2010)

Aportación personal al trabajo

Mi contribución a este trabajo consistió en la determinación de los niveles de GH e IGF-1, así como en los análisis Western de la respuesta a GH. Además, contribuí al estudio de la expresión de diversos genes y microRNAs y a la confirmación de IGF-1 como diana de miR-1. Finalmente, colaboré en la elaboración del manuscrito y las figuras.

Insulin-like growth factor 1 treatment extends longevity in a mouse model of human premature aging by restoring somatotroph axis function

Guillermo Mariño[a,1], Alejandro P. Ugalde[a,1], Álvaro F. Fernández[a], Fernando G. Osorio[a], Antonio Fueyo[b], José M. P. Freije[a], and Carlos López-Otín[a,2]

[a]Departamento de Bioquímica y Biología Molecular and [b]Biología Funcional, Facultad de Medicina, Instituto Universitario de Oncología, Universidad de Oviedo, 33006 Oviedo, Spain

Edited by Cynthia Kenyon, University of California, San Francisco, CA, and approved August 4, 2010 (received for review March 2, 2010)

Zmpste24 (also called FACE-1) is a metalloproteinase involved in the maturation of lamin A, an essential component of the nuclear envelope. Zmpste24-deficient mice exhibit multiple defects that phenocopy human accelerated aging processes such as Hutchinson–Gilford progeria syndrome. In this work, we report that progeroid *Zmpste24*$^{-/-}$ mice present profound transcriptional alterations in genes that regulate the somatotroph axis, together with extremely high circulating levels of growth hormone (GH) and a drastic reduction in plasma insulin-like growth factor 1 (IGF-1). We also show that recombinant IGF-1 treatment restores the proper balance between IGF-1 and GH in *Zmpste24*$^{-/-}$ mice, delays the onset of many progeroid features, and significantly extends the lifespan of these progeroid animals. Our findings highlight the importance of IGF/GH balance in longevity and may be of therapeutic interest for devastating human progeroid syndromes associated with nuclear envelope abnormalities.

laminopathy | microRNA | progeria | protease | cancer

Aging is a natural process that affects most biological functions and appears to be a consequence of the accumulative action of different types of stressors. Among these, oxidative damage, telomere attrition, and the decline of DNA repair and protein turnover systems are thought to be major causes of aging (1, 2). Over the last few years, our knowledge of the molecular basis of aging has gained mechanistic insight from studies on progeroid syndromes in which features of human aging are manifested precociously or in an exacerbated form. The vast majority of progeroid syndromes are a consequence of inefficient DNA repair mechanisms or defective nuclear envelope assembly, which ultimately lead to DNA damage accumulation and chromosome instability (3). Thus, mutations in the gene encoding lamin A (an essential component of the nuclear envelope) or in *Zmpste24* (encoding a metalloproteinase involved in the maturation of lamin A) are responsible for several devastating human progeroid syndromes, including Hutchinson–Gilford progeria, atypical Werner syndrome, restrictive dermopathy, and mandibuloacral dysplasia (3–7). The elucidation of the molecular mechanisms underlying these diseases has been facilitated by the generation and analysis of *Lmna*- and *Zmpste24*-deficient mice, which exhibit profound nuclear architecture abnormalities and multiple histopathological defects that phenocopy human progeroid syndromes (8–12).

In recent years, somatotroph [i.e., growth hormone (GH)/insulin-like growth factor 1 (IGF-1)] signaling has been identified as a major regulator of longevity from nematodes to man (13). Paradoxically, studies have shown that reduced somatotroph signaling is a common feature of both long-lived model organisms and progeroid mice harboring alterations in DNA-repair mechanisms (14, 15). However, to date no studies have been undertaken to evaluate whether the down-regulation of IGF-1 signaling observed in premature aging is a beneficial adaptive response or a detrimental event that directly contributes to the development of progeroid features. In the present work, we report that *Zmpste24*$^{-/-}$ mice, which constitute an appropriate murine model of Hutchinson–Gilford progeria, demonstrate a clear dysregulation of somatotroph axis signaling. In addition, we show that this alteration is detrimental, given that *Zmpste24*$^{-/-}$ mice treated with recombinant IGF-1 show a clear amelioration of progeroid features and significantly extended longevity compared with untreated *Zmpste24*$^{-/-}$ mice.

Results

To gain insight into the alterations associated with the premature aging phenotype observed in *Zmpste24*$^{-/-}$ mice, and considering the increasing evidence for the importance of somatotroph axis regulation in longevity, we analyzed IGF-1 plasma levels in 1-, 2- and 4-mo-old progeroid mice. As shown in Fig. 1*A*, 1-mo-old *Zmpste24*$^{-/-}$ mice—which do not yet exhibit any obvious progeroid features—already demonstrate a significant reduction in circulating IGF-1 levels, which progressively declines as the mice prematurely age. Given that IGF-1 synthesis is regulated mainly by circulating GH, we measured plasma GH concentration in the same *Zmpste24*$^{-/-}$ mice. As shown in Fig. 1*A*, we found that although 1-mo-old mutant mice show circulating GH levels comparable to those from age-matched WT littermates, 2- and 4-mo-old progeroid mice show a drastic, progressive increase in circulating GH (~5- and 11-fold, respectively). To test whether the somatotroph alterations of mutant mice could be simply a consequence of their premature aging, we measured plasma levels of IGF and GH in 1- and 2-y-old WT mice from the same genetic background. As shown in Fig. 1*A*, the alterations in circulating IGF-1 and GH levels seen in *Zmpste24*$^{-/-}$ mice were not observed in aged WT controls. This suggests that the somatotroph deregulation of progeroid mice is not just a secondary consequence of their premature aging, but rather an early pathological situation that could contribute to the development of the progeroid phenotype and reduced lifespan characteristic of *Zmpste24*$^{-/-}$ mice. Reduced IGF-1 and increased circulating GH are common features of GH resistance, also known as Laron syndrome (LS) (16). Interestingly, some pathological features of LS are also found among the complex phenotypic manifestations of these progeroid mice. Both *Zmpste24*$^{-/-}$ mice and LS patients have reduced muscle development, strength, and endurance, as well as decreased bone mineral density, and both exhibit alopecia, skin atrophy, and hypoglycemia (8, 16, 17).

As a first step to elucidating the molecular determinants for the GH/IGF-1 axis alteration observed in *Zmpste24*$^{-/-}$ mice, we performed a detailed analysis of our previously reported transcriptome data of liver from these progeroid mice (9). In addition to the reported

Author contributions: G.M., A.P.U., J.M.P.F., and C.L.-O. designed research; G.M., A.P.U., Á.F.F., F.G.O., and A.F. performed research; G.M., A.P.U., F.G.O., A.F., J.M.P.F., and C.L.-O. analyzed data; and G.M., A.P.U., and C.L.-O. wrote the paper.

The authors declare no conflict of interest.

This article is a PNAS Direct Submission.

[1]G.M. and A.P.U. contributed equally to this work.

[2]To whom correspondence should be addressed. E-mail: clo@uniovi.es.

This article contains supporting information online at www.pnas.org/lookup/suppl/doi:10.1073/pnas.1002696107/-/DCSupplemental.

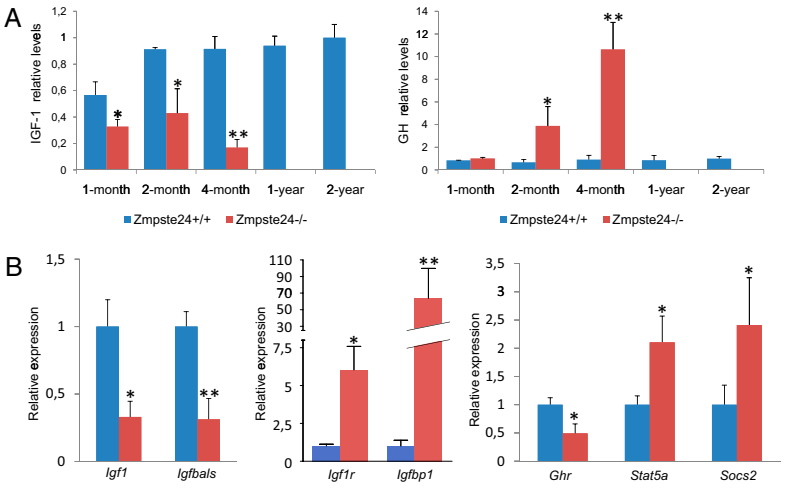

Fig. 1. Somatotroph axis alterations in *Zmpste24*$^{-/-}$ mice. (*A*) Plasma concentration of IGF-1 (*Left*) and GH (*Right*) in WT mice (blue bars) and *Zmpste24*$^{-/-}$ mice (red bars). The depicted values indicate a progressive reduction of circulating IGF-1 together with a progressive increase of plasma GH in *Zmpste24*$^{-/-}$ mice. (*B*) qPCR evaluation of mRNA levels of key genes for somatotroph axis in liver. Blue bars represent WT mice, whereas red bars correspond to *Zmpste24*$^{-/-}$ mice. Error bars indicate the SEM between replicates. At least eight WT and eight mutant animals were used for each assay. **P* < 0.05; ***P* < 0.005, one-tailed *t* test.

changes in glucose and lipid metabolism genes (17, 18) and the marked up-regulation of components of the p53-signaling pathway (9), we observed that many genes involved in somatotroph axis signaling were transcriptionally altered in the liver of *Zmpste24*$^{-/-}$ mice (Table 1). To further evaluate these results, we performed a quantitative PCR (qPCR) analysis of selected GH/IGF-1 axis genes in liver samples from *Zmpste24*$^{-/-}$ mice. As shown in Fig. 1*B*, mRNA levels of *IGF-1* were significantly lower in mutant mice compared with their control littermates. Similarly, mutant mice showed reduced levels of *Igfals* transcripts encoding the IGF-binding protein acid labile subunit, which has been associated with reduced levels of circulating IGF-1 in vivo (19, 20). In contrast, *Igfbp1*, the up-regulation of which is also associated with a reduced effective IGF-1 concentration (21), was transcriptionally up-regulated in *Zmpste24*$^{-/-}$ mice. Likewise, *IGF-1r* (IGF-1 receptor) mRNA levels were markedly increased in mutant mice, possibly reflecting a compensatory attempt to amplify the IGF-1 signaling. We also found alterations in genes involved in GH-mediated signaling. In fact, although liver mRNA levels of *Ghr* (growth hormone receptor) in *Zmpste24*$^{-/-}$ mice were lower than those found in WT animals, *Stat5a* (signal transducer and activator of transcription 5a) and *Socs2* (suppressor of cytokine signaling 2) mRNA levels were up-regulated in these progeroid mice (Fig. 2*B*). Although the functions of these two genes are antagonistic (*Socs2* down-regulates GH signaling, whereas *Stat5a* is one of the main transducers of this pathway), both genes are transcriptionally up-regulated in response to GH in the liver (22, 23). Therefore, the finding of increased mRNA levels for both factors in *Zmpste24*$^{-/-}$ progeroid mice is likely linked to the abnormally high circulating GH levels. Taken collectively, the transcriptional alterations in components of the somatotroph axis seen in *Zmpste24*$^{-/-}$ progeroid mice, together with the fact that *IGF-1* mRNA and protein levels remain reduced in presence of high circulating GH levels, point to a situation of GH resistance similar to that reported for some humans with Hutchinson–Gilford progeria (24). The finding that *Zmpste24*$^{-/-}$ male mice have very low levels of major urinary proteins (MUPs) (8) is also consistent with this situation, given that the synthesis of these proteins is dependent on somatotroph signaling (25, 26).

Considering the complexity of the somatotroph axis alterations found in *Zmpste24*$^{-/-}$ mice, we decided to evaluate in more detail the putative GH resistance observed in these progeroid animals. Thus, we analyzed the protein levels and relative phosphorylation of Jak2, Stat3, Stat5, and

Table 1. Liver transcriptome analysis of *Zmpste24*$^{-/-}$ reveals somatotroph axis transcriptional alterations

Gene name	Gene symbol	*Zmpste24*$^{-/-}$ vs. WT fold change
Signal transducer and activator of transcription 5B	*Stat5b*	7.55
IGF-binding protein 1	*Igfbp1*	6.37
Suppressor of cytokine signaling 3	*Socs3*	4.61
IGF-binding protein 3	*Igfbp3*	3.17
Suppressor of cytokine signaling 2	*Socs2*	2.20
Protein tyrosine phosphatase, nonreceptor type substrate 1	*Ptpns1*	2.09
Estrogen-related receptor, alpha	*Esrra*	1.84
Janus kinase 2	*Jak2*	1.28
Suppressor of cytokine signaling 1	*Socs1*	−1.28
Suppressor of cytokine signaling 5	*Socs5*	−1.41
Fibroblast growth factor receptor 4	*Fgfr4*	−1.52
Fibroblast growth factor 4	*Fgf4*	−1.67
Cytokine-inducible SH2-containing protein	*Cish*	−1.71
Insulin-like growth factor 1	*IGF-1*	−1.76
Growth hormone receptor	*Ghr*	−1.82
Insulin-like growth factor binding protein 5	*Igfbp5*	−1.98
Deiodinase, iodothyronine, type I	Dio1	−4.46
IGF-binding protein, acid labile subunit	Igfals	−7.24

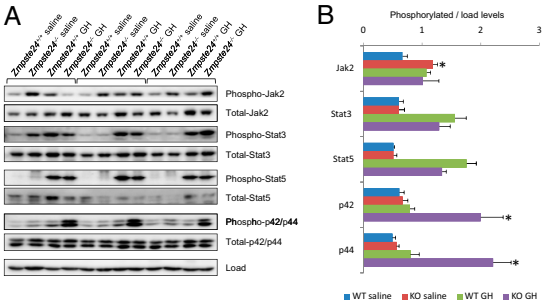

Fig. 2. GH-dependent transduction pathways analysis in *Zmpste24*$^{-/-}$ mice. Human recombinant GH was injected i.v. in overnight-fasted *Zmpste24*$^{+/+}$ and *Zmpste24*$^{-/-}$ mice. After 10 min, the mice were euthanized, and their livers were collected and flash-frozen. Liver response to GH was further analyzed by immunoblotting against major components of GH-induced signaling cascades. (*A*) Immunoblotting against total and phosphorylated forms of Jak2, Stat3, Stat5, and Erk1/2 in WT and *Zmpste24*$^{-/-}$ mice livers. (*B*) Densitometry analysis of the phosphorylated forms of GH-related signaling transducers shown in *A*. At least three WT and six mutant animals were used for each assay. $*P < 0.05$, two-tailed *t* test.

Erk1/2, all of which have been reported to be main effectors of GH stimulation (25), in response to i.v. GH injection. As shown in Fig. 2, stimulation with GH induced similar Jak2, Stat3, and Stat5 phosphorylation in the livers of both WT and *Zmpste24*$^{-/-}$ mice. However, whereas the GH-treated WT mice displayed only slight Erk1/2 activation, the GH-treated mutant mice exhibited strong phosphorylation of these proteins. Interestingly, we also found increased basal phosphorylation of Jak2 in *Zmpste24*$^{-/-}$ mice, which is consistent with the high levels of circulating GH in these animals. Conversely, basal phosphorylation levels of Stat3 and Stat5 were comparable in the mutant mice and WT livers. Taken together, these complex results indicate a nonuniform response among the multiple downstream effectors of GH and are likely a result of the multiple signaling alterations previously described in *Zmpste24*$^{-/-}$ mice (9, 17, 27). In this regard, the higher *Socs2* transcription levels displayed by mutant mice could specifically explain the absence of changes in Stat3 and Stat5, because Socs2 blocks the binding of Stat to GH receptor (28). Previous studies have shown that GH-mediated *IGF-1* transcription in vivo is dependent mainly on Stat5 activity (29); however, in vitro studies have shown that Mek inhibition stimulates *IGF-1* expression (30). Likewise, somatostatin has been reported to inhibit IGF-1 expression by activating the ERK-signaling pathway (31). Finally, the fact that human GH demonstrates a certain degree of lactogenic activity in mice must be considered (32). Thus, we cannot totally exclude the possibility that some of the complex and nonuniform signaling responses observed in progeroid mice after treatment with recombinant GH could be influenced by this phenomenon. Taken together, these results help explain the *IGF-1* mRNA down-regulation found in *Zmpste24*$^{-/-}$ mice. Nevertheless, it is likely that other signaling pathways also may contribute to the somatotroph axis changes seen in these mutant mice.

Additional signaling alterations, such as the previously described hyperactivation of p53 signaling (9) and down-regulation of the Wnt pathway (27), as well as the profound changes in glucose and lipid metabolism seen in *Zmpste24*$^{-/-}$ mice (18) might contribute to the observed decrease in *IGF-1* mRNA synthesis even in the presence of abnormally increased levels of circulating GH. Taking this into consideration, and given the increasing relevance of microRNAs (miRs) in the regulation of most physiological and pathological processes (33), we performed an exhaustive search of putative miRs predicted to target *Igf1*, because deregulation of miRs function could possibly help explain the observed paradoxical reduction in *Igf1* mRNA. Interestingly, we found that several miRs (miR-1, miR-26a and miR-27b) were predicted to target *IGF-1* (Fig. 3*A*). Consequently, we analyzed the transcriptional levels of these miRs in liver tissues from WT and progeroid mice. As shown in Fig. 3*A*, the expression levels of miR-26a and miR-27b in *Zmpste24*$^{-/-}$ mice liver tissues were similar to those seen in WT mice. In contrast, the expression of miR-1 was significantly higher in the liver, kidney, and muscle tissue of *Zmpste24*$^{-/-}$ mice compared with their WT littermates (Fig. 3*B*). Accordingly, we decided to analyze in more detail whether or not miR-1 is able to repress IGF-1. For this, we performed luciferase assays using a fusion of the 3′-UTR of murine *Igf1* downstream of the cDNA of Renilla luciferase. As shown in Fig. S1, we confirmed a functional binding site for miR-1 in the 3′-UTR of *IGF-1*. In addition, a 2-nt substitution in the putative seed sequence of miR-1 was sufficient to significantly reduce miR-1 repressive effect over the 3′-UTR of *IGF-1*, thus confirming that *IGF-1* is a bona fide target for miR-1. During the preparation of this manuscript, and consistent with our findings, it has been reported that miR-1 is able to target *IGF-1* in the context of cardiac and skeletal muscle physiology (34, 35), which supports our results. To further examine this putative link among miR-1, IGF-1, and progeroid syndromes, we analyzed miR-1 expression levels in cultured fibroblasts derived from patients with Hutchinson–Gilford progeria syndrome. As shown in Fig. 3*C*, these human progeroid cells also exhibited a marked transcriptional up-regulation of miR-1 compared with control fibroblasts. Interestingly, cultured murine fibroblasts subjected to persistent DNA damage also exhibited increased miR-1 mRNA levels (Fig. 3*D*). This finding also agrees with previous reports of reduced *IGF-1* expression in WT mice exposed to a low dose of chronic genotoxic stress (36), as well as with the fact that cells from both Hutchinson–Gilford progeria patients and *Zmpste24*$^{-/-}$ mice show increased DNA damage (37). Taken together, these findings suggest that miR-1 up-regulation occurs in both progeroid mice and human Hutchinson–Gilford progeria cells and likely contributes to somatotroph axis suppression by reducing IGF-1 synthesis, even in the presence of elevated circulating GH levels.

Finally, in this work we explored whether the detailed characterization of the somatotroph axis alterations observed in *Zmpste24*$^{-/-}$ mice could lead to the development of therapeutic strategies for human progeroid syndromes. We decided to first evaluate the effect of recombinant human IGF-1 (rIGF-1) treatment on *Zmpste24*$^{-/-}$ mice to test whether somatotroph axis restoration could ameliorate or aggravate their progeroid phenotype, including their reduced longevity. To provide continuous rIGF-1 delivery, we used subcutaneous osmotic pumps, which ensure uniform drug delivery into the systemic circulation. The successful delivery of rIGF-1 was further verified by ELISA analysis of human IGF-1 levels in treated mice (Fig. 4). Interestingly, *Zmpste24*$^{-/-}$ mice treated with rIGF-1 demonstrated substantial recovery of progeroid phenotypes (Fig. 4). Thus, rIGF-1 treatment improved body weight, increased the amount of subcutaneous fat, reduced the degree of kyphosis and alopecia, and significantly extended the longevity of *Zmpste24*$^{-/-}$ mice ($P = 0.025$, log-rank test) (Fig. 4). The median survival of treated *Zmpste24*$^{-/-}$ mice was extended from 123 d to 145 d, and the maximum survival was extended from 151 d to 187 d. Notably, all phenotypes rescued in *Zmpste24*$^{-/-}$ progeroid mice represent characteristic features of Hutchinson–Gilford progeria in humans. Moreover, 4-mo-old rIGF-1–treated mice had similar GH levels as WT mice, whereas age-matched saline-treated progeroid mice had dramatically increased circulating GH levels, suggesting that rIGF-1 treatment restored the observed somatotroph axis alterations of *Zmpste24*$^{-/-}$ mice. In fact, the 4-mo-old treated mice had normal MUP concentrations in urine (Fig. 4), providing additional support to the restoration of the GH/IGF-1 function in mutant mice treated with rIGF-1.

Discussion

In recent years, the effect of somatotroph axis alterations on lifespan extension has been a subject of extensive analysis (38). The first evidence pointing to a longevity regulatory role of IGF-1 signaling was reported in nematodes. In fact, worms lacking *Daf2*, the ortholog of mammalian insulin/IGF-1 receptor, have a dramatically increased lifespan (39). Similarly, flies harboring inactivating mutations in *InR* (the ortholog of *C. elegans Daf2* and mammalian *IR* and *IGF-1R*) have

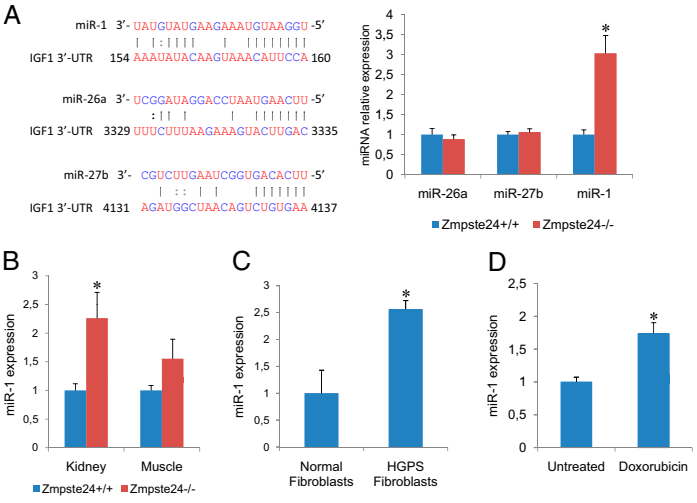

Fig. 3. miR-1 expression analysis in *Zmpste24*$^{-/-}$ mice and Hutchinson–Gilford progeria cells. (*A*) qPCR analysis of putative IGF-1 microRNAs. A selection of TargetScan-predicted microRNAs targeting IGF-1 (*Left*) were analyzed by qPCR in liver samples (*Right*) from WT (blue bars) and *Zmpste24*$^{-/-}$ mice (red bars). (*B*) miR-1 expression studies were extended to the indicated tissues from WT and *Zmpste24*$^{-/-}$ mice. (*C*) miR-1 expression levels in in human fibroblasts from patients with Hutchinson–Gilford progeria syndrome. (*D*) miR-1 expression levels in WT fibroblasts untreated and treated with 0.5 μM doxorubicin for 24 h.

a significantly increased lifespan (40). In mammals, both reduced insulin and IGF-1 signaling are commonly found in long-lived organisms. Thus, a reduction in IGF-1 signaling alone is sufficient to significantly extend the lifespan, at least in mice (41). More surprisingly, a pathological condition such as LS, which is associated with GH resistance and growth retardation, extends longevity in mice and confers some degree of cancer protection in humans (42). Notably, and despite their reduced growth rate and body size, LS mice exhibit reduced circulating IGF-1 levels and increased blood GH content and greater longevity compared with control animals (43). Thus, the finding that *Zmpste24*$^{-/-}$ progeroid mice present features of GH resistance similar to those seen in LS mice, as well as additional alterations associated with lifespan extension, such as increased autophagy (17), is both paradoxical and intriguing.

Previous reports have noted a number of unexpected similarities between phenotypic alterations found in murine models of premature aging and long-lived organisms, including reduced circulating IGF-1 levels (36, 44, 45). All these alterations seem to be part of an adaptive stress response aimed at preserving organism viability under compromising circumstances (14, 15). These features common to both long-lived and premature-aged individuals have been proposed to arise from a progressive and age-dependent accumulation of DNA damage, which is highly exacerbated in progeroid syndromes (46). In addition, DNA damage induction in vivo has been shown to lead to a series of alterations similar to those observed in both progeroid and long-lived animals (14, 44). Thus, it seems reasonable that long-lived organisms that have been able to overcome cancer, cardiovascular, or other life-threatening pathologies accumulate DNA damage with aging that eventually elicits an adaptive stress response similar to that observed at an early age in progeroid individuals. This response is aimed at reallocating resources from growth to somatic preservation, given that normal growth or proliferation rates in cells that accumulate a critical amount of DNA damage will unequivocally lead to replication defects, chromosomal instability, nuclear envelope abnormalities, and, finally, the development of cancer (15). It is tempting to speculate that if this putative adaptive response fails to counteract the detrimental effects of DNA damage accumulation, then progeroid mice will finally succumb to cancer. Conversely, if this strategy is successful, then progeroid mice that have acquired features of long-lived organisms will exhibit reduced metabolic and growth rates, but not the characteristic lifespan reduction. This could be due to overactivation of antiproliferative pathways induced by the massive accumulation of DNA damage, which leads to a systemic senescent state and finally to premature death. The somatotroph axis alterations found in *Zmpste24*$^{-/-}$ progeroid mice could constitute a clear example of redundant oversuppression of a growth-

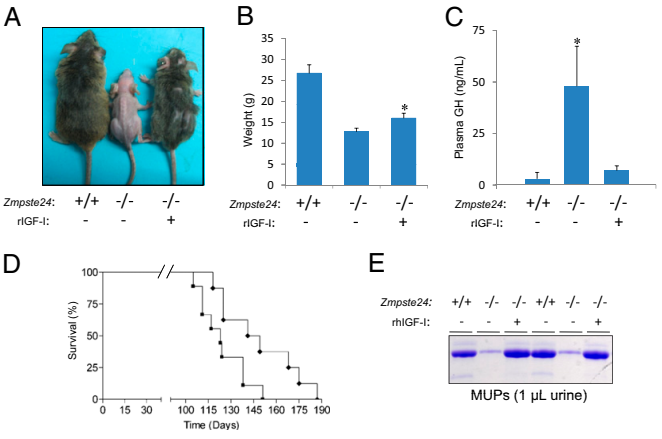

Fig. 4. Recombinant IGF-1 treatment ameliorates *Zmpste24*-deficient mice progeroid phenotypes. (*A*) Representative photographs of 4-mo-old *Zmpste24*$^{+/+}$ and *Zmpste24*$^{-/-}$ mice untreated and treated with recombinant human IGF-1. (*B*) Total body weight of 3-mo-old *Zmpste24*$^{+/+}$ ($n = 6$), *Zmpste24*$^{-/-}$ ($n = 8$), and treated *Zmpste24*$^{-/-}$ ($n = 8$) mice. The treated mice exhibit a significant recovery of the total body weight. (*C*) Recombinant IGF-1 treatment restores GH levels of 4-mo-old *Zmpste24*$^{-/-}$ mice to those observed in their age-matched WT littermates. (*D*) Kaplan-Meier graph showing a significant increment of the maximum life span in IGF-1–treated *Zmpste24*$^{-/-}$ mice (diamonds; $n = 8$) compared with untreated mice (squares; $n = 8$). (*E*) Representative SDS/PAGE gel showing normal MUPs urine content in 4-mo-old *Zmpste24*$^{-/-}$ mice treated with recombinant IGF-1.

promoting pathway. In fact, progeroid mice show alterations in multiple regulators of GH-mediated signaling, including up-regulation of *Socs2* and *Igfbp1* together with down-regulation of *Igfl*, *Igfals*, and *Ghr* genes, clearly pointing to an strategy of growth suppression. Moreover, the marked up-regulation of miR-1 observed in both *Zmpste24*$^{-/-}$ mice and Hutchinson-Gilford Progeria syndrome cells likely contributes to the exacerbated suppression of liver IGF-1 synthesis observed in progeroid mice, even in the presence of high circulating GH levels.

The possibility that the dramatically increased circulating GH levels could constitute one of the main determinants of the premature aging of *Zmpste24*$^{-/-}$ mice should be considered as well. In fact, although progeroid mice demonstrate liver GH resistance in terms of IGF-1 synthesis, they show no significant alteration in Jak/Stat pathway activation after i.v. GH injection. Thus, it is possible that the observed supraphysiological circulating GH levels could directly elicit a variety of detrimental responses in peripheral tissues, which could contribute to the development of premature aging. Interestingly, liver-specific knockout mice with reduced IGF-1 and increased GH circulating levels exhibited metabolic defects that could be corrected by the administration of a GH antagonist (47). This demonstrates that high levels of circulating GH can be detrimental and contribute to a shortened lifespan. Moreover, giant GH transgenic mice were found to have several features of accelerated aging (48), supporting the idea that the increased GH levels in *Zmpste24*$^{-/-}$ mice could contribute to the organismal wasting that accompanies accelerated aging. In contrast, the increased longevity seen in LS mice indicates that somatotroph axis-linked regulation of longevity is precisely fine-tuned. Consistently, our finding that rIGF-1 administration extends longevity and ameliorates several progeroid features of *Zmpste24*$^{-/-}$ mice suggests that the intensity of the systemic adaptive response seen in premature aging conditions is excessive and must be modulated to extend longevity. Thus, although the complete elimination of the antiproliferative alterations observed in progeroid mice would likely result in cancer, the selective modification of some signaling pathways in these mice could be beneficial for extending longevity. Accordingly, we have previously shown that a reduction in p53 signaling delays the onset of progeroid features and increases the lifespan in *Zmpste24*$^{-/-}$ mice (9). Our observation that rIGF-1–mediated restoration of somatotroph axis status—altered in both accelerated aging models and some progeria patients (24, 45)—extends longevity in mice points in the same direction. IGF-1 has proven effective in treating GH-refractory somatotroph alterations in humans with no significant detrimental effects (49). Accordingly, rIGF-1 treatment, alone or in combination with other drugs, such as statins and bisphosphonates (50), merits exploration as a therapeutic approach to slow disease progression in children with progeria.

Materials and Methods

Transgenic Animals. Mutant mice deficient in Zmpste24 metalloproteinase have been described previously (8). All animal experiments were conducted in accordance with the guidelines of the University of Oviedo's Committee on Animal Experimentation.

Recombinant IGF-1 Administration. Mice were treated with recombinant human IGF-1 (Prospec) at a daily dose of 1 mg/kg of body mass. IGF-1 dissolved in 10 mmol/L of HCl and sterile isotonic saline at a concentration of 8.3 mg/mL was loaded into a miniosmotic pump (model 1004; Alzet) that had a pumping rate of 0.125 μL/h (3 μL/d) for 28 d. Loaded pumps were primed in isotonic saline at 37 °C for 24 h before implantation. Mice assigned to receive IGF-1 were anesthetized with isoflurane such that they were unresponsive to tactile stimuli, whereupon an incision was made in the skin in the middle of the spinal curvature and an s.c. pocket was created via blunt dissection with surgical scissors. Pumps were inserted into the s.c. space with the flow regulator cap directed distally, and the incision was closed with Michel clips. After 28 d of continuous IGF-1 administration, the pumps were replaced with freshly loaded and primed units to enable a further 28 d of treatment by the same procedure. On removal, the pumps were aspirated to ensure that fouling had not occurred and that the contents had been administered appropriately.

Immunoblot Analysis. After extraction, mouse tissues were immediately frozen in liquid nitrogen and then homogenized in a 20 mM Tris buffer (pH 7.4) containing 150 mM NaCl, 1% Triton X-100, and 10 mM EDTA, Complete Protease Inhibitor Mixture (Roche Applied Science), and phosphatase inhibitors (200 μM sodium orthovanadate, 1 mM β-glycerophosphate). Once homogenized, tissue extracts were centrifuged at 12,000 × *g* and 4 °C, and supernatants were collected. Supernatant protein concentration was evaluated by the bicinchoninic acid technique (Pierce BCA Protein Assay Kit). Then 25 μg of each protein sample was loaded onto 8% SDS-polyacrylamide gels. After electrophoresis, the gels were electrotransferred onto nitrocellulose filters, and the filters were then blocked with 5% nonfat dried milk in PBT (PBS with 0.05% Tween 20) and incubated with primary antibodies in 5% BSA in PBT. After three washes with PBT, filters were incubated with HRP-conjugated goat anti-rabbit IgG at a 1:10,000 dilution in 1.5% milk in PBT, and developed with a West Pico enhanced chemiluminescence kit (Pierce). All of the antibodies used in this work were obtained from Cell Signaling.

Blood and Plasma Parameters. The mice were starved for 5 h to avoid any possible alteration in blood parameters due to food intake before measurements. After the mice were anesthetized with isoflurane, blood was extracted directly from the heart. Plasma was obtained as described previously (17). In brief, blood was centrifuged immediately after collection at 3,000 × *g* and 4 °C, and the supernatant was collected and stored at −70 °C until analysis. Plasma IGF-1 concentration was determined using the R&D Systems Quantikine ELISA kit, whereas plasma GH concentration was measured using the Linco ELISA kit, according to the manufacturer's instructions.

RNA Preparation. Collected tissue was immediately homogenized in TRIzol reagent (Invitrogen) and processed on the same day through alcohol precipitation. RNA pellets were then washed in cold 80% ethanol and stored at −80 °C until further use. After resuspension of RNA in nuclease-free water (Ambion), the samples were quantified and evaluated for purity (260 nm/280 nm ratio) using a NanoDrop ND-1000 spectrophotometer, and 100 μg of each sample was further purified using Qiagen RNeasy spin columns according to the manufacturer's instructions.

Analysis of Liver Response to GH Injection. Recombinant human GH was injected i.v. with a 5 mg/kg dose in 3.5-mo-old *Zmpste24* WT and KO mice fasted overnight. At 10 min after GH injection, the mice were killed, and their livers were collected and flash-frozen in liquid nitrogen. Liver response to GH was analyzed by immunoblotting using antibodies against major components of GH-induced signaling cascades.

Quantitative RT-PCR Analysis. cDNA was synthesized using 1–5 μg of total RNA, 0.14 mM oligo(dT) (22-mer) primer, 0.2 mM concentrations of each dNTP, and SuperScript II reverse transcriptase (Invitrogen). Quantitative RT-PCR (qRT-PCR) was carried out in triplicate for each sample using 20 ng of cDNA, TaqMan Universal PCR Master Mix (Applied Biosystems), and 1 μL of the specific TaqMan custom gene expression assay for the gene of interest (Applied Biosystems). To quantify gene expression, PCR was performed at 95 °C for 10 min and at 50 °C for 2 min, followed by 40 cycles of 95 °C for 15 s and 60 °C for 1 min, using an Applied Biosystems 7300 real-time PCR system. As an internal control for the amount of template cDNA used, gene expression was normalized to the mouse β-actin gene using the mouse β-actin endogenous control (VIC/MGB probe; primer limited) TaqMan gene expression assay (Applied Biosystems). Relative expression of the distinct analyzed genes was calculated according to the manufacturer's instructions. In brief, the analyzed gene expression was normalized to β-actin in WT or *Zmpste24*$^{-/-}$ derived samples, using the following formula: the mean values of $2^{\Delta CTgene\ (gene\ of\ interest)-\Delta CTgene\ (\beta\text{-}actin)}$ for at least six different WT animals were considered 100% for each analyzed gene, and the same values for *Zmpste24*$^{-/-}$ mice tissues were referred to those values, as described previously (51).

Luciferase Assays. Computational prediction of the conserved miR-binding sites in the mouse *IGF-1* 3′-UTR was carried out using TargetScan software (http://www.targetscan.org). The entire 3′-UTR sequence of *IGF-1* was cloned into psiCHECK-2 plasmid (Promega) downstream of the Renilla luciferase ORF using the restriction enzymes XhoI and NotI. HEK-293 cells were seeded 6 h before transfection in 24-well plates at 50% of confluence in growth media without antibiotics. Tranfections were performed using Lipofectamine 2000 (Invitrogen), 250 ng of each psiCHECK-2 construct, and 20 pmol of miR-1 or control miR molecules (Ambion), following the manufacturer's instructions. Transfection was carried out for 4 h, after which the medium was removed and cells were left to recover for 18 h. Luciferase activity was measured using the Promega Dual-Luciferase Reporter Assay System. In brief, cells on 24-well plates were washed with PBS and lysed by pipetting up and down in the well using 80 μL of the passive lysis buffer. Then both Renilla (reporter gene) and

firefly (endogenous control) luciferase activity of each sample were measured in a Turner Biosystems TD-20/20 luminometer. Each assay was carried out in triplicate, and Renilla activity was normalized to the firefly activity detected in the same sample.

miRNA analysis. Total RNA was prepared using the Ambion miRVANA miRNA Isolation Kit, and RNA samples were quantified and evaluated for purity (260 nm/280 nm ratio) using a NanoDrop ND-1000 spectrophotometer. miRNA detection was performed using TaqMan miRNA expression assays (Applied Biosystems). In brief, 10 ng of total RNA was reverse-transcribed using the TaqMan miRNA Reverse-Transcription Kit (Applied Biosystems) and PCR-amplified using the Applied Biosystems 7300 Real-Time PCR System. As an internal control, miRNA expression was normalized to snoRNA202 for mouse samples and to RNU6B for human samples, using TaqMan Gene Expression Assays (Applied Biosystems). All of the protocols were carried out according to the manufacturer's instructions.

Cell Culture. Human Hutchinson–Gilford progeria syndrome cells (AG11498) were obtained from the Coriell Cell Repository. Cultures were maintained in DMEM (Gibco) supplemented with 10% FBS and 1% penicillin-streptomycin-glutamine (Gibco). Murine fibroblasts were extracted from 12-wk-old mice ears. The ears were sterilized with ethanol, washed with PBS, and triturated with razor blades. The resulting samples were incubated with 600 μL of 4-mg/mL collagenase D (Roche) and 4 mg/mL of dispase II (Roche) in DMEM for 45 min in 5% CO_2 at 37 °C. After filtering and washing, 6 mL of DMEM with 10% FBS and 1% antibiotic-antimycotic were added, and the mixture was incubated in 5% CO_2at 37 °C. Approximately 10^6 cells were passed in a 10-cm plate every 3 d and cultured under standard conditions. For DNA damage induction, murine fibroblasts were seeded in six-well plates; after 24 h, doxorubicin (Sigma-Aldrich) was added to the growing media at 0.5 μM, and 24 h later, RNA was extracted and miR-1 expression analyzed.

Statistical Analysis. All experimental data are reported as means; error bars represent SEM. Statistical analysis was performed with the nonparametric Student *t* test using GraphPad Prism version 4.0. Kaplan-Meier survival analysis was performed using the MedCalc statistical package.

ACKNOWLEDGMENTS. We thank Drs. A. Astudillo and A. J. Ramsay for helpful comments and F. Rodríguez, S. Álvarez, M. Fernández, and D. Álvarez for excellent technical assistance. This work was supported by grants from Ministerio de Ciencia e Innovación-Spain, Fundación "M. Botín," and European Union (FP7 MicroEnviMet). The Instituto Universitario de Oncología is supported by Obra Social Cajastur and Acción Transversal del Cáncer-Red Temática de Investigación Cooperativa en Cáncer.

1. Kirkwood TB (2005) Understanding the odd science of aging. *Cell* 120:437–447.
2. Vijg J, Campisi J (2008) Puzzles, promises and a cure for ageing. *Nature* 454:1065–1071.
3. Ramírez CL, Cadiñanos J, Varela I, Freije JM, López-Otín C (2007) Human progeroid syndromes, aging and cancer: New genetic and epigenetic insights into old questions. *Cell Mol Life Sci* 64:155–170.
4. Hennekam RC (2006) Hutchinson–Gilford progeria syndrome: Review of the phenotype. *Am J Med Genet A* 140:2603–2624.
5. Kudlow BA, Kennedy BK, Monnat RJ, Jr. (2007) Werner and Hutchinson–Gilford progeria syndromes: Mechanistic basis of human progeroid diseases. *Nat Rev Mol Cell Biol* 8:394–404.
6. Pereira S, et al. (2008) HGPS and related premature aging disorders: From genomic identification to the first therapeutic approaches. *Mech Ageing Dev* 129:449–459.
7. Gruenbaum Y, Margalit A, Goldman RD, Shumaker DK, Wilson KL (2005) The nuclear lamina comes of age. *Nat Rev Mol Cell Biol* 6:21–31.
8. Pendás AM, et al. (2002) Defective prelamin A processing and muscular and adipocyte alterations in Zmpste24 metalloproteinase-deficient mice. *Nat Genet* 31:94–99.
9. Varela I, et al. (2005) Accelerated ageing in mice deficient in Zmpste24 protease is linked to p53 signalling activation. *Nature* 437:564–568.
10. Osorio FG, Obaya AJ, López-Otín C, Freije JM (2009) Accelerated ageing: From mechanism to therapy through animal models. *Transgenic Res* 18:7–15.
11. Bergo MO, et al. (2002) *Zmpste24* deficiency in mice causes spontaneous bone fractures, muscle weakness, and a prelamin A processing defect. *Proc Natl Acad Sci USA* 99:13049–13054.
12. Sullivan T, et al. (1999) Loss of A-type lamin expression compromises nuclear envelope integrity leading to muscular dystrophy. *J Cell Biol* 147:913–920.
13. Russell SJ, Kahn CR (2007) Endocrine regulation of ageing. *Nat Rev Mol Cell Biol* 8: 681–691.
14. Garinis GA, et al. (2009) Persistent transcription-blocking DNA lesions trigger somatic growth attenuation associated with longevity. *Nat Cell Biol* 11:604–615.
15. Hoeijmakers JH (2009) DNA damage, aging, and cancer. *N Engl J Med* 361:1475–1485.
16. Laron Z (2004) Laron syndrome (primary growth hormone resistance or insensitivity): The personal experience 1958–2003. *J Clin Endocrinol Metab* 89:1031–1044.
17. Mariño G, et al. (2008) Premature aging in mice activates a systemic metabolic response involving autophagy induction. *Hum Mol Genet* 17:2196–2211.
18. Mariño G, López-Otín C (2008) Autophagy and aging: New lessons from progeroid mice. *Autophagy* 4:807–809.
19. Ueki I, et al. (2000) Inactivation of the acid labile subunit gene in mice results in mild retardation of postnatal growth despite profound disruptions in the circulating insulin-like growth factor system. *Proc Natl Acad Sci USA* 97:6868–6873.
20. Domené HM, Bengolea SV, Jasper HG, Boisclair YR (2005) Acid-labile subunit deficiency: Phenotypic similarities and differences between human and mouse. *J Endocrinol Invest* 28 (5):Suppl):43–46.
21. Gay E, et al. (1997) Liver-specific expression of human insulin-like growth factor binding protein-1 in transgenic mice: Repercussions on reproduction, ante- and perinatal mortality and postnatal growth. *Endocrinology* 138:2937–2947.
22. Ortiz BL, Sánchez-Gómez M, Norstedt G (2000) Comparison of STAT5 mRNA levels in GH-treated male and female rats analysed by a solution hybridization assay. *Growth Horm IGF Res* 10:236–241.
23. Tollet-Egnell P, Flores-Morales A, Stavréus-Evers A, Sahlin L, Norstedt G (1999) Growth hormone regulation of SOCS-2, SOCS-3, and CIS messenger ribonucleic acid expression in the rat. *Endocrinology* 140:3693–3704.
24. Abdenur JE, Brown WT, Friedman S, Smith M, Lifshitz F (1997) Response to nutritional and growth hormone treatment in progeria. *Metabolism* 46:851–856.
25. Rowland JE, et al. (2005) In vivo analysis of growth hormone receptor signaling domains and their associated transcripts. *Mol Cell Biol* 25:66–77.
26. Norstedt G, Palmiter R (1984) Secretory rhythm of growth hormone regulates sexual differentiation of mouse liver. *Cell* 36:805–812.
27. Espada J, et al. (2008) Nuclear envelope defects cause stem cell dysfunction in premature-aging mice. *J Cell Biol* 181:27–35.
28. Flores-Morales A, Greenhalgh CJ, Norstedt G, Rico-Bautista E (2006) Negative regulation of growth hormone receptor signaling. *Mol Endocrinol* 20:241–253.
29. Barclay JL, et al. (2010) In vivo targeting of the growth hormone receptor (GHR) Box1 sequence demonstrates that the GHR does not signal exclusively through JAK2. *Mol Endocrinol* 24:204–217.
30. Frost RA, Nystrom GJ, Lang CH (2002) Regulation of IGF-1 mRNA and signal transducers and activators of transcription-3 and -5 (Stat-3 and -5) by GH in C2C12 myoblasts. *Endocrinology* 143:492–503.
31. Hagemeister AL, Sheridan MA (2008) Somatostatin inhibits hepatic growth hormone receptor and insulin-like growth factor I mRNA expression by activating the ERK and PI3K signaling pathways. *Am J Physiol Regul Integr Comp Physiol* 295:R490–R497.
32. Fuh G, Colosi P, Wood WI, Wells JA (1993) Mechanism-based design of prolactin receptor antagonists. *J Biol Chem* 268:5376–5381.
33. Bushati N, Cohen SM (2007) MicroRNA functions. *Annu Rev Cell Dev Biol* 23:175–205.
34. Shan ZX, et al. (2009) Up-regulated expression of miR-1/miR-206 in a rat model of myocardial infarction. *Biochem Biophys Res Commun* 381:597–601.
35. Elia L, et al. (2009) Reciprocal regulation of microRNA-1 and insulin-like growth factor-1 signal transduction cascade in cardiac and skeletal muscle in physiological and pathological conditions. *Circulation* 120:2377–2385.
36. van der Pluijm I, et al. (2007) Impaired genome maintenance suppresses the growth hormone—insulin-like growth factor 1 axis in mice with Cockayne syndrome. *PLoS Biol* 5:e2.
37. Liu B, et al. (2005) Genomic instability in laminopathy-based premature aging. *Nat Med* 11:780–785.
38. Bartke A (2005) Minireview: Role of the growth hormone/insulin-like growth factor system in mammalian aging. *Endocrinology* 146:3718–3723.
39. Kenyon C, Chang J, Gensch E, Rudner A, Tabtiang R (1993) A *C. elegans* mutant that lives twice as long as wild type. *Nature* 366:461–464.
40. Tatar M, et al. (2001) A mutant *Drosophila* insulin receptor homolog that extends life span and impairs neuroendocrine function. *Science* 292:107–110.
41. Holzenberger M, et al. (2003) IGF-1 receptor regulates lifespan and resistance to oxidative stress in mice. *Nature* 421:182–187.
42. Laron Z (2008) The GH-IGF-1 axis and longevity: The paradigm of IGF-1 deficiency. *Hormones (Athens)* 7:24–27.
43. Coschigano KT, et al. (2003) Deletion, but not antagonism, of the mouse growth hormone receptor results in severely decreased body weights, insulin, and insulin-like growth factor I levels and increased life span. *Endocrinology* 144:3799–3810.
44. Niedernhofer LJ, et al. (2006) A new progeroid syndrome reveals that genotoxic stress suppresses the somatotroph axis. *Nature* 444:1038–1043.
45. van de Ven M, et al. (2006) Adaptive stress response in segmental progeria resembles long-lived dwarfism and calorie restriction in mice. *PLoS Genet* 2:e192.
46. Garinis GA, van der Horst GT, Vijg J, Hoeijmakers JH (2008) DNA damage and ageing: New-age ideas for an age-old problem. *Nat Cell Biol* 10:1241–1247.
47. Yakar S, et al. (2004) Inhibition of growth hormone action improves insulin sensitivity in liver IGF-1–deficient mice. *J Clin Invest* 113:96–105.
48. Wolf E, et al. (1993) Effects of long-term elevated serum levels of growth hormone on life expectancy of mice: Lessons from transgenic animal models. *Mech Ageing Dev* 68: 71–87.
49. Clemmons DR (2007) Modifying IGF-1 activity: An approach to treat endocrine disorders, atherosclerosis and cancer. *Nat Rev Drug Discov* 6:821–833.
50. Varela I, et al. (2008) Combined treatment with statins and aminobisphosphonates extends longevity in a mouse model of human premature aging. *Nat Med* 14:767–772.
51. Livak KJ, Schmittgen TD (2001) Analysis of relative gene expression data using real-time quantitative PCR and the 2(-Delta Delta C(T)) method. *Methods* 25:402–408.

Supporting Information

Mariño et al. 10.1073/pnas.1002696107

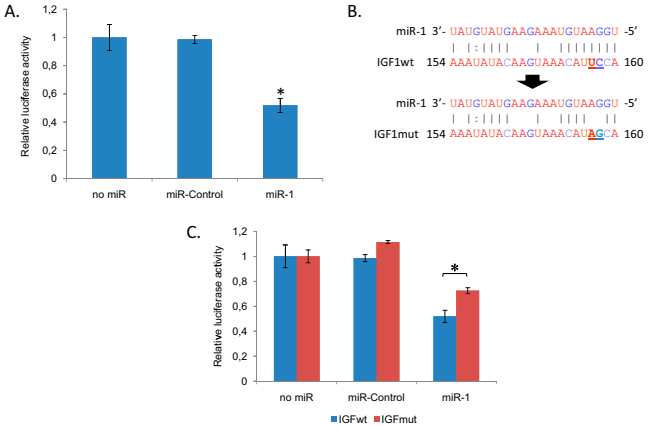

Fig. S1. The 3′-UTR of mouse *IGF-1* presents a functional binding site for miR-1. (*A*) The 3′-UTR of mouse *IGF-1* was cloned downstream the ORF of Renilla luciferase, and the plasmid was transfected alone or together with a control miR or miR-1 precursor molecules. Renilla luciferase activity was measured 18 h later, and data were normalized against firefly luciferase activity. (*B*) Pairwise alignment between miR-1 and the WT and mutated 3′-UTR of *IGF-1* (IGF-1mut), in which bases at positions 3 and 4 of the seed region were mutated (underlined bases). (*C*) Luciferase assays using the WT (blue bars) or mutated (red bars) 3′-UTR of mouse *IGF-1* alone or together with a control miR or miR-1 precursor molecules. All of the experiments were carried out in triplicate.

VI. Efecto rejuvenecedor de la señalización somatotrofa en el envejecimiento acelerado

Aunque clásicamente se ha asociado la disminución de la señalización del eje somatotrofo con un aumento de la longevidad de los organismos, el descubrimiento de que los organismos con envejecimiento acelerado presentan igualmente una señalización disminuida de esta ruta ha resultado sin duda paradójico. En este sentido, nuestro laboratorio ha contribuido a la elucidación del papel del eje somatotrofo en el envejecimiento acelerado con el descubrimiento de que los ratones progeroides deficientes en la metaloproteasa Zmpste24 presentan un marcado descenso en la señalización de IGF-1. Asimismo, se demostró que la restauración de este defecto extiende la longevidad de los ratones progeroides y mejora varios de sus síntomas (Mariño y col., 2010). En este artículo de opinión se resumen las principales observaciones del trabajo y se discute la importancia de esta ruta en la modulación del envejecimiento, así como el posible desarrollo de una estrategia terapéutica para el tratamiento de los síndromes progeroides humanos.

Artículo 6: **Alejandro P. Ugalde**, Guillermo Mariño y Carlos López-Otín. "Rejuvenating somatotropic signaling: a therapeutical opportunity for premature aging?"

Aging **2**(12):1017-1022 (2010)

Aportación personal al trabajo

En este artículo de opinión colaboré junto con el Dr. Guillermo Mariño en la recopilación de la información referente a la participación del eje somatotrofo en el envejecimiento y en la elaboración del manuscrito y las figuras, bajo la supervisión del Dr. Carlos López-Otín.

www.impactaging.com AGING, December 2010, Vol. 2. No 12

Research Perspective

Rejuvenating somatotropic signaling: a therapeutical opportunity for premature aging?

Alejandro P. Ugalde, Guillermo Mariño and Carlos López-Otín

Departamento de Bioquímica y Biología Molecular, Facultad de Medicina, Instituto Universitario de Oncología, Universidad de Oviedo, 33006-Oviedo, Spain

Key words: *progeria, cancer, growth hormone, insulin-like growth factor, longevity*
Received: *12/22/10; Accepted: 12/22/10; Published: 12/26/10*
Correspondence: *with Carlos Lopez-Otin, PhD to clo@uniovi.es*
Contribution: *Ugalde AP and Guillermo Mariño G have equally contributed to the work*
© Ugalde et al. This is an open-access article distributed under the terms of the Creative Commons Attribution License, which permits unrestricted use, distribution, and reproduction in any medium, provided the original author and source are credited

Abstract: We have recently reported that progeroid *Zmpste24*$^{-/-}$ mice, which exhibit multiple defects that phenocopy Hutchinson-Gilford progeria syndrome, show a profound dysregulation of somatotropic axis, mainly characterized by the occurrence of very high circulating levels of growth hormone (GH) and a drastic reduction in insulin-like growth factor-1 (IGF-1). We have also shown that restoration of the proper GH/IGF-1 balance in *Zmpste24*$^{-/-}$ mice by treatment with recombinant IGF-1 delays the onset of many progeroid features in these animals and significantly extends their lifespan. Here, we summarize these observations and discuss the importance of GH/IGF-1 balance in longevity as well as its modulation as a putative therapeutic strategy for the treatment of human progeroid syndromes.

Somatotropic regulation of aging

Although the maximal lifespan of an organism is probably genetically determined, the combined accumulative action of different types of stressors, such as oxidative damage, telomere attrition and the decline of DNA repair and protein turnover systems determines the real lifespan and contributes to the so-called aging process [1,2]. Currently, the dynamics of aging is far from being completely understood, but our knowledge of the molecular basis of this complex process has considerably increased in recent years. Among the different processes and pathways involved in lifespan regulation, GH/IGF somatotropic signaling has gained relevance as one of the major determinants of longevity in different and evolutionary distant species, including mammals [3,4]. The pivotal role of somatotropic axis in the regulation of lifespan was first shown by Kenyon and colleagues, who observed that mutation of specific genes essential for IGF-related signaling was able to considerably extend longevity in nematodes [5]. Currently, it is widely accepted that the downregulation of IGF-related signaling extends lifespan in a wide variety of model organisms and it is also a common feature of long-lived individuals [6,7].

Almost two decades after the first evidence on the somatotropic axis role in lifespan regulation, many other signaling pathways and metabolic routes have been shown to participate in the aging process [8-14]. Remarkably, some of these advances in the understanding of aging have been boosted by the study of both accelerated aging syndromes and progeroid animal models [15-17]. Progeroid syndromes are dramatic diseases in which certain features of human aging are prematurely developed, leading to a considerable reduction in the lifespan of patients, although the specific features and impact on longevity are highly dependent on the molecular nature of the disease. Many progeroid syndromes are caused by defects in DNA repair mechanisms but others derive from defects in nuclear envelope maintenance [18-21]. In fact, mutations in the *LMNA* gene encoding lamin A –a fundamental constituent of the nuclear envelope– or in that encoding the metalloproteinase ZMPSTE24 involved in the proteolytic processing of lamin A– cause dramatic human progeroid

syndromes, such as Hutchinson-Gilford progeria syndrome (HGPS), atypical Werner syndrome, mandibuloacral dysplasia and restrictive dermopathy [20,22,23]. The clarification of the molecular mechanisms underlying these devastating diseases has been impulsed by studies of *Lmna*- and *Zmpste24*-deficient mice, which show nuclear architecture aberrations and a number of histopathological alterations that phenocopy human syndromes of accelerated aging [24-26].

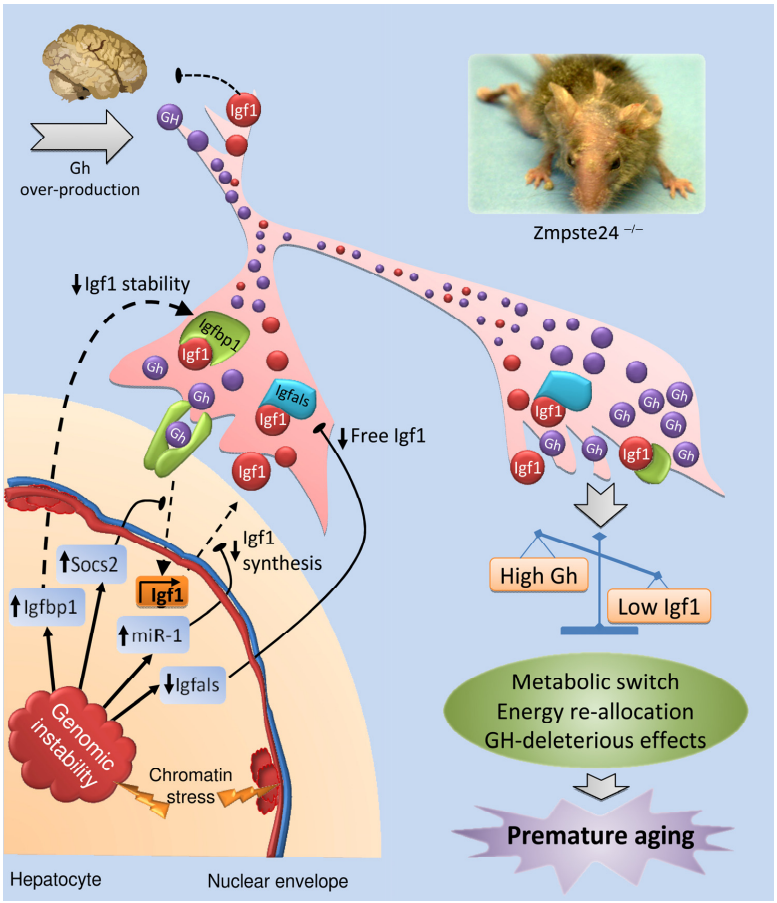

Figure 1. Proposed model for the somatotroph axis alterations of *Zmpste24*$^{-/-}$ progeroid mice. Nuclear envelope abnormalities present in *Zmpste24*-deficient cells cause chromatin detachment from the nuclear envelope and a profound structural disorganization. This genomic instability activates a chronic DNA damage response, which in turn triggers an adaptive response aimed at re-allocating resources from growth to somatic preservation. Hepatocytes are involved in this adaptive response through its ability to modulate the somatotropic axis and respond to the chronic DNA damage altering the expression of some key genes that affect Igf1-signaling at several levels. First, the reduced growth-hormone receptor (Ghr) transcription and the up-regulation of suppressor of cytokine signaling-2 (Socs2), diminishes the Gh-mediated Igf1 transcription. In addition, miR-1 over-activation represses Igf1 synthesis, reinforcing the already reduced Igf1 transcription and compromising the circulating levels of Igf1. The availability and stability of free Igf1 is reduced through up-regulation of insulin-like growth factor binding protein-1 (Igfbp1) and down-regulation of Igfbp-acid labile subunit (Igfals), respectively. Consequently, Igf1- signaling is diminished in the whole organism, which in turn leads to a metabolic switch towards somatic maintenance at the expense of somatic growth. In parallel, the low levels of Igf1 fail to inhibit Gh secretion at the pituitary gland, generating the high levels of circulating Gh present in these progeroid mice, which could aggravate the situation through its deleterious effects. Dotted lines represent disrupted pathways and blunt arrows indicate inhibitory actions.

Somatotropic signaling in progeria

Given the prominent and evolutionarily conserved role of IGF-1-related signaling in lifespan regulation, we have recently examined the somatotropic axis in mice deficient in the Zmpste24 metalloproteinase, which present a strong progeroid phenotype and exhibit many features observed in HGPS patients [25]. We have found that *Zmpste24*$^{-/-}$ mice show a profound dysregulation of GH/IGF-1 balance, mainly characterized by the progressive reduction of blood IGF-1 levels, the progressive increase in circulating GH levels and the generation of marked transcriptional alterations in key genes for somatotropic signaling [27]. In fact, genes coding for proteins involved in IGF-1 stability or in IGF-1 signaling – such as *Igfbals, Ghr, and Igf1* itself– are transcriptionally downregulated in livers from *Zmpste24*-deficient mice. Conversely, genes encoding proteins involved in IGF-1 signaling suppression such as *Igfbp1*, *Socs2* and *Socs3* are significantly upregulated in progeroid mice, especially in the case of *Igfbp1*, whose mRNA levels are more than 50-fold higher as compared with wild-type mice values. The finding of these marked alterations of somatotropic axis components in *Zmpste24*$^{-/-}$ mice, and the observation of reduced *Igf1* mRNA and protein levels even in the presence of high circulating GH levels, was indicative of a GH resistance process similar to that described in some HGPS patients [28]. However, after analyzing the status of the main transduction pathways activated by GH in response to intravenously injected recombinant GH, we excluded the possibility that the transcriptional downregulation of *Igf1* observed in *Zmpste24*$^{-/-}$ mice is caused by a liver-specific GH-resistance derived from signal transduction abnormalities in archetypal pathways [27].

Based on these findings, we next explored different possibilities which could explain the observed decrease of *Igf1* mRNA levels in progeroid mice, assuming that this should be the initial and major event accounting for the dysregulation of somatotropic axis found in *Zmpste24*$^{-/-}$ progeroid mice [27]. After an exhaustive search for alterations that could be responsible for the observed reduction in *Igf1* mRNA, we found that miR-1 –a microRNA predicted to target *Igf1*– was significantly upregulated in a variety of tissues from *Zmpste24*$^{-/-}$ mice. Interestingly, we also observed that this microRNA was significantly upregulated in fibroblasts from HGPS patients, which also show profound nuclear envelope abnormalities. Since these experimental findings suggested a causal relationship between nuclear envelope defects and miR-1 upregulation, we decided to characterize in more detail the putative relevance of miR-1 as a specific microRNA involved in *Igf1* control. After performing a series of specific luciferase assays, usually employed for microRNAs target validation, we could confirm that the 3'-UTR of *Igf1* contains a functional binding site for miR-1, thereby demonstrating that miR-1 is a *bona fide* microRNA targeting *Igf1* regulator [27,29]. Accordingly, it is tempting to speculate that the characteristic nuclear lamina abnormalities present in both HGPS and *Zmpste24*$^{-/-}$ cells induce –by a yet unknown mechanism– an upregulation of miR-1, which in turn leads to a reduction in *Igf1* mRNA cellular content and finally, to a decrease in circulating IGF-1 (Figure 1). As a consequence of this decrease, blood GH levels start to rise in an attempt to increase IGF-1 synthesis. However, and although GH is able to stimulate the *Igf1* mRNA transcription in progeroid cells, the increased levels of miR-1 may contribute to block IGF-1 protein synthesis. Taken together, all these events may initially lead to the observed dysregulation in the essential GH/IGF-1 balance, which in turn probably accounts for all the other alterations in somatotropic axis components found in *Zmpste24*$^{-/-}$ progeroid mice (Figure 1).

To test this hypothesis and to evaluate whether a restoration of circulating IGF-1 levels in *Zmpste24*$^{-/-}$ mice could have a positive effect on the lifespan and progeroid features of these prematurely aged mice, we treated mutant mice with recombinant IGF-1 through the use of osmotic pumps which allowed a constant and stable delivery of the recombinant protein to bloodstream. Surprisingly, exogenous administration of IGF-1 not only restored the GH/IGF-1 balance, but also significantly extended mutant mice lifespan and ameliorated or delayed the onset of many of their progeroid features [27]. These findings strongly suggest that the dysregulation of somatotropic axis observed in *Zmpste24*$^{-/-}$ progeroid mice is a detrimental phenomenon, rather than a successful adaptive strategy.

Concluding remarks and perspectives

Although most of the physiological and pathological features of progeroid individuals resemble those found in aged individuals, recent studies on prematurely-aged mice have facilitated the identification of surprising and paradoxical similarities between progeria patients and individuals with exceptional lifespan [30,31]. Among these similarities, the fact that circulating IGF-1 levels of progeroid mice are similar to those observed in long-lived or calorie-restricted individuals is remarkable, given the profound implications of IGF-1 signaling in lifespan regulation. Apparently, these paradoxical similarities between prematurely-aged and long-lived animals could derive from an adaptive effort to adjust the values of many biologic parameters to those which are compatible with a maximal lifespan, perhaps in an

attempt to slow down the onset of premature aging. However, the precise physiological significance of these surprising alterations has not been studied in detail so far. It seems that this kind of metabolic and hormonal reprogramming is elicited when DNA damage or chromosomal instability signals reach a certain threshold. In fact, similar changes to those observed in prematurely-aged, calorie-restricted or long-lived individuals in terms of somatotropic axis dysregulation are seen in wild-type mice subjected to chronic oxidative or genotoxic stress [32-34]. It seems reasonable that in these conditions, which probably mimic those present in progeroid mice, a massive cellular induction of checkpoint and anti-proliferative responses would lead to a general endocrine and metabolic shift at the organismal level. This type of metabolic reprogramming would re-allocate resources from growth to somatic preservation in an attempt to reduce replication defects, chromosomal instability, nuclear envelope abnormalities and finally, the risk of developing cancer [31]. Hence, in transient situations of excessive genotoxic damage, a systemic metabolic reprogramming towards preservation rather than proliferation would be of pivotal importance in order to survive until problems are solved. Similarly, during physiological aging, DNA damage accumulation would progressively induce a similar endocrine and metabolic shift – although in a much slower fashion– that is only observed in long-lived individuals who have not succumbed to cancer or to any other age-associated diseases.

A similar situation likely applies to individuals subjected to calorie restriction regimes, in which nutrients scarcity and the subsequent reduction of available ATP, would be the driving forces accounting for a general metabolic reprogramming which would contribute to extend longevity. However, if anti-proliferative signals are too strong and prolonged in time, as presumably occurs in premature aging syndromes, a chronic over-activation of this initially protective reprogramming could be detrimental for the organism, leading to a systemic senescent state and finally, to premature death. In this sense, the somatotropic axis alterations found in *Zmpste24*$^{-/-}$ progeroid mice represent an example of over-suppression of a growth-promoting pathway, as they show multiple and probably redundant alterations in regulators of GH-mediated signaling. In addition, the observed up-regulation of miR-1 likely contributes to the exacerbated suppression of liver IGF-1 synthesis, even in the presence of high circulating GH levels. In fact, it is possible that these elevated levels of circulating GH could directly elicit detrimental responses in peripheral tissues, which could contribute to the development of accelerated aging. Interestingly, conditional mutant mice with liver-specific *Igf1*-deficiency have reduced IGF-1 levels and increased GH circulating levels, as well as a series of concomitant metabolic defects that can be ameliorated by treatment with a GH antagonist [35]. Moreover, giant GH transgenic mice exhibit several characteristic features of premature aging [36]. Accordingly, it is reasonable to speculate that an initially protective response involving a downregulation of IGF-1 signaling may lead to detrimental effects when it is chronically over-activated and causes a profound dysregulation of somatotropic axis.

Our finding that restoration of somatotropic balance by recombinant IGF-1 administration not only ameliorates several progeroid features of *Zmpste24*$^{-/-}$ mice, but also extends their longevity, strongly supports this hypothesis. Consequently, and although an uncontrolled IGF-1 treatment could lead to the massive blockade of the anti-proliferative responses characteristic of *Zmpste24*$^{-/-}$ mice and favor cancer development, a selective modification of some altered signaling pathways could be beneficial for extending longevity without increasing the risk of malignancies. In this regard, it is remarkable that a reduction in p53 signaling increases lifespan and delays the onset of progeroid features in *Zmpste24*$^{-/-}$ mice [26]. Thus, given that somatotropic axis status is altered in some types of progeria and that recombinant IGF-1 treatment is effective for treating GH-refractory somatotropic alterations without significant detrimental effects [37], it is reasonable to consider recombinant IGF-1 treatment, alone or in combination with other drugs [38], as an experimental therapeutic strategy for children with progeria. Further studies with improved murine models of human progeria [16] will be necessary before this possibility can be translated into a clinical reality.

ACKNOWLEDGEMENTS

This work has been supported by grants from Ministerio de Ciencia e Innovación-Spain, Fundación "M. Botín", and European Union (FP7 MicroEnviMet). The Instituto Universitario de Oncología is supported by Obra Social Cajastur and Acción Transversal del Cáncer-RTICC.

CONFLICT OF INTERESTS STATEMENT

The authors of this manuscript have no conflict of interest to declare.

REFERENCES

1. Vijg J and Campisi J. Puzzles, promises and a cure for ageing. Nature. 2008; 454: 1065-1071.

2. Blagosklonny MV, Campisi J, Sinclair DA. Aging: past, present and future. Aging. 2009; 1: 1-5.
3. Russell SJ and Kahn CR. Endocrine regulation of ageing. Nat Rev Mol Cell Biol. 2007; 8: 681-691.
4. Rozing MP, Westendorp RG, Frolich M, de Craen AJ, Beekman M, Heijmans BT, Mooijaart SP, Blauw GJ, Slagboom PE, van Heemst D. Human insulin/IGF-1 and familial longevity at middle age. Aging. 2009; 1: 714-722.
5. Kenyon C, Chang J, Gensch E, Rudner A, Tabtiang R. A C. elegans mutant that lives twice as long as wild type. Nature. 1993; 366: 461-464.
6. Liang H, Masoro EJ, Nelson JF, Strong R, McMahan CA, Richardson A. Genetic mouse models of extended lifespan. Exp Gerontol. 2003; 38: 1353-1364.
7. Bartke A. Growth hormone, insulin and aging: The benefits of endocrine defects. Exp Gerontol. 2010; In Press.
8. Guarente L and Kenyon C. Genetic pathways that regulate ageing in model organisms. Nature. 2000; 408: 255-262.
9. Espada J, Varela I, Flores I, Ugalde AP, Cadinanos J, Pendas AM, Stewart CL, Tryggvason K, Blasco MA, Freije JM, Lopez-Otin C. Nuclear envelope defects cause stem cell dysfunction in premature-aging mice. J Cell Biol. 2008; 181: 27-35.
10. Finkel T, Deng CX, Mostoslavsky R. Recent progress in the biology and physiology of sirtuins. Nature. 2009; 460: 587-591.
11. Kapahi P, Chen D, Rogers AN, Katewa SD, Li PW, Thomas EL, Kockel L. With TOR, less is more: a key role for the conserved nutrient-sensing TOR pathway in aging. Cell Metab. 2010; 11: 453-465.
12. Marino G, Fernandez AF, Lopez-Otin C. Autophagy and aging: lessons from progeria models. Adv Exp Med Biol. 2010; 694: 61-68.
13. Raffaello A and Rizzuto R. Mitochondrial longevity pathways. Biochim Biophys Acta. 2010;
14. Sahin E and Depinho RA. Linking functional decline of telomeres, mitochondria and stem cells during ageing. Nature. 2010; 464: 520-528.
15. Haithcock E, Dayani Y, Neufeld E, Zahand AJ, Feinstein N, Mattout A, Gruenbaum Y, Liu J. Age-related changes of nuclear architecture in Caenorhabditis elegans. Proc Natl Acad Sci U S A. 2005; 102: 16690-16695.
16. Osorio FG, Obaya AJ, Lopez-Otin C, Freije JM. Accelerated ageing: from mechanism to therapy through animal models. Transgenic Res. 2009; 18: 7-15.
17. Pegoraro G and Misteli T. The central role of chromatin maintenance in aging. Aging. 2009; 1: 1017-1022.
18. Ramirez CL, Cadinanos J, Varela I, Freije JM, Lopez-Otin C. Human progeroid syndromes, aging and cancer: new genetic and epigenetic insights into old questions. Cell Mol Life Sci. 2007; 64: 155-170.
19. Musich PR and Zou Y. Genomic instability and DNA damage responses in progeria arising from defective maturation of prelamin A. Aging. 2009; 1: 28-37.
20. Burtner CR and Kennedy BK. Progeria syndromes and ageing: what is the connection? Nat Rev Mol Cell Biol. 2010; 11: 567-578.
21. Osorio FG, Varela I, Lara E, Puente XS, Espada J, Santoro R, Freije JM, Fraga MF, Lopez-Otin C. Nuclear envelope alterations generate an aging-like epigenetic pattern in mice deficient in Zmpste24 metalloprotease. Aging Cell. 2010; 9: 947-957.
22. Hennekam RC. Hutchinson-Gilford progeria syndrome: review of the phenotype. Am J Med Genet A. 2006; 140: 2603-2624.
23. Pereira S, Bourgeois P, Navarro C, Esteves-Vieira V, Cau P, De Sandre-Giovannoli A, Levy N. HGPS and related premature aging disorders: from genomic identification to the first therapeutic approaches. Mech Ageing Dev. 2008; 129: 449-459.
24. Sullivan T, Escalante-Alcalde D, Bhatt H, Anver M, Bhat N, Nagashima K, Stewart CL, Burke B. Loss of A-type lamin expression compromises nuclear envelope integrity leading to muscular dystrophy. J Cell Biol. 1999; 147: 913-920.
25. Pendas AM, Zhou Z, Cadinanos J, Freije JM, Wang J, Hultenby K, Astudillo A, Wernerson A, Rodriguez F, Tryggvason K, Lopez-Otin C. Defective prelamin A processing and muscular and adipocyte alterations in Zmpste24 metalloproteinase-deficient mice. Nat Genet. 2002; 31: 94-99.
26. Varela I, Cadinanos J, Pendas AM, Gutierrez-Fernandez A, Folgueras AR, Sanchez LM, Zhou Z, Rodriguez FJ, Stewart CL, Vega JA, Tryggvason K, Freije JM, Lopez-Otin C. Accelerated ageing in mice deficient in Zmpste24 protease is linked to p53 signalling activation. Nature. 2005; 437: 564-568.
27. Marino G, Ugalde AP, Fernandez AF, Osorio FG, Fueyo A, Freije JM, Lopez-Otin C. Insulin-like growth factor 1 treatment extends longevity in a mouse model of human premature aging by restoring somatotroph axis function. Proc Natl Acad Sci U S A. 2010; 107: 16268-16273.
28. Abdenur JE, Brown WT, Friedman S, Smith M, Lifshitz F. Response to nutritional and growth hormone treatment in progeria. Metabolism. 1997; 46: 851-856.
29. Elia L, Contu R, Quintavalle M, Varrone F, Chimenti C, Russo MA, Cimino V, De Marinis L, Frustaci A, Catalucci D, Condorelli G. Reciprocal regulation of microRNA-1 and insulin-like growth factor-1 signal transduction cascade in cardiac and skeletal muscle in physiological and pathological conditions. Circulation. 2009; 120: 2377-2385.
30. Marino G, Ugalde AP, Salvador-Montoliu N, Varela I, Quiros PM, Cadinanos J, van der Pluijm I, Freije JM, Lopez-Otin C. Premature aging in mice activates a systemic metabolic response involving autophagy induction. Hum Mol Genet. 2008; 17: 2196-2211.
31. Hoeijmakers JH. DNA damage, aging, and cancer. N Engl J Med. 2009; 361: 1475-1485.
32. Niedernhofer LJ, Garinis GA, Raams A, Lalai AS, Robinson AR, Appeldoorn E, Odijk H, Oostendorp R, Ahmad A, van Leeuwen W, Theil AF, Vermeulen W, van der Horst GT, Meinecke P, Kleijer WJ, Vijg J, Jaspers NG, Hoeijmakers JH. A new progeroid syndrome reveals that genotoxic stress suppresses the somatotroph axis. Nature. 2006; 444: 1038-1043.
33. van der Pluijm I, Garinis GA, Brandt RM, Gorgels TG, Wijnhoven SW, Diderich KE, de Wit J, Mitchell JR, van Oostrom C, Beems R, Niedernhofer LJ, Velasco S, Friedberg EC, Tanaka K, van Steeg H, Hoeijmakers JH, van der Horst GT. Impaired genome maintenance suppresses the growth hormone--insulin-like growth factor 1 axis in mice with Cockayne syndrome. PLoS Biol. 2007; 5: e2.
34. Garinis GA, Uittenboogaard LM, Stachelscheid H, Fousteri M, van Ijcken W, Breit TM, van Steeg H, Mullenders LH, van der Horst GT, Bruning JC, Niessen CM, Hoeijmakers JH, Schumacher B. Persistent transcription-blocking DNA lesions trigger somatic

growth attenuation associated with longevity. Nat Cell Biol. 2009; 11: 604-615.

35. Yakar S, Setser J, Zhao H, Stannard B, Haluzik M, Glatt V, Bouxsein ML, Kopchick JJ, LeRoith D. Inhibition of growth hormone action improves insulin sensitivity in liver IGF-1-deficient mice. J Clin Invest. 2004; 113: 96-105.

36. Wolf E, Kahnt E, Ehrlein J, Hermanns W, Brem G, Wanke R. Effects of long-term elevated serum levels of growth hormone on life expectancy of mice: lessons from transgenic animal models. Mech Ageing Dev. 1993; 68: 71-87.

37. Clemmons DR. Modifying IGF1 activity: an approach to treat endocrine disorders, atherosclerosis and cancer. Nat Rev Drug Discov. 2007; 6: 821-833.

38. Varela I, Pereira S, Ugalde AP, Navarro CL, Suarez MF, Cau P, Cadinanos J, Osorio FG, Foray N, Cobo J, de Carlos F, Levy N, Freije JM, Lopez-Otin C. Combined treatment with statins and aminobisphosphonates extends longevity in a mouse model of human premature aging. Nat Med. 2008; 14: 767-772.

VII. Análisis de la función de los miRNAs en el envejecimiento

Aunque se ha descrito la implicación de los miRNAs en una amplia variedad de procesos fisiológicos y patológicos, todavía no se abordado en profundidad su posible papel regulador del envejecimiento. En este trabajo empleamos los ratones deficientes en la metaloproteasa Zmpste24 para estudiar la expresión de los miRNAs en el envejecimiento acelerado. Estos estudios revelaron la desregulación en los ratones mutantes de varios miRNAs, entre los cuales centramos nuestra investigación en la familia de miR-29, con el hallazgo de que estos miRNAs se encuentran sobreexpresados tanto en el envejecimiento acelerado como fisiológico. Además, observamos que su expresión responde a estrés en el DNA en una manera dependiente del supresor de tumores p53. Finalmente, identificamos algunos de sus mRNAs diana, entre los que destaca el correspondiente a la fosfatasa Ppm1d, que desfosforila entre otras proteínas, a p53. En base a estas y otras observaciones proponemos un modelo por el cual la acumulación de daño en el DNA o el envejecimiento activan un circuito de regulación que implica a miR-29 y p53.

Artículo 6: **Alejandro P. Ugalde**, Andrew J. Ramsay, Jorge de la Rosa, Ignacio Varela, Guillermo Mariño, Juan Cadiñanos, Jun Lu, José M. P. Freije y Carlos López-Otín. "Aging and chronic DNA damage response activate a regulatory pathway involving miR-29 and p53"

The EMBO Journal, **30**(11):2219-2232 (2011)

Aportación personal al trabajo

En este trabajo participé activamente en el diseño, realización y análisis de los niveles de expresión de miRNAs en tejidos de ratón y líneas celulares bajo distintos tratamientos, así como en la predicción y validación de los genes diana. Además, colaboré en los ensayos de proliferación de fibroblastos y en los experimentos funcionales de miRNAs en células. Finalmente, cooperé en la elaboración del manuscrito y las figuras.

The EMBO Journal (2011), 1–14 | © 2011 European Molecular Biology Organization | All Rights Reserved 0261-4189/11
www.embojournal.org

THE EMBO JOURNAL

Aging and chronic DNA damage response activate a regulatory pathway involving miR-29 and p53

Alejandro P Ugalde[1], Andrew J Ramsay[1], Jorge de la Rosa[2], Ignacio Varela[1], Guillermo Mariño[1], Juan Cadiñanos[2], Jun Lu[3], José MP Freije[1] and Carlos López-Otín[1,*]

[1]Departamento de Bioquímica y Biología Molecular, Instituto Universitario de Oncología, Universidad de Oviedo, Oviedo, Spain, [2]Laboratorio de Medicina Molecular, Instituto de Medicina Oncológica y Molecular de Asturias, Oviedo, Spain and [3]Department of Genetics, Yale University, Yale Stem Cell Center, New Haven, CT, USA

Aging is a multifactorial process that affects most of the biological functions of the organism and increases susceptibility to disease and death. Recent studies with animal models of accelerated aging have unveiled some mechanisms that also operate in physiological aging. However, little is known about the role of microRNAs (miRNAs) in this process. To address this question, we have analysed miRNA levels in *Zmpste24*-deficient mice, a model of Hutchinson–Gilford progeria syndrome. We have found that expression of the miR-29 family of miRNAs is markedly upregulated in *Zmpste24*$^{-/-}$ progeroid mice as well as during normal aging in mouse. Functional analysis revealed that this transcriptional activation of miR-29 is triggered in response to DNA damage and occurs in a p53-dependent manner since *p53*$^{-/-}$ murine fibroblasts do not increase miR-29 expression upon doxorubicin treatment. We have also found that miR-29 represses Ppm1d phosphatase, which in turn enhances p53 activity. Based on these results, we propose the existence of a novel regulatory circuitry involving miR-29, Ppm1d and p53, which is activated in aging and in response to DNA damage.

The EMBO Journal advance online publication, 26 April 2011; doi:10.1038/emboj.2011.124
Subject Categories: RNA; genome stability & dynamics; molecular biology of disease
Keywords: cancer; microRNA; phosphatase; progeria; tumour suppressor

Introduction

Aging is a complex process that progressively compromises most of the biological functions of the organism, resulting in an increased susceptibility to disease and death. Although a considerable effort has been made to unveil the causes of aging, there is no consensus theory to completely explain this process (Vijg and Campisi, 2008). Nevertheless, there is some agreement that a common feature of aging is the progressive accumulation of cellular damage. Several stressors have been proposed to contribute to this cell damage, such as oxidative reactions, telomere attrition, or the decline of DNA repair and protein turnover systems (Kirkwood, 2005). Evidence for the association of DNA damage with aging is supported by the identification of gene mutations that lead to an accelerated development of many age-related features. Most of these mutations were originally found in genes encoding proteins directly implicated in DNA repair (Hoeijmakers, 2009), but recent studies have revealed that alterations in other processes that affect genomic integrity, such as nuclear envelope formation and dynamics, are also responsible for the development of premature aging syndromes (Hasty *et al*, 2003; Cadinanos *et al*, 2005; Broers *et al*, 2006). Thus, mice with mutations in lamin A or deficient in the Zmpste24 metalloprotease involved in its maturation, display multiple features of premature aging (Osorio *et al*, 2009). This phenotype is associated with an increased genomic instability as a consequence of the nuclear envelope network disruption and is supported by the transcriptional upregulation of p53 target genes and the decline in the function of somatic stem cells (Pendas *et al*, 2002; Varela *et al*, 2005; Espada *et al*, 2008). On this basis, it has been proposed that the same mechanisms that detect damage and protect cells from malignant transformation may have a deleterious effect in aged tissues, thereby providing a good example of the principle of antagonistic pleiotropy (Campisi, 2005; Kirkwood, 2005).

Over the last decade, miRNAs have emerged as new and fundamental actors in the gene regulation scenario. These ~21–24 nucleotide RNA molecules are able to bind to specific sites typically present in the 3′-UTR region of their target genes and mediate either mRNA decay or translational blockade (Flynt and Lai, 2008). Although the function of only a small percentage of the identified miRNAs is known, computational predictions have estimated that at least 20–30% of transcripts are susceptible to miRNA-mediated regulation (Lewis *et al*, 2005). miRNAs were initially associated with development regulation, but numerous studies have revealed that these small RNA molecules have essential roles in a wide variety of physiological and cellular processes (Bushati and Cohen, 2007). As a consequence, miRNA dysregulation is a common feature found in cancer, and several members of this family of regulatory RNAs have been proposed to act as oncogenes or tumour suppressors (He *et al*, 2007; Shenouda and Alahari, 2009; Garzon *et al*, 2009a).

At present, very little is known about the implication of miRNAs during mammalian aging. In contrast, several miRNAs have been associated with aging in *Caenorhabditis elegans* and it has been shown that knockdown of *lin-4* miRNA extends lifespan in these nematodes (Boehm and Slack, 2005; Williams *et al*, 2007). In vertebrates, profiling studies in liver and skeletal muscle from aged mice have revealed changes in miRNA expression during aging,

*Corresponding author. Departamento de Bioquímica y Biología Molecular, Facultad de Medicina, Universidad de Oviedo, Fernando Bongera s/n Edificio Santiago Gascon, Oviedo 33006, Spain. Tel.: +34 985 104201; Fax: +34 985 103564; E-mail: clo@uniovi.es

Received: 26 July 2010; accepted: 30 March 2011

©2011 European Molecular Biology Organization

although no differences have been identified in lung (Williams *et al*, 2007; Drummond *et al*, 2008; Maes *et al*, 2008). Additionally, several miRNAs have been found to be dysregulated in the Ames dwarf mice, and miR-27 has been proposed to have a role in the delayed aging observed in these mice (Bates *et al*, 2010). However, to date, no such studies have been performed in premature aging mice. In this work, we have evaluated for the first time the miRNA expression levels in a mouse model of human Hutchinson–Gilford progeria. We report that the expression of the miR-29 family of miRNAs is dysregulated in both pathological and physiological aging. In addition, we have found that miR-29 miRNAs form part of a new signalling pathway involving the Ppm1d/Wip1 phosphatase and the p53 tumour suppressor, which is activated in aging and during chronic DNA damage response.

Results

Dysregulation of miRNAs in Zmpste24$^{-/-}$ progeroid mice

To identify miRNAs that could be implicated in normal or pathological aging processes, we first analysed the miRNA transcriptome of *Zmpste24*-null mice, a mouse model of Hutchinson–Gilford progeria that exhibits accelerated aging and recapitulates many symptoms of normal aging (Varela *et al*, 2005). To this purpose, we used a bead-based flow cytometric platform covering the complete set of mouse and human miRNAs to profile miRNA expression levels in liver from *Zmpste24*-deficient mice (Lu *et al*, 2005). This analysis revealed the differential expression of a series of miRNAs, which were significantly upregulated or downregulated in these progeroid mice. Interestingly, three of the miRNAs whose expression levels were altered in *Zmpste24*-deficient mice (miR-29a, miR-29b and miR-29c) belong to the same family (Figure 1A). Accordingly, we next proceeded to further validate these flow cytometry-based miR-29 expression results by stem loop quantitative PCR miRNA assays. As shown in Figure 1B, we confirmed the upregulation of all three members of the miR-29 family in *Zmpste24*$^{-/-}$-deficient mice, with values for miR-29a, -29b and -29c being 1.6-, 2.7- and 1.6-fold increased when compared with normal tissues. As a control, we assayed in parallel the expression levels of miR-23b, which shows no changes between normal and mutant liver in the array-based profiling analysis (Figure 1B).

Next, we extended the miRNA expression study to other tissues from *Zmpste24*$^{-/-}$ mice, such as muscle, which displays considerable alterations in this mouse model (Pendas *et al*, 2002). As shown in Figure 1C, miR-29 levels were dramatically altered in this tissue, as assessed by the finding of a 9.7-fold induction for miR-29b in *Zmpste24*$^{-/-}$ mice (Figure 1C). Likewise, miR-29a and -29c levels were also markedly increased in muscle from *Zmpste24*$^{-/-}$ mice when compared with wild-type littermates (5.1- and 4.4-fold, respectively). Because *Zmpste24*-null mice phenocopy many alterations characteristic of normal aging, we next asked whether these miRNAs could also be dysregulated in aged mice. To evaluate this hypothesis, we analysed miR-29 expression levels in tissues from 2-year-old mice. As can be seen in Figure 1B and C, the expression levels of miR-29a, -29b and -29c in liver and muscle from wild-type

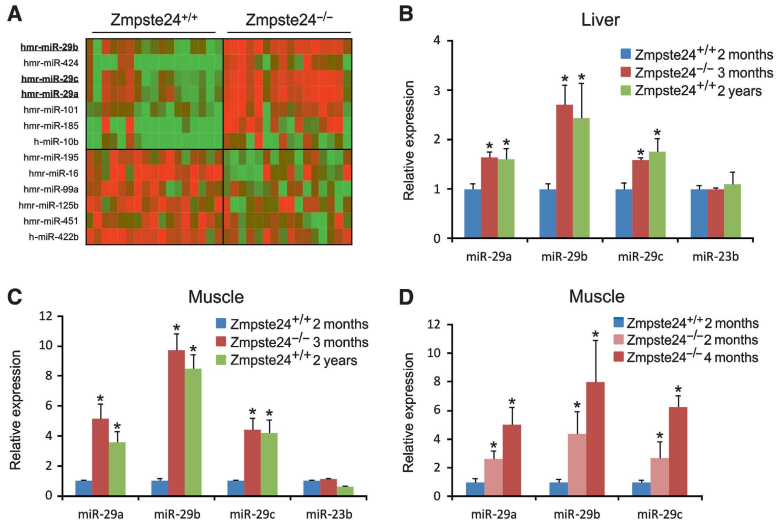

Figure 1 miRNA expression analysis in tissues from *Zmpste24*$^{-/-}$ mice. (**A**) A total of 17 and 16 *Zmpste24*$^{-/-}$ and *Zmpste24*$^{+/+}$ liver samples were analysed through a bead-based flow cytometry platform that covers the complete set of human and mouse miRNAs. miRNAs with significant fold induction were plotted as a colour heat map, with the miR-29 family miRNAs underlined (P-value<0.05, $0.75 \geqslant$fold induction$\geqslant 1.25$). (**B**) miR-29a, -29b and -29c upregulation in *Zmpste24*$^{-/-}$ was confirmed through stem loop qPCR in liver samples. Expression analysis in liver from aged mice shows similar levels of miR-29 miRNAs than in samples from *Zmpste24*$^{-/-}$ mice. As a control, levels of miR-23b that shows no changes in the profiling study were analysed. (**C**) qPCR analysis of the miR-29 family in muscle revealed eight-fold induction in samples from *Zmpste24*$^{-/-}$ and aged *Zmpste24*$^{+/+}$, compared with young *Zmpste24*$^{-/-}$. (**D**) Correlation between miR-29 levels and phenotype development in *Zmpste24*$^{-/-}$ muscle samples. For all the experiments, a minimum of three animals were analysed. *Significantly different from 2-month-old wild-type mice, $P<0.05$.

 ©2011 European Molecular Biology Organization

aged mice were higher than those of young mice and very similar to those present in the same tissues from 2-month-old *Zmpste24*$^{-/-}$ mice (3.6-, 8.5- and 4.2-fold, respectively). Finally, we examined the putative correlation between miR-29 levels and phenotype development in *Zmpste24*$^{-/-}$ muscle samples, with the finding that 2-month-old mice, which are almost indistinguishable from their wild-type littermates, present significantly lower levels of miR-29 compared with 4-month-old mice, which display the most severe phenotype, as assessed by an extensive hair and weight loss and a prominent kyphosis (Figure 1D). This observation suggests that the miR-29 family upregulation is an early event in the development of *Zmpste24*-deficient mice phenotype rather than a consequence of the multiple alterations present in these progeroid mice.

Additionally, we analysed the putative changes in miR29-expression levels in some available tissues from progeroid mice deficient in other genes implicated in DNA repair, including *XPF*- (Tian *et al*, 2004), *CSB/XPA*- (van der Pluijm *et al*, 2007) and *ATM*-deficient mice (Elson *et al*, 1996), as well as *ATR-Seckel* mice (Murga *et al*, 2009). However, no significant changes in the miR-29 family were found in any of the DNA repair deficiency models. Overall, these data would suggest that the miR-29 increase in the *Zmpste24*$^{-/-}$ model is dependent upon a chronic DNA damage due to a very specific genotoxic stress caused by nuclear envelope dysfunction, but not initiated in response to intrinsic genomic stress derived from repair machinery impairment. Taken together, these data associate the miR-29 family with normal and pathological aging, and reinforce the relevance of *Zmpste24*-null mice as a model to study the molecular links between miRNA dysregulation and aging processes.

miR-29 induction is linked to DNA damage response

We have previously shown that *Zmpste24*-null mice present nuclear abnormalities linked to altered chromatin architecture and p53 pathway activation, a situation which suggests the existence of a chronic response to genomic damage (Liu *et al*, 2005; Varela *et al*, 2005; Espada *et al*, 2008). On this basis, we hypothesized that the miR-29 upregulation observed in aging tissues could be triggered as a result of genomic damage. As a first step to evaluate this hypothesis, we analysed miR-29 expression during successive passages of *Zmpste24*$^{-/-}$ primary fibroblasts until they reached replicative senescence. As shown in Figure 2A, miR-29a, -29b and -29c levels are consistently higher at passage six and correlate with the significant accumulation of senescence-associated β-galactosidase (SA-βGal)-positive cells and a considerable increase in the levels of the DNA damage marker γ-H2AX in comparison to initial passage controls (Figure 2C and D). To evaluate whether this phenomenon is an exclusive feature of mutant mice fibroblasts, we extended the analysis to wild-type fibroblasts, finding that these cells undergo the same grade of miR-29 upregulation at serial passage six (Figure 2B) and show no significant differences at passage one or six compared with *Zmpste24*$^{-/-}$ fibroblasts under the same

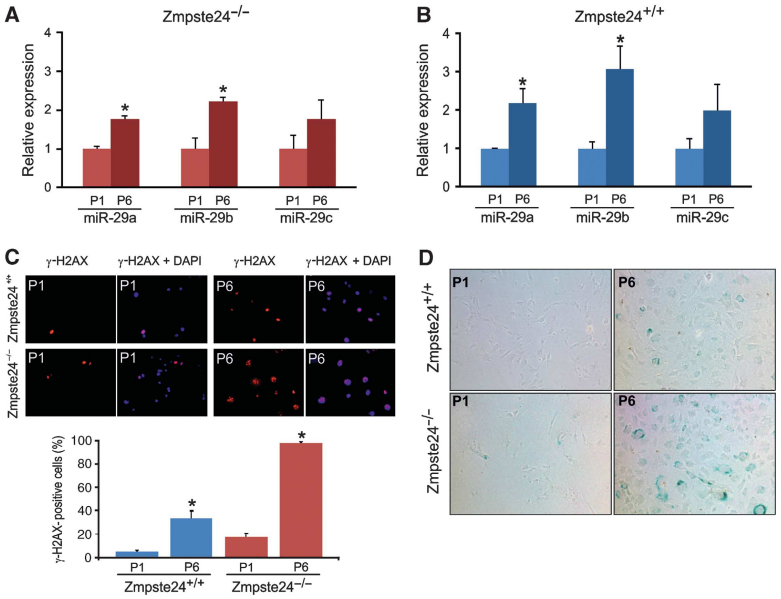

Figure 2 miR-29 expression is associated with DNA damage and cell senescence. Levels of miR-29 increase with serial passages of *Zmpste24*$^{-/-}$ (**A**) and *Zmpste24*$^{+/+}$ (**B**) primary ear fibroblasts in culture. Total RNA from three independent *Zmpste24*$^{-/-}$ and *Zmpste24*$^{+/+}$ fibroblast cell lines was extracted at passages 1 and 6 and the miR-29a, -29b and -29c levels were analysed by qPCR. *Significantly different from passage 1 fibroblasts, $P<0.05$. (**C**) Representative images and quantification (lower chart) of γ-H2AX staining in the three *Zmpste24*$^{-/-}$ and *Zmpste24*$^{+/+}$ fibroblast cell lines at passages 1 and 6. *Significantly different from passage 1 fibroblasts, $P<0.05$. (**D**) Senescence-associated β-galactosidase activity (SA-βGAL) representative images from *Zmpste24*$^{-/-}$ and *Zmpste24*$^{+/+}$ primary fibroblasts at passages 1 and 6. Both wild-type and *Zmpste24*-mutant primary fibroblasts show an increase in γ-H2AX foci and SA-βGal activity at passage 6, evidencing the genotoxic stress induced by the *in vitro* serial passage of primary fibroblasts.

©2011 European Molecular Biology Organization

culture conditions. Senescence and DNA damage studies in wild-type fibroblasts demonstrated that although there is a progressive accumulation of SA-βGal and γ-H2AX during serial passaging, which clearly correlates miR-29 upregulation with cellular conditions of increased DNA damage, both markers are significantly increased in *Zmpste24*-deficient fibroblasts (Figure 2C and D). This observation can conceivably be attributed to multiple additional pathway alterations present in the mutant fibroblasts.

To clarify further if genomic damage is responsible for this miR-29 activation, growing wild-type fibroblasts were treated with doxorubicin, a DNA topoisomerase inhibitor that generates a DNA damage that is difficult to repair and induces the expression of miRNAs implicated in the p53 pathway, such as miR-34 (L'Ecuyer *et al*, 2006; Rokhlin *et al*, 2008). As can be seen in Figure 3A, miR-29 expression was induced in wild-type fibroblasts, after 24 h treatment with 1 μM doxorubicin. In contrast, treatment with drugs that induce transient oxidative damage, such as H_2O_2, or UV-like lesions, like those attributed to 4-nitroquinolone-1-oxide (4-NQO) (Eller *et al*, 1996) failed to induce the expression of this family of miRNAs (Figure 3B), suggesting that the main stimulus for miR-29 transcriptional activation is the accumulation of chronic, difficult to repair DNA lesions. To further explore whether the observed miR-29 upregulation is associated with p53 signalling activation, we performed similar experiments with $p53^{-/-}$ fibroblasts, with the finding that the deletion of p53 abolishes miR-29 induction after doxorubicin treatment (Figure 3A). Moreover, and in agreement with these data, we have found that *p53*-deficient primary mouse fibroblasts fail to upregulate miR-29 expression during successive passages of cell culture, providing further evidence of the connection between p53, miR-29 and replicative senescence, as $p53^{-/-}$ fibroblasts never enter a non-growing senescent phase (Harvey *et al*, 1993; Supplementary Figure S1A). Further, we extended these experiments to fibroblasts defective in ATM or containing the ATR-Seckel mutation, demonstrating that disruption of both DNA damage response pathways abolishes miR-29 upregulation under an equivalent dosage of doxorubicin (Supplementary Figure S1A). Interestingly, high concentrations of doxorubicin induced miR-29 transcriptional activation even in the absence of functional ATM or ATR proteins, indicating that other regulatory mechanisms are operating under these conditions.

Having established that p53 deficiency in fibroblasts attenuates the increase of the miR-29 family in response to doxorubicin-induced DNA damage, we next analysed if p53 is required for the initiation of promoter activity of both the hsa-miR-29b-1∼29a and hsa-miR-29b-2∼29c clusters. Accordingly, ∼4 kb of the promoter sequence of both

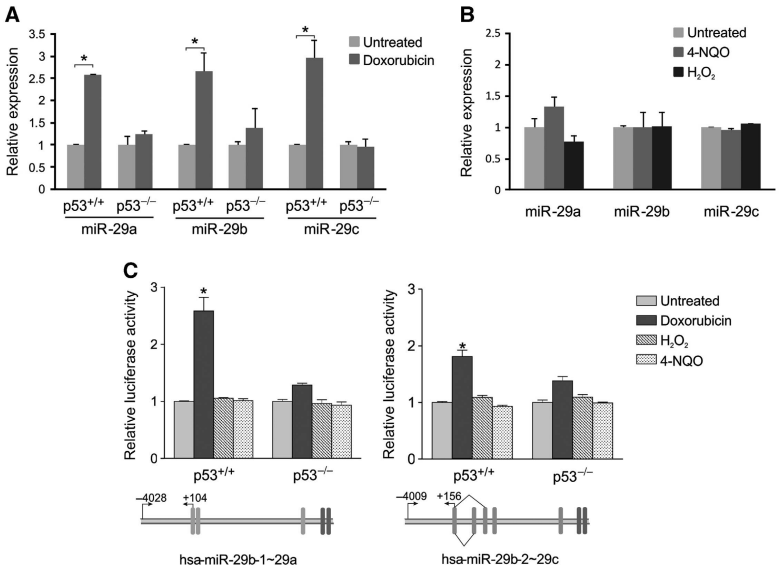

Figure 3 miR-29 induction is linked to DNA damage response. (**A**) miR-29 expression is activated during DNA damage in a p53-dependent manner. Primary ear fibroblasts from $p53^{+/+}$ and $p53^{-/-}$ mice were treated for 24 h with doxorubicin or left untreated in parallel, and miR-29 expression was analysed by qPCR ($n=2$ biological replicates). (**B**) Transient damage induced by H_2O_2 or UV-like lessons caused by 4-nitroquinolone-1-oxide (4-NQO) show no effect on miR-29 transcription. Primary ear fibroblasts were treated with 80 μM H_2O_2 or 0.8 μM 4-NQO for 24 h and miR-29 levels were analysed by qPCR ($n=2$ biological replicates). Untreated samples in (**A**) and (**B**) were taken at the same time points as in treated cells. (**C**) Transcriptional regulation of miR-29 promoters. Approximately 4 kb of the promoter sequence of both hsa-miR-29b-1∼29a and hsa-miR-29b-2∼29c clusters were cloned upstream the firefly luciferase coding sequence of the pGL3-basic plasmid (diagrams below the chart). Promoter constructs were transfected in wild-type *or* $p53^{-/-}$ HCT-116 cells and treated with 1 μM doxorubicin or left untreated for 36 h. In all transfections, a plasmid expressing *Renilla* luciferase was included for normalization. The normalized luciferase activity relative to the untreated sample is represented. p53 deficiency abolishes or strongly reduces the promoter activity of hsa-miR-29b-1∼29a and hsa-miR-29b-2∼29c upon doxorubicin treatment, respectively. Additionally, 4-NQO and H_2O_2 treatments were included as a negative control. *Significantly different from the indicated condition, $P<0.05$.

 ©2011 European Molecular Biology Organization

hsa-miR-29b-1∼29a and hsa-miR-29b-2∼29c clusters were cloned upstream the firefly luciferase coding sequence of the pGL3-basic plasmid (Figure 3C, lower panels). Promoter constructs were transfected in parallel with a *Renilla* luciferase expressing construct (normalization control) into wild-type or $p53^{-/-}$ HCT-116 cells and treated with 1 μM doxorubicin or left untreated for 36 h. In complete agreement with quantitative PCR experiments of wild-type mouse fibroblasts exposed to various DNA damaging agents (Figure 3A and B), only doxorubicin treatment was able to activate promoter activity of the hsa-miR-29b-1∼29a and hsa-miR-29b-2∼29c clusters in wild-type HCT-116 cells (Figure 3C, left side of upper panels). Importantly, in a further confirmation of experiments in *p53*-deficient fibroblasts, absence of p53 in the HCT-116 cell line abolished doxorubicin-stimulated promoter activity of the hsa-miR-29b-1∼29a and hsa-miR-29b-2∼29c clusters (Figure 3C, right side of upper panels). Collectively, these experiments indicate that miR-29 transcriptional induction in response to chronic DNA damage is dependent on p53 signalling, an observation that is supported by the study made by Tarasov *et al* (2007) showing that miR-29a is a direct transcriptional target for p53.

Identification of miR-29 targets of potential interest in aging processes

To try to establish the specific role of miR-29 miRNAs in normal and pathological aging, we next performed a computational search of candidate targets that could be subjected to translational repression by members of this miRNA family. Combining the results yielded by the different predictive software available, we first elaborated a list of genes containing putative miR-29 binding sites in their 3′-UTRs and then performed luciferase assays to validate the predicted targets. To this end, the 3′-UTRs of each candidate gene were cloned upstream the ORF of *Renilla* luciferase and the luminescence emission was measured after transfection in HEK-293 cells together with miR-29 precursor molecules or a control miRNA. The different targets showing more than a 50% repression ratio between the miRNA control and any of the miR-29 miRNAs are shown in Figure 4A. Interestingly, all three miR-29 family members exhibited similar activity in the repression ratio of the different targets. These targets include protein phosphatases such as Ppm1d (also called Wip1) and Dusp2, the interferon-inducible protein Ifi30, the transcriptional repressor Hbp1, the prelamin A interacting protein Narf, the Adamts18 metalloproteinase and the Mycn proto-oncogene (Figure 4B). To further validate these findings, we performed similar luciferase-based experiments with the mutated forms of the 3′-UTR of *Narf* and *Ppm1d*, in which we generated a mismatch in the seed region of the putative binding site for miR-29 miRNAs (Figure 5A). We selected these two targets because, in addition to their potential functional relevance in the analysed process, both have a unique binding site for miR-29, which facilitates the mutagenesis experiments and simplifies the analysis of the repression effects. In both mRNAs, the disruption of the

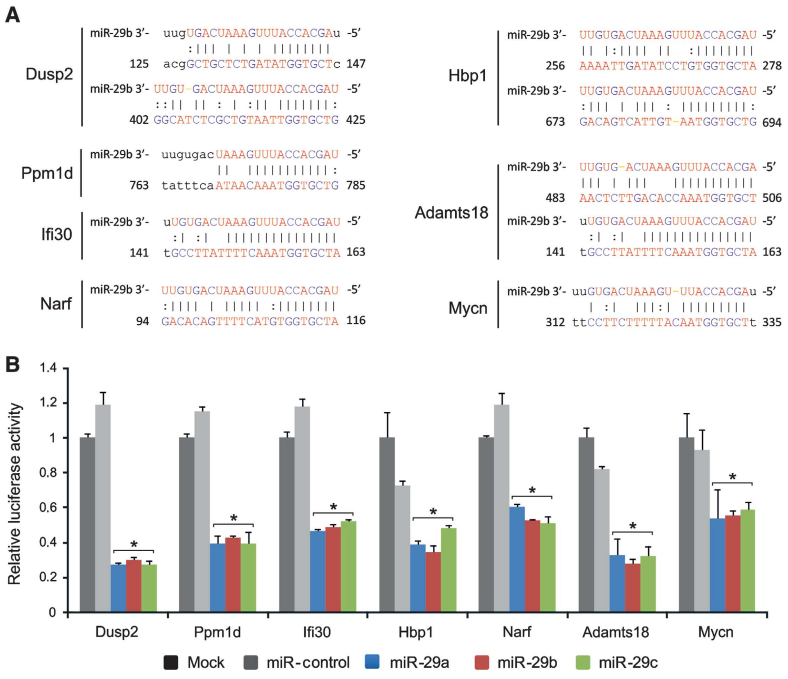

Figure 4 miR-29 target prediction and validation. (**A**) Pairwise alignment of predicted miR-29 targets. Base pair numbers on each 3′-UTR are indicated. (**B**) Luciferase assays in HEK-293 cells. The 3′-UTR of each predicted target was cloned downstream of the ORF of *Renilla* luciferase and transfected into HEK-293 cells alone or together with miR-29a, -29b or -29c or a control miRNA. Data were normalized to the firefly luciferase and experiments were carried out in triplicate. *Significantly different from HEK-293 cells transfected with no miRNA, $P<0.05$.

©2011 European Molecular Biology Organization

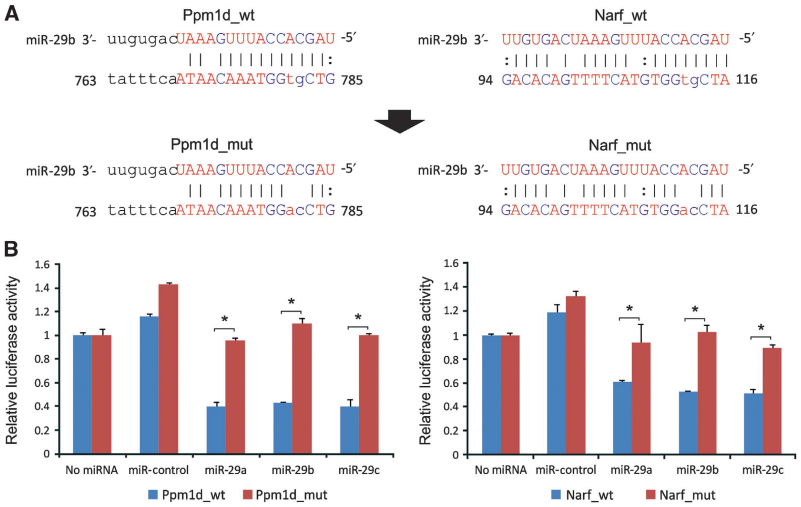

Figure 5 Mutation of the miRNA binding site abolishes miRNA repression. (**A**) Pairwise alignment between miR-29b and the wild-type and mutated 3′-UTR of *Narf* and *Ppm1d* (Narf_mut and Ppm1d_mut), in which bases at positions 4 and 5 of the seed region were mutated and are highlighted in grey. (**B**) Luciferase experiments with the wild-type and the mutated 3′-UTR of *Narf* and *Ppm1d*. Mutation of the seed region of the 3′-UTR binding site abolishes the repression triggered by either of the three miR-29 miRNAs, confirming the presence of functional miRNA binding sites in the 3′-UTR of *Narf* and *Ppm1d*. *Significantly different, $P<0.05$.

Watson–Crick miRNA–mRNA complementarity within the seed region of the binding site was sufficient to abolish the repression effect caused by any of the three miR-29 miRNAs in luciferase experiments (Figure 5B).

As a different approach to validate these results and place them in the context of the DNA damage response, HEK-293 cells transfected with the *Ppm1d* and *Narf* luciferase constructs were treated for 24 h with doxorubicin, and the luminescence emission was assayed (Figure 6A and B). Doxorubicin treatment strongly repressed the luminescence emission of cells transfected with the wild-type *Ppm1d* and *Narf* 3′-UTRs compared with untreated cells. In contrast, transfection of miR-29 inhibitory molecules (anti-miR 29) together with the 3′-UTRs of these targets abolished (Figure 6A) or significantly reverted (Figure 6B) the translational repression induced by doxorubicin. Several studies have reported the influence of mRNA structure in the miRNA-mediated repression. To rule out any interference of the mRNA structure and visualize the translational repression at the protein level, we extended the above analysis to the complete mRNA of *Ppm1d* and *Narf* genes, including the 3′-UTR. To achieve this goal, we cloned the complete *Ppm1d* and *Narf* mRNAs in a mammalian expression vector and transfected each of them with either a mixture of the three miR-29 miRNAs or a control miRNA (Figure 6C and D). In both cases, protein synthesis resulted strongly inhibited when miR-29 miRNAs were present, thereby confirming the functionality of the miR-29 binding sites predicted within the 3′-UTR of *Ppm1d* and *Narf*. On the basis of these results, we conclude that the DNA damage response can mediate the repression of these targets through members of the miR-29 family of miRNAs.

Finally, and also in relation to the identified targets of miR-29 in cells from *Zmpste24* progeroid mice, it is remarkable that a comparative analysis of the skeletal muscle transcriptome of *Zmpste24*$^{-/-}$ mice (Varela *et al*, 2005) with expression levels of predicted miR-29 targets demonstrated significant overlap in the analysed data sets (Supplementary Figure S1B). Further, RT–PCR expression analysis of genes such as *Ppm1d, Hbp1* and *Narf*, which were not represented in the available transcriptomic data, revealed a clear downregulation of *Narf* expression levels and no significant changes in *Hbp1* and *Ppm1d* mRNA levels, although a trend towards downregulation in the mutant tissues was observed for all transcripts (Supplementary Figure S1C).

miR-29 family reduces proliferation and enhances cell senescence

Among the selected miR-29 targets of potential relevance in aging processes, we focused our attention on the Ppm1d/Wip1 phosphatase, since it has been previously reported that this protein is a key regulator of the DNA damage response through its ability to dephosphorylate a wide variety of proteins such as p53, Chk1, Chk2, p38, γ-H2AX and ATM (Lu *et al*, 2008a; Cha *et al*, 2010). According to this, and given that this family of miRNAs is regulated by the DNA damage response and miR-29 levels are progressively accumulated during cell senescence, we asked whether miR-29 family could modulate cell viability in culture fibroblasts. As a first attempt to evaluate this hypothesis, we transfected three different primary fibroblast cell lines with a combination of miR-29a, -29b and -29c precursor molecules and we measured cell proliferation during three passages by cell counting. As shown in Figure 7A, exogenous addition of miR-29 compromises cell proliferation in primary fibroblasts. In addition, analysis of cell senescence in miR-29 overexpressing fibroblasts demonstrated a consistent accumulation of SA-βGal-positive cells and increased levels of γ-H2AX compared with control cells at the end point of this experi-

 ©2011 European Molecular Biology Organization

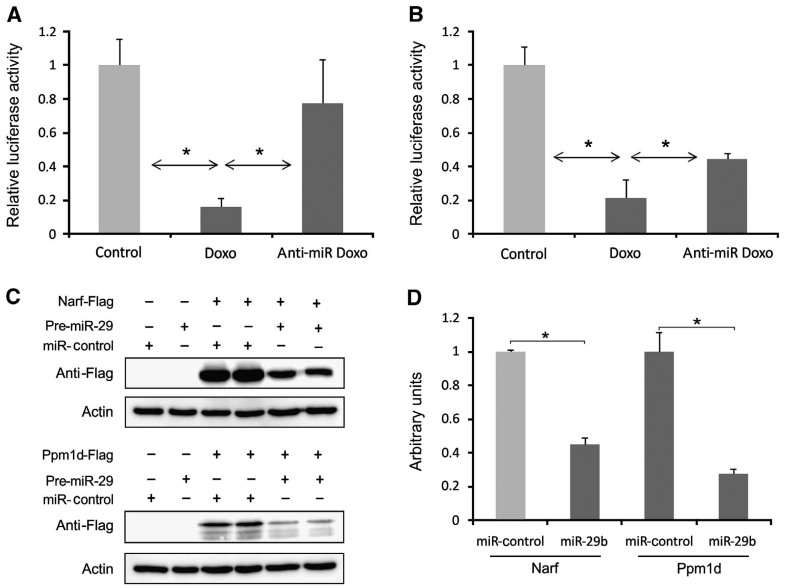

Figure 6 Doxorubicin treatment represses Ppm1d and Narf synthesis through miR-29. Doxorubicin treatment decreases luminescence emission in cells transfected with the wild-type 3′-UTR of *Ppm1d* (**A**) and *Narf* (**B**). Transfection of miR-29 inhibitory molecules abolishes the translational repression over the 3′-UTRs of *Ppm1d* and *Narf* after doxorubicin treatment ($n=3$ biological replicates). (**C**) Immunoblotting of HEK-293 cells transfected with pcDNA-flag-Narf or pcDNA-flag-Ppm1d in combination with miR-29 microRNA precursor molecules or a microRNA control. The full-length mRNAs of both *Narf* and *Ppm1d*, including the 3′-UTR were cloned into pcDNA vector in frame with a flag epitope for immunoblot detection with an anti-Flag antibody. (**D**) Densitometry analysis of the immunoblots shown in (**A**). Overexpression of miR-29 reduces the protein levels of Narf and Wip1 by 55 and 72%, respectively. *Significantly different, $P<0.05$.

ment (Figure 7A). Given these results, we asked whether miR-29 inhibition could delay replicative senescence in *Zmpste24*$^{-/-}$ fibroblasts by transfection of antagomiR molecules against miR-29. As expected, we observed a marked increase in proliferative potential of the anti-miR-29-transfected cell cultures in comparison to scrambled anti-miR-transfected cell lines (Figure 7B). Moreover, anti-miR-29 transfection of *Zmpste24*$^{-/-}$ fibroblasts yielded a significant increase in both the number of senescent and γ-H2AX-positive cells (Figure 7B). To further confirm these results, cell proliferation in wild-type fibroblasts transfected with miR-29 precursor molecules and *Zmpste24*$^{-/-}$ fibroblasts transfected with inhibitor molecules was assessed by MTT assays at different time points (Supplementary Figure S2A). These experiments corroborated and reinforced the previous observations. Additionally, we examined whether augmented miR-29 levels can enhance sensitivity to DNA damage drugs in fibroblasts. To achieve this goal, control or miR-29-transfected fibroblasts were treated with doxorubicin and cell viability was measured using an MTT assay. As shown in Figure 7C, miR-29-transfected fibroblasts were more sensitive to doxorubicin treatment, showing a considerable reduction in cell viability. On the other hand, reduction of miR-29 levels in *Zmpste24*$^{-/-}$ fibroblasts by transfection of anti-miR molecules resulted in augmented cell viability under doxorubicin conditions in comparison to scrambled anti-miR-transfected cells. To confirm that these observations can be extended to other cellular systems, we analysed the impact of miR-29 on the proliferation potential of U2OS human osteosarcoma cells. To achieve this goal, we used a different approach which consists of the overexpression of the miR-29b and -29c levels by using a lentiviral vector that expresses the miR-29b-2∼29c cluster. Consistent with observations in fibroblasts, U2OS cells transduced with the miR-29 lentiviral vector showed a marked reduction in proliferation potential in comparison to cells transduced with the empty vector (Supplementary Figure S2B). Furthermore, we were able to demonstrate that transfection of anti-miR-29 molecules restored the proliferation potential of U2OS cells that overexpress miR-29. Collectively, these results demonstrate that the miR-29 family modulates cell viability through regulation of cell proliferation and senescence, features that perfectly correlate with the phenotype alterations observed in *Zmpste24*$^{-/-}$ progeroid mice.

miR-29 regulates p53 phosphorylation through Ppm1d repression

Since *Ppm1d* is a *bona fide* target of miR-29 and a well-known regulator of p53, we proceeded to analyse the impact of miR-29 on the p53 pathway. For this purpose, wild-type primary fibroblasts were transfected with miR-29 precursors or inhibitory molecules or their corresponding scrambled controls, and p53 phosphorylation was analysed by western blot in both untreated and doxorubicin-treated conditions (Figure 8A). Although in untreated conditions there were no clear differences, we observed a strong correlation in the phosphorylation status of p53 at serine 15—the residue targeted by Ppm1d—and miR-29 levels in doxorubicin-treated

©2011 European Molecular Biology Organization

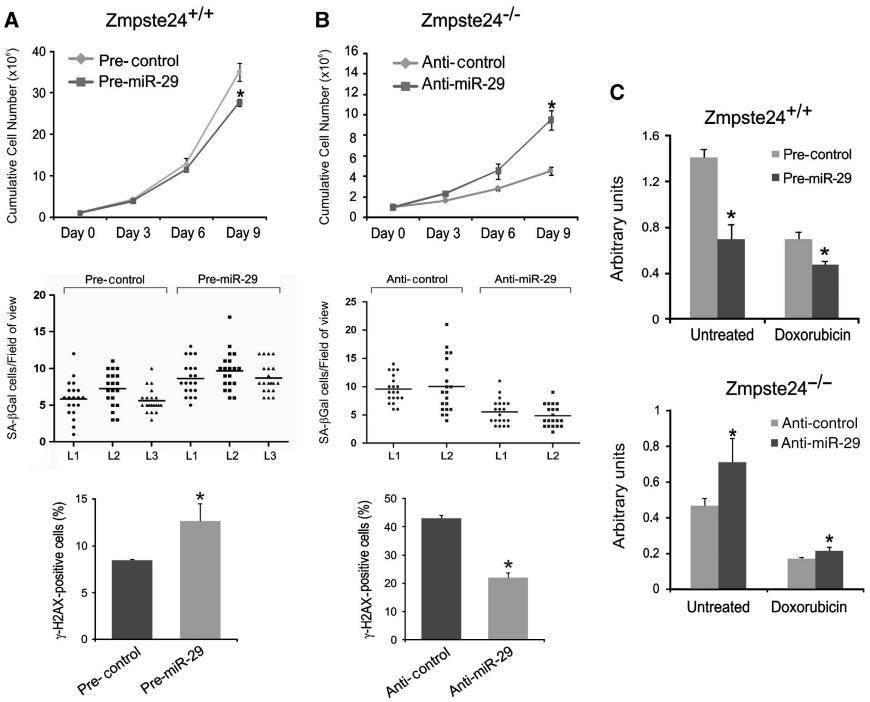

Figure 7 miR-29 overexpression reduces cell proliferation and viability and increases senescence. (**A**) Effects of miR-29 on cell proliferation and senescence. Passage 2 wild-type primary fibroblasts were transfected with a combination of miR-29a, -29b and -29c or control precursor miRNA (pre-miR-29 or pre-control) A million cells growing in 10 cm dishes were transfected with the indicated molecules and every 3 days cell populations were determined by cell counting using a hemocytometer (top panel). At each passage, a million cells were re-seeded and this procedure was repeated during three passages (three wild-type and three mutant mice fibroblasts were used in each condition). Additionally, SA-βGal activity (middle panel) and γ-H2AX (bottom panel) markers at the end point of the experiment were analysed. (**B**) The same experiment was carried out with passage 4 *Zmpste24*$^{-/-}$ fibroblast using inhibitory molecules (anti-miR-29 or anti-control). (**C**) MTT assay of cell viability under doxorubicin treatment. Primary wild-type fibroblasts (top panel) transfected with miR-29 or control precursor molecules and *Zmpste24*-deficient mice fibroblast transfected with miR-29 or control inhibitor molecules (bottom panel) were treated with 1 μM doxorubicin or left untreated for 72 h and cell viability was measured by MTT assay ($n = 3$ biological replicates). *Significantly different from pre- or anti-control transfected cells, $P < 0.05$.

cells. Thus, transfection of precursor molecules resulted in elevated levels of phospho-p53 whereas in anti-miR-transfected fibroblasts, there was a marked reduction in phosphorylated p53. Accordingly, we tried to reduce the phosphorylation levels of p53 in *Zmpste24*$^{-/-}$ fibroblasts by transfection of miR-29 inhibitor molecules (Figure 8B). Interestingly, miR-29 inhibition successfully reduced the levels of phosphorylated p53 in both untreated and doxorubicin-treated cells in comparison to the scrambled anti-miR-transfected cells. Due to antibody specificity limitations, we were unable to perform a reliable measure of Ppm1d protein levels in murine systems. Consequently, we moved to a human system by using U2OS osteosarcoma cells, which display normal PPM1D levels and p53 responsiveness. As shown in Figure 8C, U2OS cells transfected with miR-29 precursor molecules display a strong reduction in PPM1D protein levels, which correlates with an increase in phospho-p53 levels, while total-p53 showed no substantial changes. However, in this system, miR-29 inhibition did not result in consistent changes in *PPM1D* expression, which could be explained by repression by other miRNAs whose expression is altered in this cell line.

To further correlate miR-29 levels with *Ppm1d* repression and p53 phosphorylation, we used a different approach involving infection of U2OS cells with a lentiviral vector expressing the miR-29b-2-c cluster or the empty vector, followed by analysis of the p53 response in both basal and doxorubicin-treatment conditions. As can be seen in Figure 8D, miR-29 expressing cells presented diminished basal levels of PPM1D and higher levels of p53 phosphorylation, and displayed an exacerbated response to DNA damage that also correlates with the PPM1D levels. These results are consistent with previous works describing that miR-29 enhances p53 responsiveness through p53 stabilization, which agrees well with our results since phosphorylation stabilizes this tumour suppressor protein and prevents its proteasome-mediated degradation (Lavin and Gueven, 2006).

Discussion

Since the discovery of miRNA-mediated translational regulation, a wide variety of functions have been associated with this process. Compared with protein–protein interactions, in which a single protein interacts with a reduced number of

 ©2011 European Molecular Biology Organization

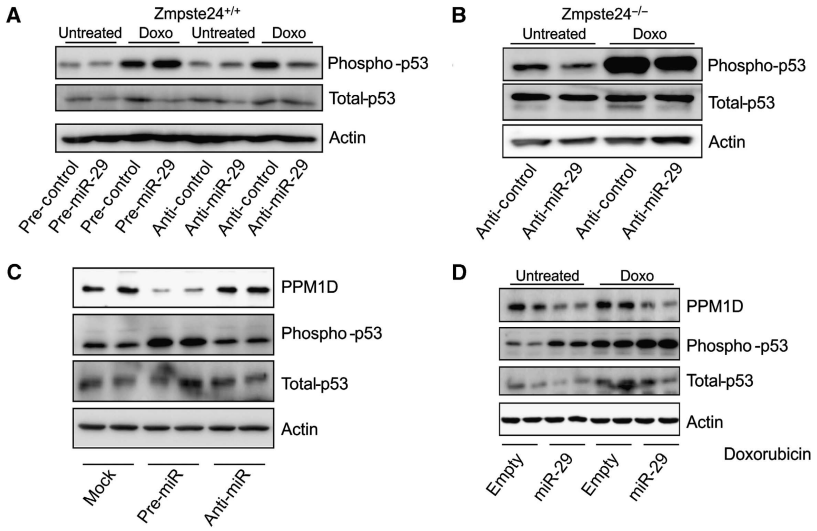

Figure 8 miR-29 modulates the DNA damage response through Ppm1d. (**A**) Wild-type mouse ear fibroblasts were transfected with a combination of pre- or anti-miR-29 molecules, left to recover for 24 h and treated with 0.5 μM doxorubicin or left untreated for 24 h. Then, cells were harvested and phospho-(S15)-p53, total-p53 and β-actin protein levels were analysed by western blot using specific antibodies. (**B**) Western blot of *Zmpste24*$^{-/-}$ primary fibroblasts transfected with control or miR-29 inhibitor molecules in untreated or doxorubicin-treated conditions. After transfection, cells were left to recover for 24 h, and then treated with 0.5 μM doxorubicin or left untreated for 24 h. (**C**) Western blot analysis of U2OS cells transfected with a combination of pre-miR-29 or anti-miR-29 molecules. After 48 h, transfection cells were harvested and protein levels were assessed by western blot using anti-PPM1D, anti-phospho-(S15)-p53, anti-total-p53 and anti-β-actin antibodies. (**D**) Western blot analysis of U2OS cells infected with a lentiviral vector that expresses miR-29-b-c (miR-29) cluster or the empty vector (empty). Cells were treated with 0.1 μM doxorubicin for 90 min and after 3 h cells were harvested and proteins were separated on SDS–PAGE and probed with anti-PPM1D, anti-phospho-(S15)-p53, anti-total-p53 and anti-β-actin antibodies.

proteins, each miRNA has the potential ability to repress the translation of hundreds of transcripts (Grigoriev, 2003; Lewis *et al*, 2005). Accordingly, dysregulation of miRNA expression could also contribute to the numerous alterations present in a very complex and multifactorial process such as aging. Previous works have analysed the expression of miRNAs in different tissues from young and old mice (Williams *et al*, 2007; Maes *et al*, 2008) as well as in mice with delayed aging (Bates *et al*, 2010), but the role of miRNAs in mice with accelerated aging is still unknown. Our results show that *Zmpste24*-deficient mice, a mouse model of human Hutchinson–Gilford progeria, display dysregulated miRNA expression in liver and muscle. Among those miRNAs whose expression is altered in these progeroid mice, we have identified three miRNAs belonging to the miR-29 family which are significantly overexpressed in tissues from *Zmpste24*$^{-/-}$ mice. miR-29 upregulation was especially relevant in muscle from *Zmpste24*$^{-/-}$ mice, showing up to ~10-fold higher levels than those of control animals. Further studies of miR-29 levels in liver and muscle samples from old mice demonstrated that the changes observed in these premature aging mice also occur during physiological aging. Notably, a recent exhaustive study of the age-related miRNA changes in the human and macaque brain cortex has identified the miR-29 family among those miRNAs with high age-correlated expression (Somel *et al*, 2010). Additionally, miR-29 levels are downregulated in Ames dwarf mice, which display a delay in the onset of aging (Bates *et al*, 2010), thus suggesting a more general role for this miRNA family in the regulation of processes associated with normal and pathological aging.

Functional analysis aimed at the characterization of the molecular mechanisms underlying the observed links between miR-29 and aging has revealed that the miR-29 upregulation is associated with the DNA damage response (Figure 9). We had previously described that tissues from *Zmpste24*-deficient mice present an accumulation of senescent cells and a marked transcriptional activation of p53 downstream targets (Varela *et al*, 2005). Additionally, these progeroid mice present genomic instability and a profound stem cell dysfunction (Liu *et al*, 2005; Espada *et al*, 2008; Marino *et al*, 2008). These previous findings prompted us to consider that the transcriptional activation of *miR-29* family members could be part of the DNA damage response against genomic instability. Consistent with this hypothesis, we have found that miR-29 expression is progressively increased during passage of *Zmpste24*$^{-/-}$ primary cultures from mouse ear fibroblasts, with the highest levels being detected when cells reach replicative senescence. Interestingly, this phenomenon was not an exclusive property of *Zmpste24*-mutant mice fibroblasts, since miR-29 undergoes a similar upregulation in wild-type fibroblasts in serial passage. This observation, together with the finding that both wild-type and mutant mice fibroblasts display similar levels of miR-29 at first passage, indicates that miR-29 changes cannot fully explain the proliferation differences between wild-type and mutant fibroblasts in cell culture. However, the increased levels of senescence and DNA damage markers during serial passage

©2011 European Molecular Biology Organization

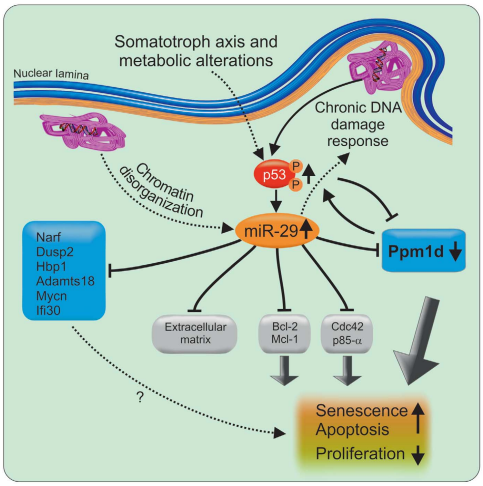

Figure 9 Model for the miR-29 regulatory network in *Zmpste24*$^{-/-}$ progeroid mice. Nuclear lamina alterations of *Zmpste24*$^{-/-}$ cells induce a genomic instability situation that it is recognized by these cells as a chronic DNA damage, thereby activating the p53 signalling pathway. Additionally, nuclear lamina abnormalities disrupt the chromatin–lamina attachment patterns causing profound changes in chromatin structure. These alterations, putatively reinforced by the somatotroph axis and metabolic alterations present in these mice (dotted line), lead to an abnormal miR-29 activation and a subsequent repression of their target genes. These targets include several genes with pro-survival roles, like *Bcl-2*, *Mcl-1*, *Cdc42*, *p85-α* and *Ppm1d/Wip1*, whose downregulation leads to a decrease of cell proliferation and an increase of cell senescence and apoptosis, processes that finally result in the loss of tissue and organism homoeostasis. Moreover, Ppm1d repression diminishes the ratio of p53 dephosphorylation, which positively feedbacks the p53 loop, exacerbating the initial situation. Additionally, increased miR-29 levels may directly participate in further exacerbating DNA damage. Dotted lines indicate hypothetical links.

of both wild-type and mutant mice, although at different extent, link the genotoxic stress with the progressive accumulation of miR-29.

Further confirmation of this association came from the treatment of wild-type fibroblasts with different genotoxic drugs. These experiments have revealed that doxorubicin, a DNA topoisomerase inhibitor that causes double-strand breaks and generates a kind of chronic DNA damage, also induces the transcriptional activation of either miR-29a, -29b, and -29c, in contrast with the treatment with H_2O_2 or 4-NQO, which induce transient oxidative damage or UV-like lesions, respectively. According to these results, only the chronic or difficult to repair DNA damage induces the expression of this family of miRNAs. Furthermore, we have found that this upregulation occurs in a p53-dependent manner, since *p53*$^{-/-}$ murine fibroblasts failed to increase miR-29 expression during successive cell culture passages and upon doxorubicin treatment. Likewise, *ATM*-deficient and *ATR-Seckel* murine fibroblasts failed to induce miR-29 expression when using equivalent concentrations of doxorubicin, which further confirms the link between DNA damage response and miR-29 regulation. More interestingly, high concentrations of doxorubicin activated the expression of miR-29 in both *ATM*-deficient and *ATR-Seckel* fibroblasts, which suggests that other regulatory mechanisms could be operating depending on the extent of DNA damage. In this regard, two recent works have identified c-myc and NF-κB as repressor factors of these miRNAs (Liu *et al*, 2010; Mott *et al*, 2010). Collectively, all these data associate the miR-29 family upregulation present in both *Zmpste24*-deficient mice and normal aging with the DNA damage response activation.

To identify miR-29 targets which could contribute to the observed effects related to aging and DNA damage response in *Zmpste24*$^{-/-}$ progeroid mice, we followed an experimental approach based on the combination of target prediction by different algorithms with luciferase-based validation assays of the predicted targets. This strategy led us to identify seven transcripts subjected to repression by miR-29a, -29b or -29c. Interestingly, we did not observe different repression ratios by any of the three miRNAs of the miR-29 family, which suggests that they are not specialized in different functions and may perform redundant activities in the regulation of the identified targets. These targets include protein phosphatases (Ppm1d/Wip1 and Dusp2), oncogenes (Mycn), interferon-inducible proteins (Ifi30), transcriptional repressors (Hbp1), nuclear envelope proteins (Narf) and metalloproteases (Adamts18). Among all of them, we focused on Ppm1d phosphatase and prelamin A interacting protein Narf, which had been previously associated with processes of interest in relation to DNA damage and aging. Thus, Ppm1d dephosphorylates a variety of proteins involved in DNA damage response, such as p53, Chk1, Chk2, p38, γ-H2AX and ATM (Lu *et al*, 2008a; Cha *et al*, 2010). Moreover, *Ppm1d* is transcriptionally activated by p53 upon DNA damage and participates in a negative regulatory feedback with ATM (Batchelor *et al*, 2008, 2009). On the other hand, Narf interacts with prelamin A, whose accumulation at the nuclear envelope of *Zmpste24*$^{-/-}$ cells is the pathological hallmark underlying the accelerated aging process exhibited by these mice (Varela *et al*, 2008). Consequently, we evaluated the presence of miR-29 binding sites in these two targets, with the finding that a 2-nt mutation in the putative seed sequences of *Ppm1d* and *Narf* 3′-UTR abolishes the translational repression by miR-29 in luciferase assays. We also found that co-expression of the full-length mRNA of *Ppm1d* or *Narf* together with *miR-29* precursor molecules in HEK-293 cells, significantly reduces Narf and Ppm1d protein levels compared with cells transfected with a control miRNA. These experiments confirm that *Ppm1d* and *Narf* transcripts contain functional miR-29 binding sites and that these miRNAs repress the translation of both targets. The lack of appropriate antibodies for Narf precluded further work to explore miR-29 effects on the endogenous protein, but parallel experiments demonstrated that miR-29 family members are able to inhibit endogenous Ppm1d protein production and that this effect has a special impact on the phosphorylation of p53.

According to the above results, it was tempting to speculate that miR-29 upregulation, as a likely consequence of the progressive accumulation of DNA damage, reduces Ppm1d protein levels, a key regulatory phosphatase of the DNA damage response that dephosphorylates a wide variety of proteins such as p53, Chk1, Chk2, p38, γ-H2AX and ATM, important for the control of cell viability (Lu *et al*, 2008a; Cha *et al*, 2010; Le Guezennec and Bulavin, 2010). Experiments aimed to further evaluate this hypothesis confirmed that increased levels of miR-29 through transfection of

 ©2011 European Molecular Biology Organization

miRNA precursor molecules reduce fibroblasts proliferation and enhance cell senescence. Furthermore, γ-H2AX levels were increased in these cells, which demonstrated the increased sensitivity to DNA damage, an observation that was also confirmed by MTT assays of wild-type fibroblasts transfected with miR-29 precursor, although the possibility of a positive feedback in which miR-29 increases DNA damage cannot be discarded (Figure 9). Importantly, we were also able to reverse the proliferation defects in *Zmpste24*$^{-/-}$ fibroblasts by the transfection of antagomiR molecules against miR-29. Thus, miR-29 inhibition in these cells resulted in a strong increase in proliferation potential accompanied by a significant decrease in both the number of SA-βGal- and γ-H2AX-positive cells. Likewise, we could demonstrate that the sensitivity of *Zmpste24*$^{-/-}$ fibroblasts to doxorubicin treatment is significantly diminished when miR-29 is downregulated by transfection of miRNA inhibitor molecules. Also in agreement with our proposal of a role for miR-29 in the modulation of cell viability, we have found higher phosphorylation levels of p53 at Ser15—the residue targeted by Ppm1d—in mouse fibroblasts transfected with miR-29 precursor molecules. Conversely, inhibitory molecules against miR-29 yielded the opposite effect, decreasing the levels of p53 phosphorylation in doxorubicin-treated wild-type fibroblasts. Moreover, a similar experiment with *Zmpste24*-deficient mouse fibroblasts showed that miR-29 inhibition decrease the levels of phosphorylated p53 in both basal and doxorubicin conditions. Furthermore, we were able to correlate the p53 phosphorylation status with the PPM1D protein levels in basal and doxorubicin-treated U2OS human cells. These results are also consistent with previous data showing that miR-29 induces apoptosis in a p53-dependent manner and increases the levels of total-p53 (Park *et al*, 2009), because p53 phosphorylation stabilizes the protein preventing its degradation by the proteasome (Lavin and Gueven, 2006). Likewise, the observation that Ppm1d dephosphorylates Mdm2 and prevents p53 proteasome degradation (Lu *et al*, 2008b), is consistent with our finding that miR-29 targets *Ppm1d* and influences levels and activity of the p53 tumour suppressor.

Collectively, these data together with additional observations from the literature, strongly support our proposal that miR-29 is an aging-related miRNA. First, several reports have described a tumour suppressor role for miR-29 family members in several human cancers including haematological malignancies, rhabdomyosarcoma, pleural mesothelioma and hepatocellular carcinoma (Pekarsky *et al*, 2006; Wang *et al*, 2008; Garzon *et al*, 2009b; Pass *et al*, 2010; Xiong *et al*, 2010; Zhao *et al*, 2010). This tumour suppressive function of miR-29 family members is consistent with a pro-aging role for them, since a growing number of tumour suppressor genes have a negative role during aging through a process known as antagonistic pleiotropy (Campisi, 2005; Kirkwood, 2005). In fact, *Zmpste24*$^{-/-}$ progeroid mice exhibit a chronic hyperactivation of p53 signalling as well as a marked overexpression of other tumour suppressors such as p16/INK4A (Varela *et al*, 2005; Espada *et al*, 2008). Moreover, functions attributed to miR-29 include reduction of cell proliferation and induction of apoptosis, two features associated with the diminished capacity to maintain tissue homoeostasis which is a characteristic feature of aging processes (Mott *et al*, 2007; Muniyappa *et al*, 2009). Notably, it has also been reported that miR-29b induces global DNA hypomethylation by targeting different demethylases (Garzon *et al*, 2009b), another observation that links miR-29 functions and aging, since epigenetic alterations are characteristic features of the aging process (Gravina and Vijg, 2010; Osorio *et al*, 2010). Finally, miR-29 family members show increased expression during aging and an inverse relationship with expression levels of a group of cancer-related genes in human and macaque brain (Somel *et al*, 2010).

In conclusion, we propose that miR-29 has a pivotal role in the regulation of cell survival and proliferation through the modulation of the DNA damage response (Figure 9); thus, making these miRNAs very interesting in the context of both cancer and aging. Disruption of the DNA damage response is a hallmark of cancer progression that is achieved by many tumours through mutations in p53. However, tumours can amplify PPM1D as an alternative way to inhibit p53 activity and, interestingly, these tumours rarely harbour p53 mutations (Bulavin *et al*, 2002). According to our results, miR-29 downregulation could constitute another way for tumours to reduce p53 signalling, thus allowing tumours to escape from apoptosis and growth arrest. Finally, the observation that miR-29 accumulates during aging provides an additional evidence for the implication of miRNAs in the development of the complex process of aging.

Materials and methods

Transgenic animals

Mutant mice deficient in Zmpste24 metalloproteinase have been previously described (Pendas *et al*, 2002). *ATM*$^{-/-}$ and *ATR*$^{s/s}$ mice were kindly provided by Dr Oscar Fernandez-Capetillo (CNIO, Madrid, Spain), and *XPF*$^{-/-}$ and *CSB/XPA*$^{-/-}$ mice by Dr Jan Hoeijmakers (Erasmus University, Rotterdam, The Netherlands). Animal experiments were conducted in accordance with the guidelines of the Committee on Animal Experimentation of the Universidad de Oviedo, Oviedo, Spain.

Luciferase assays

For miR-29 target validation, the entire 3′-UTR murine sequence of each predicted target gene was PCR amplified and cloned into psiCHECK-2 plasmid (kindly provided by Dr A Rodriguez, The Welcome Trust Sanger Institute, Cambridge, UK) downstream of the Renilla luciferase ORF using the restriction enzymes *Xho*I and *Not*I. HEK-293 cells were seeded 6 h before transfection in 24-well plates at 50% of confluence. Transfections were performed using lipofectamine 2000 (Invitrogen), 250 ng of each psiCHECK-2 constructs and 20 pmol of miR-29a, -29b, -29c or control miRNA molecules (Ambion), following the manufacturer's instructions. Transfection was carried out for 4 h, and then medium was removed and cells were left to recover for 18 h. For promoter analysis, the indicated genomic regions of each cluster were cloned into pGL3-basic plasmid (Promega) using the restriction enzyme *Sma*I. In all, 250 ng of the resulting plasmids was transfected in HCT-116 cells growing in 24-well plates in combination with 12.5 ng of the pRLTK plasmid (Promega) using lipofectamine 2000 (Invitrogen). Transfections were carried out for 4 h, and then medium was replaced by fresh medium alone or containing 0.5 μM doxorubicin, 0.5 μM 4-nitroquinolone-1-oxide or 20 μM H_2O_2. Determination of luciferase activity was performed using Dual-luciferase® Reporter Assay System (Promega). Briefly, cells on 24-well plates were washed with PBS and lysed by pipetting mixing using 80 μl of the passive lysis buffer. Then, both Renilla and Firefly luciferase activity of each sample were measured in a TD-20/20 luminometer (Turner Biosystems).

Immunoblotting analysis

Cell cultures were washed with PBS and homogenized in an appropriate volume of 20 mM Tris buffer pH 7.4, containing 150 mM NaCl, 1% Triton X-100, 10 mM EDTA, Complete® protease inhibitor cocktail (Roche Applied Science), and phosphatase inhibitors

©2011 European Molecular Biology Organization

(200 μM sodium orthovanadate, 1 mM β-glycerophosphate). Once homogenized, cell extracts were sonicated and subsequently centrifuged at 12 000 *g* at 4°C, with the resulting supernatants being collected. The protein concentration of the supernatant was evaluated by bicinchoninic acid (BCA protein assay kit, Pierce Biotechnology, Rockford, IL) and 4 μg of each cell extract was loaded onto SDS–polyacrylamide gels. After electrophoresis, gels were electrotransferred onto nitrocellulose membranes, and then the membranes were blocked with 5% non-fat dried milk in PBT (phosphate buffered saline with 0.05% Tween-20) and incubated with primary antibodies in 5% BSA in PBT. After three washes with PBT, membranes were incubated with horseradish peroxidase-conjugated goat anti-rabbit IgG at a 1:10 000 dilution in 1.5% milk in PBT, and developed with a West Pico enhanced chemiluminescence kit (Pierce Biotechnology). For immunoblotting, the following antibodies were used: anti-PPM1D (Bethyl Laboratories), anti-S15-phospho-p53 (Cell Signaling), anti-total-p53 (Cell Signaling), anti-flag (Sigma-Aldrich) and anti-β-actin (Sigma-Aldrich).

microRNA analysis

microRNA profiling was performed as previously described (Lu *et al*, 2005) using total RNA extracted with TRIzol (Invitrogen). For qPCR analysis, total RNA was prepared using miRVANA™ miRNA isolation Kit (Ambion, Austin, TX) and RNA samples were quantified and evaluated for purity (260 nm/280 nm ratio) using a NanoDrop ND-1000 spectrophotometer. miRNA detection was performed using Taqman® miRNA expression assays (Applied Biosystems). Briefly, 10 ng of total RNA was reverse transcribed using Taqman® miRNA reverse transcription kit (Applied Biosystems) and PCR amplified using an Applied Biosystems 7300 Real-Time PCR system. As an internal control, miRNA expression was normalized to snoRNA202 for mouse samples and to RNU6B for human samples, using Taqman® Gene Expression Assays (Applied Biosystems). All protocols were carried out according to the manufacturer's instructions.

Cell culture

HCT-116 cells were kindly provided by Dr B Vogelstein (Ludwig Center, Baltimore, MD, USA), HEK-293T and U2OS cells by Dr PP Durán (CNIO) and p53-deficient cells by Dr M Serrano (CNIO). Cultures were maintained in Dulbecco's modified Eagle's medium (DMEM, Gibco) supplemented with 10% fetal bovine serum (FBS) and 1% penicillin–streptomycin–glutamine (Gibco). Murine fibroblasts were extracted from 12-week-old mice ears. Ears were sterilized with ethanol, washed with PBS, and triturated with razor blades. Samples were then incubated with 600 μl of 4 mg/ml collagenase D (Roche) and 4 mg/ml dispase II (Roche) in DMEM for 45 min at 37°C and 5% CO_2. After filtering and washing, 6 ml of DMEM with 10% FBS and 1% antibiotic-antimycotic were added, and the mixture was incubated at 37°C and 5% CO_2. Cell numbers were determined using a hemocytometry and 10^6 cells were passed into a 10-cm plate every 3 days and cultured under standard conditions. For DNA damage induction, cells were seeded in 6-well plates and after 24 h, doxorubicin (Sigma) was added to the growing media. After a 24-h period, RNA was extracted and microRNA expression was analysed. Cell counting was performed using a Bright-Line hemacytometer (Hausser Scientific) following the manufacturer's instructions.

Cell transfections

Transfection of the U2OS cell line was carried out using lipofectamine RNAiMAX (Invitrogen) following manufacturer's instructions. U2OS cells were seeded in 6-well plates and the miRNA precursor or inhibitory molecules (from Dharmacon Inc) were transfected at a final concentration of 25 nM. For primary fibroblast transfections, two rounds of consecutive transfections were performed using lipofectamine RNAiMAX. miRNA inhibition was carried out using a control or miR-29b mercury LNA™ power inhibitors from Exiqon at a final concentration of 20 nM. miRNA over-expression in fibroblasts was performed using a mixture of miR-29a, -29b and -29c or control precursor molecules from Dharmacon Inc at a final concentration of 25 nM.

Viral package and cell infection

Lentiviruses were packaged in HEK-293T cells using a VSVG-based package system kindly provided by Dr JM Silva (Columbia University, New York, USA). Cells were seeded in 6-well plates 24 h before transfection. The next day, cells were transfected using TransIT®-LT1 Transfection Reagent (Mirus) and a mixture of 2 μg of the desired plasmid and 1 μg of each lentiviral helper, following the manufacturer's instructions. Transfection medium was removed 24 h after transfection and fresh medium was added to the plate. Cell supernatants were collected at 24 and 48 h, cleared by centrifugation at 1200 r.p.m. for 10 min and filtered through a 0.45-μm sterile filter. U2OS cells were seeded in 6-well plate at 20–30% confluence 24 h before the infection. The following day, 1 ml of viral supernatant was added to growing media supplemented with 5 μg/ml of polybrene (Millipore), centrifuged at 1000 r.p.m. for 1 h at room temperature and incubated for 8 h. This step was repeated twice and cells were left recovering for 24 h in growing media before drug selection. Cells infected with pLemiR or pMSCV constructs were selected with 2 μg/ml of puromycin (Sigma) or 100 μg/ml of hygromycin (Invitrogen), respectively.

Cell senescence analysis

Cell senescence was assessed by detecting the senescence-associated β-galactosidase activity at pH 6.0 (SA-βGal) using the Senescence β-galactosidase kit from Cell Signaling. Staining was performed in 6-well plates and the SA-βGal-positive cells were detected by phase contrast microscopy using a Zeiss Axiovert 200M fluorescence microscope (Zeiss). Quantification was performed by counting the positive cells present in 20 independent fields of view at ×10 magnification, and images were captured and processed using Adobe Photoshop CS3 and displayed using CorelDraw.

Immunofluorescence

Cells were seeded on glass coverslips, allowed to recover for 24 h and then fixed for 10 min at room temperature in 4% p-formaldehyde-buffered solution, followed by permeabilization with 0.5% Triton X-100 for 5 min. Cell preparations were blocked for 45 min at room temperature in 0.5% bovine serum albumin in PBS. Cells were incubated with anti-γH2AX antibody (1:250, Millipore) overnight at 4°C, and then with the appropriate fluorescence-conjugated secondary antibodies (Invitrogen) for 1 h at room temperature. Nuclei were stained by incubating cells with 4′,6-diamidino-2-phenylindole (DAPI), after which, coverslips were mounted on slides and cells imaged with a Zeiss Axiovert 200M fluorescence microscope (Zeiss). Images were processed using Adobe Photoshop CS3 and displayed using CorelDraw.

MTT assay

For MTT assay, 2500 fibroblasts or 5000 U2OS cells per well were seeded in 96-well plates. Transfection of miRNA precursor or inhibitor molecules was performed at the time of seeding using lipofectamine RNAiMAX (Invitrogen) according to the reverse protocol provided by the manufacturer. After transfection, medium was changed and MTT assay was performed at different time points using the Cell Titer 96 Non-Radioactive Cell Proliferation Assay (Promega). At each time point, 15 μl of dye solution was added to the medium for 2 h followed by an addition of 100 μl of solubilization solution. After 1 h incubation at 37°C, absorbance at 570 nm was measured using a powerWave XS spectrophotometer (Biotek).

Statistical and bioinformatics analysis

For computational prediction of the miR-29 targets, a combination of the following software was used: TargetScan (http://www.targetscan.org), Microcosm (http://www.ebi.ac.uk/enright-srv/microcosm/htdocs/targets/v5/) and PicTar (http://pictar.mdc-berlin.de/). All experimental data are reported as mean values and the error bars represent the s.e.m.. Statistical analysis was performed by the non-parametric Student's *t* test, using the Prism program v4.0 (GraphPad software, Inc).

Supplementary data

Supplementary data are available at *The EMBO Journal* Online (http://www.embojournal.org).

Acknowledgements

We thank M Fernández and C Garabaya for excellent technical assistance and Drs J Hoeijmakers, B Vogelstein, PP Durán, M Serrano,

 ©2011 European Molecular Biology Organization

JM Silva and O Fernández-Capetillo for providing cells, tissues and reagents. This work has been supported by grants from Ministerio de Ciencia e Innovación-Spain and European Union (FP7 MicroEnviMet). The Instituto Universitario de Oncología is supported by Obra Social Cajastur and Acción Transversal del Cáncer-RTICC. JR is supported by a fellowship from Fundación María Cristina Masaveu Peterson. CLO is an Investigator of the Botín Foundation.

Author contributions: APU designed and carried out most of the experiments and co-wrote the paper. AJR performed and analysed the immunofluorescence and SA-βGAL assays, collaborated in the promoter experiments and co-wrote the paper. JRS carried out some of the qPCR experiments and luciferase assays. IV provided mice biopsies and advised in cell culture. GM advised in immunoblotting experiments and experimental design. JC collaborated in the microRNA profiling and experimental design. JL carried out the microRNA profiling. JMPF analysed most data and advised in some experiments. CLO conceived and supervised the work and co-wrote the paper.

Conflict of interest

The authors declare that they have no conflict of interest.

References

Batchelor E, Loewer A, Lahav G (2009) The ups and downs of p53: understanding protein dynamics in single cells. *Nat Rev Cancer* **9:** 371–377

Batchelor E, Mock CS, Bhan I, Loewer A, Lahav G (2008) Recurrent initiation: a mechanism for triggering p53 pulses in response to DNA damage. *Mol Cell* **30:** 277–289

Bates DJ, Li N, Liang R, Sarojini H, An J, Masternak MM, Bartke A, Wang E (2010) MicroRNA regulation in Ames dwarf mouse liver may contribute to delayed aging. *Aging Cell* **9:** 1–18

Boehm M, Slack F (2005) A developmental timing microRNA and its target regulate life span in C. elegans. *Science* **310:** 1954–1957

Broers JL, Ramaekers FC, Bonne G, Yaou RB, Hutchison CJ (2006) Nuclear lamins: laminopathies and their role in premature ageing. *Physiol Rev* **86:** 967–1008

Bulavin DV, Demidov ON, Saito S, Kauraniemi P, Phillips C, Amundson SA, Ambrosino C, Sauter G, Nebreda AR, Anderson CW, Kallioniemi A, Fornace Jr AJ, Appella E (2002) Amplification of PPM1D in human tumors abrogates p53 tumor-suppressor activity. *Nat Genet* **31:** 210–215

Bushati N, Cohen SM (2007) microRNA functions. *Annu Rev Cell Dev Biol* **23:** 175–205

Cadinanos J, Varela I, Lopez-Otin C, Freije JM (2005) From immature lamin to premature aging: molecular pathways and therapeutic opportunities. *Cell Cycle* **4:** 1732–1735

Campisi J (2005) Aging, tumor suppression and cancer: high wire-act!. *Mech Ageing Dev* **126:** 51–58

Cha H, Lowe JM, Li H, Lee JS, Belova GI, Bulavin DV, Fornace Jr AJ (2010) Wip1 directly dephosphorylates gamma-H2AX and attenuates the DNA damage response. *Cancer Res* **70:** 4112–4122

Drummond MJ, McCarthy JJ, Fry CS, Esser KA, Rasmussen BB (2008) Aging differentially affects human skeletal muscle microRNA expression at rest and after an anabolic stimulus of resistance exercise and essential amino acids. *Am J Physiol Endocrinol Metab* **295:** E1333–E1340

Elson A, Wang Y, Daugherty CJ, Morton CC, Zhou F, Campos-Torres J, Leder P (1996) Pleiotropic defects in ataxia-telangiectasia protein-deficient mice. *Proc Natl Acad Sci USA* **93:** 13084–13089

Eller MS, Ostrom K, Gilchrest BA (1996) DNA damage enhances melanogenesis. *Proc Natl Acad Sci USA* **93:** 1087–1092

Espada J, Varela I, Flores I, Ugalde AP, Cadinanos J, Pendas AM, Stewart CL, Tryggvason K, Blasco MA, Freije JM, Lopez-Otin C (2008) Nuclear envelope defects cause stem cell dysfunction in premature-aging mice. *J Cell Biol* **181:** 27–35

Flynt AS, Lai EC (2008) Biological principles of microRNA-mediated regulation: shared themes amid diversity. *Nat Rev Genet* **9:** 831–842

Garzon R, Calin GA, Croce CM (2009a) MicroRNAs in cancer. *Annu Rev Med* **60:** 167–179

Garzon R, Liu S, Fabbri M, Liu Z, Heaphy CE, Callegari E, Schwind S, Pang J, Yu J, Muthusamy N, Havelange V, Volinia S, Blum W, Rush LJ, Perrotti D, Andreeff M, Bloomfield CD, Byrd JC, Chan K, Wu LC *et al* (2009b) MicroRNA-29b induces global DNA hypomethylation and tumor suppressor gene reexpression in acute myeloid leukemia by targeting directly DNMT3A and 3B and indirectly DNMT1. *Blood* **113:** 6411–6418

Gravina S, Vijg J (2010) Epigenetic factors in aging and longevity. *Pflugers Arch* **459:** 247–258

Grigoriev A (2003) On the number of protein-protein interactions in the yeast proteome. *Nucleic Acids Res* **31:** 4157–4161

Harvey M, Sands AT, Weiss RS, Hegi ME, Wiseman RW, Pantazis P, Giovanella BC, Tainsky MA, Bradley A, Donehower LA (1993) *In vitro* growth characteristics of embryo fibroblasts isolated from p53-deficient mice. *Oncogene* **8:** 2457–2467

Hasty P, Campisi J, Hoeijmakers J, van Steeg H, Vijg J (2003) Aging and genome maintenance: lessons from the mouse? *Science* **299:** 1355–1359

He L, He X, Lowe SW, Hannon GJ (2007) microRNAs join the p53 network–another piece in the tumour-suppression puzzle. *Nat Rev Cancer* **7:** 819–822

Hoeijmakers JH (2009) DNA damage, aging, and cancer. *N Engl J Med* **361:** 1475–1485

Kirkwood TB (2005) Understanding the odd science of aging. *Cell* **120:** 437–447

L'Ecuyer T, Sanjeev S, Thomas R, Novak R, Das L, Campbell W, Heide RV (2006) DNA damage is an early event in doxorubicin-induced cardiac myocyte death. *Am J Physiol Heart Circ Physiol* **291:** H1273–H1280

Lavin MF, Gueven N (2006) The complexity of p53 stabilization and activation. *Cell Death Differ* **13:** 941–950

Le Guezennec X, Bulavin DV (2010) WIP1 phosphatase at the crossroads of cancer and aging. *Trends Biochem Sci* **35:** 109–114

Lewis BP, Burge CB, Bartel DP (2005) Conserved seed pairing, often flanked by adenosines, indicates that thousands of human genes are microRNA targets. *Cell* **120:** 15–20

Liu B, Wang J, Chan KM, Tjia WM, Deng W, Guan X, Huang JD, Li KM, Chau PY, Chen DJ, Pei D, Pendas AM, Cadinanos J, Lopez-Otin C, Tse HF, Hutchison C, Chen J, Cao Y, Cheah KS, Tryggvason K *et al* (2005) Genomic instability in laminopathy-based premature aging. *Nat Med* **11:** 780–785

Liu S, Wu LC, Pang J, Santhanam R, Schwind S, Wu YZ, Hickey CJ, Yu J, Becker H, Maharry K, Radmacher MD, Li C, Whitman SP, Mishra A, Stauffer N, Eiring AM, Briesewitz R, Baiocchi RA, Chan KK, Paschka P *et al* (2010) Sp1/NFkappaB/HDAC/miR-29b regulatory network in KIT-driven myeloid leukemia. *Cancer Cell* **17:** 333–347

Lu J, Getz G, Miska EA, Alvarez-Saavedra E, Lamb J, Peck D, Sweet-Cordero A, Ebert BL, Mak RH, Ferrando AA, Downing JR, Jacks T, Horvitz HR, Golub TR (2005) MicroRNA expression profiles classify human cancers. *Nature* **435:** 834–838

Lu X, Nguyen TA, Moon SH, Darlington Y, Sommer M, Donehower LA (2008a) The type 2C phosphatase Wip1: an oncogenic regulator of tumor suppressor and DNA damage response pathways. *Cancer Metastasis Rev* **27:** 123–135

Lu X, Nguyen TA, Zhang X, Donehower LA (2008b) The Wip1 phosphatase and Mdm2: cracking the "Wip" on p53 stability. *Cell Cycle* **7:** 164–168

Maes OC, An J, Sarojini H, Wang E (2008) Murine microRNAs implicated in liver functions and aging process. *Mech Ageing Dev* **129:** 534–541

Marino G, Ugalde AP, Salvador-Montoliu N, Varela I, Quiros PM, Cadinanos J, van der Pluijm I, Freije JM, Lopez-Otin C (2008) Premature aging in mice activates a systemic metabolic response involving autophagy induction. *Hum Mol Genet* **17:** 2196–2211

Mott JL, Kobayashi S, Bronk SF, Gores GJ (2007) mir-29 regulates Mcl-1 protein expression and apoptosis. *Oncogene* **26:** 6133–6140

Mott JL, Kurita S, Cazanave SC, Bronk SF, Werneburg NW, Fernandez-Zapico ME (2010) Transcriptional suppression of mir-29b-1/mir-29a promoter by c-Myc, hedgehog, and NF-kappaB. *J Cell Biochem* **110:** 1155–1164

©2011 European Molecular Biology Organization

Muniyappa MK, Dowling P, Henry M, Meleady P, Doolan P, Gammell P, Clynes M, Barron N (2009) MiRNA-29a regulates the expression of numerous proteins and reduces the invasiveness and proliferation of human carcinoma cell lines. *Eur J Cancer* **45:** 3104–3118

Murga M, Bunting S, Montana MF, Soria R, Mulero F, Canamero M, Lee Y, McKinnon PJ, Nussenzweig A, Fernandez-Capetillo O (2009) A mouse model of ATR-Seckel shows embryonic replicative stress and accelerated aging. *Nat Genet* **41:** 891–898

Osorio FG, Obaya AJ, Lopez-Otin C, Freije JM (2009) Accelerated ageing: from mechanism to therapy through animal models. *Transgenic Res* **18:** 7–15

Osorio FG, Varela I, Lara E, Puente XS, Espada J, Santoro R, Freije JM, Fraga MF, Lopez-Otin C (2010) Nuclear envelope alterations generate an aging-like epigenetic pattern in mice deficient in Zmpste24 metalloprotease. *Aging Cell* **9:** 947–957

Park SY, Lee JH, Ha M, Nam JW, Kim VN (2009) miR-29 miRNAs activate p53 by targeting p85 alpha and CDC42. *Nat Struct Mol Biol* **16:** 23–29

Pass HI, Goparaju C, Ivanov S, Donington J, Carbone M, Hoshen M, Cohen D, Chajut A, Rosenwald S, Dan H, Benjamin S, Aharonov R (2010) hsa-miR-29c* is linked to the prognosis of malignant pleural mesothelioma. *Cancer Res* **70:** 1916–1924

Pekarsky Y, Santanam U, Cimmino A, Palamarchuk A, Efanov A, Maximov V, Volinia S, Alder H, Liu CG, Rassenti L, Calin GA, Hagan JP, Kipps T, Croce CM (2006) Tcl1 expression in chronic lymphocytic leukemia is regulated by miR-29 and miR-181. *Cancer Res* **66:** 11590–11593

Pendas AM, Zhou Z, Cadinanos J, Freije JM, Wang J, Hultenby K, Astudillo A, Wernerson A, Rodriguez F, Tryggvason K, Lopez-Otin C (2002) Defective prelamin A processing and muscular and adipocyte alterations in Zmpste24 metalloproteinase-deficient mice. *Nat Genet* **31:** 94–99

Rokhlin OW, Scheinker VS, Taghiyev AF, Bumcrot D, Glover RA, Cohen MB (2008) MicroRNA-34 mediates AR-dependent p53-induced apoptosis in prostate cancer. *Cancer Biol Ther* **7:** 1288–1296

Shenouda SK, Alahari SK (2009) MicroRNA function in cancer: oncogene or a tumor suppressor? *Cancer Metastasis Rev* **28:** 369–378

Somel M, Guo S, Fu N, Yan Z, Hu HY, Xu Y, Yuan Y, Ning Z, Hu Y, Menzel C, Hu H, Lachmann M, Zeng R, Chen W, Khaitovich P (2010) MicroRNA, mRNA, and protein expression link development and aging in human and macaque brain. *Genome Res* **20:** 1207–1218

Tarasov V, Jung P, Verdoodt B, Lodygin D, Epanchintsev A, Menssen A, Meister G, Hermeking H (2007) Differential regulation of microRNAs by p53 revealed by massively parallel sequencing: miR-34a is a p53 target that induces apoptosis and G1-arrest. *Cell Cycle* **6:** 1586–1593

Tian M, Shinkura R, Shinkura N, Alt FW (2004) Growth retardation, early death, and DNA repair defects in mice deficient for the nucleotide excision repair enzyme XPF. *Mol Cell Biol* **24:** 1200–1205

van der Pluijm I, Garinis GA, Brandt RM, Gorgels TG, Wijnhoven SW, Diderich KE, de Wit J, Mitchell JR, van Oostrom C, Beems R, Niedernhofer LJ, Velasco S, Friedberg EC, Tanaka K, van Steeg H, Hoeijmakers JH, van der Horst GT (2007) Impaired genome maintenance suppresses the growth hormone–insulin-like growth factor 1 axis in mice with Cockayne syndrome. *PLoS Biol* **5:** e2

Varela I, Cadinanos J, Pendas AM, Gutierrez-Fernandez A, Folgueras AR, Sanchez LM, Zhou Z, Rodriguez FJ, Stewart CL, Vega JA, Tryggvason K, Freije JM, Lopez-Otin C (2005) Accelerated ageing in mice deficient in Zmpste24 protease is linked to p53 signalling activation. *Nature* **437:** 564–568

Varela I, Pereira S, Ugalde AP, Navarro CL, Suarez MF, Cau P, Cadinanos J, Osorio FG, Foray N, Cobo J, de Carlos F, Levy N, Freije JM, Lopez-Otin C (2008) Combined treatment with statins and aminobisphosphonates extends longevity in a mouse model of human premature aging. *Nat Med* **14:** 767–772

Vijg J, Campisi J (2008) Puzzles, promises and a cure for ageing. *Nature* **454:** 1065–1071

Wang H, Garzon R, Sun H, Ladner KJ, Singh R, Dahlman J, Cheng A, Hall BM, Qualman SJ, Chandler DS, Croce CM, Guttridge DC (2008) NF-kappaB-YY1-miR-29 regulatory circuitry in skeletal myogenesis and rhabdomyosarcoma. *Cancer Cell* **14:** 369–381

Williams AE, Perry MM, Moschos SA, Lindsay MA (2007) microRNA expression in the aging mouse lung. *BMC Genomics* **8:** 172

Xiong Y, Fang JH, Yun JP, Yang J, Zhang Y, Jia WH, Zhuang SM (2010) Effects of microRNA-29 on apoptosis, tumorigenicity, and prognosis of hepatocellular carcinoma. *Hepatology* **51:** 836–845

Zhao JJ, Lin J, Lwin T, Yang H, Guo J, Kong W, Dessureault S, Moscinski LC, Rezania D, Dalton WS, Sotomayor E, Tao J, Cheng JQ (2010) microRNA expression profile and identification of miR-29 as a prognostic marker and pathogenetic factor by targeting CDK6 in mantle cell lymphoma. *Blood* **115:** 2630–2639

 ©2011 European Molecular Biology Organization

Aging and chronic DNA damage response activate a regulatory pathway involving miR-29 and p53

Ugalde et al, The EMBO Journal (2011)

Supplementary information

Supplementary Figure 1. (A) miR-29 expression analysis by qPCR of two independent *p53*$^{-/-}$ fibroblast cell lines at passages 2 and 8, and of mouse *ATM*$^{-/-}$ and *ATR*$^{s/s}$ fibroblasts treated with two different concentration of doxorubicin. (n=2 biological replicates). *Significantly different from untreated cells, $p<0.05$. (**B**) Table showing the mRNA levels of validated miR-29 target genes in whole transcriptome analysis of *Zmpste24*$^{-/-}$ muscle samples. Data represent the normalized fold change in deficient mice. (**C**) qPCR analysis of *Narf*, *Ppm1d* and *Hbp1* mRNA levels in muscle from wild-type and mutant mice (n = 6 mice of each genotype). * Significantly different from wild-type mice, $p<0.05$.

Supplementary Figure 2. (A) Wild type (**left panel**) or *Zmpste24*$^{-/-}$ (**right panel**) primary mouse fibroblasts were seeded in 96-well plates and transfected with miR-29 or control precursor or inhibitor molecules, respectively. Cell proliferation was assessed by MTT assay at different time points (n = 3 biological replicates). **(B)** MTT assay of U2OS over-expressing miR-29. U2OS cells transduced with a lentiviral vector expressing the miR-29b-2~29c cluster were seeded in 96-well plates and transfected with control or miR-29 inhibitor molecules and cell proliferation was assessed by MTT assay at different time points (n = 3 biological replicates). * significantly different from empty vector transduced cells, p-value < 0.05. # significantly different from control transfected cells, p-value < 0.05.

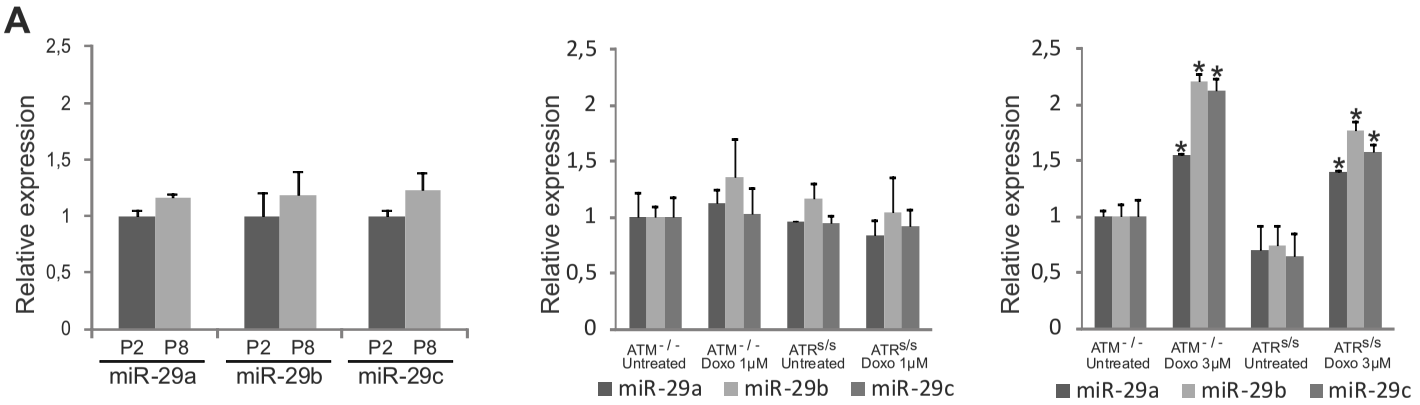

B

Target Gene	Fold
Bcl2	-2,68
Col3a1	-2,10
Dnmt1	-1,87
Dnmt3a	-1,53
Col1a2	-1,52
Col1a1	-1,35
Fbn1	-1,28
Sp1	-1,20
Nmyc1	-1,16
Eln	-1,13
Mcl1	-1,05
Yy1	1,09
Cdc42	1,11
Dusp2	1,42
Pik3r1	1,58
Ifi30	2,30

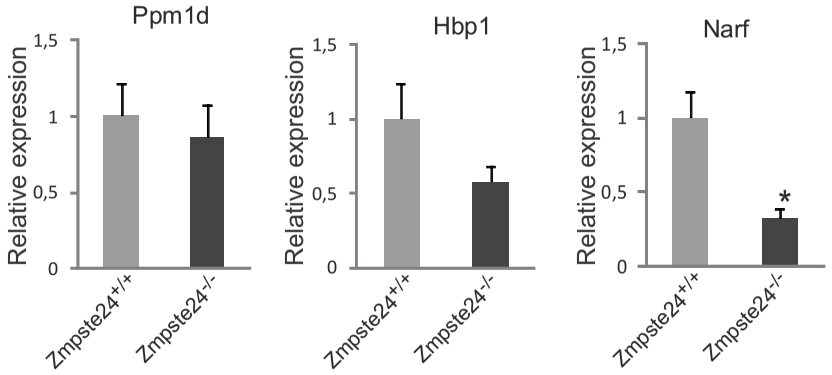

Suppl. Fig. 1 Ugalde et al

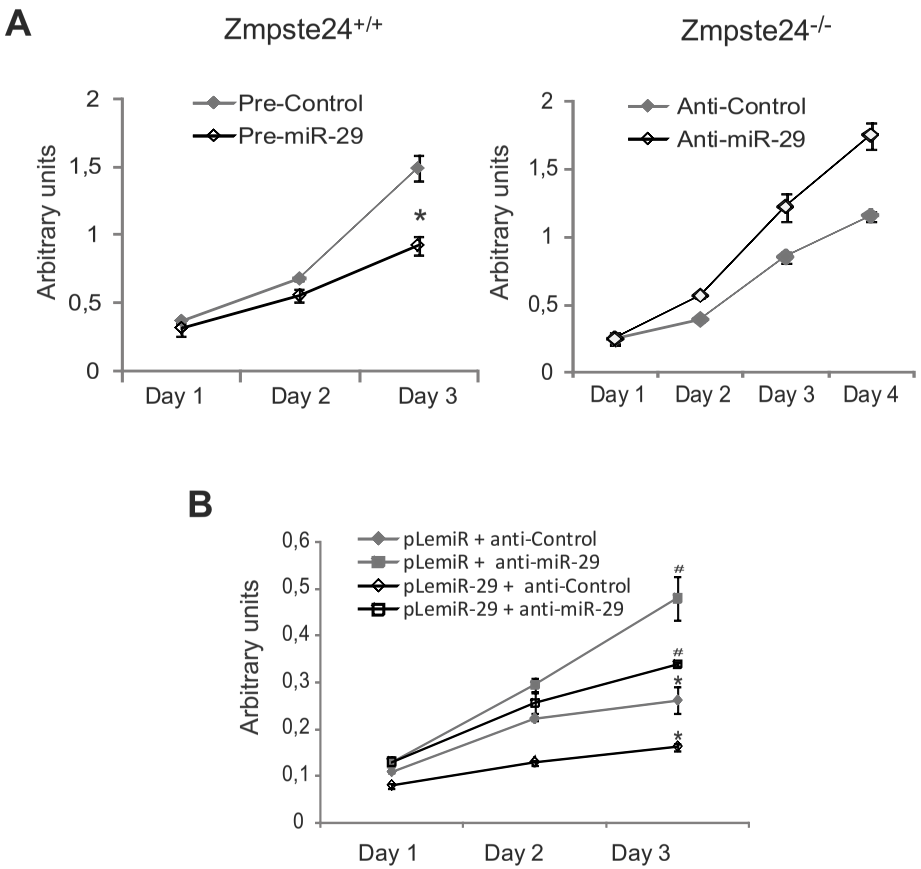

Suppl. Fig. 2 Ugalde et al

VIII. Otros trabajos relacionados con la Tesis

Durante el desarrollo de esta Tesis Doctoral he tenido la oportunidad de participar en otras líneas de investigación encaminadas al estudio de distintos aspectos del envejecimiento acelerado de los ratones deficientes en Zmpste24. Estos trabajos han dado lugar a las siguientes publicaciones:

Artículo 8: Jesús Espada, Ignacio Varela, Ignacio Flores, **Alejandro P. Ugalde**, Juan Cadiñanos, Alberto M. Pendás, Colin L. Stewart, Karl Tryggvason, María A. Blasco, José M. P. Freije y Carlos López-Otín. "Nuclear envelope defects cause stem cell dysfunction in premature-aging mice" *J Cell Biol*, **181**(1): 27-35 (2008).

Artículo 9: Guillermo Mariño, **Alejandro P. Ugalde**, Natalia Salvador-Montoliu, Ignacio Varela, Pedro M. Quirós, Juan Cadiñanos, Ingrid van der Pluijm, José M. P. Freije y Carlos López-Otín, C. "Premature aging in mice activates a systemic metabolic response involving autophagy induction" *Hum Mol Genet* **17**(14): 2196-2211 (2008).

Artículo 10: Ignacio Varela, Sandra Pereira, **Alejandro P. Ugalde**, Claire L. Navarro, María F. Suárez, Pierre Cau, Juan Cadiñanos, Fernando G. Osorio, Nicolas Foray, Juan Cobo, Félix de Carlos, Nicolas Levy, José M. P. Freije y Carlos López-Otín. "Combined treatment with statins and aminobisphosphonates extends longevity in a mouse model of human premature aging" *Nature Med* **14**(7): 767-772 (2008).

DISCUSIÓN

En las últimas décadas, los grandes avances que se han producido en el conocimiento de los sistemas proteolíticos han modificado nuestra consideración clásica de las funciones de estos enzimas. En el primer capítulo de la presente Tesis Doctoral hemos realizado una revisión de los distintos aspectos de los enzimas proteolíticos que han llevado a su caracterización como un complejo sistema de regulación post-traduccional, para posteriormente profundizar en la descripción del conocimiento actual sobre el grupo de las metaloproteasas **(I)**. Uno de los principales aspectos que han impulsado la investigación sobre este conjunto de enzimas ha sido la sucesiva acumulación de datos que han puesto de manifiesto que las proteasas son capaces de llevar a cabo reacciones altamente específicas que modifican una amplia variedad de características de las proteínas y provocan un gran impacto en la biología celular. Así, el número de trabajos que han descrito la implicación del procesamiento proteolítico en la regulación de múltiples aspectos de la biología de los organismos ha ido creciendo exponencialmente. Igualmente, se ha encontrado una amplia variedad de patologías humanas relacionadas con la desregulación de las actividades proteolíticas y se han descrito más de 90 enfermedades humanas hereditarias asociadas a mutaciones en genes de proteasas (Quesada y col., 2009). Otra de las observaciones que manifiesta la importancia de estos enzimas es el elevado número de genes de enzimas proteolíticos presentes en los genomas de los organismos, que alcanzan el 2% del total de genes codificantes de proteínas en el genoma humano. En este mismo sentido, es también relevante que, aunque todas las proteasas catalizan la misma reacción química, la actividad proteolítica ha surgido y evolucionado independientemente en diversas ocasiones, dando lugar a una amplia variedad de enzimas con distintos mecanismos de catálisis. Entre las distintas clases de enzimas proteolíticos, las metaloproteasas constituyen uno de los grupos más numerosos en distintos organismos **(I)**. Además, esta clase catalítica contiene algunas de las familias de mayor extensión, diversidad y relevancia en la fisiología y patología humanas, entre las que destacan las MMPs, las ADAMs, las ADAMTSs y las aminopeptidasas. Por todas estas razones, en la primera parte de la presente Tesis Doctoral y coincidiendo con los dos primeros objetivos planteados al comienzo de la misma, hemos tratado de contribuir al conocimiento de los sistemas proteolíticos mediante la identificación y

caracterización de nuevas metaloproteasas. Así, siguiendo esta estrategia, hemos identificado una nueva aminopeptidasa del subclan de las gluzinquinas **(II y III)** y dos metaloproteasas no descritas hasta el momento de iniciar nuestro trabajo y cuya identificación y caracterización nos ha permitido definir una nueva familia de metzinquinas humanas **(IV)**.

La estrategia seguida para la identificación de la aminopeptidasa-O humana (AP-O) **(II)** se basó en una búsqueda genómica de secuencias con similitud a aquellas que codifican el domino catalítico de aminopeptidasas conocidas, como las denominadas APA, APN, APB o LTA4H. Tras la identificación de secuencias candidatas en el genoma humano y la realización de una serie de amplificaciones por PCR utilizando una genoteca de cDNA humano, se consiguió finalmente aislar el cDNA completo de la AP-O humana, lo que nos permitió su posterior clonación y secuenciación. El análisis computacional de la estructura derivada de la secuencia clonada reveló que esta proteína presentaba una organización caracterizada por una región amino terminal similar a la región equivalente de la LTA4H, un domino catalítico central, una pequeña región con secuencias de reconocimiento SH3 y una extensión carboxilo terminal con plegamiento tipo armadillo (ARM). Por similitud con la LTA4H, cuya estructura tridimensional ha sido determinada, la región amino terminal de la AP-O podría adquirir un plegamiento equivalente, caracterizado por una extensa superficie cóncava expuesta al solvente que participa en el reconocimiento y especificidad de sustratos (Thunnissen y col., 2001). Tras esta región, la AP-O humana posee un dominio catalítico típico de la familia M1 de metaloproteasas, determinado por la conservación del motivo característico del subclan de las gluzinquinas, $HEXXHX_{(18)}E$, y de la mayor parte de residuos aminoacídicos característicos de la familia de aminopeptidasas que se han asociado al reconocimiento del sustrato o a la catálisis enzimática (Laustsen y col., 2001; Thompson y col., 2003). Sin embargo, es destacable que la AP-O humana carece de varios de los residuos que forman parte del motivo aminoacídico específico de la familia M1, GXMEN, al que se le ha atribuido un papel esencial en la catálisis (Luciani y col., 1998; Vazeux y col., 1998). Seguidamente, el dominio catalítico de la AP-O se conecta con la región carboxilo terminal a través de una región que contiene un

bucle hidrofóbico rico en prolina similar a dominios SH3 de reconocimiento presentes en otras aminopeptidasas y que podría constituir una zona óptima para la interacción con otras proteínas (Thunnissen y col., 2001; Pham y col., 2007). Finalmente, el análisis computacional de la región carboxilo terminal de la AP-O predice la existencia de un plegamiento similar a repeticiones tipo ARM o tipo HEAT. Estas repeticiones se caracterizan por una estructura tridimensional en forma de superhélice compuesta normalmente de 3 a 36 pares de hélices alfa. Esta peculiar estructura se cree que participa en interacciones entre proteínas, aunque cabe destacar que las aminopeptidasas presentan una versión de menor tamaño a la encontrada en las proteínas armadillo o huntingtina, en las cuales se han caracterizado los dominios ARM y HEAT, respectivamente (Andrade y col., 2001). La presencia de este domino ARM en la AP-O, así como en las aminopeptidasas LTA4H, APB y APB-2, nos impulsó a proponer la clasificación de estas proteínas en un subgrupo de metaloproteasas M1 al que hemos llamado aminopeptidasas ARM.

En este trabajo también analizamos la distribución de la AP-O en tejidos humanos y de ratón. Estos estudios nos permitieron detectar la expresión del gen *AP-O* en varios tejidos, principalmente en páncreas, placenta, hígado, corazón y testículos, lo que sugiere que la AP-O está implicada en el desarrollo o fisiología de estos órganos. Curiosamente, el análisis de expresión de la AP-O en testículo de ratones de diferentes edades reveló un pico de expresión en muestras de ratones de 30-35 días, que coincide con la etapa de maduración sexual. Este resultado sugiere la posible implicación de esta nueva aminopeptidasa en el desarrollo del testículo, de manera análoga a lo descrito para la APB (Cadel y col., 1997).

Continuando con la caracterización de la AP-O y para profundizar en el estudio de sus implicaciones fisiológicas, llevamos a cabo un análisis funcional del enzima recombinante producido en *E. coli*. Este análisis reveló que dicha proteína es una aminopeptidasa catalíticamente activa y que su actividad es suprimida tanto por inhibidores generales de metaloproteasas como por inhibidores específicos de aminopeptidasas. Además, estos experimentos pusieron de manifiesto que la AP-O muestra preferencia por arginina-AMC y

carece de actividad frente a lisina-AMC, a diferencia de la APN o la PAP que, en experimentos similares, mostraron capacidad para procesar eficientemente ambos aminoácidos. El valor calculado de K_m para la AP-O en ensayos enzimáticos frente a arginina-AMC fue aproximadamente 100 veces menor que el valor deducido para las aminopeptidasas APN y PAP en las mismas condiciones. Este resultado apoyaría la posibilidad de que la eliminación de arginina de los extremos amino terminal catalizada por la AP-O podría ser de relevancia *in vivo*. Basándonos en esta observación y considerando la expresión de *AP-O* en corazón y testículo, tejidos donde el sistema renina-angiotensina desempeña un papel importante, nos planteamos analizar la posibilidad de que la AP-O estuviera involucrada en el procesamiento de péptidos de este sistema. El sistema renina-angiotensina controla numerosos procesos del organismo, tanto a nivel sistémico como local, aunque su principal función es la regulación de la presión sanguínea y la homeostasis de los fluidos corporales (Leung y Carlsson, 2001). El principal efector de esta ruta hormonal es la angiotensina, que se genera como angiotensina I y II a partir del precursor angiotensinógeno mediante la acción sucesiva de la endopeptidasa renina y la carboxipeptidasa ACE (enzima convertidor de angiotensina). La angiotensina II es un octapéptido involucrado en la homeostasis y regulación hemodinámica, que se convierte por la acción de una aminopeptidasa, probablemente la APA, en angiotensina III, un heptapéptido implicado en la fisiología cerebral y cardiovascular. Finalmente, la angiotensina III se transforma en angiotensina IV mediante el procesamiento por otras aminopeptidasas, entre las que se encuentra la APN. Consistente con la especificidad de la AP-O recombinante, este enzima es capaz de eliminar *in vitro* el residuo de arginina del extremo amino terminal de la angiotensina III, mientras que no muestra actividad frente a la angiotensina I o II. Este hallazgo podría significar que la AP-O forma parte del grupo de enzimas involucrados en el procesamiento de la angiotensina que desempeñan un papel importante en los procesos biológicos que dependen de la generación de angiotensina IV en tejidos como páncreas, cerebro, testículos y corazón (Leung y Carlsson, 2001; Leung y Sernia, 2003; Fyhrquist y Saijonmaa, 2008). Sin embargo, debe tenerse en cuenta que estos experimentos se han llevado a cabo con el domino catalítico recombinante de la AP-O, mientras que el procesamiento de la angiotensina III por APN se

realizó utilizando un enzima purificado de origen natural. Este hecho podría además explicar los bajos valores de K_{cat} obtenidos para la AP-O en el procesamiento de arginina-AMC, así como la lenta conversión de la angiotensina III que mostró este enzima.

Por otra parte, cabe señalar que la AP-O podría también procesar otros péptidos con actividad angiogénica que se han asociado a la progresión tumoral, tal y como se ha descrito para otras aminopeptidasas (Ino y col., 2004; Inagaki y col., 2010). En este sentido, la región 9q22 donde se localiza el gen que codifica la AP-O se ha encontrado asociada a pérdida de heterocigosidad en diferentes tumores, incluyendo carcinomas de ovario, vejiga y esófago (Simoneau y col., 2000; Byrom y col., 2004; Lichun y col., 2004; Obermann y col., 2004). Además, se ha detectado una asociación entre la amplificación de esta región y la resistencia a cisplatino en cáncer de testículo (Rao y col., 1998). Asimismo, resulta interesante el hecho de que el gen *AP-O* contiene en su último intrón la secuencia codificante de un clúster de miRNAs compuesto por miR-23b, miR-27b y miR-24-1. En este sentido, un trabajo reciente ha descrito la participación de miR-27b en el desarrollo del corazón en ratones mediante la modulación de la expresión de Mef2c, demostrando además que, tanto este miRNA como el gen de la *AP-O*, presentan un patrón temporal de expresión análogo en el corazón, caracterizado por la activación transcripcional en E12.5 y su mantenimiento en neonatos (Chinchilla y col., 2011).

Recientemente, se ha podido profundizar en ciertos aspectos de la AP-O mediante el uso de ratones que portaban una inserción en el gen que la codifica (Axton y col., 2008). Estos estudios, revisados en el capítulo **III**, han revelado que la AP-O podría estar implicada en la biología del sistema vascular. Utilizando una metodología de trampa génica (del inglés “gene trap”) que emplea un cebo con un marcador fluorescente, Axton y colaboradores han identificado el gen *AP-O* como un posible candidato en un cribado de genes que se expresan en la diferenciación a cardiomiocitos. Los ratones generados a partir de células embrionarias portadoras de la inserción en el gen *AP-O* son totalmente normales, lo que podría indicar un fenómeno de redundancia, común en otras familias de proteasas (López-Otín y Bond, 2008). Sin embargo,

los autores también han señalado la posibilidad de que la inserción no interfiera en la funcionalidad de la proteína, puesto que ocurre en el extremo 3' del gen, dando lugar a una fusión proteica que conserva la mayor parte de la secuencia codificante de AP-O. De todas formas, estos mismos autores han encontrado que la AP-O murina se expresa en la vasculatura embrionaria y en la de diversos tejidos adultos, incluyendo hígado, corazón, cerebro, pulmón, músculo y riñón, observación que es totalmente consistente con nuestros resultados. Además, Axton y colaboradores han descrito la existencia de una secuencia aminoacídica que dirige la localización de AP-O hacia el nucleosoma. Asimismo, se han identificado varios eventos de ayuste alternativo del gen *AP-O* que afectan a esta secuencia y al dominio catalítico, y que, por lo tanto, podrían controlar la actividad y localización celular de esta proteína (Axton y col., 2008).

En resumen, hemos clonado y caracterizado la AP-O, una nueva aminopeptidasa de la familia M1 que muestra una organización similar a otros miembros de la familia, aunque también presenta peculiaridades estructurales. Curiosamente, hemos identificado secuencias ortólogas en ratón y rata, pero no en *C. elegans* o *D. melanogaster*, pese a que sus genomas contienen ortólogos para el resto de genes de la familia M1. Asimismo, hemos mostrado que la AP-O es proteolíticamente activa y muestra un perfil de actividad y sensibilidad a inhibidores característico de metaloproteasas. Finalmente, la combinación de nuestros datos con trabajos adicionales de otros grupos, sugiere que la AP-O podría desempeñar un papel en el desarrollo y fisiología cardiacas, así como en la vasculatura de otros órganos, mediante el procesamiento de péptidos biológicamente activos como la angiotensina.

Continuando con los dos primeros objetivos de la presente Tesis Doctoral, la búsqueda de nuevos genes del degradoma humano nos permitió la identificación y caracterización de dos nuevas proteasas humanas a las que hemos denominado arqueometzinquinas 1 y 2 **(IV)**. De acuerdo con sus características estructurales y enzimáticas, estas proteínas pertenecen a una nueva familia de metaloproteasas caracterizada por la presencia de un motivo conservado ($HEXXHXXGX_3CX_4CXMX_{17}CXXC$) que contiene el sitio consenso

de unión a zinc de las metzinquinas y cuatro residuos de cisteína que contribuyen a definir los determinantes específicos de esta nueva familia de metaloproteasas. Además, los ensayos enzimáticos realizados con las AMZs recombinantes humanas han aportado las primeras evidencias de que estas proteínas son metaloproteasas catalíticamente activas que muestran una especificidad de sustrato y sensibilidad a inhibidores compatible con la idea de que ambas podrían actuar predominantemente como aminopeptidasas.

Una característica adicional de esta familia de metaloproteasas es la compleja serie de acontecimientos evolutivos que han contribuido a su creación y diversificación en diferentes organismos. De hecho, nuestros análisis bioinformáticos han revelado que estos enzimas están ampliamente distribuidos en vertebrados y arqueobacterias, pero están ausentes en los genomas de un amplio número de organismos modelo como *E. coli*, *S. cerevisiae*, *A. thaliana*, *D. melanogaster* y *C. elegans*. La existencia de genes compartidos por procariotas y vertebrados, pero ausentes en otros eucariotas, es frecuentemente considerada como un indicativo de acontecimientos de transferencia génica lateral desde procariotas a vertebrados (Lander y col., 2001). En este sentido, las AMZs podrían representar un nuevo ejemplo de este peculiar evento evolutivo. Sin embargo, la acumulación de observaciones cuestionando numerosos casos de transferencia génica lateral al linaje de vertebrados nos impulsó a realizar una exhaustiva búsqueda bioinformática de genes *AMZ* en los genomas disponibles (Stanhope y col., 2001). Este análisis nos permitió identificar secuencias relacionadas con *AMZ* en diversos organismos eucariotas no vertebrados y en dos especies de bacterias, así como poner de manifiesto una serie de complejos sucesos evolutivos subyacentes a la formación de esta familia de metaloproteasas. De acuerdo con los análisis filogenéticos, la explicación más probable de la historia evolutiva de las AMZs podría corresponder a un escenario en el que el gen *AMZ* primordial, relacionado con los actuales genes *AMZ2*, surgió en un ancestro común de arqueobacterias y eucariotas. La pérdida de genes *AMZ* en prácticamente todos los genomas bacterianos analizados podría ser consistente con el modelo propuesto, según el cual las AMZs surgieron tras la aparición del organismo primordial de bacterias. La presencia de una AMZ en

Aquifex aeolicus, una bacteria hipertermófila que ocupa un nicho ecológico dominado por arqueas, podría explicarse por transferencia génica lateral desde arqueobacterias. Además, la clara relación filogenética entre la AMZ2 de *A. aeolicus* y las AMZs de arqueas apoya el posible acontecimiento propuesto de transferencia lateral. De forma similar, el hallazgo de secuencias AMZ en *M. xanthus* podría derivar de la transferencia lateral desde arqueas, aunque en este caso, este suceso fue seguido de una rápida acumulación de mutaciones, lo que podría explicar su localización como un grupo externo en el árbol filogenético. La historia evolutiva de las AMZs en los organismos eucariotas incluye también una serie de diversos acontecimientos desde su separación del ancestro común con arqueas. Primero, la ausencia de genes *AMZ* en plantas, nematodos o insectos es destacable, sugiriendo la ocurrencia de múltiples eventos de pérdida génica en estos organismos. Consistente con esta propuesta, el análisis del uso de codones o la composición de nucleótidos de los genes *AMZ* no apoya la posibilidad de la transferencia lateral desde arqueas a vertebrados. Finalmente, el análisis filogenético también ha revelado que la AMZ1 eucariota divergió de la AMZ2 recientemente por duplicación génica, lo que ilustra una vez más la plasticidad genómica de esta familia de metaloproteasas.

Para analizar en profundidad la relevancia funcional de AMZ1 y AMZ2, realizamos un análisis enzimático de ambas proteínas recombinantes producidas en *E. coli*. Este análisis reveló que los enzimas recombinantes son catalíticamente activos y que sus actividades parecen corresponder al tipo aminopeptidasa. Sin embargo, las dos nuevas metaloproteasas humanas muestran diferentes preferencias de sustrato. Mientras la AMZ1 procesa preferentemente sustratos que contienen alanina en su extremo amino terminal, la AMZ2 hidroliza principalmente sustratos con arginina en esa posición. En consonancia con estos resultados, la AMZ1 es capaz de hidrolizar la alanina amino terminal de la neurogranina, mientras que la AMZ2 hidroliza la arginina amino terminal de la angiotensina III. Además, los enzimas recombinantes no mostraron actividad frente a péptidos sintéticos como QF35 y QF41, frecuentemente utilizados para el análisis de metaloendopeptidasas. La actividad de ambos enzimas pudo ser abolida por inhibidores generales de

metaloproteasas, como o-fenantrolina o batimastato, y por inhibidores específicos de aminopeptidasas, como amastatina, hecho que apoya su clasificación como aminopeptidasas. Además, en este sentido, es destacable que la actividad de los dominios catalíticos recombinantes de AMZs es relativamente bajo, lo cual es en cierto grado similar a la limitada actividad proteolítica de los dominios catalíticos de las ADAMTSs, aunque contrasta con el domino catalítico de las MMPs, que hidroliza eficientemente péptidos lineales y gelatina (Fanjul-Fernández y col., 2010). En base a estas observaciones, se podría especular que las AMZs y las ADAMTSs podrían tener estrictos requerimientos en términos de la presencia de motivos adicionales o dominios para mostrar todo su potencial proteolítico.

En este trabajo, también hemos analizado la distribución de la AMZ1 y AMZ2 en tejidos humanos. Estos estudios nos han permitido detectar la expresión predominante de *AMZ1* en hígado y corazón, mientras que el mRNA de *AMZ2* se detecta principalmente en corazón y testículos. Este patrón de expresión sugiere que ambas AMZs están implicadas en el desarrollo o fisiología de estos órganos. De todas formas, será necesario realizar aproximaciones adicionales, como la determinación de su estructura tridimensional o la generación de ratones deficientes en los genes *AMZ*, para profundizar en las implicaciones fisiológicas de estos enzimas en la biología humana. En este sentido, cabe mencionar que hemos realizado varios intentos de generación de ratones deficientes en los genes *AMZ*, mediante la electroporación de vectores de reemplazamiento génico en células madre embrionarias, aunque esta aproximación no ha ofrecido resultados positivos hasta el momento.

Coincidiendo con la finalización de los dos primeros objetivos de la presente Tesis Doctoral, el extraordinario auge de los estudios sobre los miRNAs como sistema de regulación y la creciente implicación del eje somatotrofo en el control del envejecimiento, nos impulsaron a diseñar una serie de aproximaciones encaminadas a valorar la contribución de estos dos sistemas de regulación en procesos de envejecimiento mediante la utilización del modelo de ratón progeroide deficiente en Zmpste24 generado en nuestro

laboratorio (Pendás y col., 2002). Así, siguiendo esta estrategia, que se enmarca en el tercer objetivo de la presente Tesis Doctoral, hemos podido demostrar la desregulación de ambos sistemas en nuestro modelo de envejecimiento y su asociación con las alteraciones presentes en estos ratones.

En los últimos años, el efecto de las alteraciones del eje somatotrofo en la extensión de la longevidad se ha sometido a un exhaustivo análisis. La primera evidencia que señaló la implicación del papel regulador de la ruta de IGF-1 en la longevidad surgió en nematodos. En este organismo, la pérdida del gen *daf2*, el ortólogo en mamíferos del receptor de insulina/IGF-1, condujo a un incremento significativo de su esperanza de vida (Kenyon y col., 1993). De forma similar, también se describió que moscas portadoras de mutaciones inactivantes en *InR* (el gen ortólogo de *daf2* en nematodos y del receptor de insulina/IGF-1 en mamíferos) mostraban un incremento en la longevidad (Tatar y col., 2001). Igualmente, se ha probado que la reducción de la señalización de IGF-1 en ratones provoca un aumento de la longevidad (Holzenberger y col., 2003). Sorprendentemente, la condición patológica del síndrome de Laron, que se asocia a resistencia a GH y retraso en el crecimiento, extiende la longevidad en ratones y confiere cierto grado de protección frente al cáncer en humanos (Laron, 2008; Guevara-Aguirre y col., 2011). Notablemente, pese a su reducida tasa de crecimiento y tamaño corporal, los ratones con síndrome de Laron muestran niveles reducidos de IGF-1 y altos niveles de GH en sangre, y muestran una mayor longevidad en comparación con los animales control (Coschigano y col., 2003). En este sentido, el hallazgo de que los ratones progeroides deficientes en Zmpste24 presentan características de resistencia a GH similares a las observadas en los ratones con síndrome de Laron, así como alteraciones asociadas a individuos longevos, como un incremento en la autofagia, es a la vez intrigante y paradójico (Mariño y col., 2008) **(V y VI)**.

En trabajos anteriores se han descrito inesperadas similitudes entre las alteraciones fenotípicas encontradas en modelos murinos de envejecimiento prematuro y en organismos con longevidad extendida, incluyendo niveles reducidos de IGF-1 circulante (Niedernhofer y col., 2006; van de Ven y col.,

2006; van der Pluijm y col., 2007). Estas alteraciones se cree que son parte de una respuesta adaptativa a estrés encaminada a preservar la viabilidad de los organismos bajo circunstancias comprometidas (Garinis y col., 2009; Hoeijmakers, 2009). Estas características, comunes a individuos longevos y progeroides, se ha propuesto que surgen de la progresiva acumulación de daño en el DNA, proceso que se encuentra exacerbado en los síndromes progeroides (Garinis y col., 2008). Adicionalmente, se ha descrito que la inducción de daño en el DNA *in vivo* conlleva una serie de alteraciones similares a las observadas en individuos progeroides y longevos (Niedernhofer y col., 2006; Garinis y col., 2009). Así, resulta razonable pensar que los organismos con longevidad extendida que evaden el cáncer, los fallos cardiacos u otras alteraciones de la edad, acumulan daño en el DNA con el paso del tiempo desencadenando una respuesta adaptativa frente al estrés similar a la observada a edades tempranas de individuos progeroides. Esta respuesta estaría destinada a redistribuir los recursos energéticos del crecimiento a la preservación somática, dado que la proliferación y crecimiento en células que acumulan un nivel crítico de daño en el DNA llevaría inequívocamente a defectos en la replicación, inestabilidad cromosómica, anomalías en la envuelta nuclear y finalmente al desarrollo de cáncer (Hoeijmakers, 2009). Es posible especular que si esta respuesta adaptativa no consiguiese combatir los efectos perjudiciales de la acumulación de daño en el DNA, los ratones progeroides sucumbirían al cáncer. En sentido contrario, si esta estrategia tuviera éxito, los ratones progeroides que han adquirido características de organismos longevos mostrarían ritmos metabólicos y de crecimiento reducidos, pero no mostrarían una disminución de la esperanza de vida.

Las alteraciones del eje somatotrofo encontradas en ratones progeroides deficientes en Zmpste24 podrían constituir un claro ejemplo de una supresión redundante y exagerada de una ruta promotora del crecimiento. De hecho, los ratones progeroides muestran alteraciones en múltiples reguladores de la señalización mediada por GH, incluyendo la sobreexpresión de *Socs2* y *Igfbp1* junto con una reducción de la expresión de *Igf1*, *Igf1als* y *Ghr*, lo cual apunta hacia la existencia de una estrategia de supresión del crecimiento (**Figura 4**).

Además, el análisis de los niveles de expresión de varios miRNAs que incluyen a IGF-1 entre sus posibles dianas reveló una marcada sobreexpresión de miR-1 en varios tejidos de ratones deficientes en Zmpste24, así como en fibroblastos de pacientes con el síndrome de Hutchinson-Gilford. Asimismo, la realización de experimentos basados en el empleo de luciferasa ha confirmado la presencia de sitios funcionales de represión por miR-1 en el 3'UTR de *Igf-1*. Estos datos sugieren que los elevados niveles de miR-1 podrían estar contribuyendo a la exacerbada supresión de la síntesis de IGF-1 observada en ratones progeroides, incluso en presencia de altos niveles circulantes de GH.

Por otra parte, también debe considerarse la posibilidad de que el gran incremento de los niveles de GH circulante en los ratones deficientes en

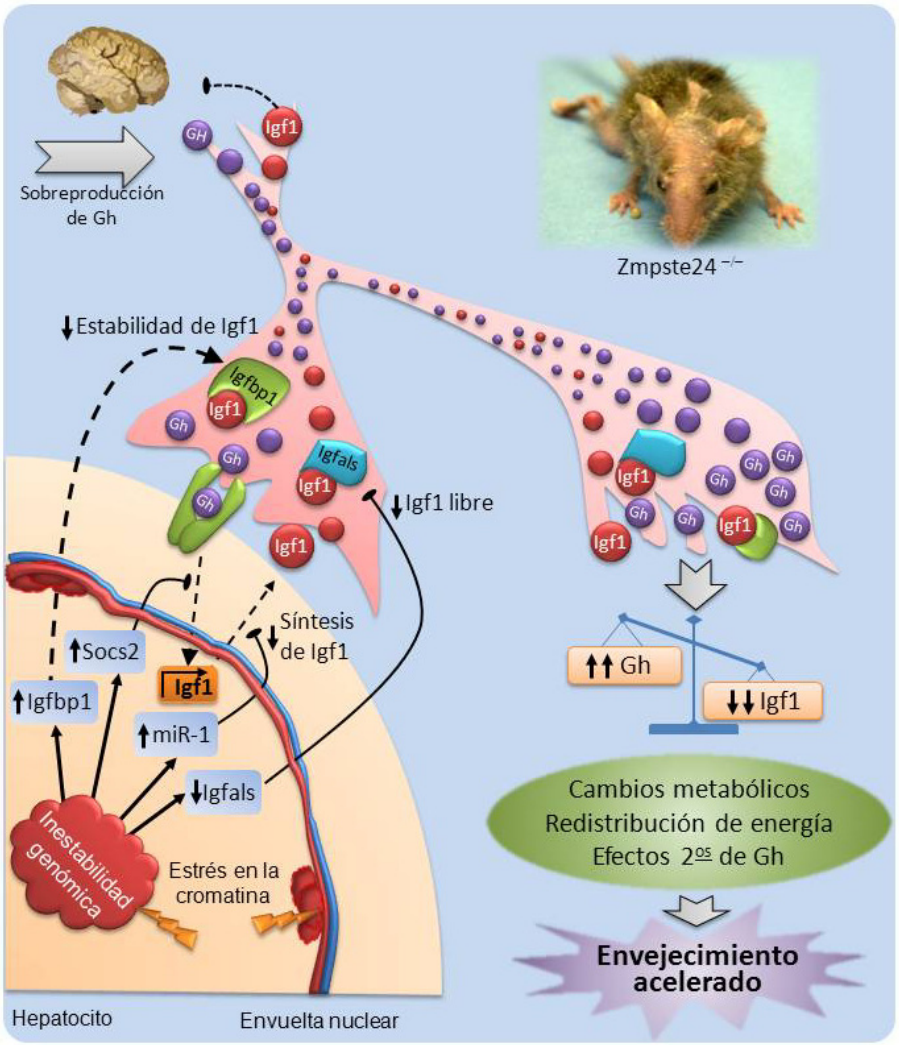

Figura 4. Modelo de las alteraciones del eje somatotrofo en el envejecimiento acelerado de los ratones deficientes en Zmpste24.

Zmpste24 pueda constituir uno de los mayores determinantes del envejecimiento prematuro de estos animales (**Figura 4**). De hecho, aunque estos ratones muestran resistencia a GH en términos de síntesis de IGF-1, no presentan ninguna alteración significativa en la activación de la ruta Jak/Stat tras la inyección intravenosa de GH. Así, es posible que los niveles elevados de GH pudieran provocar directamente una variedad de respuestas perjudiciales en tejidos periféricos, lo cual podría contribuir al desarrollo de un proceso de envejecimiento acelerado. Curiosamente, los ratones condicionales deficientes en IGF-1 hepático presentan niveles reducidos de IGF-1 y un incremento en los niveles circulantes de GH, y muestran defectos metabólicos que pueden ser corregidos por administración de un agonista de GH (Yakar y col., 2004). Este hecho demuestra que los altos niveles circulantes de GH pueden ser perjudiciales y contribuir a la reducida longevidad. Es más, los ratones gigantes que sobreexpresan GH presentan varias características progeroides, lo cual apoya la idea de que los altos niveles de GH presentes en los ratones deficientes en Zmpste24 podrían contribuir a los defectos que acompañan al envejecimiento acelerado (Wolf y col., 1993). En contraposición, el incremento de longevidad observado en los ratones con síndrome de Laron indica que la regulación asociada al eje somatotrofo está regulada con gran precisión. Consistentemente, nuestro hallazgo de que la administración de IGF-1 recombinante aumenta la longevidad y mejora varios síntomas asociados al envejecimiento acelerado sugiere que la intensidad de la respuesta adaptativa sistémica observada en condiciones de envejecimiento prematuro es excesiva y debe ser modulada para aumentar la longevidad. Además, aunque la completa eliminación de las alteraciones antiproliferativas observadas en estos ratones podría generar cáncer, la modificación selectiva de algunas rutas de señalización en estos ratones podría ser beneficiosa para extender la longevidad. De acuerdo con estas observaciones, en nuestro laboratorio hemos demostrado previamente que la reducción en la señalización de p53 retrasa la aparición de los síntomas progeroides e incrementa la longevidad de los ratones mutantes (Varela y col., 2005). Nuestro hallazgo de que el tratamiento con IGF-1 recombinante restablece el estado del eje somatotrofo y extiende la longevidad en ratones apunta en la misma dirección. El IGF-1 se ha utilizado con notable eficacia para el tratamiento de alteraciones del eje somatotrofo

resistentes a GH en humanos sin efectos secundarios significativos (Clemmons, 2007). De acuerdo con estos hechos, el tratamiento con IGF-1, solo o en combinación con otros fármacos, como las estatinas y los bifosfonatos, podría tener interés como posible tratamiento para disminuir la progresión de la enfermedad en pacientes con progeria.

Tras el descubrimiento de la regulación de la expresión génica mediada por miRNAs, se han descrito una amplia variedad de funciones asociadas con este proceso. Comparado con las interacciones proteína-proteína, en las cuales una proteína interacciona con un grupo reducido de elementos, cada miRNA tiene el potencial de reprimir la traducción de cientos de transcritos (Grigoriev, 2003; Lewis y col., 2005). Estas características, junto con nuestras observaciones previas **(V y VI)**, sugieren que la desregulación de la expresión de miRNAs podría contribuir a las numerosas alteraciones presentes en procesos multifactoriales tan complejos como el envejecimiento. Aunque trabajos anteriores han abordado el estudio comparativo de la expresión de miRNAs entre ratones jóvenes y de edad avanzada, así como en ratones con longevidad extendida, la función de los miRNAs en el envejecimiento acelerado todavía no se había analizado (Williams y col., 2007; Maes y col., 2008; Bates y col., 2010). Para tratar de abordar esta cuestión, realizamos un análisis de los niveles globales de miRNAs en tejidos de ratones progeroides deficientes en Zmpste24 **(VII)**. Esta aproximación reveló que dichos ratones, que representan un modelo murino de la progeria de Hutchinson-Gilford, muestran una expresión desregulada de miRNAs en hígado y músculo. Entre los miRNAs con expresión alterada, hemos identificado tres miRNAs pertenecientes a la familia de miR-29 que se encuentran sobreexpresados significativamente en tejidos de ratones mutantes. La desregulación de esta familia de miRNAs es especialmente relevante en el músculo de ratones deficientes en Zmpste24, mostrando niveles de expresión hasta 10 veces superior a los de los ratones control. Además, estudios de expresión llevados a cabo con ratones de edad avanzada han revelado que esta desregulación es una característica común al envejecimiento fisiológico. Apoyando estos resultados, es destacable que un estudio reciente de la expresión de miRNAs asociada a la edad en humanos y macacos ha identificado la familia de miR-29 entre los miRNAs cuya expresión

en el córtex cerebral se relaciona con la edad de los individuos (Somel y col., 2010). Asimismo, otro trabajo reciente ha puesto de manifiesto que los niveles de miR-29 se encuentran disminuidos en los ratones Ames, caracterizados por un retraso en la longevidad (Bates y col., 2010). Estos hechos sugieren un papel general de la familia de miR-29 en la regulación de los procesos asociados al envejecimiento, tanto en condiciones fisiológicas como patológicas.

Para profundizar en la conexión entre la familia de miR-29 y el envejecimiento, realizamos una serie de estudios funcionales que revelaron que la activación transcripcional de miR-29 está asociada a la respuesta a daño en el DNA. Las observaciones previas de que los ratones deficientes en Zmpste24 presentan una marcada inestabilidad genómica asociada a un fenotipo de senescencia sistémica y una sobreexpresión de dianas de p53, así como a defectos en las células madre adultas, nos impulsaron a plantearnos la posibilidad de que la sobreactivación de miR-29 formase parte de la respuesta a daño en el DNA presente en estos ratones (Varela y col., 2005; Espada y col., 2008). A favor de esta hipótesis, hemos encontrado que la expresión de miR-29 se incrementa progresivamente durante el cultivo primario de fibroblastos de ratones *Zmpste24*$^{-/-}$, alcanzando el nivel máximo cuando los cultivos entran en senescencia. Sin embargo, este fenómeno no es un hecho exclusivo de las células de ratones progeroides, puesto que los fibroblastos de ratones controles experimentaron una activación similar de miR-29. Esta observación, junto con el hecho de que no existan diferencias significativas en los niveles de miR-29 entre fibroblastos de ratones progeroides y ratones controles en los primeros pases de cultivo *in vitro*, sugieren que la familia de miR-29 no es la única responsable de los defectos proliferativos de los fibroblastos mutantes. Sin embargo, el incremento de los marcadores de senescencia y daño en el DNA durante el cultivo continuado, tanto de fibroblastos deficientes en Zmpste24 como de ratones controles, aunque en distinta proporción, asocia el estrés genotóxico con la progresiva acumulación de miR-29.

Otra observación que sugiere la conexión de miR-29 y la respuesta a

daño en el DNA es el hecho de que el tratamiento de fibroblastos control con doxorrubicina, un inhibidor de topoisomerasas que induce roturas de doble hebra en el DNA y genera un escenario de daño crónico en el DNA, induce la activación transcripcional de miR-29a, -29b y -29c. Por el contrario, el tratamiento con H_2O_2 o 4-NQO, que inducen daño transitorio o lesiones similares a las producidas por radiación UV, respectivamente, no afecta a la expresión de estos miRNAs. De acuerdo con estos resultados, parece que solo el daño crónico o difícil de reparar en el DNA induce la expresión de la familia de miR-29. Además, estos experimentos funcionales también han puesto de manifiesto que la inducción de miR-29 es dependiente de p53, uno de los principales mediadores de la respuesta a daño en el DNA, ya que los fibroblastos deficientes en esta proteína carecen de la capacidad de sobreexpresar miR-29 en respuesta al tratamiento con doxorrubicina. De igual forma, los fibroblastos deficientes en ATM o portadores de la mutación del síndrome de Seckel en ATR (Barlow y col., 1997; Murga y col., 2009), proteínas profundamente implicadas en la elaboración de la respuesta a daño en el DNA, tampoco activan la expresión de miR-29 en respuesta al tratamiento con doxorrubicina. Sin embargo, resulta interesante la observación de que el tratamiento de estas células con altas concentraciones de doxorrubicina se traduce en un aumento de los niveles de miR-29, sugiriendo que existen otros mecanismos de regulación que podrían participar en condiciones de excesivo daño en el DNA. En este sentido, cabe destacar que dos trabajos recientes han identificado a las proteínas c-myc y NF-κB como factores represores de estos miRNAs (Liu y col., 2010; Mott y col., 2010). En conjunto, todas estas observaciones asocian la activación de la familia de miR-29 en los ratones deficientes en Zmpste24 y en ratones envejecidos con la respuesta al daño en el DNA.

Para identificar dianas de miR-29 que pudiesen contribuir a los defectos relacionados con el envejecimiento y la respuesta al daño en el DNA de los ratones progeroides deficientes en Zmpste24, realizamos una serie de aproximaciones basadas en la predicción computacional de dianas de miRNAs, combinadas con la validación experimental mediante ensayos de luciferasa. Esta estrategia nos permitió identificar 7 transcritos sujetos a represión por la

familia de miR-29. Curiosamente, no observamos ninguna diferencia en los niveles de represión de los genes diana entre los distintos miembros de la familia de miR-29, lo que podría indicar que no están especializados en distintas funciones, sino que operan de forma redundante en la regulación de sus genes diana. Estos genes diana incluyen los que codifican diversas fosfatasas (Ppm1d/Wip1 y Dusp2), oncoproteínas (Mycn), proteínas inducidas por interferón (Ifi30), represores transcripcionales (Hbp1), proteínas de la envuelta nuclear (Narf) y metaloproteasas (Adamts18). Entre estas dianas, nos centramos en la fosfatasa Ppm1d y la proteína de interacción con prelamina A Narf, ya que ambas se habían asociado previamente a procesos de interés en relación con el daño en el DNA y el envejecimiento. Ppm1d desfosforila una amplia variedad de proteínas involucradas en la respuesta a daño en el DNA, como p53, Chk1, Chk2, p38, γ-H2AX y ATM (Lu y col., 2007; Cha y col., 2010). Además, Ppm1d se activa en respuesta al daño en el DNA en una manera dependiente de p53 y participa en un bucle de retroalimentación negativa con ATM (Batchelor y col., 2008; Batchelor y col., 2009). Por otro lado, Narf interacciona con la prelamina A, cuya acumulación en la envuelta nuclear de las células deficientes en Zmpste24 es la principal responsable de los defectos observados en los ratones (Barton y Worman, 1999; Varela y col., 2005). En base a estos precedentes decidimos comprobar la existencia de sitios funcionales de unión de miR-29 en estos dos genes mediante experimentos de mutagénesis dirigida. Estos estudios revelaron que la sustitución de dos nucleótidos de la región semilla de los MBS de miR-29 en estos transcritos abolía la capacidad de represión de estos miRNAs en experimentos de luciferasa. Adicionalmente, comprobamos que la transfección simultánea de construcciones que expresaban *Ppm1d* o *Narf* junto con miméticos de miR-29, condujo a una disminución en la producción de las respectivas proteínas. Estos experimentos confirman que los transcritos de Ppm1d y Narf contienen sitios funcionales de unión de miR-29 y que estos miRNAs reprimen la producción de ambas proteínas. La carencia de anticuerpos apropiados frente a Narf nos obligó a abandonar la exploración en profundidad del efecto de miR-29 en la proteína endógena, pero experimentos paralelos nos permitieron demostrar que miR-29 es capaz de inhibir la producción endógena de Ppm1d y que este efecto tiene consecuencias sobre la fosforilación de p53.

De acuerdo con los resultados anteriores, nos planteamos la hipótesis de que la sobreexpresión de miR-29, como consecuencia de la progresiva acumulación de daño en el DNA, reduciría los niveles de Ppm1d, un regulador clave de la respuesta a daño en el DNA que a su vez desfosforila una amplia variedad de proteínas como p53, Chk1, Chk2, p38, γ-H2AX y ATM, ejerciendo un importante papel en el control de la viabilidad celular (**Figura 5**). Para evaluar esta hipótesis realizamos una serie de experimentos que demostraron que la elevación de los niveles de miR-29 mediante transfección de moléculas miméticas reduce la proliferación de fibroblastos *in vitro* y aumenta la senescencia celular. Además, observamos que esas mismas células presentaban niveles elevados de γ-H2AX, apoyando la existencia de un incremento de la sensibilidad al daño en el DNA, observación que se sustenta también en ensayos MTT de fibroblastos control transfectados con miméticos de miR-29 y tratados con doxorrubicina. Sin embargo, no se puede descartar la posibilidad de que exista un bucle de retroalimentación negativa por el cual

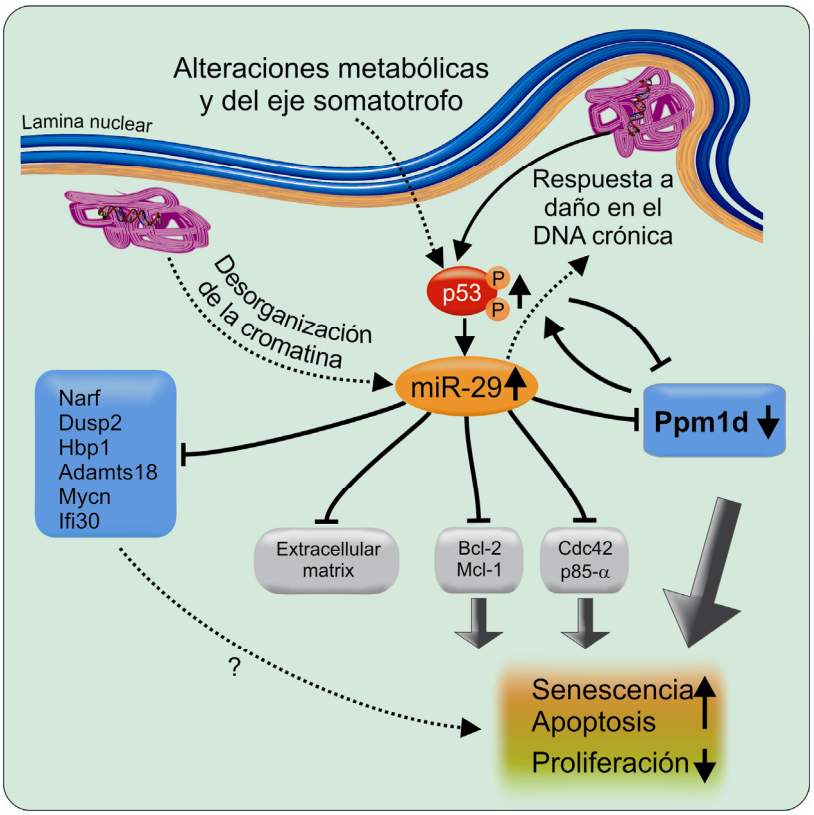

Figura 5. Modelo de regulación de miR-29 en los ratones deficientes en Zmpste24.

miR-29, a través de otros genes diana, incremente el daño en el DNA. De acuerdo con los resultados anteriores, hemos podido demostrar que el tratamiento con moléculas inhibidoras de miR-29 revierte los defectos proliferativos presentes en fibroblastos deficientes en Zmpste24. Así, la inhibición de miR-29 en estas células provocó un importante aumento de la proliferación celular, acompañado por un significativo descenso de los marcadores de senescencia y daño al DNA. De igual forma, hemos podido demostrar que la sensibilidad a doxorrubicina de los fibroblastos deficientes en Zmpste24 transfectados con inhibidores de miR-29 se encuentra disminuida. Además, de acuerdo con el modelo propuesto, la transfección de miméticos de miR-29 en fibroblastos control provoca un aumento en los niveles de fosforilación de p53 en la serina 15, el residuo diana de Ppm1d. Asimismo, la inhibición de miR-29 en fibroblastos produjo el resultado inverso, disminuyendo los niveles de fosforilación de p53 en fibroblastos tratados con doxorrubicina. En este mismo sentido, un experimento similar realizado con fibroblastos deficientes en Zmpste24 causó una disminución de la fosforilación de p53 tanto en células sin tratar como tratadas con doxorrubicina. Finalmente, utilizando células de osteosarcoma humano U2OS, hemos podido demostrar una relación inversa entre Ppm1d y la fosforilación de p53 al transfectar moléculas miméticas o inhibidoras de miR-29. Estos resultados son consistentes con observaciones previas que han mostrado que miR-29 induce apoptosis de forma dependiente de p53 y aumenta los niveles totales de esta proteína, ya que la fosforilación de p53 la estabiliza bloqueando su degradación en el proteasoma (Lavin y Gueven, 2006; Park y col., 2009). Además, también se ha descrito que Ppm1d desfosforila directamente la proteína MDM2, previniendo la degradación proteasomal de p53, observación que encaja con nuestro modelo por el cual miR-29 reprime *Ppm1d* influyendo en los niveles y actividad de p53 (Lu y col., 2008).

Colectivamente, nuestros datos, así como observaciones adicionales de la literatura, apoyan la posibilidad de que miR-29 sea una familia de miRNAs asociada al envejecimiento. En primer lugar, varios trabajos han descrito un papel supresor de tumores para miR-29 en varios cánceres humanos, incluyendo rabdomiosarcomas, neoplasias hematológicas, mesoteliomas

pleurales y carcinomas hepáticos (Pekarsky y col., 2006; Wang y col., 2008; Garzon y col., 2009; Pass y col., 2010; Xiong y col., 2010; Zhao y col., 2010). Esta función supresora de tumores de los miembros de la familia de miR-29 es consistente con un papel promotor del envejecimiento de estos miRNAs, dado que numerosos supresores de tumores se han asociado a una función negativa durante el envejecimiento, fenómeno que se conoce como antagonismo pleiotrópico (Kirkwood y Holliday, 1979). De hecho, los ratones progeroides deficientes en Zmpste24 muestran una hiperactivación crónica de la señalización de p53, así como una marcada sobreexpresión de supresores tumorales como p16/INK4A (Varela y col., 2005; Espada y col., 2008). Por otra parte, entre las funciones atribuidas a miR-29 se encuentran la reducción de la proliferación y el aumento de la apoptosis, dos procesos asociados con una disminución en la capacidad de los tejidos de mantener su homeostasis, un fenómeno característico del envejecimiento (Mott y col., 2007; Muniyappa y col., 2009). Por otra parte, también se ha descrito que miR-29 induce la hipometilación global del DNA mediante la represión de varias proteínas desmetilantes, otra observación que asocia la función de miR-29 y el envejecimiento, ya que las alteraciones epigenéticas también se han descrito en el envejecimiento (Gravina y Vijg, 2010; Osorio y col., 2010). Finalmente, los miembros de la familia de miR-29 muestran elevados niveles de expresión en cerebro humano y de macaco durante el envejecimiento y una relación inversa con los niveles de expresión de un grupo de genes relacionados con el cáncer (Somel y col., 2010).

En conclusión, proponemos que miR-29 ejerce un papel clave en la regulación de la supervivencia y proliferación celular a través de la modulación de la respuesta a daño en el DNA, convirtiendo estos miRNAs en importantes reguladores tanto del cáncer como del envejecimiento. La abolición de la respuesta a daño en el DNA es una característica común en el cáncer, que en una gran proporción de casos se adquiere mediante mutaciones inactivantes de p53. Asimismo, se ha observado que ciertos tumores pueden adquirir esta ventaja mediante la amplificación de *PPM1D* como forma alternativa (Bulavin y col., 2002). De acuerdo con nuestros resultados, la disminución de los niveles de miR-29 podría constituir otra vía alternativa para que los tumores reduzcan

la señalización de p53, permitiéndoles escapar de la apoptosis o la senescencia celular. Finalmente, la observación de que los niveles de miR-29 aumentan con la edad ofrece una evidencia adicional de la implicación de los miRNAs en el desarrollo de un proceso tan complejo como el del envejecimiento.

En resumen, en esta Tesis Doctoral hemos tratado de contribuir al conocimiento de los sistemas de regulación mediados por proteasas y miRNAs mediante la búsqueda de nuevos genes codificantes de enzimas proteolíticos y el análisis de la participación de los miRNAs en el envejecimiento acelerado. Siguiendo la primera estrategia hemos identificado tres nuevas metaloproteasas y hemos caracterizado algunas de sus propiedades. Así, hemos demostrado que la AP-O es un enzima catalíticamente activo del tipo aminopeptidasa que podría participar en el desarrollo y la fisiología de órganos como el corazón mediante el procesamiento de péptidos biológicamente activos como la angiotensina. Igualmente, hemos descubierto y caracterizado bioquímicamente dos nuevas metaloproteasas, la AMZ1 y AMZ2, que definen una nueva familia de metzinquinas humanas con una peculiar historia evolutiva. Asimismo, la segunda estrategia nos ha permitido identificar una serie de miRNAs con expresión desregulada en los ratones deficientes en Zmpste24 y profundizar en algunos aspectos de sus funciones. Así, hemos podido demostrar que miR-1 regula la producción de IGF-1 y que su sobreexpresión en los ratones progeroides está asociada a una profunda desregulación del eje somatotrofo. Finalmente, hemos descubierto que el daño crónico en el DNA, como el presente en los ratones deficientes en Zmpste24, activa la expresión de los miRNAs de la familia de miR-29. Además, hemos identificado el gen que codifica la fosfatasa Ppm1d como una diana de este miRNA y hemos podido demostrar que miR-29 ejerce un papel clave en la regulación de la proliferación y viabilidad celular a través de la modulación de la respuesta al daño en el DNA.

CONCLUSIONES

1. Hemos identificado una nueva metaloproteasa humana a la que hemos denominado aminopeptidasa-O y hemos confirmado su actividad hidrolítica de tipo aminopeptidasa con preferencia por sustratos que contienen arginina en el extremo amino terminal.

2. Hemos identificado y caracterizado enzimáticamente dos nuevas metaloproteasas que constituyen una nueva familia de metzinquinas humanas con una compleja historia evolutiva y a las que hemos denominado arqueometzinquinas 1 y 2.

3. Los ratones con envejecimiento acelerado deficientes en la metaloproteasa Zmpste24 presentan graves alteraciones en la señalización del eje somatotrofo caracterizadas por un pronunciado incremento de los niveles de GH y un marcado descenso en los niveles de IGF-1 en sangre.

4. Hemos identificado el miRNA miR-1 como un nuevo elemento regulador del eje somatotrofo que actúa a través de la represión de la síntesis de IGF-1 y hemos demostrado su activación transcripcional en los tejidos de ratones deficientes en Zmpste24 y en células de pacientes con el síndrome de Hutchinson-Gilford.

5. La administración de IGF-1 recombinante a los ratones progeroides deficientes en Zmpste24 restablece el balance de GH e IGF-1, mejora sus síntomas de envejecimiento y extiende su longevidad.

6. El análisis global de los niveles de miRNAs en los ratones deficientes en Zmpste24 ha revelado la sobreexpresión en hígado y músculo de los tres miembros de la familia miR-29 de miRNAs.

7. La activación transcripcional de miR-29 acontece también en el envejecimiento fisiológico en ratones y se asocia a la respuesta a daño en el DNA de una manera dependiente del supresor tumoral p53.

8. Los miRNAs de la familia miR-29 regulan la proliferación y viabilidad celular mediante la represión del gen *Ppm1d*, que codifica una fosfatasa reguladora de varias proteínas clave en la respuesta a daño en el DNA.

BIBLIOGRAFÍA

Albiston, A. L., McDowall, S. G., Matsacos, D., Sim, P., Clune, E., Mustafa, T., Lee, J., Mendelsohn, F. A., Simpson, R. J., Connolly, L. M. y Chai, S. Y. (2001). "Evidence that the angiotensin IV (AT(4)) receptor is the enzyme insulin-regulated aminopeptidase" *J Biol Chem* **276**(52): 48623-6.

Ambros, V. (1989). "A hierarchy of regulatory genes controls a larva-to-adult developmental switch in C. elegans" *Cell* **57**(1): 49-57.

Andrade, M. A., Petosa, C., O'Donoghue, S. I., Muller, C. W. y Bork, P. (2001). "Comparison of ARM and HEAT protein repeats" *J Mol Biol* **309**(1): 1-18.

Axton, R., Wallis, J. A., Taylor, H., Hanks, M. y Forrester, L. M. (2008). "Aminopeptidase O contains a functional nucleolar localization signal and is implicated in vascular biology" *J Cell Biochem* **103**(4): 1171-82.

Barlow, C., Brown, K. D., Deng, C. X., Tagle, D. A. y Wynshaw-Boris, A. (1997). "Atm selectively regulates distinct p53-dependent cell-cycle checkpoint and apoptotic pathways" *Nat Genet* **17**(4): 453-6.

Bartel, D. P. (2009). "MicroRNAs: target recognition and regulatory functions" *Cell* **136**(2): 215-33.

Barton, R. M. y Worman, H. J. (1999). "Prenylated prelamin A interacts with Narf, a novel nuclear protein" *J Biol Chem* **274**(42): 30008-18.

Batchelor, E., Mock, C. S., Bhan, I., Loewer, A. y Lahav, G. (2008). "Recurrent initiation: a mechanism for triggering p53 pulses in response to DNA damage" *Mol Cell* **30**(3): 277-89.

Batchelor, E., Loewer, A. y Lahav, G. (2009). "The ups and downs of p53: understanding protein dynamics in single cells" *Nat Rev Cancer* **9**(5): 371-7.

Bates, D. J., Li, N., Liang, R., Sarojini, H., An, J., Masternak, M. M., Bartke, A. y Wang, E. (2010). "MicroRNA regulation in Ames dwarf mouse liver may contribute to delayed aging" *Aging Cell* **9**(1): 1-18.

Blasco, M. A., Lee, H. W., Hande, M. P., Samper, E., Lansdorp, P. M., DePinho, R. A. y Greider, C. W. (1997). "Telomere shortening and tumor formation by mouse cells lacking telomerase RNA" *Cell* **91**(1): 25-34.

Brase, J. C., Wuttig, D., Kuner, R. y Sultmann, H. (2010). "Serum microRNAs as non-invasive biomarkers for cancer" *Mol Cancer* **9**: 306.

Brown-Borg, H. M. (2009). "Hormonal control of aging in rodents: the somatotropic axis" *Mol Cell Endocrinol* **299**(1): 64-71.

Bulavin, D. V., Demidov, O. N., Saito, S., Kauraniemi, P., Phillips, C., Amundson, S. A., Ambrosino, C., Sauter, G., Nebreda, A. R., Anderson, C. W., Kallioniemi, A., Fornace, A. J., Jr. y Appella, E. (2002). "Amplification of PPM1D in human tumors abrogates p53 tumor-suppressor activity" *Nat Genet* **31**(2): 210-5.

Byrom, J., Mudaliar, V., Redman, C. W., Jones, P., Strange, R. C. y Hoban, P. R. (2004). "Loss of heterozygosity at chromosome 9q22-31 is a frequent and early event in ovarian tumors" *Int J Oncol* **24**(5): 1271-7.

Cadel, S., Foulon, T., Viron, A., Balogh, A., Midol-Monnet, S., Noel, N. y Cohen, P. (1997). "Aminopeptidase B from the rat testis is a bifunctional enzyme structurally related to leukotriene-A4 hydrolase" *Proc Natl Acad Sci U S A* **94**(7): 2963-8.

Cadiñanos, J., Varela, I., López-Otín, C. y Freije, J. M. (2005). "From immature lamin to premature aging: molecular pathways and therapeutic opportunities" *Cell Cycle* **4**(12): 1732-5.

Calin, G. A., Sevignani, C., Dumitru, C. D., Hyslop, T., Noch, E., Yendamuri, S., Shimizu, M., Rattan, S., Bullrich, F., Negrini, M. y Croce, C. M. (2004). "Human microRNA genes are frequently located at fragile sites and genomic regions involved in cancers" *Proc Natl Acad Sci U S A* **101**(9): 2999-3004.

Ciccia, A. y Elledge, S. J. (2010). "The DNA damage response: making it safe to play with knives" *Mol Cell* **40**(2): 179-204.

Clemmons, D. R. (2007). "Modifying IGF1 activity: an approach to treat endocrine disorders, atherosclerosis and cancer" *Nat Rev Drug Discov* **6**(10): 821-33.

Collado, M., Blasco, M. A. y Serrano, M. (2007). "Cellular senescence in cancer and aging" *Cell* **130**(2): 223-33.

Coschigano, K. T., Holland, A. N., Riders, M. E., List, E. O., Flyvbjerg, A. y Kopchick, J. J. (2003). "Deletion, but not antagonism, of the mouse growth hormone receptor results in severely decreased body weights, insulin, and insulin-like growth factor I levels and increased life span" *Endocrinology* **144**(9): 3799-810.

Cha, H., Lowe, J. M., Li, H., Lee, J. S., Belova, G. I., Bulavin, D. V. y Fornace, A. J., Jr. (2010). "Wip1 directly dephosphorylates gamma-H2AX and attenuates the DNA damage response" *Cancer Res* **70**(10): 4112-22.

Chen, J. H., Hales, C. N. y Ozanne, S. E. (2007). "DNA damage, cellular senescence and organismal ageing: causal or correlative?" *Nucleic Acids Res* **35**(22): 7417-28.

Chew, A., Buck, E. A., Peretz, S., Sirugo, G., Rinaldo, P. y Isaya, G. (1997). "Cloning, expression, and chromosomal assignment of the human mitochondrial intermediate peptidase gene (MIPEP)" *Genomics* **40**(3): 493-6.

Chinchilla, A., Lozano, E., Daimi, H., Esteban, F. J., Crist, C., Aranega, A. E. y Franco, D. (2011). "MicroRNA profiling during mouse ventricular maturation: a role for miR-27 modulating Mef2c expression" *Cardiovasc Res* **89**(1): 98-108.

Chomczynski, P. y Sacchi, N. (1987). "Single-step method of RNA isolation by

acid guanidinium thiocyanate-phenol-chloroform extraction" *Anal Biochem* **162**(1): 156-9.

Danilczyk, U., Eriksson, U., Crackower, M. A. y Penninger, J. M. (2003). "A story of two ACEs" *J Mol Med* **81**(4): 227-34.

Danziger, R. S. (2008). "Aminopeptidase N in arterial hypertension" *Heart Fail Rev* **13**(3): 293-8.

Deng, S., Calin, G. A., Croce, C. M., Coukos, G. y Zhang, L. (2008). "Mechanisms of microRNA deregulation in human cancer" *Cell Cycle* **7**(17): 2643-6.

Donehower, L. A., Harvey, M., Slagle, B. L., McArthur, M. J., Montgomery, C. A., Jr., Butel, J. S. y Bradley, A. (1992). "Mice deficient for p53 are developmentally normal but susceptible to spontaneous tumours" *Nature* **356**(6366): 215-21.

Elmen, J., Lindow, M., Schutz, S., Lawrence, M., Petri, A., Obad, S., Lindholm, M., Hedtjarn, M., Hansen, H. F., Berger, U., Gullans, S., Kearney, P., Sarnow, P., Straarup, E. M. y Kauppinen, S. (2008). "LNA-mediated microRNA silencing in non-human primates" *Nature* **452**(7189): 896-9.

Espada, J., Varela, I., Flores, I., Ugalde, A. P., Cadiñanos, J., Pendás, A. M., Stewart, C. L., Tryggvason, K., Blasco, M. A., Freije, J. M. y López-Otín, C. (2008). "Nuclear envelope defects cause stem cell dysfunction in premature-aging mice" *J Cell Biol* **181**(1): 27-35.

Fanjul-Fernández, M., Folgueras, A. R., Cabrera, S. y López-Otín, C. (2010). "Matrix metalloproteinases: evolution, gene regulation and functional analysis in mouse models" *Biochim Biophys Acta* **1803**(1): 3-19.

Feinberg, A. P. (2007). "Phenotypic plasticity and the epigenetics of human disease" *Nature* **447**(7143): 433-40.

Folgueras, A. R., Pendás, A. M., Sánchez, L. M. y López-Otín, C. (2004). "Matrix metalloproteinases in cancer: from new functions to improved inhibition strategies" *Int J Dev Biol* **48**(5-6): 411-24.

Friedman, R. C., Farh, K. K., Burge, C. B. y Bartel, D. P. (2009). "Most mammalian mRNAs are conserved targets of microRNAs" *Genome Res* **19**(1): 92-105.

Fyhrquist, F. y Saijonmaa, O. (2008). "Renin-angiotensin system revisited" *J Intern Med* **264**(3): 224-36.

Garcia-Cao, I., Garcia-Cao, M., Martin-Caballero, J., Criado, L. M., Klatt, P., Flores, J. M., Weill, J. C., Blasco, M. A. y Serrano, M. (2002). ""Super p53" mice exhibit enhanced DNA damage response, are tumor resistant and age normally" *EMBO J* **21**(22): 6225-35.

Garinis, G. A., van der Horst, G. T., Vijg, J. y Hoeijmakers, J. H. (2008).

"DNA damage and ageing: new-age ideas for an age-old problem" *Nat Cell Biol* **10**(11): 1241-7.

Garinis, G. A., Uittenboogaard, L. M., Stachelscheid, H., Fousteri, M., van Ijcken, W., Breit, T. M., van Steeg, H., Mullenders, L. H., van der Horst, G. T., Bruning, J. C., Niessen, C. M., Hoeijmakers, J. H. y Schumacher, B. (2009). "Persistent transcription-blocking DNA lesions trigger somatic growth attenuation associated with longevity" *Nat Cell Biol* **11**(5): 604-15.

Garzon, R., Heaphy, C. E., Havelange, V., Fabbri, M., Volinia, S., Tsao, T., Zanesi, N., Kornblau, S. M., Marcucci, G., Calin, G. A., Andreeff, M. y Croce, C. M. (2009). "MicroRNA 29b functions in acute myeloid leukemia" *Blood* **114**(26): 5331-41.

Gatza, C. E., Dumble, M., Kittrell, F., Edwards, D. G., Dearth, R. K., Lee, A. V., Xu, J., Medina, D. y Donehower, L. A. (2008). "Altered mammary gland development in the p53+/m mouse, a model of accelerated aging" *Dev Biol* **313**(1): 130-41.

Gomis-Ruth, F. X. (2003). "Structural aspects of the metzincin clan of metalloendopeptidases" *Mol Biotechnol* **24**(2): 157-202.

Gravina, S. y Vijg, J. (2010). "Epigenetic factors in aging and longevity" *Pflugers Arch* **459**(2): 247-58.

Greer, E. L. y Brunet, A. (2005). "FOXO transcription factors at the interface between longevity and tumor suppression" *Oncogene* **24**(50): 7410-25.

Grigoriev, A. (2003). "On the number of protein-protein interactions in the yeast proteome" *Nucleic Acids Res* **31**(14): 4157-61.

Grimson, A., Farh, K. K., Johnston, W. K., Garrett-Engele, P., Lim, L. P. y Bartel, D. P. (2007). "MicroRNA targeting specificity in mammals: determinants beyond seed pairing" *Mol Cell* **27**(1): 91-105.

Gruenbaum, Y., Margalit, A., Goldman, R. D., Shumaker, D. K. y Wilson, K. L. (2005). "The nuclear lamina comes of age" *Nat Rev Mol Cell Biol* **6**(1): 21-31.

Guevara-Aguirre, J., Balasubramanian, P., Guevara-Aguirre, M., Wei, M., Madia, F., Cheng, C. W., Hwang, D., Martin-Montalvo, A., Saavedra, J., Ingles, S., de Cabo, R., Cohen, P. y Longo, V. D. (2011). "Growth hormone receptor deficiency is associated with a major reduction in pro-aging signaling, cancer, and diabetes in humans" *Sci Transl Med* **3**(70): 70ra13.

Guttman, M., Amit, I., Garber, M., French, C., Lin, M. F., Feldser, D., Huarte, M., Zuk, O., Carey, B. W., Cassady, J. P., Cabili, M. N., Jaenisch, R., Mikkelsen, T. S., Jacks, T., Hacohen, N., Bernstein, B. E., Kellis, M., Regev, A., Rinn, J. L. y Lander, E. S. (2009). "Chromatin signature reveals over a thousand highly conserved large non-coding RNAs in mammals" *Nature* **458**(7235): 223-7.

Haeggstrom, J. Z., Wetterholm, A., Vallee, B. L. y Samuelsson, B. (1990).

"Leukotriene A4 hydrolase: an epoxide hydrolase with peptidase activity" *Biochem Biophys Res Commun* **173**(1): 431-7.

Haigis, M. C. y Yankner, B. A. (2010). "The aging stress response" *Mol Cell* **40**(2): 333-44.

Hallberg, M. (2009). "Targeting the insulin-regulated aminopeptidase/AT4 receptor for cognitive disorders" *Drug News Perspect* **22**(3): 133-9.

Hayflick, L. y Moorhead, P. S. (1961). "The serial cultivation of human diploid cell strains" *Exp Cell Res* **25**: 585-621.

Hinkal, G. y Donehower, L. A. (2008). "How does suppression of IGF-1 signaling by DNA damage affect aging and longevity?" *Mech Ageing Dev* **129**(5): 243-53.

Hoeijmakers, J. H. (2009). "DNA damage, aging, and cancer" *N Engl J Med* **361**(15): 1475-85.

Holzenberger, M., Dupont, J., Ducos, B., Leneuve, P., Geloen, A., Even, P. C., Cervera, P. y Le Bouc, Y. (2003). "IGF-1 receptor regulates lifespan and resistance to oxidative stress in mice" *Nature* **421**(6919): 182-7.

Hoogervorst, E. M., van Steeg, H. y de Vries, A. (2005). "Nucleotide excision repair- and p53-deficient mouse models in cancer research" *Mutat Res* **574**(1-2): 3-21.

Huntzinger, E. y Izaurralde, E. (2011). "Gene silencing by microRNAs: contributions of translational repression and mRNA decay" *Nat Rev Genet* **12**(2): 99-110.

Inagaki, Y., Tang, W., Zhang, L., Du, G., Xu, W. y Kokudo, N. (2010). "Novel aminopeptidase N (APN/CD13) inhibitor 24F can suppress invasion of hepatocellular carcinoma cells as well as angiogenesis" *Biosci Trends* **4**(2): 56-60.

Ino, K., Shibata, K., Kajiyama, H., Kikkawa, F. y Mizutani, S. (2004). "Regulatory role of membrane-bound peptidases in the progression of gynecologic malignancies" *Biol Chem* **385**(8): 683-90.

Iturrioz, X., Rozenfeld, R., Michaud, A., Corvol, P. y Llorens-Cortes, C. (2001). "Study of asparagine 353 in aminopeptidase A: characterization of a novel motif (GXMEN) implicated in exopeptidase specificity of monozinc aminopeptidases" *Biochemistry* **40**(48): 14440-8.

Jacob, F. y Monod, J. (1961). "Genetic regulatory mechanisms in the synthesis of proteins" *J Mol Biol* **3**: 318-56.

Keller, S. R., Scott, H. M., Mastick, C. C., Aebersold, R. y Lienhard, G. E. (1995). "Cloning and characterization of a novel insulin-regulated membrane aminopeptidase from Glut4 vesicles" *J Biol Chem* **270**(40): 23612-8.

Kenyon, C., Chang, J., Gensch, E., Rudner, A. y Tabtiang, R. (1993). "A C. elegans mutant that lives twice as long as wild type" *Nature* **366**(6454): 461-4.

Kenyon, C. J. (2010). "The genetics of ageing" *Nature* **464**(7288): 504-12.

Kirkwood, T. B. y Holliday, R. (1979). "The evolution of ageing and longevity" *Proc R Soc Lond B Biol Sci* **205**(1161): 531-46.

Koppen, M. y Langer, T. (2007). "Protein degradation within mitochondria: versatile activities of AAA proteases and other peptidases" *Crit Rev Biochem Mol Biol* **42**(3): 221-42.

Lachance, C., Arbour, N., Cashman, N. R. y Talbot, P. J. (1998). "Involvement of aminopeptidase N (CD13) in infection of human neural cells by human coronavirus 229E" *J Virol* **72**(8): 6511-9.

Lagos-Quintana, M., Rauhut, R., Lendeckel, W. y Tuschl, T. (2001). "Identification of novel genes coding for small expressed RNAs" *Science* **294**(5543): 853-8.

Lander, E. S., Linton, L. M., Birren, B., Nusbaum, C., Zody, M. C., Baldwin, J., Devon, K., Dewar, K., Doyle, M., FitzHugh, W., Funke, R., Gage, D., Harris, K., Heaford, A., Howland, J., Kann, L., Lehoczky, J., LeVine, R., McEwan, P., McKernan, K. y col. (2001). "Initial sequencing and analysis of the human genome" *Nature* **409**(6822): 860-921.

Laron, Z. (2008). "The GH-IGF1 axis and longevity. The paradigm of IGF1 deficiency" *Hormones (Athens)* **7**(1): 24-7.

Lau, N. C., Lim, L. P., Weinstein, E. G. y Bartel, D. P. (2001). "An abundant class of tiny RNAs with probable regulatory roles in Caenorhabditis elegans" *Science* **294**(5543): 858-62.

Laustsen, P. G., Vang, S. y Kristensen, T. (2001). "Mutational analysis of the active site of human insulin-regulated aminopeptidase" *Eur J Biochem* **268**(1): 98-104.

Lavin, M. F. y Gueven, N. (2006). "The complexity of p53 stabilization and activation" *Cell Death Differ* **13**(6): 941-50.

Lee, R. C., Feinbaum, R. L. y Ambros, V. (1993). "The C. elegans heterochronic gene lin-4 encodes small RNAs with antisense complementarity to lin-14" *Cell* **75**(5): 843-54.

Lee, R. C. y Ambros, V. (2001). "An extensive class of small RNAs in Caenorhabditis elegans" *Science* **294**(5543): 862-4.

Leung, P. S. y Carlsson, P. O. (2001). "Tissue renin-angiotensin system: its expression, localization, regulation and potential role in the pancreas" *J Mol Endocrinol* **26**(3): 155-64.

Leung, P. S. y Sernia, C. (2003). "The renin-angiotensin system and male

reproduction: new functions for old hormones" *J Mol Endocrinol* **30**(3): 263-70.

Levy, G. G., Nichols, W. C., Lian, E. C., Foroud, T., McClintick, J. N., McGee, B. M., Yang, A. Y., Siemieniak, D. R., Stark, K. R., Gruppo, R., Sarode, R., Shurin, S. B., Chandrasekaran, V., Stabler, S. P., Sabio, H., Bouhassira, E. E., Upshaw, J. D., Jr., Ginsburg, D. y Tsai, H. M. (2001). "Mutations in a member of the ADAMTS gene family cause thrombotic thrombocytopenic purpura" *Nature* **413**(6855): 488-94.

Lewis, B. P., Burge, C. B. y Bartel, D. P. (2005). "Conserved seed pairing, often flanked by adenosines, indicates that thousands of human genes are microRNA targets" *Cell* **120**(1): 15-20.

Li, M., Marin-Muller, C., Bharadwaj, U., Chow, K. H., Yao, Q. y Chen, C. (2009). "MicroRNAs: control and loss of control in human physiology and disease" *World J Surg* **33**(4): 667-84.

Lichun, Y., Ching Tang, C. M., Wai Lau, K. y Lung, M. L. (2004). "Frequent loss of heterozygosity on chromosome 9 in Chinese esophageal squamous cell carcinomas" *Cancer Lett* **203**(1): 71-7.

Lim, E. J., Sampath, S., Coll-Rodríguez, J., Schmidt, J., Ray, K. y Rodgers, D. W. (2007). "Swapping the substrate specificities of the neuropeptidases neurolysin and thimet oligopeptidase" *J Biol Chem* **282**(13): 9722-32.

Liu, H., Bravata, D. M., Olkin, I., Nayak, S., Roberts, B., Garber, A. M. y Hoffman, A. R. (2007). "Systematic review: the safety and efficacy of growth hormone in the healthy elderly" *Ann Intern Med* **146**(2): 104-15.

Liu, N., Bezprozvannaya, S., Williams, A. H., Qi, X., Richardson, J. A., Bassel-Duby, R. y Olson, E. N. (2008). "microRNA-133a regulates cardiomyocyte proliferation and suppresses smooth muscle gene expression in the heart" *Genes Dev* **22**(23): 3242-54.

Liu, S., Wu, L. C., Pang, J., Santhanam, R., Schwind, S., Wu, Y. Z., Hickey, C. J., Yu, J., Becker, H., Maharry, K., Radmacher, M. D., Li, C., Whitman, S. P., Mishra, A., Stauffer, N., Eiring, A. M., Briesewitz, R., Baiocchi, R. A., Chan, K. K., Paschka, P. y col. (2010). "Sp1/NFkappaB/HDAC/miR-29b regulatory network in KIT-driven myeloid leukemia" *Cancer Cell* **17**(4): 333-47.

Locke, D. P., Hillier, L. W., Warren, W. C., Worley, K. C., Nazareth, L. V., Muzny, D. M., Yang, S. P., Wang, Z., Chinwalla, A. T., Minx, P., Mitreva, M., Cook, L., Delehaunty, K. D., Fronick, C., Schmidt, H., Fulton, L. A., Fulton, R. S., Nelson, J. O., Magrini, V., Pohl, C. y col. (2011). "Comparative and demographic analysis of orang-utan genomes" *Nature* **469**(7331): 529-33.

López-Contreras, A. J. y Fernández-Capetillo, O. (2010). "The ATR barrier to replication-born DNA damage" *DNA Repair (Amst)* **9**(12): 1249-55.

López-Otín, C. y Overall, C. M. (2002). "Protease degradomics: a new challenge for proteomics" *Nat Rev Mol Cell Biol* **3**(7): 509-19.

López-Otín, C. y Matrisian, L. M. (2007). "Emerging roles of proteases in tumour suppression" *Nat Rev Cancer* **7**(10): 800-8.

López-Otín, C. y Bond, J. S. (2008). "Proteases: multifunctional enzymes in life and disease" *J Biol Chem* **283**(45): 30433-7.

López-Otín, C. y Hunter, T. (2010). "The regulatory crosstalk between kinases and proteases in cancer" *Nat Rev Cancer* **10**(4): 278-92.

Lu, J., Getz, G., Miska, E. A., Alvarez-Saavedra, E., Lamb, J., Peck, D., Sweet-Cordero, A., Ebert, B. L., Mak, R. H., Ferrando, A. A., Downing, J. R., Jacks, T., Horvitz, H. R. y Golub, T. R. (2005). "MicroRNA expression profiles classify human cancers" *Nature* **435**(7043): 834-8.

Lu, X., Ma, O., Nguyen, T. A., Jones, S. N., Oren, M. y Donehower, L. A. (2007). "The Wip1 Phosphatase acts as a gatekeeper in the p53-Mdm2 autoregulatory loop" *Cancer Cell* **12**(4): 342-54.

Lu, X., Nguyen, T. A., Zhang, X. y Donehower, L. A. (2008). "The Wip1 phosphatase and Mdm2: cracking the "Wip" on p53 stability" *Cell Cycle* **7**(2): 164-8.

Luciani, N., Marie-Claire, C., Ruffet, E., Beaumont, A., Roques, B. P. y Fournie-Zaluski, M. C. (1998). "Characterization of Glu350 as a critical residue involved in the N-terminal amine binding site of aminopeptidase N (EC 3.4.11.2): insights into its mechanism of action" *Biochemistry* **37**(2): 686-92.

Llamazares, M., Cal, S., Quesada, V. y López-Otín, C. (2003). "Identification and characterization of ADAMTS-20 defines a novel subfamily of metalloproteinases-disintegrins with multiple thrombospondin-1 repeats and a unique GON domain" *J Biol Chem* **278**(15): 13382-9.

Machwe, A., Xiao, L., Groden, J. y Orren, D. K. (2006). "The Werner and Bloom syndrome proteins catalyze regression of a model replication fork" *Biochemistry* **45**(47): 13939-46.

Maes, O. C., An, J., Sarojini, H. y Wang, E. (2008). "Murine microRNAs implicated in liver functions and aging process" *Mech Ageing Dev* **129**(9): 534-41.

Mariño, G., Ugalde, A. P., Salvador-Montoliu, N., Varela, I., Quiros, P. M., Cadiñanos, J., van der Pluijm, I., Freije, J. M. y López-Otín, C. (2008). "Premature aging in mice activates a systemic metabolic response involving autophagy induction" *Hum Mol Genet* **17**(14): 2196-211.

Mariño, G., Ugalde, A. P., Fernández, A. F., Osorio, F. G., Fueyo, A., Freije, J. M. y López-Otín, C. (2010). "Insulin-like growth factor 1 treatment extends longevity in a mouse model of human premature aging by restoring somatotroph axis function" *Proc Natl Acad Sci U S A* **107**(37): 16268-73.

Mott, J. L., Kobayashi, S., Bronk, S. F. y Gores, G. J. (2007). "mir-29 regulates Mcl-1 protein expression and apoptosis" *Oncogene* **26**(42): 6133-40.

Mott, J. L., Kurita, S., Cazanave, S. C., Bronk, S. F., Werneburg, N. W. y Fernández-Zapico, M. E. (2010). "Transcriptional suppression of mir-29b-1/mir-29a promoter by c-Myc, hedgehog, and NF-kappaB" *J Cell Biochem* **110**(5): 1155-64.

Muniyappa, M. K., Dowling, P., Henry, M., Meleady, P., Doolan, P., Gammell, P., Clynes, M. y Barron, N. (2009). "MiRNA-29a regulates the expression of numerous proteins and reduces the invasiveness and proliferation of human carcinoma cell lines" *Eur J Cancer* **45**(17): 3104-18.

Murga, M., Bunting, S., Montana, M. F., Soria, R., Mulero, F., Canamero, M., Lee, Y., McKinnon, P. J., Nussenzweig, A. y Fernández-Capetillo, O. (2009). "A mouse model of ATR-Seckel shows embryonic replicative stress and accelerated aging" *Nat Genet* **41**(8): 891-8.

Niedernhofer, L. J., Garinis, G. A., Raams, A., Lalai, A. S., Robinson, A. R., Appeldoorn, E., Odijk, H., Oostendorp, R., Ahmad, A., van Leeuwen, W., Theil, A. F., Vermeulen, W., van der Horst, G. T., Meinecke, P., Kleijer, W. J., Vijg, J., Jaspers, N. G. y Hoeijmakers, J. H. (2006). "A new progeroid syndrome reveals that genotoxic stress suppresses the somatotroph axis" *Nature* **444**(7122): 1038-43.

Obermann, E. C., Meyer, S., Hellge, D., Zaak, D., Filbeck, T., Stoehr, R., Hofstaedter, F., Hartmann, A. y Knuechel, R. (2004). "Fluorescence in situ hybridization detects frequent chromosome 9 deletions and aneuploidy in histologically normal urothelium of bladder cancer patients" *Oncol Rep* **11**(4): 745-51.

Ordoñez, G. R., Hillier, L. W., Warren, W. C., Grutzner, F., López-Otín, C. y Puente, X. S. (2008). "Loss of genes implicated in gastric function during platypus evolution" *Genome Biol* **9**(5): R81.

Osorio, F. G., Obaya, A. J., López-Otín, C. y Freije, J. M. (2009). "Accelerated ageing: from mechanism to therapy through animal models" *Transgenic Res* **18**(1): 7-15.

Osorio, F. G., Varela, I., Lara, E., Puente, X. S., Espada, J., Santoro, R., Freije, J. M., Fraga, M. F. y López-Otín, C. (2010). "Nuclear envelope alterations generate an aging-like epigenetic pattern in mice deficient in Zmpste24 metalloprotease" *Aging Cell* **9**(6): 947-57.

Overall, C. M. y López-Otín, C. (2002). "Strategies for MMP inhibition in cancer: innovations for the post-trial era" *Nat Rev Cancer* **2**(9): 657-72.

Park, C. Y., Choi, Y. S. y McManus, M. T. (2010). "Analysis of microRNA knockouts in mice" *Hum Mol Genet* **19**(R2): R169-75.

Park, S. Y., Lee, J. H., Ha, M., Nam, J. W. y Kim, V. N. (2009). "miR-29 miRNAs activate p53 by targeting p85 alpha and CDC42" *Nat Struct Mol Biol* **16**(1): 23-9.

Pasquinelli, A. E., Reinhart, B. J., Slack, F., Martindale, M. Q., Kuroda, M. I.,

Maller, B., Hayward, D. C., Ball, E. E., Degnan, B., Muller, P., Spring, J., Srinivasan, A., Fishman, M., Finnerty, J., Corbo, J., Levine, M., Leahy, P., Davidson, E. y Ruvkun, G. (2000). "Conservation of the sequence and temporal expression of let-7 heterochronic regulatory RNA" *Nature* **408**(6808): 86-9.

Pass, H. I., Goparaju, C., Ivanov, S., Donington, J., Carbone, M., Hoshen, M., Cohen, D., Chajut, A., Rosenwald, S., Dan, H., Benjamin, S. y Aharonov, R. (2010). "hsa-miR-29c* is linked to the prognosis of malignant pleural mesothelioma" *Cancer Res* **70**(5): 1916-24.

Pekarsky, Y., Santanam, U., Cimmino, A., Palamarchuk, A., Efanov, A., Maximov, V., Volinia, S., Alder, H., Liu, C. G., Rassenti, L., Calin, G. A., Hagan, J. P., Kipps, T. y Croce, C. M. (2006). "Tcl1 expression in chronic lymphocytic leukemia is regulated by miR-29 and miR-181" *Cancer Res* **66**(24): 11590-3.

Pendás, A. M., Zhou, Z., Cadiñanos, J., Freije, J. M., Wang, J., Hultenby, K., Astudillo, A., Wernerson, A., Rodríguez, F., Tryggvason, K. y López-Otín, C. (2002). "Defective prelamin A processing and muscular and adipocyte alterations in Zmpste24 metalloproteinase-deficient mice" *Nat Genet* **31**(1): 94-9.

Perez, V. I., Van Remmen, H., Bokov, A., Epstein, C. J., Vijg, J. y Richardson, A. (2009). "The overexpression of major antioxidant enzymes does not extend the lifespan of mice" *Aging Cell* **8**(1): 73-5.

Pham, V. L., Cadel, M. S., Gouzy-Darmon, C., Hanquez, C., Beinfeld, M. C., Nicolas, P., Etchebest, C. y Foulon, T. (2007). "Aminopeptidase B, a glucagon-processing enzyme: site directed mutagenesis of the Zn2+-binding motif and molecular modelling" *BMC Biochem* **8**(1): 21.

Porter, S., Clark, I. M., Kevorkian, L. y Edwards, D. R. (2005). "The ADAMTS metalloproteinases" *Biochem J* **386**(Pt 1): 15-27.

Puente, X. S., Sánchez, L. M., Overall, C. M. y López-Otín, C. (2003). "Human and mouse proteases: a comparative genomic approach" *Nat Rev Genet* **4**(7): 544-58.

Puente, X. S. y López-Otín, C. (2004). "A genomic analysis of rat proteases and protease inhibitors" *Genome Res* **14**(4): 609-22.

Puente, X. S., Gutierrez-Fernández, A., Ordoñez, G. R., Hillier, L. W. y López-Otín, C. (2005). "Comparative genomic analysis of human and chimpanzee proteases" *Genomics* **86**(6): 638-47.

Puente, X. S., Quesada, V., Osorio, F. G., Cabanillas, R., Cadiñanos, J., Fraile, J. M., Ordóñez, G. R., Puente, D. A., Gutierrez-Fernández, A., Fanjul-Fernández, M., Levy, N., Freije, J. M. y López-Otín, C. (2011). "Exome Sequencing and Functional Analysis Identifies BANF1 Mutation as the Cause of a Hereditary Progeroid Syndrome" *Am J Hum Genet* **88**(5): 650-6.

Quesada, V., Ordóñez, G. R., Sánchez, L. M., Puente, X. S. y López-Otín, C. (2009). "The Degradome database: mammalian proteases and diseases of proteolysis" *Nucleic Acids Res* **37**(Database issue): D239-43.

Ramirez, C. L., Cadiñanos, J., Varela, I., Freije, J. M. y López-Otín, C. (2007). "Human progeroid syndromes, aging and cancer: new genetic and epigenetic insights into old questions" *Cell Mol Life Sci* **64**(2): 155-70.

Rao, P. H., Houldsworth, J., Palanisamy, N., Murty, V. V., Reuter, V. E., Motzer, R. J., Bosl, G. J. y Chaganti, R. S. (1998). "Chromosomal amplification is associated with cisplatin resistance of human male germ cell tumors" *Cancer Res* **58**(19): 4260-3.

Rawlings, N. D. y Barrett, A. J. (1993). "Evolutionary families of peptidases" *Biochem J* **290 (Pt 1)**: 205-18.

Reaux, A., Fournie-Zaluski, M. C., David, C., Zini, S., Roques, B. P., Corvol, P. y Llorens-Cortes, C. (1999). "Aminopeptidase A inhibitors as potential central antihypertensive agents" *Proc Natl Acad Sci U S A* **96**(23): 13415-20.

Reiss, K. y Saftig, P. (2009). "The "a disintegrin and metalloprotease" (ADAM) family of sheddases: physiological and cellular functions" *Semin Cell Dev Biol* **20**(2): 126-37.

Sambrook, J. y Russell, D. W. (2001). "Molecular cloning: a laboratory manual". *Cold Spring Harbor Laboratory Press, NY*.

Schauder, B., Schomburg, L., Kohrle, J. y Bauer, K. (1994). "Cloning of a cDNA encoding an ectoenzyme that degrades thyrotropin-releasing hormone" *Proc Natl Acad Sci U S A* **91**(20): 9534-8.

Schwarz, D. S., Hutvagner, G., Du, T., Xu, Z., Aronin, N. y Zamore, P. D. (2003). "Asymmetry in the assembly of the RNAi enzyme complex" *Cell* **115**(2): 199-208.

Serwold, T., Gonzalez, F., Kim, J., Jacob, R. y Shastri, N. (2002). "ERAAP customizes peptides for MHC class I molecules in the endoplasmic reticulum" *Nature* **419**(6906): 480-3.

Simoneau, M., LaRue, H., Aboulkassim, T. O., Meyer, F., Moore, L. y Fradet, Y. (2000). "Chromosome 9 deletions and recurrence of superficial bladder cancer: identification of four regions of prognostic interest" *Oncogene* **19**(54): 6317-23.

Somel, M., Guo, S., Fu, N., Yan, Z., Hu, H. Y., Xu, Y., Yuan, Y., Ning, Z., Hu, Y., Menzel, C., Hu, H., Lachmann, M., Zeng, R., Chen, W. y Khaitovich, P. (2010). "MicroRNA, mRNA, and protein expression link development and aging in human and macaque brain" *Genome Res* **20**(9): 1207-18.

Stanhope, M. J., Lupas, A., Italia, M. J., Koretke, K. K., Volker, C. y Brown, J. R. (2001). "Phylogenetic analyses do not support horizontal gene transfers from bacteria to vertebrates" *Nature* **411**(6840): 940-4.

Tatar, M., Kopelman, A., Epstein, D., Tu, M. P., Yin, C. M. y Garofalo, R. S. (2001). "A mutant Drosophila insulin receptor homolog that extends life-span and impairs neuroendocrine function" *Science* **292**(5514): 107-10.

Thompson, M. W., Govindaswami, M. y Hersh, L. B. (2003). "Mutation of active site residues of the puromycin-sensitive aminopeptidase: conversion of the enzyme into a catalytically inactive binding protein" *Arch Biochem Biophys* **413**(2): 236-42.

Thunnissen, M. M., Nordlund, P. y Haeggstrom, J. Z. (2001). "Crystal structure of human leukotriene A(4) hydrolase, a bifunctional enzyme in inflammation" *Nat Struct Biol* **8**(2): 131-5.

Tsujimoto, M., Mizutani, S., Adachi, H., Kimura, M., Nakazato, H. y Tomoda, Y. (1992). "Identification of human placental leucine aminopeptidase as oxytocinase" *Arch Biochem Biophys* **292**(2): 388-92.

Turner, A. J., Isaac, R. E. y Coates, D. (2001). "The neprilysin (NEP) family of zinc metalloendopeptidases: genomics and function" *Bioessays* **23**(3): 261-9.

Tyner, S. D., Venkatachalam, S., Choi, J., Jones, S., Ghebranious, N., Igelmann, H., Lu, X., Soron, G., Cooper, B., Brayton, C., Hee Park, S., Thompson, T., Karsenty, G., Bradley, A. y Donehower, L. A. (2002). "p53 mutant mice that display early ageing-associated phenotypes" *Nature* **415**(6867): 45-53.

van de Ven, M., Andressoo, J. O., Holcomb, V. B., von Lindern, M., Jong, W. M., De Zeeuw, C. I., Suh, Y., Hasty, P., Hoeijmakers, J. H., van der Horst, G. T. y Mitchell, J. R. (2006). "Adaptive stress response in segmental progeria resembles long-lived dwarfism and calorie restriction in mice" *PLoS Genet* **2**(12): e192.

van der Pluijm, I., Garinis, G. A., Brandt, R. M., Gorgels, T. G., Wijnhoven, S. W., Diderich, K. E., de Wit, J., Mitchell, J. R., van Oostrom, C., Beems, R., Niedernhofer, L. J., Velasco, S., Friedberg, E. C., Tanaka, K., van Steeg, H., Hoeijmakers, J. H. y van der Horst, G. T. (2007). "Impaired genome maintenance suppresses the growth hormone--insulin-like growth factor 1 axis in mice with Cockayne syndrome" *PLoS Biol* **5**(1): e2.

Van Raamsdonk, J. M. y Hekimi, S. (2009). "Deletion of the mitochondrial superoxide dismutase sod-2 extends lifespan in Caenorhabditis elegans" *PLoS Genet* **5**(2): e1000361.

Varela, I., Cadiñanos, J., Pendás, A. M., Gutierrez-Fernández, A., Folgueras, A. R., Sánchez, L. M., Zhou, Z., Rodríguez, F. J., Stewart, C. L., Vega, J. A., Tryggvason, K., Freije, J. M. y López-Otín, C. (2005). "Accelerated ageing in mice deficient in Zmpste24 protease is linked to p53 signalling activation" *Nature* **437**(7058): 564-8.

Varela, I., Pereira, S., Ugalde, A. P., Navarro, C. L., Suárez, M. F., Cau, P., Cadiñanos, J., Osorio, F. G., Foray, N., Cobo, J., de Carlos, F., Levy, N., Freije, J. M. y López-Otín, C. (2008). "Combined treatment with statins and

aminobisphosphonates extends longevity in a mouse model of human premature aging" *Nat Med* **14**(7): 767-72.

Vazeux, G., Iturrioz, X., Corvol, P. y Llorens-Cortes, C. (1998). "A glutamate residue contributes to the exopeptidase specificity in aminopeptidase A" *Biochem J* **334 (Pt 2)**: 407-13.

Ventura, A., Young, A. G., Winslow, M. M., Lintault, L., Meissner, A., Erkeland, S. J., Newman, J., Bronson, R. T., Crowley, D., Stone, J. R., Jaenisch, R., Sharp, P. A. y Jacks, T. (2008). "Targeted deletion reveals essential and overlapping functions of the miR-17 through 92 family of miRNA clusters" *Cell* **132**(5): 875-86.

Wang, H., Garzon, R., Sun, H., Ladner, K. J., Singh, R., Dahlman, J., Cheng, A., Hall, B. M., Qualman, S. J., Chandler, D. S., Croce, C. M. y Guttridge, D. C. (2008). "NF-kappaB-YY1-miR-29 regulatory circuitry in skeletal myogenesis and rhabdomyosarcoma" *Cancer Cell* **14**(5): 369-81.

Williams, A. E., Perry, M. M., Moschos, S. A. y Lindsay, M. A. (2007). "microRNA expression in the aging mouse lung" *BMC Genomics* **8**: 172.

Winter, J., Jung, S., Keller, S., Gregory, R. I. y Diederichs, S. (2009). "Many roads to maturity: microRNA biogenesis pathways and their regulation" *Nat Cell Biol* **11**(3): 228-34.

Wolf, E., Kahnt, E., Ehrlein, J., Hermanns, W., Brem, G. y Wanke, R. (1993). "Effects of long-term elevated serum levels of growth hormone on life expectancy of mice: lessons from transgenic animal models" *Mech Ageing Dev* **68**(1-3): 71-87.

Xiong, Y., Fang, J. H., Yun, J. P., Yang, J., Zhang, Y., Jia, W. H. y Zhuang, S. M. (2010). "Effects of microRNA-29 on apoptosis, tumorigenicity, and prognosis of hepatocellular carcinoma" *Hepatology* **51**(3): 836-45.

Yakar, S., Setser, J., Zhao, H., Stannard, B., Haluzik, M., Glatt, V., Bouxsein, M. L., Kopchick, J. J. y LeRoith, D. (2004). "Inhibition of growth hormone action improves insulin sensitivity in liver IGF-1-deficient mice" *J Clin Invest* **113**(1): 96-105.

Zhang, B., Pan, X., Cobb, G. P. y Anderson, T. A. (2007). "microRNAs as oncogenes and tumor suppressors" *Dev Biol* **302**(1): 1-12.

Zhao, J. J., Lin, J., Lwin, T., Yang, H., Guo, J., Kong, W., Dessureault, S., Moscinski, L. C., Rezania, D., Dalton, W. S., Sotomayor, E., Tao, J. y Cheng, J. Q. (2010). "microRNA expression profile and identification of miR-29 as a prognostic marker and pathogenetic factor by targeting CDK6 in mantle cell lymphoma" *Blood* **115**(13): 2630-9.